# Manipulating Triplets in Organic Semiconductors

David Martin Eric Freeman

A thesis submitted in part fulfilment towards the award of

Doctor of Philosophy

UCL

Under the Supervision of Dr. Hugo Bronstein

I, David Martin Eric Freeman, confirm that the work presented in this thesis is my own. Where information has been derived from other sources, I confirm that this has been indicated in the thesis.

# Abstract

Triplet states in organic semiconducting devices are often associated with loss processes. Radiative decay to the ground state is a spin disallowed process, which results in triplets in normal organic systems decaying primarily though non-radiative pathways. In OLEDs, where 75% of created excitons are triplets, this has a large impact on device efficiency.

The work herein focusses on the synthesis of organic polymers that utilise triplet states in some useful fashion. This was first achieved through incorporation of a heavy metal in the polymer chain, which increased spin-orbit coupling and allowed phosphorescence to occur. The heavy metal was incorporated directly into the polymer backbone as part of a porphyrin complex.

Focus then moved to organic polymers that have decreased first excited singlet-triplet energy gaps. This allows excitons to move from singlet to triplet state without the use of a heavy metal, a formally spin disallowed process. Thermally activated delayed fluorescence is observed in one polymer.

All synthetic work carried out is linked by the aim of using triplet states usefully in a resultant device. While the applications of the devices may differ, all in some way use triplet states in the movement of energy through the electronic system of the polymer. It is hoped that some of this work may form the basis of new types of materials for organic semiconducting systems.

# Impact Statement

Three publications have resulted directly from the work presented herein. At the time of submission, these works have generated 20 citations and thousands of individual page views (as of 06/06/18). The work has been presented at domestic and international scientific conferences which were attended by leaders in the fields of polymer synthesis and organic electronics as physicists, chemists and materials scientists.

The development of OLED technology has already shown benefits to society as a whole and is employed by many companies in marketable products. The further development of organic electronic materials therefore has obvious benefits in a non-academic setting. It is hoped this work may lead to further increases in efficiency for light emitting organic polymers and more efficient, more eco-friendly devices.

# Table of Contents


Abstract ..... v

Impact Statement ..... vi

Contributions ..... ix

Acknowledgments ..... x

Publications ..... xi

List of Abbreviations ..... xii

**Chapter 1: Introduction ..... 2**

1.1 Polymers ..... 2

1.2 Organic Semiconducting Devices ..... 6

1.3 Triplet states in Organic Semiconductors ..... 13

1.4 Porphyrins ..... 20

**Chapter 2: Phosphorescent Polymers: Incorporating a Covalently Bound Porphyrin in Polymers ..... 24**

2.1 Introduction ..... 24

2.2 A Platinum Containing Polyfluorene for Phosphorescent Emission: PF MPP(Pt) ..... 28

2.3 Towards a Triplet-triplet Annihilation Polymer: PDPA MPP(Pt) ..... 40

2.4 Conclusions ..... 52

**Chapter 3: Low Energy Triplet Formation for TTA Polymers: Extended Porphyrins ..... 54**

3.1 Introduction ..... 54

3.2 Synthesis of Extended Porphyrins ..... 58

3.3 Conclusions ..... 74

**Chapter 4: Reducing the Singlet-Triplet Energy Gap: Donor-Orthogonal Acceptor Polymers ..... 78**

4.1 Introduction ..... 78

4.2 Synthesis of SFCN and SFH ..... 89

4.3 Synthesis of ASFCN and ASFH ..... 96

4.4 Physical and Optical Properties of SFH, SFCN, ASFH and ASFCN ..... 104

4.5 Conclusions ..... 112

**Chapter 5: Circularly Polarised Light Emitting Polymers: Synthesis of Chiral Monomers . 116**

5.1 Introduction ..... 116

5.2 Synthesis of AB Ring System ..... 119

5.3 Synthesis of CD Ring System and Chiral Spiro Monomer ..... 126

5.4 Conclusions ..... 133

**Chapter 6: Experimental ..... 136**

6.1 General Procedures ..... 136
6.2 Synthetic Techniques for Chapter 2 ..... 141
6.3 Synthetic Techniques for Chapter 3 ..... 151
6.4 Synthetic Techniques for Chapter 4 ..... 170
6.5 Synthetic Techniques for Chapter 5 ..... 186
**References ..... 200**
**Appendices ..... 208**
Appendix 1: Deep-red electrophosphorescence from a platinum(II)–porphyrin complex copolymerised with polyfluorene for efficient energy transfer and triplet harvesting ..... 208
Appendix 2: Highly red-shifted NIR emission from a novel anthracene conjugated polymer backbone containing Pt(II) porphyrins ..... 218
Appendix 3: Synthesis and Exciton Dynamics of Donor-Orthogonal Acceptor Conjugated Polymers: Reducing the Singlet–Triplet Energy Gap ..... 230

# Contributions

Collaboration with other groups was a large part of this body of work. As a synthetic chemist, I have relied on physicists, physical chemists and materials scientists to process my polymers into devices and perform complex measurements that I was not equipped for. Where appropriate, figures or data that have been obtained by someone other than myself have been labelled in the text.

***Chapter 2:*** Giulia Tregnago and Alessandro Minotto in Franco Cacialli's group in the UCL physics department performed device fabrication and measurements on the **PF MPP(Pt)** and **PDPA MPP(Pt)** polymers respectively.

***Chapter 3:*** Jordan Shaikh in Tracey Clarke's group in the UCL chemistry department performed physical testing of **HAPPAP F8BT.** His work has not been directly discussed in this text as it is ongoing.

***Chapter 4:*** Andrew Musser in Richard Friend's group in the Cambridge physics department performed device fabrication and measurements on **SFH**, **SFCN**, **ASFH** and **ASFCN**. Jarvist Frost in the Imperial chemistry department performed computational calculations.

# Acknowledgments

Thank you to Hugo Bronstein, who has been an excellent supervisor throughout my PhD. Your unique supervisorial style is in my opinion the very best way to conduct research. I have enjoyed myself immensely and learned a great deal, this is in large part thanks to you.

Thanks also to Kealan Fallon, you probably would have preferred a longer acknowledgment. Thank you to Tom Waugh, since you like gimmicky things, here is a haiku. Oliver Ware has been around since I started, I would like to thank him for the times he wasn't.

Past and present members of the Bronstein group, thank you to all. Anastasia, Alex and Niall especially, you have all made UCL a better place by your presence, I don't care what everyone else says.

Thanks family. Hi Mum, you don't have to read the whole thing.

The following work has been in part paid for by the generous donations of the Johanna Eaden foundation for impoverished boyfriends.

# Publications

***Chapter 2 – Appendices I and II***

**Freeman D. M. E.**, Minotto A., Duffy W., Fallon K. J., McCulloch I., Cacialli F., Bronstein H. "Highly red-shifted NIR emission from a novel anthracene conjugated polymer backbone containing Pt(II) porphyrins", *Polym. Chem.*, **2016**, 7, 722-730

**Freeman D. M. E.**, Tregnago G., Rodriguez S. A., Fallon K. J., Cacialli F., Bronstein H. "Deep-red electrophosphorescence from a platinum(II)–porphyrin complex copolymerised with polyfluorene for efficient energy transfer and triplet harvesting", *J. Org. Semiconductors*, **2015**, 3, (1), 1-7

***Chapter 4 – Appendix III***

**Freeman D. M. E.**, Musser A., Frost J., Stern H., Fallon K. J., McCulloch I., Clarke T., Friend R., Bronstein H. "Donor-Orthogonal Acceptor Conjugated Polymers: Reducing the Singlet-Triplet Energy Gap in Conjugated Polymers", *J. Am. Chem. Soc.*, **2017**, *139* (32), pp 11073–11080

***As Contributing Author***

- Lin, Y. L.; Koch, M.; Brigeman, A. N.; **Freeman, D. M. E.**; Zhao, L.; Bronstein, H.; Giebink, N. C.; Scholes, G. D.; Rand, B. P. "Enhanced sub-bandgap efficiency of a solid-state organic intermediate band solar cell using triplet–triplet annihilation", *Energy Environ Sci,* **2017**, 10, 1465-1475

- Fallon K. J., Santala A., Wijeyasinghe N., Manley E. F., Goodeal N., Leventis A., **Freeman D. M. E**., Al-Hashimi M., Chen L. X., Marks T. J., Anthopoulos T. D., Bronstein H., "Effect of Alkyl Chain Branching Point on 3D Crystallinity in High N-type Mobility Indolonaphthyridine Polymers", *Adv. Funct. Mater.*, **2017**, 1704069

- Fallon K. J., Wijeyasinghe N., Manley E. F., Dimitrov S. D., Yousaf S. A., Ashraf R. S., Duffy W., **Freeman D. M. E.**, Al-Hashimi M., Durrant J. R., Chen L. X., McCulloch I., Marks T. J., Clarke T., Anthopoulos T. D., Bronstein H. "Indolo-naphthyridine-6,13-dione thiophene (INDT) building block for conjugated polymer electronics: Molecular origin of ultra-high n-type mobility", *Chem. Mater.*, **2016**, 28, (22), 8366–8378

- Fallon K. J., Wijeyasinghe N., Yaacobi-Gross N., Ashraf R. S., **Freeman D. M. E.**, Palgrave R. G., Al-Hashimi M., Marks T. J., McCulloch I., Anthopoulos T. D., Bronstein H. "A Nature-Inspired Conjugated Polymer for High Performance Transistors and Solar Cells", *Macromolecules*, **2015**, 48, (15), 5148–5154

# List of Abbreviations

| | |
|---|---|
| °C | Degrees centigrade |
| $\mu$L | Microlitre |
| $\mu$s | Microsecond |
| 3D | 3 dimensional |
| Ac | Acetyl |
| acac | Acetylacetone |
| AD | Asymmetric dihydroxylation |
| AIBN | Azobisisobutyronitrile |
| Ar | Aromatic group |
| ASFCN | *Poly*-4',4''-(4-(2-octyldodecyl)-*N*,*N*-diphenylaniline)-*alt*-2,7-(9,9'-spirobi[fluorene]-2',7'-dicarbonitrile) |
| ASFH | *Poly*-4',4''-(4-(2-octyldodecyl)-*N*,*N*-diphenylaniline)-*alt*-2,7-(9,9'-spirobi[fluorene]) |
| ASTM | American Society for Testing and Materials |
| br | Broad |
| Bu | Butyl |
| *c* | Concentration |
| calcd | Calculated |
| cat | Catalyst |
| CB | Conduction band |
| CD | Compact disk |
| Cd | Candela |
| conc | Concentrated aqueous solution |
| CPL | Circularly polarised light |
| CT | Charge transfer |
| Cyano-PPV | Poly(2,5-di(hexyloxy)cyanoterephthalylidene) |
| d | Days |
| *d* | Doublet |
| Đ | Dispersity |
| DA | Donor-acceptor |
| Da | Daltons |
| DBU | 1,8-Diazabicycloundec-7-ene |
| *dd* | Doublet of doublets |
| *ddd* | Doublet of doublet of doublets |
| *dddd* | Doublet of doublet of doublet of doublets |
| DDQ | 2,3-Dichloro-5,6-dicyano-1,4-benzoquinone |
| DEPT | Distortionless enhancement by polarization transfer |
| DFT | Density functional theory |
| DIPEA | *N*,*N*-Diisopropylethylamine |
| DME | Dimethoxyethane |
| DMF | Dimethylformamide |
| DMSO | Dimethylsulfoxide |
| DNA | Deoxyribonucleic acid |
| DoA | Donor-orthogonal acceptor |
| dppf | 1,1'-Bis(diphenylphosphino)ferrocene |
| dppp | 1,3-Bis(diphenylphosphino)propane |
| DSS | Dye sensitised solar cell |
| *dt* | Doublet of triplets |
| EDG | Electron donating group |
| *ee* | Enantiomeric excess |
| *eg* | For example |
| EL | Electroluminescence |
| eq | Equivalents |
| EQE | External quantum efficiency |
| Et | Ethyl |
| eV | Electron volts |
| EWG | Electron withdrawing group |
| F8BT | Poly(9,9-dioctylfluorene-*alt*-benzothiadiazole) |
| FRET | Fluorescence resonance energy transfer |
| g | Grams |
| GPC | Gel permeation chromatography |

| | | | |
|---|---|---|---|
| h | Hours | m.p. | Melting point |
| HAPPAP | 5,15-bis((4-bromophenyl)ethynyl)-10,20-bis(3,4,5-tris(dodecyloxy)phenyl) porphyrinato zinc(II) | *m/z* | Mass to charge ratio |
| | | mbar | Millibar |
| | | Me | Methyl |
| | | MEH-PPV | Poly[2-methoxy-5-(2-ethylhexyloxy)-1,4-phenylenevinylene] |
| HDPE | High density polyethylene | | |
| HMBC | Heteronuclear multiple-bond correlation spectroscopy | mg | Milligrams |
| | | MHz | Mega Hertz |
| HOMO | Highest occupied molecular orbital | min | Minutes |
| HPLC | High-performance liquid chromatography | mL | Millilitres |
| | | mm | Millimetres |
| HRMS | High resolution mass spectrometry | mmol | Millimoles |
| HSQC | Heteronuclear single quantum coherence spectroscopy | $M_n$ | Number Average Molecular Weight |
| | | MO | Molecular orbital |
| Hz | Hertz | MPP | 5,15-bis(4-bromophenyl)-10,20-dimesitylporphyrin |
| *i* | Iso | | |
| IC | Internal conversion | MPP(Pt) | 5,15-bis(4-bromophenyl)-10,20-dimesitylporphyrinato platinum(II) |
| IR | Infrared | | |
| ISC | Intersystem crossing | Ms | Mesyl |
| ITO | Indium tin oxide | $m_s$ | Spin component for single electron |
| IUPAC | International Union of Pure and Applied Chemistry | $M_s$ | Spin component for entire system |
| | | Mw | Molecular weight |
| *J* | Coupling constant | $M_w$ | Weight Average Molecular Weight |
| K | Kelvin | *n* | Normal |
| k | Rate constant | NBS | N-Bromosuccinimide |
| $k_B$ | Boltzmann constant | NGP | Neighbouring group participation |
| kDa | Kilo Daltons | NIR | Near infrared |
| LASER | Light amplification by stimulated emission of radiation | nm | Nanometers |
| | | NMM | *N*-Methylmorpholine |
| $LC_{50}$ | 50% lethal concentration level | NMO | *N*-Methylmorpholine *N*-oxide |
| LDA | Lithium diisopropylamide | NMR | Nuclear magnetic resonance spectroscopy |
| LDPE | Low density polyethylene | | |
| LED | Light emitting diode | NOESY | Nuclear Overhauser effect spectroscopy |
| LR-TD-DFT | Linear Response Time-Dependent Density-Functional Theory | | |
| | | ns | Nanoseconds |
| LUMO | Lowest unoccupied molecular orbital | OFET | Organic field effect transistor |
| M | Molar | OLASER | Organic LASER |
| *m* | Multiplet | OLED | Organic light emitting diode |

| | | | |
|---|---|---|---|
| OPV | Organic photovoltaic | | Overhauser effect spectroscopy |
| Ox | Oxidant | rt | Room temperature |
| PCE | Power conversion efficiency | s | Singlet (for NMR) |
| PCPDTBT | Poly[2,6-(4,4-bis-(2-ethylhexyl)-4H-cyclopenta [2,1-b;3,4-b']dithiophene)-*alt*-4,7(2,1,3-benzothiadiazole)] | *s* | Spin quantum number |
| | | $S_0$ | Ground singlet state |
| | | $S_1$ | First excited singlet state |
| PDPA | *Poly*-4',4''-(2,3,6,7-(octyloxy)-9,10-diphenylanthracene-*alt*-1,4-phenyl) | SAD | Sharpless asymmetric dihydroxylation |
| | | SEC | Size exclusion chromatography |
| PDT | Photo dynamic therapy | SFCN | *Poly*-2,7-(9,9-dihexadecyl-9H-fluoren-2-yl)-*alt*-2,7-(9,9'-spirobi[fluorene]-2',7'-dicarbonitrile) |
| PE | Polyethylene | | |
| PEBPP | 5,15-bis((4-bromophenyl)ethynyl)-10,20-bis(3,5-di-tert-butylphenyl)porphyrin | SFH | *Poly*-2,7-(9,9-dihexadecyl-9H-fluoren-2-yl)-*alt*-2,7-(9,9'-spirobi[fluorene]) |
| PEDOT | Poly(3,4-ethylenedioxythiophene) | $S_n$ | nth excited singlet state |
| PEMP | 5,15-bis((phenyl)ethynyl)-10,20-dimesitylporphyrin | $sol^n$ | Solution |
| | | SSET | Singlet-singlet energy transfer |
| PESA | Photoelectron Spectroscopy in Air | $^t$ | Tertiary |
| PF | Polyfluorene | t | Triplet (for NMR) |
| PF MPP(Pt) | Poly-9,9-dioctylfluorene-*ran*-5,15-dimesityl-10,20-diphenylporphyrinato platinum (II) | T | Temperature |
| | | $T_1$ | First excited triplet state |
| | | TADF | Thermally activated delayed fluorescence |
| PFO | Polydioctylfluorene | | |
| Ph | Phenyl | TAS | Transient absorption spectroscopy |
| PIA | Photo-induced absorption | TBAF | Tetra-*n*-butylammonium fluoride |
| PL | Photoluminescence | TD-DFT | Time-Dependent Density-Functional Theory |
| PLQY | Photoluminescence quantum yield | | |
| PP | Polypropylene | TEMP | 5,15-bis((5-bromo-3-hexylthiophen-2-yl)ethynyl)-10,20-dimesitylporphyrin |
| ppb | Parts per billion | | |
| ppm | Parts per million | TEMPO | (2,2,6,6-Tetramethylpiperidin-1-yl)oxyl |
| PS | Polystyrene | | |
| PSS | Polystyrene sulfonate | TFA | Trifluoroacetic acid |
| PVC | Polyvinyl Chloride | TFB | Poly[(9,9-dioctylfluorenyl-2,7-diyl)-*co*-(4,4'-(N-(4-sec-butylphenyl)diphenylamine)] |
| quant | Quantitative | | |
| QY | Quantum yield | | |
| $R_f$ | Retention factor | TGA | Thermogravimetric analysis |
| RHS | Right hand side (of myrcene) | THF | Tetrahydrofuran |
| RISC | Reverse intersystem crossing | TLC | Thin layer chromatography |
| ROSEY | Rotating frame nuclear | TMS | Trimethyl silyl |

| | | | |
|---|---|---|---|
| $T_n$ | $n^{th}$ excited triplet state | VB | Valence band |
| Ts | Tosyl | w/w | Weight percentage |
| TTA | Triplet–Triplet Annihilation | X | Halogen |
| TTET | Triplet triplet energy transfer | Δ | Change |
| UV | Ultraviolet | $\Delta E_{ST}$ | First excited singlet-triplet energy gap |
| V | Volts | ε | Extinction coefficient |

# Chapter 1: Introduction

## 1.1 Polymers

All the work presented in this thesis is focussed on the syntheses and properties of polymers. A polymer is formed when monomers are covalently bound together to form a larger structure. In biological systems, a common type of monomer is an amino acid, which may be bonded to other amino acids through the action of ribosomes to form proteins. In the polymer DNA, the monomers are nucleic acids. Clearly, proteins and DNA have vastly different characteristics and complexity levels compared to their small molecule building blocks. Synthetic polymers created by chemists also exhibit interesting new properties compared to their monomers like their biological counterparts. These new and interesting attributes of polymeric molecular systems are realised by virtue of their size, shape or (the attribute this thesis is most concerned with) their electronic configuration.

Synthetic polymers are ubiquitous in the developed world. Most commonly referred to as plastics, organic compounds that have been polymerised together form a large and diverse group of materials that find uses in electronics, aviation, clothing and almost every business sector in some fashion. ***Table 1.1.1*** shows some synthetic polymers that are common in everyday life. It should be noted that each polymer may be produced in different forms, depending on how it is synthesised and so may appear in different forms that are used for different applications.

The characteristics of the polymer depend on the structure of the monomers, as well as its macromolecular structure (molecular weight, degree of branching, 3D folded structure), and its intermolecular and intramolecular interactions. Chemists control how differences in the structure of the monomers will result in differences between polymers, by introducing different atoms into the structure the material will clearly be different. The macromolecular structure and intermolecular interactions however are not as easy to visualise.

Low density polyethylene and high density polyethylene (LDPE and HDPE) are synthesised from the same monomer, ethylene. By controlling the reaction conditions during the free radical polymerisation of ethylene, branching of the polymer chain as it grows can be encouraged (catalyst free, initially formed primary radicals may more easily migrate to more stable secondary and tertiary positions before reacting) or discouraged (Ziegler-Natta

catalysts for example stabilise the primary radicals on the chain ends and thereby promote linear chain growth). A linear chain with few branch points may pack more efficiently together. The macromolecular structure of HDPE therefore directly affects the intermolecular interactions between polymer molecules, resulting in a material with high tensile strength. LDPE by contrast has a lower tensile strength as its molecules do not pack together as efficiently.

| Name | Structure | Properties and Uses |
|---|---|---|
| Low Density Polyethylene (LDPE) | 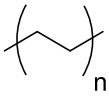 contains high degree of branching | Flexible plastics – squeeze bottles, six-pack rings |
| High Density Polyethylene (HDPE) | 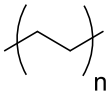 contains low degree of branching | Less flexible plastics – piping, plastic toys |
| Polypropylene (PP) | 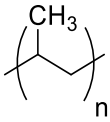 | More thermal resistance than PE – auto parts, food storage |
| Polyvinyl Chloride (PVC) | 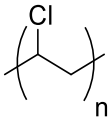 | Rigid form has weather resistance – windows, garden furniture. With plasticiser – wiring, rubber replacement |
| Polystyrene (PS) | 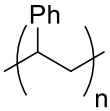 | Transparent, rigid and inexpensive – Petri dishes, CD cases |
| Nylon (generic term referring to any polyamide. Structure shown is nylon 6) | 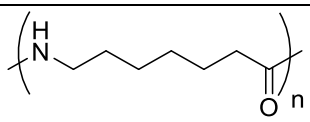 | Bio and chemi-resistant but very flexible – clothing, toothbrushes |
| Teflon (Polytetrafluoroethylene) | 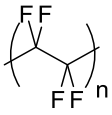 | Hydrophobic and non-reactive – non-stick pans, coating on hospital equipment |
| Kevlar | 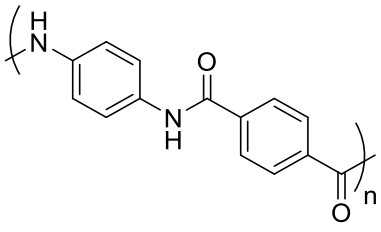 | High tensile strength to weight ratio – armour, bicycle tyres |

***Table 1.1.1:*** *Common polymers and their structures and uses.*

Polyvinyl chloride (PVC) is another polymer that is used for different applications depending on how it is synthesised. Intermolecular interactions are changed in this case more commonly through the addition of a plasticiser dopant into the material. After the polymer has been synthesised, plasticisers such as derivatives of phthalic acid are added to increase desirable properties such as heat or UV resistance, based on the material's end use.

The majority of polymers produced commercially are synthesised by radical polymerisation of alkenes. The polymer composition is dependant on the reaction conditions, as discussed above, so may be changed based on the choice of initiator, pressure, temperature etc. This type of polymerisation is the most widely used in terms of total amount of polymer created (the most common synthetic polymers, PE, PVC and PS, are all made through this method). More complex systems are difficult to realise with this method however. The control necessary to form defined structures with multiple monomers, or to use monomers with additional aromatic functionality, is realised with metal catalysed cross coupling polymerisation reactions.

| Name | Reaction | Primary uses |
|---|---|---|
| Suzuki | 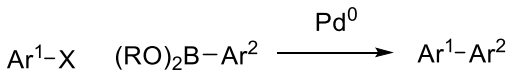 | Aryl-aryl bond formation. Polymerisations |
| Stille | 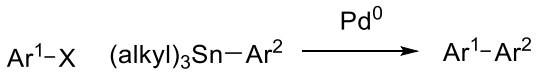 | Aryl-aryl bond formation. Polymerisations |
| Sonogashira | 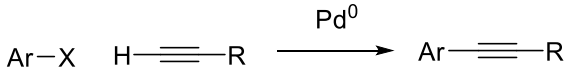 | Terminal alkyne to aryl bond formation. |
| Heck | 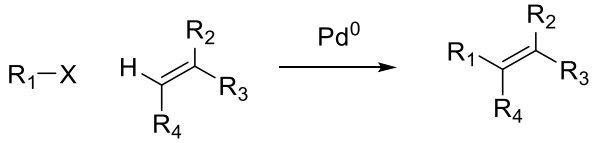 | Alkene to aryl bond formation. |
| Buchwald-Hartwig | 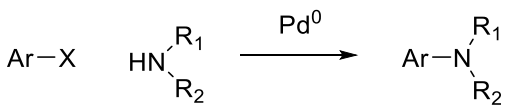 | Formation of aryl amines or aryl ethers |

***Table 1.1.2:*** *Cross coupling reactions used in this work. Ar – aromatic, R – H, aliphatic or aromatic.*

The method of creating complex polymers made of several multifunctional monomers in this work is through metal catalysed cross coupling polymerisation reaction. This work uses almost exclusively the Suzuki reaction for polymerisations, although some work used the Stille reaction. These are not the only cross coupling reactions available to polymer chemists

however, other types of this reaction were often used in the synthesis of monomers. ***Table 1.1.2*** summarises these reactions, note that the reactions are meant as a guide only. There are many exceptions to the aryl and alkyl groups, for example the Stille reaction is often performed on alkenes.

Because of the conjugated nature of the polymers described in this work, the method of polymerisation must be one in which a conjugated product is formed. This normally means the coupling of aryl groups (alkynes and alkenes also give conjugated products, but are employed less by semiconducting polymer chemists), which is why the Suzuki or Stille reactions are utilised. A Negishi reaction is another viable alternative for polymerisations using aryl zinc compounds, however this was never attempted for any synthesis herein.

The polymers described in this work are named according to IUPAC convention in the experimental section, but are given alternative, acronym based names in the main text for readability.[1]

## 1.2 Organic Semiconducting Devices

Semiconductors are an integral part of the modern world. Electronic devices contain billions of transistors, light-emitting diodes (LEDs) are used for many lighting and display applications and the solar energy industry relies on the light absorbing properties of semiconducting materials in solar cells. Semiconductors have a conductivity between that of metals and insulators, a result of their particular energy level structure. In the ground state, filled energy levels in a valence band are separated in terms of energy by a band gap that is of comparable energy to the device energy input to a conduction band of unfilled energy levels. An excited electron in a conduction band may move through the semiconductor, as may a hole in the valence band. An electron-hole pair is known as an exciton.

Silicon, germanium and compounds of gallium are the most commonly used materials for semiconducting devices. They are tuned for use usually *via* doping with, for example, boron or phosphorus compounds to create p and n-type semiconductors. This creates a material that is either rich or poor in electron density and allows electrons or holes to move more freely across the semiconductor. Blending p and n-type semiconductors together is the basis of many types of semiconducting materials, as electrons in a valence band (VB) may be excited into a conduction band (CB) and thus create partially filled energy levels and allow conduction. The difference between the VB and CB is known as the band gap.

An alternative to inorganic metalloid systems is to use organic semiconductors. Organic semiconductors are conjugated π-systems that are made from primarily carbon and hydrogen with various amounts of oxygen, nitrogen and sulphur. Organic π-conjugated polymers and their electronic properties have been of interest to polymer scientists for many years and in recent years have seen significant advances.[2] The band-gap of organic semiconductors is obtained and controlled through extended conjugation, ***Figure 1.2.1***.

As conjugation length is increased from ethene to octatetrene, the HOMO increases in energy while the LUMO decreases in energy. When the conjugation length is taken to a very large value, as in polyacetylene, the energy difference between individual filled and unfilled levels becomes small and the energy levels form bands that are analogous to inorganic semiconductors. The difference in energy between the two bands, filled (VB) and unfilled (CB), is known as the bandgap.

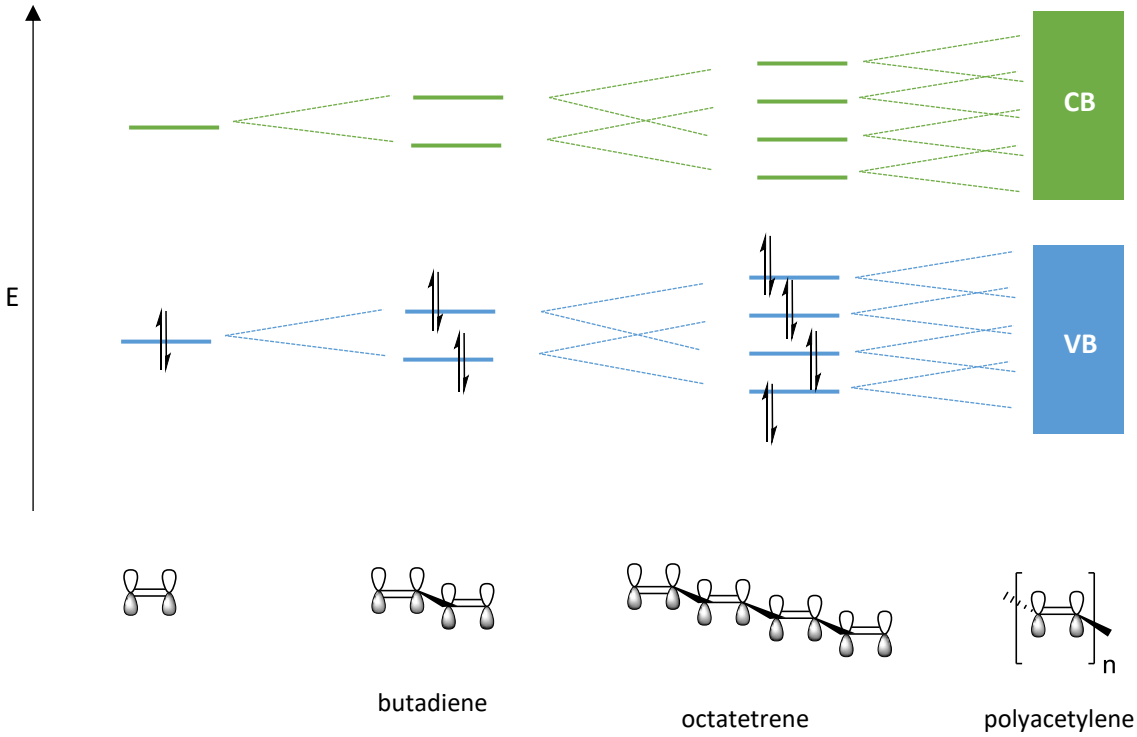


***Figure 1.2.1:*** *Energy levels of simple π-conjugated systems of increasing length. Green energy levels represent non-populated, mainly antibonding orbitals and blue energy levels represent populated, mainly bonding orbitals. Molecular orbitals shown on structures are lowest lying frontier orbitals.*

The synthetic approach to the creation of these types of semiconductor imbue them with various advantages over inorganic counterparts. Using organic molecules in this field has the advantage of tunability by molecular modification. This allows for optoelectronic functions and material properties to be minutely controlled as the molecular structure of these systems is changed. Processability is also much larger; soluble organic polymers may be easily spin coated or even printed onto devices with the result of much reduced processing costs of manufacture. New physical properties of devices are also made available; as well as being light in weight an organic polymer may be bent and twisted or made to be transparent, properties that are challenging to realise in inorganic systems and desirable for versatile applications and device durability.

Research in this area has resulted in the 2000 Nobel prize in chemistry being awarded to Alan Heeger, Alan MacDiarmid and Hideki Shirakawa who initially reported the high conductivity of iodine doped polyacetylene in 1977.[3] The semiconducting ability of conjugated polymers allows for several optoelectronic functions, including their incorporation into organic light

emitting diodes (OLEDs) and organic photovoltaics (OPVs). A simple OLED device structure is shown in ***Figure 1.2.2***, in which a battery is joined through two electrode layers to a photon emitting layer, the semiconducting polymer. This device structure is similar to one published in 1990 by Holmes *et al.* that was among the first reported OLED devices.[4]

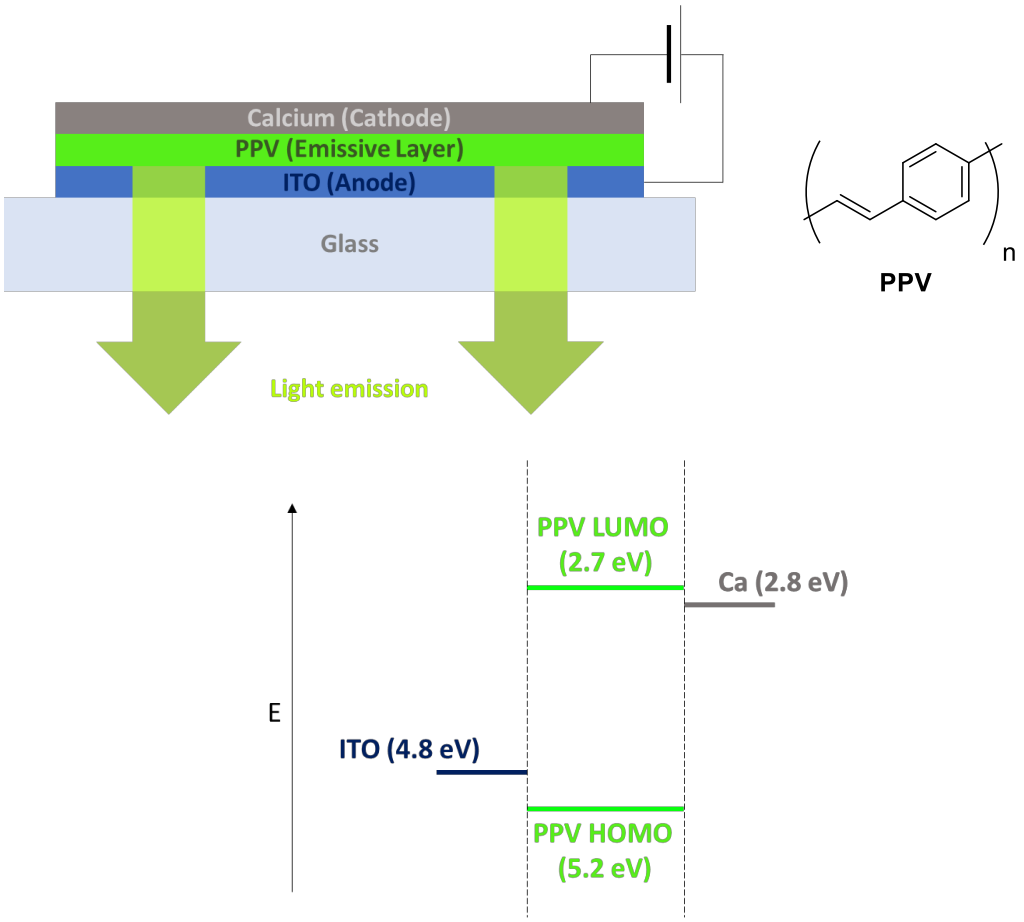


***Figure 1.2.2:*** *Device structure (top) and energy level diagram (bottom) of simple OLED device based on poly(1,4-phenylene vinylene) (PPV). Absolute energy levels are estimates included to show relative relationships.*

Electrons injected from the low work function cathode and holes injected from the high work function anode are transferred to the semiconducting layer, where they meet and form an exciton. The radiative decay of this exciton results in the emission of a photon with energy equivalent to the band gap of PPV, 2.5 eV or 496 nm (5.2 eV – 2.7 eV). The anode and cathode are chosen so that their wavefunctions match the LUMO (for the cathode) and HOMO (for the anode) of the emissive polymer. At least one electrode must also fulfil the criteria of being transparent, so as to allow photons created by the semiconductor to escape the device. In

most cases, indium tin oxide (ITO) is utilised as the anode. ITO is a transparent and processable material with a convenient wavefunction energy of 4.8 eV.

OLEDs have seen the most commercial success of any organic semiconducting material application, their uses include mobile phone screens, televisions and low energy lighting.[5-6] Other uses that are not currently a large part of their respective markets, but may be in the future, are photovoltaics (OPVs)[7], field effect transistors (OFETs)[8] and LASERs (OLASERs)[9]. Some of these applications will be discussed briefly in terms of a generic semiconductor. As the focus of most of this work, most time is spent on OLEDs.

For OLEDs, the semiconducting polymer layer will be comprised of an organic molecule that exhibits strong light emission upon electrical excitation. The molecular design of the polymer and the incorporation of various dopants can tune the frequency of emitted light and allows for the development of red, green and blue emitters, necessary for the production of colour displays. More recently there has been interest around near-infrared (NIR) emitters, which may find uses as night-vision-readable displays or certain types of sensors.[10]

***Figure 1.2.2*** has already shown how a simple OLED may operate. Modern devices however are normally more complex and contain additional layers that aid the device operation in various ways. ***Figure 1.2.3*** shows how the device in ***Figure 1.2.2*** may be improved upon. This device is based on a subsequent device reported by Holmes *et al.* but modified to show more layers for the purposes of this introduction to OLED device structure.[11]

Two additional layers have been added into the device structure in ***Figure 1.2.3***, a layer of PEDOT:PSS and an additional, modified PPV layer. PEDOT:PSS is often added to the ITO anode in fabricated devices. It forms a smooth layer that holes may be injected onto that has good compatibility with other organic layers added subsequently. Like the anode, it is important that this layer be transparent to allow light to escape the device.[12-13]

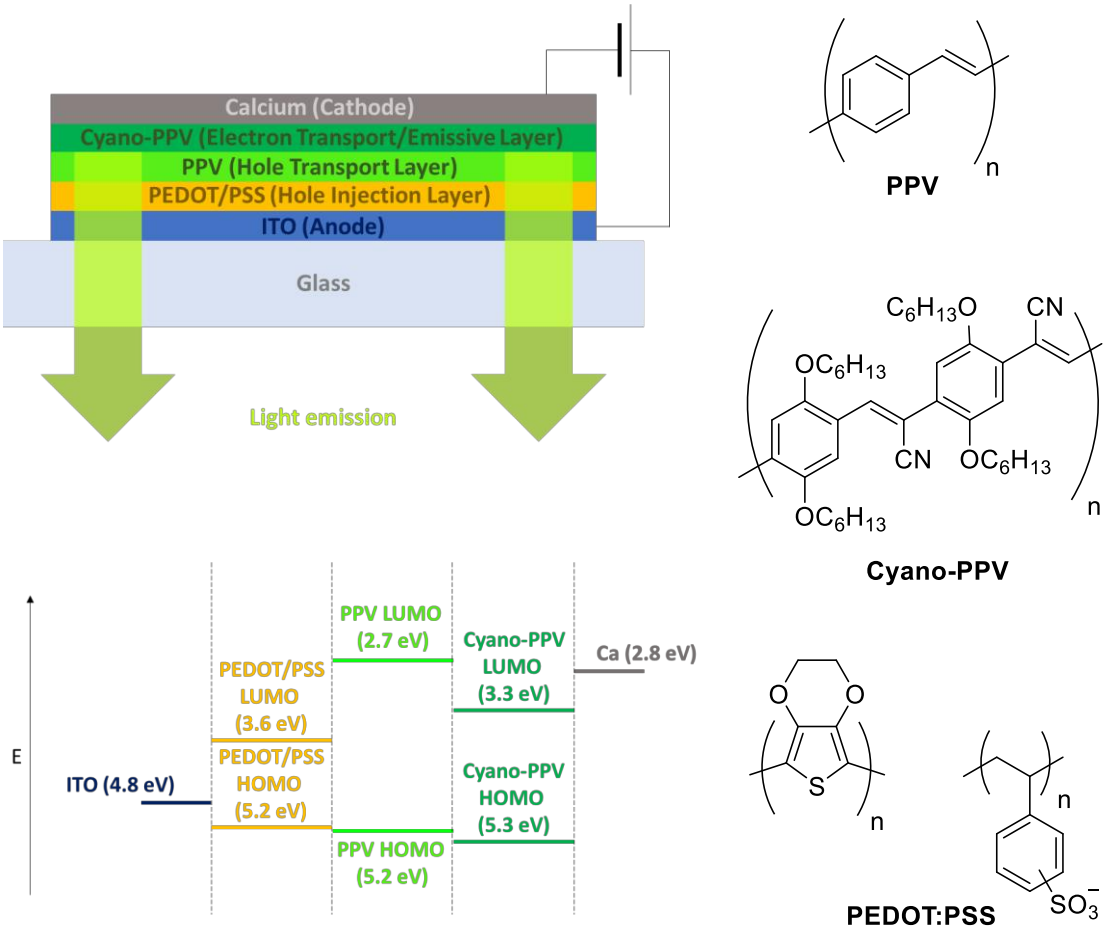


***Figure 1.2.3:*** *Improved OLED device structure (top) and energy level diagram (bottom) with structures of relevant components (right). Absolute energy levels are estimates included to show relative relationships.*

The second modification is the addition of a modified PPV layer. The addition of solubilising alkyl groups aids processability of the polymer (PPV is insoluble in most solvents so thin, well defined films are challenging to achieve). The addition of electron withdrawing groups cause the HOMO and LUMO to both decrease, although the LUMO is more largely affected resulting in a smaller bandgap and therefore a red-shifted electroluminescence. This means that electron injection from the cathode onto the LUMO is facilitated and the colour of emission is changed to red (2.05 eV reported).[11] Electron injection onto cyano-PPV single layer devices (no PPV layer) was found to be efficient with a variety of cathode materials; calcium, aluminium and to a lesser extent gold. By including a PPV layer, holes are transported to the PPV/cyano-PPV interface (to the highest HOMO) and electrons are blocked (confined on the lowest lying LUMO). This results in the confinement of charges on the cyano-PPV layer and efficiency was seen to increase from 0.15% (single layer cyano-PPV) to 4% (PPV/cyano-PPV).

This shows how device structure influences the overall operation of the device, and how an understanding of the characteristics of each layer leads to more efficient devices.

Other types of layers and materials are sometimes incorporated into OLED devices.[14] By blocking or transporting holes and/or electrons, materials scientists may intelligently design a device to be more efficient than its predecessors. The work presented here is concerned mostly with the modification of the semiconducting polymer however, rather than the device as a whole.

The ability of chemists to modify existing structures in order to tune in desirable characteristics is one of the greatest advantages of organic systems for semiconducting applications. This advantage is not limited to OLEDs however, all organic semiconducting devices share this benefit.

The basic structure of an OPV device is similar to an OLED. ***Figure 1.2.4*** shows how Holmes *et al.* used the same cyano-PPV polymer (blended with a related polymer, MEH-PPV) for light absorbing applications that had been used for light emitting applications previously (***Figure 1.2.3***).[15] Rather than injecting charge onto the semiconductor however, charge is created when light is shone upon the semiconducting layer which is then separated into holes and electrons and collected by the electrodes. The separation of charge is important for these devices, so a common motif is a donor-acceptor blended structure. Hence a blend of two polymers is used in ***Figure 1.2.4***. An exciton is separated in this motif as the component parts, an electron and a hole, are more stable on different parts of the system.

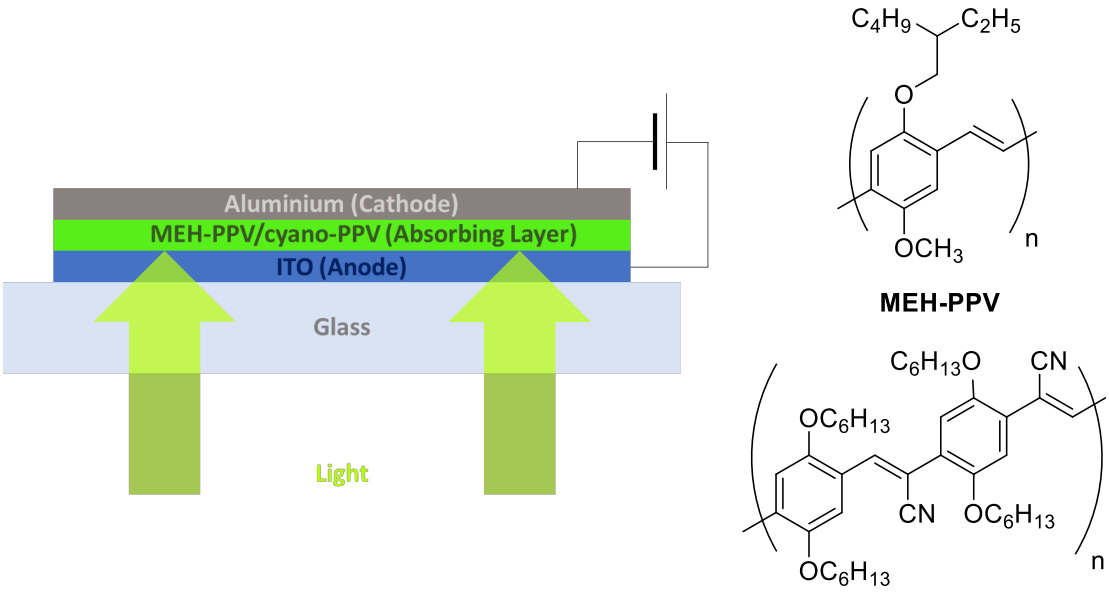


***Figure 1.2.4:*** *Device structure of OPV.*[15]

In the case of OPVs, devices are usually created using a blend of semiconducting polymer as a donor and a fullerene acceptor, although other accepting layers are possible (as in ***Figure 1.2.4***). The donor absorbs light and the blended system as a whole creates a separation of charges. This separation of charge may then result in a voltage across the system and therefore the flow of electricity. In the last decade power conversion efficiencies (PCEs) of single junction OPVs have been increased from less than 1% to over 9%.[16]

OFET device structure differs from OLEDs and OPVs, and relies upon the gate effect for its operation. ***Figure 1.2.5*** shows how a simple OFET may be designed.

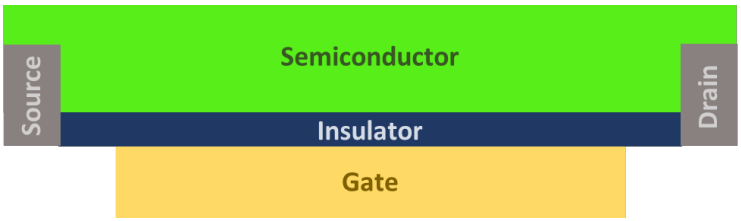


***Figure 1.2.5:*** *OFET device structure.*

A transistor allows the amount of charge carriers moving through a system from the source electrode to the drain to be controlled by varying the potential applied to the gate. If a negative potential is applied at the gate electrode, a build up of negative charge will accumulate at the interface with the insulating layer. The field effect causes a proportional build up of positive charge in the semiconductor, again at the interface with the insulator. This increases the hole mobility across the semiconductor. By controlling the potential applied to the gate, the amount of charge carriers that may move from the source to the drain electrode is thus modulated. Many architectures of OFET device are possible, but all contain the same basic relationship between source, drain and gate electrodes.

The work presented herein is concerned with the design and synthesis of organic semiconducting polymers. This is usually rationalised by thinking of the resultant device as an OLED, or in some cases as an OPV. While it is helpful to think in terms of an end product, the immediate objectives of the projects described were more fundamental and academic. The aim in the case of each project was not to create a highly efficient device, but rather to create a new type of device. What links the projects together is how this would be achieved: by utilising triplet states.

## 1.3 Triplet states in Organic Semiconductors

The HOMO of an organic semiconductor in its ground state is populated by 2 paired electrons that are necessarily of equal and opposite spins due to the Pauli exclusion principle. When one electron is promoted to the LUMO to form an exciton, the ground and excited electrons need not be paired, as they now occupy separate orbitals. This leads to 4 possible configurations of the electrons relative to each other, 3 in which the spins are parallel and 1 in which they are antiparallel. These describe the exciton in triplet and singlet states respectively. ***Figure 1.3.1*** shows graphically how this occurs.

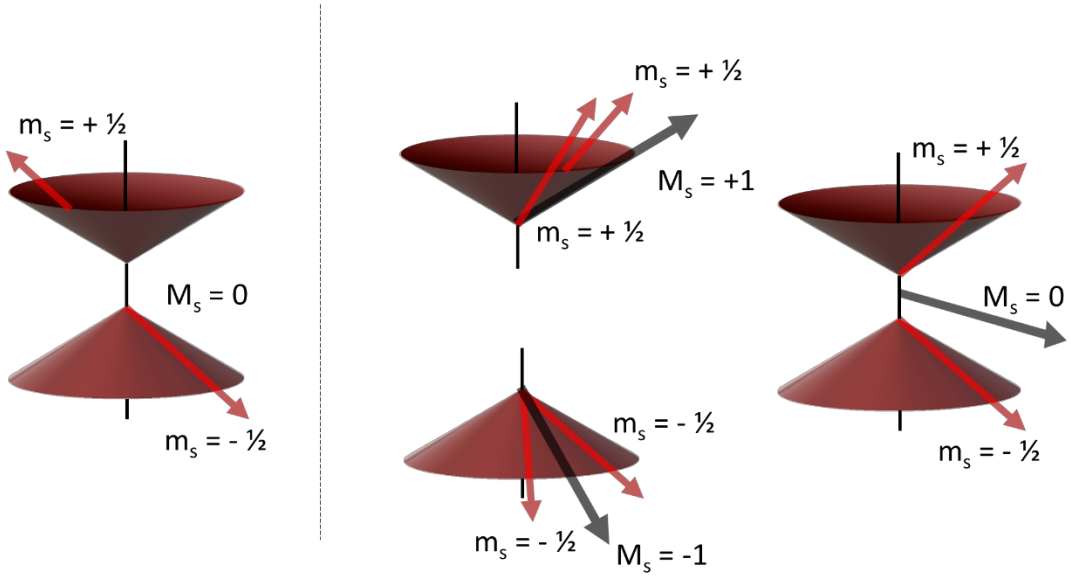


***Figure 1.3.1:*** *Singlet (left) and triplet (right) vector representations of an electronically excited two electron system. The singlet system has a spin quantum number (S) of 0 and a spin component of the system ($M_s$, found by combining the spin components of the electrons in the system) of 0. The triplet systems all have S = 1 (lying along the black vector) and may have $M_s$ = 1, 0 or -1.*

In the singlet case, the two spin momenta of the electrons in the system are antiparallel and cancel each other out, resulting in a system with an overall spin quantum number of 0. There is only 1 possible way of achieving this result, when the vectors lie in opposite directions. There are 3 ways of forming a triplet state however, which has an overall spin quantum number (s) of 1 and may have a spin component ($M_s$) of 1, 0 or -1. While the vectors of the individual electrons of the triplet states point in different directions, the angle between them

is always the same in each case which leads to the constant spin quantum number of 1 for all triplet states.

***Figure 1.3.2*** shows a Jablonski diagram in which a singlet exciton decays to the lowest excited singlet state $S_1$ through vibrational relaxation and then through fluorescence to its ground state $S_0$. An exciton in its singlet state may decay radiatively, losing a quanta of energy through the emission of a photon. This is possible only because the electrons are orientated to already be able to occupy the same orbital. This process is therefore fast.

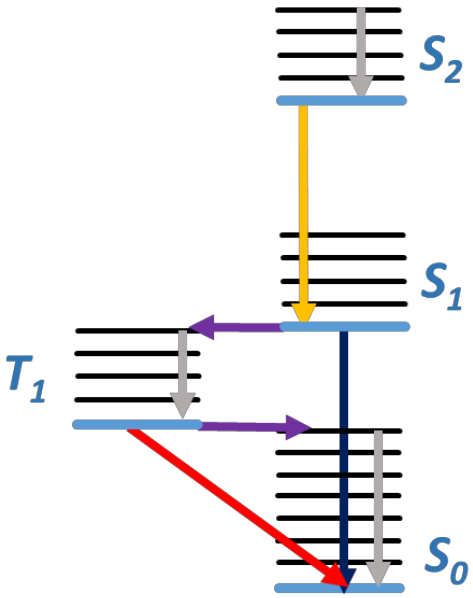


***Figure 1.3.2:*** *Jablonski diagram showing first excited singlet and triplet states for a generic system and their decay pathways to the ground state. Processes shown are fluorescence (blue), phosphorescence (red), intersystem crossing (purple), internal conversion (orange) and vibrational relaxation within an electronic state (grey).*

The pathway of decay for an exciton in a triplet state is a much slower process. According to Hund's rule, the first excited triplet state ($T_1$) for a system will be lower in energy than the first excited singlet ($S_1$) as this maximises the multiplicity of the system ($2S+1$ where $S$ is the total spin angular momentum for all electrons). This is important as it means that the process of an excited electron undergoing intersystem crossing from $S_1 \rightarrow T_1$ is more favoured compared to the reverse (reverse intersystem crossing, RISC, $S_1 \leftarrow T_1$), as a more stable system is formed. Radiative decay from $T_1 \rightarrow S_0$ is known as phosphorescence. This is a spin disallowed process, as the electrons in the excited and ground orbitals of the exciton do not have antiparallel spins and so may not occupy the same orbital unless the spin of one is changed. This process is slow

in normal systems and radiative decay from $T_1$ is not observed unless a part of the system exhibits strong spin orbit coupling that allows for an excited electron to change spin. For this reason, the formation of triplet excitons is often associated with a loss of efficiency in a device, as energy stored in these states is generally lost through non-radiative processes.

In a fluorescent organic material suitable for an OLED device such as PPV and its derivatives, an excited singlet exciton may decay to its ground state and emit a photon with energy equivalent to the band gap of the material. Spin statistics show that injection of holes from the anode and electrons from the cathode will result in the creation of exited states where 25% are singlets and 75% are triplets. Fluorescent based OLEDs therefore may only have a maximum internal quantum efficiency of 25%, since 75% of excited states do not decay radiatively. The development of phosphorescent materials containing heavy metals has allowed the development of high efficiency OLEDs that may harvest triplet excitons. Triplet states do not typically decay radiatively to a singlet ground state because this would result in an overall change in spin, *s*, which is a forbidden transition in terms of quantum mechanics. Heavy metals such as platinum (II) or iridium (III) are large enough to exhibit spin-orbit coupling, distorting the system and allowing radiative transitions where $\Delta S \neq 0$. Therefore, by doping a blue emitting OLED material with a blue absorbing phosphorescent material, energy may be transferred from a fluorescent material with low electroluminescent efficiency to a phosphorescent material with high electroluminescent efficiency *via* FRET.

***Figure 1.3.3*** shows an energy level cartoon in which an OLED doped with a heavy metal containing phosphorescent material, in this case a porphyrin, transfers energy from polymer backbone to dopant which in turn emits light. The red arrows from $S_0$ to $S_1$ and $S_0$ to $T_1$ of the polymer represent electrical excitation and the formation of a singlet exciton (25% of injected charge) and a triplet exciton (75%). In a standard system the singlet exciton may then decay back to the ground state with emission of light equivalent in energy to the $S_0 \rightarrow S_1$ gap; the bandgap of the polymer. If either exciton is sufficiently close in space to (and has the required mobility to reach) the dopant molecule, triplet-triplet energy transfer (TTET) and singlet-singlet energy transfer (SSET) may occur (orange arrows) in which an excited exciton from the polymer transfers to an excited state on the dopant (singlet to singlet and triplet to triplet, $\Delta S = 0$). Providing the $S_1$ or $T_1$ level of the dopant is below that of the polymer, this will be a favourable transition. Since the dopant contains a heavy metal and therefore exhibits substantial spin-orbit coupling, intersystem crossing (ISC) may rapidly place the singlet exciton into a triplet exited state on the dopant, $T_1$, shown as a purple arrow. Phosphorescence, shown as a red arrow, emits a photon with energy equivalent to the $S_0$ to $T_1$ gap of the dopant,

again facilitated by the spin orbit coupling of the heavy metal. Note that without the phosphorescent dopant, only the initially formed singlet would be able to emit light *via* fluorescence. All triplet excitons formed would not contribute to the emission of light but would rather decay non-radiatively which limits the internal quantum efficiency of the system to 25%.

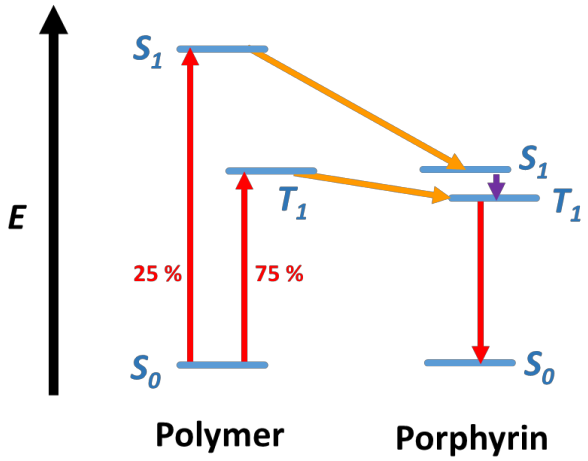


***Figure 1.3.3:*** *Jablonski type diagram showing possible radiative decay pathway of OLED doped with phosphorescent material (porphyrin).*

OPVs can also benefit from phosphorescent dopants. ***Figure 1.3.4*** shows an OPV device in which a triplet excited state is formed from low energy light which is then transferred to $T_1$ of the polymer, and subsequently undergoes triplet-triplet annihilation (TTA) upconversion with a second triplet excited state to form a higher energy excited singlet state. Low energy light is absorbed by the dopant and promotes an electron to the $S_1$ excited state (red arrow). Light absorption always results in a singlet state, because it is created from the promotion of a paired electron rather than by charge injection. Note that this is a relatively low lying excited state, the $S_1$ of the polymer backbone being much higher in energy. This means that the low energy light that was absorbed by the dopant would not be electronically absorbed by the polymer. Intersystem crossing (purple arrow) to a more stable $T_1$ state of the porphyrin is facilitated by the heavy metal exhibiting spin orbit coupling. The excited electron is then transferred to the main polymer backbone *via* internal conversion (intramolecular process) or TTET (intermolecular process) (orange arrow). TTA may occur (dark blue arrow) if two triplet excited states are close to each other, resulting in one ground state and one high energy (compared to the initially absorbed energy) singlet state.[17-18]

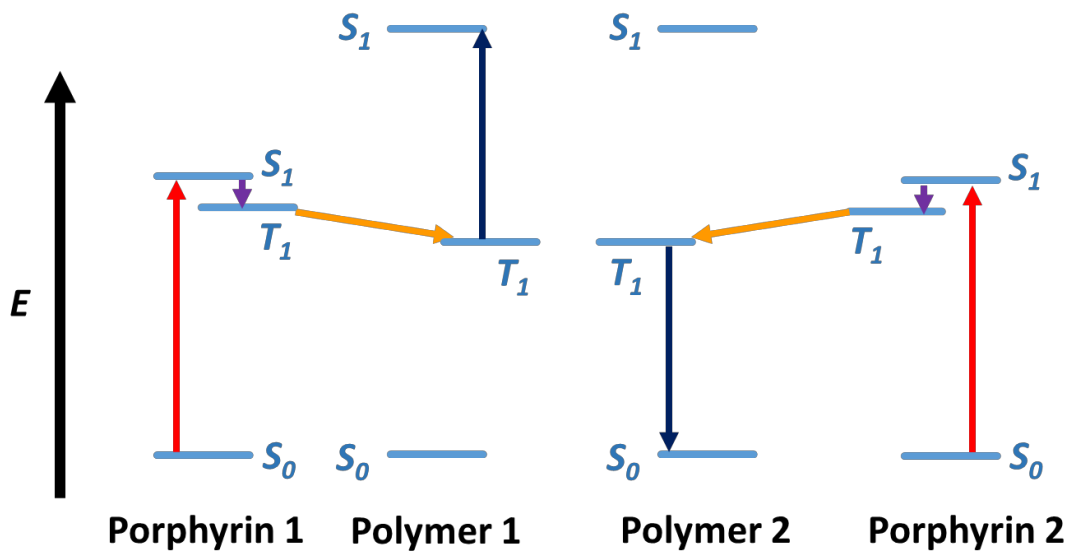


***Figure 1.3.4:*** *Possible utilisation of triplet states for OPV applications.*

One advantage of absorbing low energy light is that more of the solar spectrum becomes available for absorption, ***Figure 1.3.5***. As in the case of the OLED device, the heavy metal complexed dopant singlet excited state may decay to the lower lying triplet state by ISC (purple arrow) promoted by spin-orbit coupling. TTET to $T_1$ of the polymer, similar in energy to $T_1$ of the dopant, transfers the excited state onto the polymer backbone (orange arrow). If two $T_1$ excited states are in close enough proximity on the polymer backbone, upconversion may occur (dark blue arrows).[19] Upconversion results in one excited state decaying to the ground $S_0$ state and another being promoted to a higher energy state, in this case $S_1$. The energy of the excited $S_1$ state may then be harvested by the solar device through charge separation. In this way it becomes possible to utilise light of low energy to create a voltage of high energy. These wavelengths of light would otherwise have not been usefully absorbed.

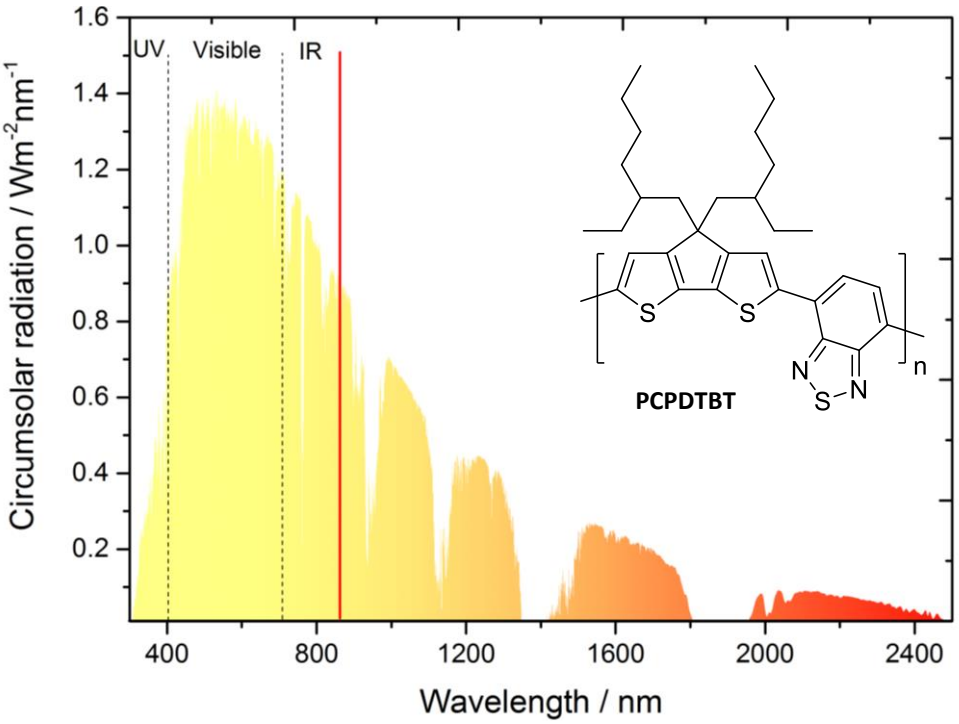


***Figure 1.3.5:*** *Solar spectrum annotated with band gap energy, shown as a red line, of poly[2,6-(4,4-bis-(2-ethylhexyl)-4H-cyclopenta[2,1-b;3,4-b]-dithiophene)-alt-4,7-(2,1,3-benzothiadiazole)] (PCPDTBT) 1. Data obtained from the American Society for Testing and Materials (ASTM).*

***Figure 1.3.5*** shows the solar spectrum. This represents all the available energy that a solar cell may absorb, with higher energy photons on the left with lower wavelengths and lower energy photons on the right with higher wavelengths. Also shown is **PCPDTBT**, an OPV semiconducting polymer that has been shown to have up to 5.5% PCE with a bandgap of 1.46 eV (850 nm). **PCPDTBT** is one of the most successful OPV semiconducting polymers.[20] This bandgap means that photons with wavelength of ≤850 nm (≥1.46 eV) may be electronically absorbed by the polymer, creating an excited state that may produce a voltage equivalent to that bandgap (=1.46 eV). The red line in ***Figure 1.3.5*** shows where the bandgap of **PCPDTBT** lies in relation to the solar spectrum. **PCPDTBT** can successfully absorb photons that have a wavelength lower than 850 nm, all those to the left of the red line. The lower energy photons that appear to the right of the red line do not have enough energy to excite the polymer and are therefore not electronically absorbed. If the bandgap is decreased, more photons will be absorbed, but since the bandgap is smaller, the voltage output will also be smaller. This trade-off between amount of solar spectrum absorbed and voltage output leads to a theoretical maximum efficiency of a solar cell, known as the Shockley–Queisser limit. The limit describes

the maximum possible PCE for a single junction solar cell with an ideal bandgap of 1.34 eV as 33.7%.[21]

One way to increase this limit is by incorporating heavy metal complexes that are capable of upconversion. By adding a dopant as in ***Figure 1.3.4***, the bandgap of the polymer may remain high while the dopant absorbs low energy photons and transfers that energy onto the polymer. Upconversion has previously been shown to work for blends of materials where a semiconducting polymer is simply blended with a heavy metal complexed molecule with the required energy levels.[19, 22-23] There are problems to overcome with blends however. The materials tend to be fairly crystalline which results in aggregation and phase separation; this means an exciton is less likely to reach a phase boundary so charge separation does not occur.

To overcome the problems associated with blends, this work in part considers covalently incorporating the dopant directly into a polymer backbone. While synthetically more challenging, having the dopant covalently bonded to the polymer will both increase the rate of energy transfer and reduce loss processes by maintaining the absorbing and emitting moieties at fixed distances. ***Figure 1.3.6*** shows how energy transfer can occur over a shorter distance by covalently linking the dopant within the polymer backbone. Another advantage is an increase in solubility of the whole system, meaning the whole film could potentially be spin coated or printed, much reducing the cost of production on a commercial scale while simultaneously lessening aggregation effects.

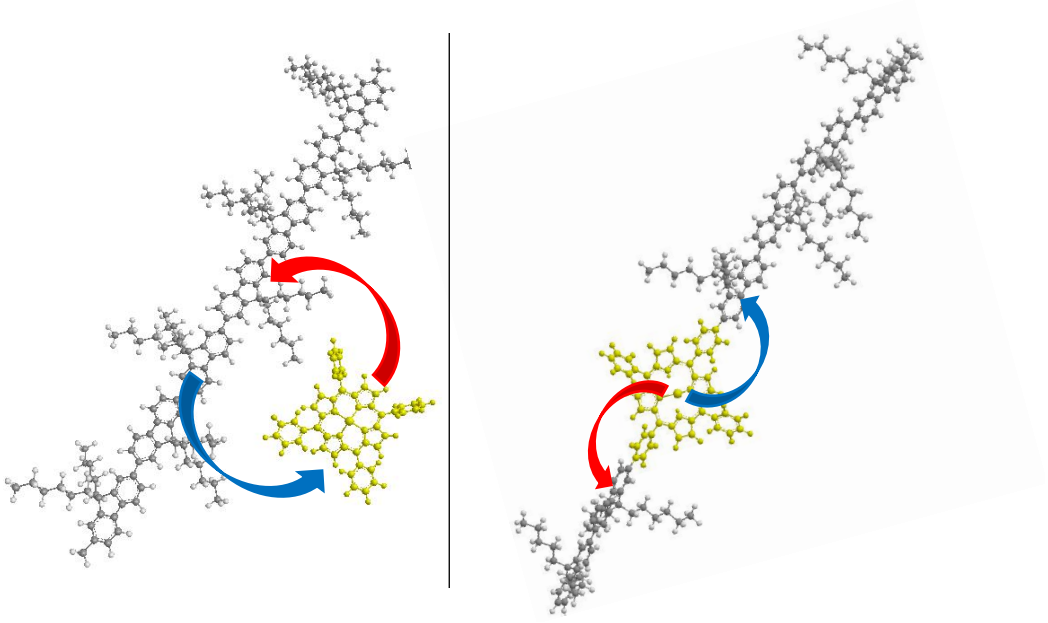

***Figure 1.3.6:*** *Blend of polymer (grey) and dopant (yellow) (left) vs dopant covalently linked into polymer (right). Red and blue arrows represent energy transfer.*

## 1.4 Porphyrins

One promising group of materials to be used as phosphorescent dopants in OPVs and OLEDs are porphyrins.[24] In most biological light absorbing systems, solar energy is absorbed and the energy efficiently transported and converted to chemical energy by a porphyrin containing chromophore, most commonly chloropyhll.[25] Good electrical properties, arising from the porphyrin π system, have led to a wide range of applications such as dye-sensitised solar cells (DSS) (12.3% efficiency measured)[26], bioimaging[27] and photodynamic therapy (PDT)[28].

Porphyrins generally absorb very strongly in the 410-430 nm region and may emit over a fairly large area. Both absorption and emission maxima may be tuned synthetically by varying the degree of substitution on the β and *meso* positions and by metal complexation. They also exhibit efficient energy transfer; uptake or loss of charge tends to result in very minimal structural changes.[29]

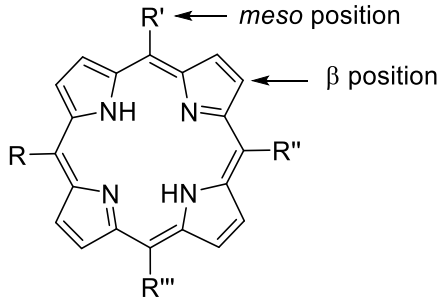


| | |
|---|---|
| R = R’ = R’’ = R’’’ | $A_4$-porphyrin |
| R = R’’ ≠ R’ = R’’’ | *trans*-$A_2B_2$-porphyrin |
| R = R’ ≠ R’’ = R’’’ | *cis*-$A_2B_2$-porphyrin |
| R ≠ R’ ≠ R’’ ≠ R’’’ | ABCD-porphyrin |

***Figure 1.4.1:*** *Labelling and nomenclature of porphyrins. This work is concerned mainly with* trans-$A_2B_2$ *porphyrins that may be built into polymers.*

These properties have resulted in very encouraging research. Porphyrins have found utility in both OLEDs[30] (as small molecules) and OPVs[31-32] (as a unit of the main polymer chain). The work contained in this report focusses on the direct incorporation of porphyrin units into semiconducting polymer chains.

Lindsey published the first facile synthesis of tetraaryl $A_4$-porphyrins which allows porphyrins to be synthesised under mild conditions with excellent functional group tolerance, ***Scheme 1.4.1***.[33-35] Pyrrole and an aldehyde are stirred together in the presence of acid. The 2 position of pyrrole attacks the aldehyde with eventual loss of water, under the right conditions this can

result in the formation of a porphyrinogen ring, **1.4.1**, which may then be oxidised to a porphyrin **1.4.2**. The synthesis becomes more complicated when trans $A_2B_2$-porphyrins **1.4.4** are desired, the general strategy being to react a dipyrromethane **1.4.3** with an aldehyde in an analogous reaction to $A_4$-porphyrin synthesis again using mild conditions, and then to further derivatise once the porphyrin framework has been built.

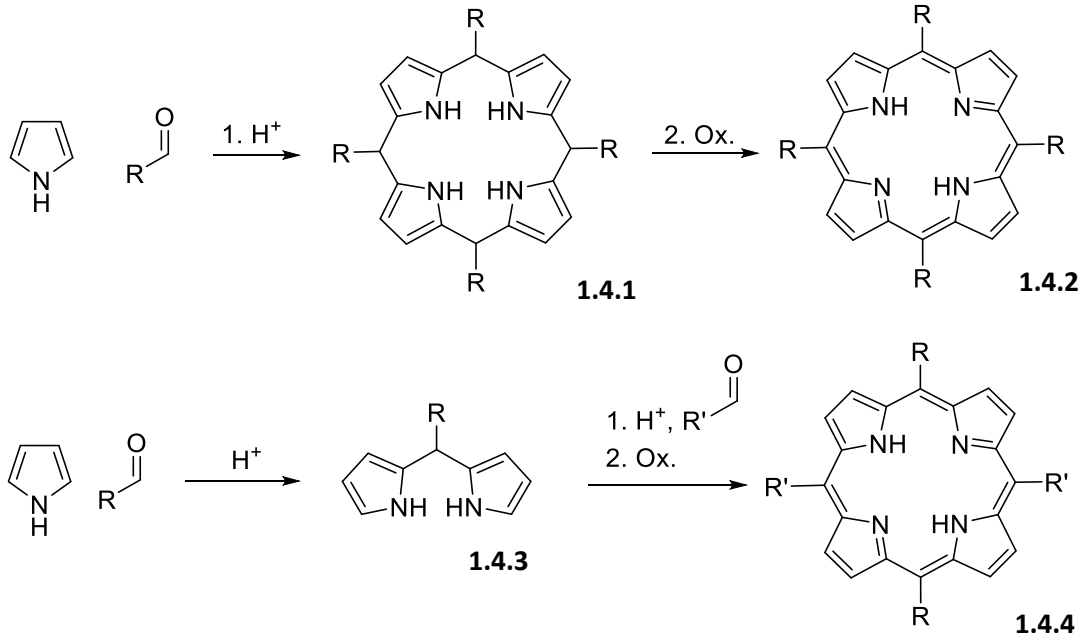


***Scheme 1.4.1:*** *General syntheses of $A_4$- (top) and trans $A_2B_2$-porphyrins (bottom).*

One problem with Lindsey's synthesis of $A_2B_2$-porphyrins is the possibility of scrambling. Under the acidic conditions necessary for reaction, multiple $A_xB_{(4-x)}$-porphyrin products may be formed as shown in ***Figure 1.4.2***.[36-37]

While it is relatively easy to separate the desired porphyrin from other reaction side products (generally, small molecules are removed by washing the sparingly soluble porphyrin and larger oligomers are removed by short silica plug), it is very difficult to separate a mixture of similar porphyrins. Similar solubilities and polarities ($R_f$ values) cause difficulties in both chromatography and recrystallisation and as a result scrambling often realistically equates to a failed reaction.[38]

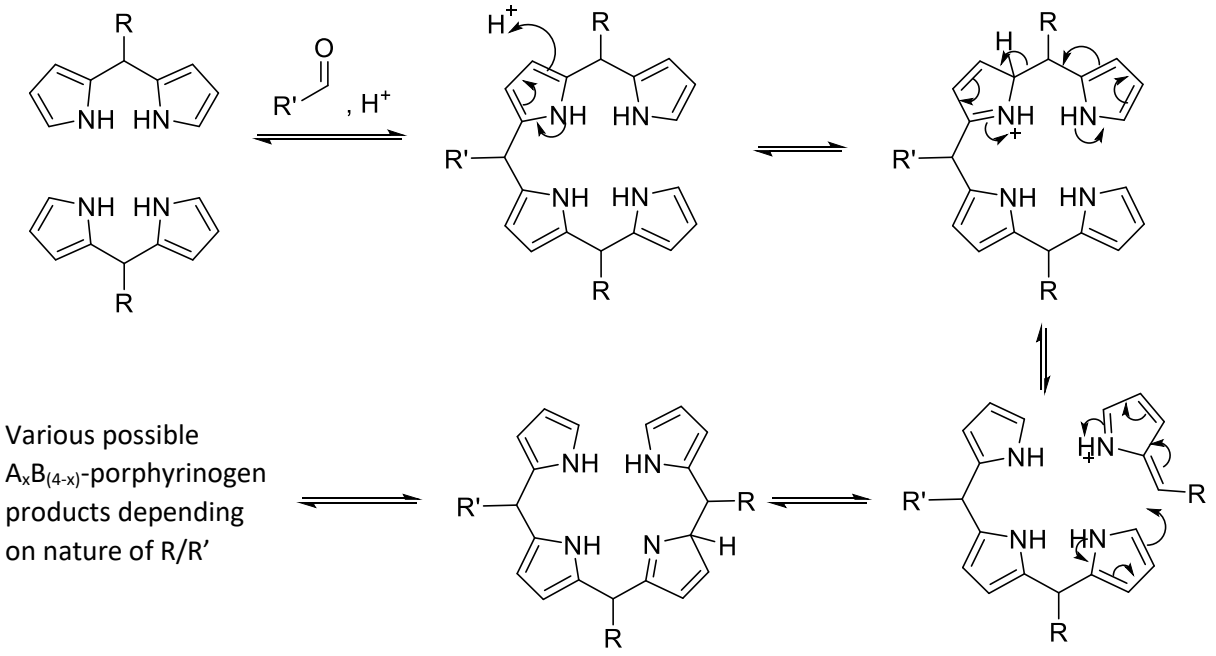


***Figure 1.4.2:*** *Mechanism of porphyrin scrambling under acidic conditions.*

As well as being capable of metal coordination, porphyrins also exhibit interesting absorbance properties. ***Figure 1.4.3*** shows the absorbance spectrum of 5,15-dimesityl-10,20-diphenylporphyrinato platinum(II) (**MPP(Pt)**), a *trans*-$A_2B_2$ porphyrin synthesised in chapter 2. The main absorbance band at 400 nm is known as the Soret band (sometimes labelled as the B band) and may be attributed to absorption from the ground state into the second excited singlet state, $S_0 \rightarrow S_2$.[39] Two additional bands are observed at 510 nm and 540 nm, these are known as Q bands. Q(0,0) represents absorption from the lowest vibrational level of the ground state into the lowest vibrational level of the first excited singlet state. Q(1,0) has an additional quanta of vibrational energy. This splitting of the Q bands is observed for metal-coordinated porphyrins. For free base porphyrins, the absorbance spectra shows four Q bands. Symmetry is broken across the x and y axes due to the additional two protons in the free base porphyrins, and so the vibrations that are degenerate in the metal-coordinated porphyrin are now split in energy. In free base porphyrin absorbance spectra, the Q bands are therefore labelled as $Q_x(0,0)$, $Q_y(0,0)$, $Q_x(1,0)$ and $Q_y(1,0)$.[39]

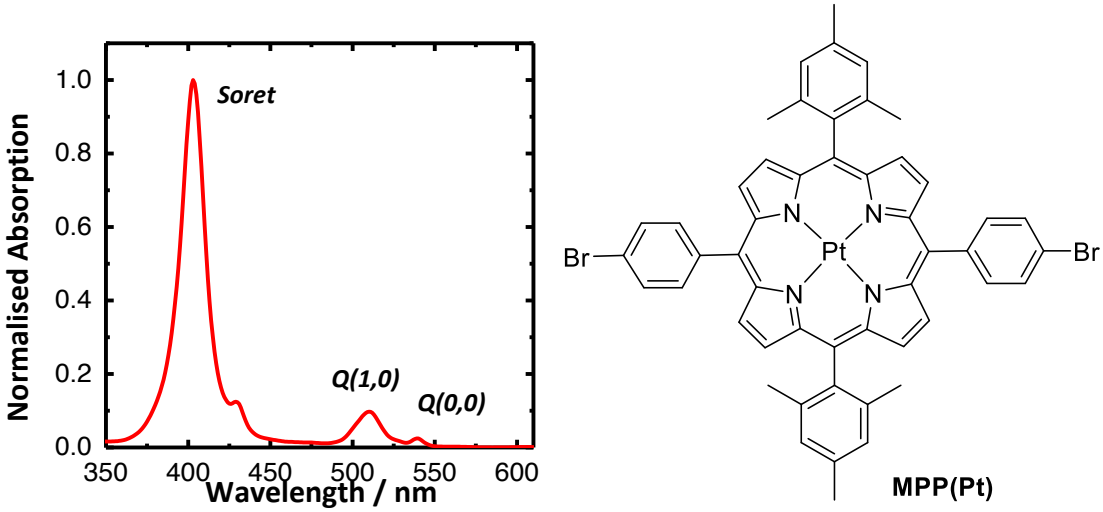


***Figure 1.4.3:*** *Normalised UV-Vis absorbance spectrum of* trans-$A_2B_2$ *porphyrin* ***MPP(Pt)***.

The Q bands of porphyrins are an important low energy absorption and emission pathway. Absorbance and emission of low energy red light as well as the strong spin-orbit coupling of platinum complexed porphyrins are useful properties that have been the basis of the subsequent two chapters in this body of work.

# Chapter 2: Phosphorescent Polymers: Incorporating a Covalently Bound Porphyrin in Polymers

## 2.1 Introduction

This chapter will deal with everything pertaining to the first porphyrin synthesised in this body of work; 5,15-dimesityl-10,20-diphenylporphyrinato platinum(II) (**MPP(Pt)**). **MPP(Pt)** is an $A_2B_2$ porphyrin-platinum complex with a strong spin orbit coupling due to its heavy metal centre. This results in a metal-complexed molecule that radiatively decays primarily through phosphorescence ($T_1 \rightarrow S_0$, 1.83 eV, 678 nm). Absorbance is observed at 405 nm and 510 nm through the Soret and Q bands respectively. Our aims relating to the work presented in this chapter were to covalently incorporate **MPP(Pt)** into varying host polymers in order to enhance, optimise and/or change the performance of the porphyrin.

Phosphorescent emitters are of interest for application in OLEDs, as 100% internal quantum efficiency is possible.[40] Porphyrins have been used in this context as a blended system where a phosphorescent porphyrin is blended with a polymeric host material. The first blends of semiconducting materials and platinum complexes were reported in 1998.[41] Since then many such systems have been reported. Blends have inherent disadvantages however; dopant aggregation and phase separation are common causes of increased phosphorescent quenching.[42-43] With increased synthetic effort, the phosphorescent dopant may be covalently bound to the host backbone, which has been shown to mitigate these disadvantages.[44-45] Pt(II) porphyrins have been covalently bound to polymeric systems before, most commonly as pendant groups into MEH-PPV to create deep-red emitting OLEDS for application in biomedical, security and communication industries.[46-53]

Incorporating the porphyrin directly into the polymer backbone is less studied however.[54] Cao *et al.* have incorporated a porphyrin into polymers *via* the β-pyyrolic positions, ***Figure 2.1.1***.[55-56]

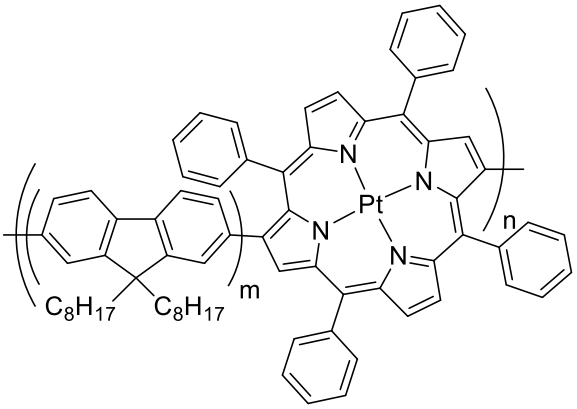


***Figure 2.1.1:*** *Polyfluorene with covalently bound porphyrin through β-positions.*[55-56]

Xiang *et al.* have synthesised a *meso* incorporated porphyrin-polymer complex, but prepared the polymer *via* a less controlled Yamamoto reaction and have only reported the properties of the polymer in terms of oxygen sensing, ***Figure 2.1.2***.

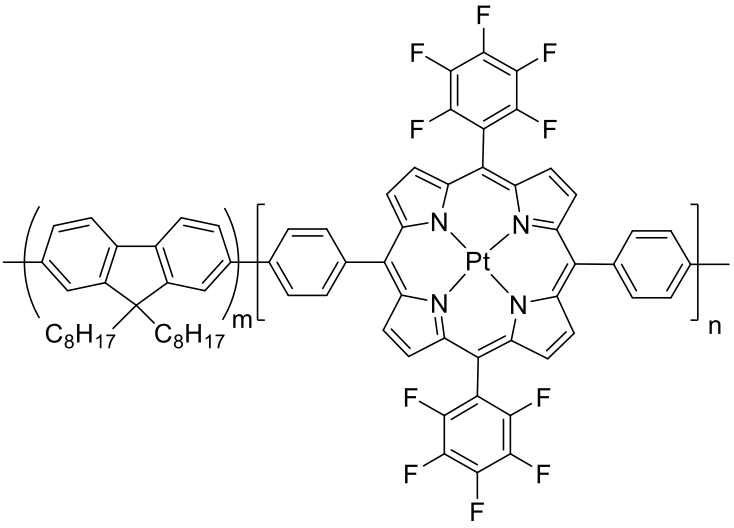


***Figure 2.1.2:*** Meso *linked porphyrin-polyfluorene complex.*

Incorporation of a porphyrin into any system is normally done to promote or utilise triplet formation. For the case of OLEDs, porphyrins are incorporated in order to utilise triplets *via* phosphorescence. Our first aim was therefore to synthesise a polymer that could utilise any triplet excitons formed when used as an OLED.

PFO is a well-studied and highly luminescent blue-emitting polymer. It has been used for many applications (OLED, OPV, OFET, biosensors)[57-60] and may be tuned to emit lower energy light

(in the case of OLEDs), as copolymerisation with a lower bandgap comonomer results in efficient FRET. Copolymerisation with **MPP(Pt)** was expected to result in a polymer that may form a singlet or triplet exciton on the polyfluorene backbone, which would then undergo energy transfer ($\Delta S = 0$) to the **MPP(Pt)** moiety where it would be emitted from a state related to $T_1$ of the porphyrin. Note that due to the heavy metal of the porphyrin, Jahn-Teller-like distortions allow for the otherwise forbidden process of inter system crossing ($\Delta S \neq 0$) to occur from singlet to triplet. In this way, all excitons formed on the backbone may be emissive regardless of original spin. ***Figure 2.1.3*** shows a representation of the energy levels of this type of system.

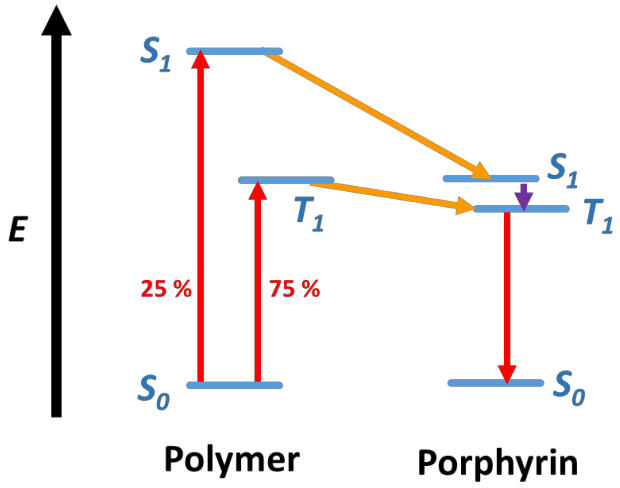


***Figure 2.1.3:*** *Singlet and triplet excited states formed from charge injection may both undergo FRET to the porphyrin which may emit from its lowest energy triplet state.*

Polyfluorene (PF) polymers have been widely studied as suitable semiconducters in OLED devices due to their high photo- and electroluminescence efficiencies (PL and EL), solubility in organic solvents and thermal stability.[57] As PF homopolymers are blue light emitters, doping or copolymerisation with a lower bandgap material that absorbs in the blue region will result in energy transfer to, and subsequent emission from the dopant. The emissive state will be the lowest possible (allowed and accessible) excited state of the system as a whole, provided energy transfer occurs efficiently from host to dopant. Due to spin orbit coupling, a porphyrin such as **MPP(Pt)** may emit from its $T_1$ state, and moreover may convert from $S_1$ (and therefore from $S_n$) to $T_1$. Any excited state on the porphyrin may therefore be assumed to ultimately emit from the $T_1$ state. This effectively allows for emission from all electronically excited states (not just from singlet states as in conventional systems) as both singlets and triplets formed

on the backbone are eventually emitted from $T_1$ of the porphyrin. This potentially boosts the efficiency of an OLED system from a maximum of 25% (only singlets emit) to 100% (all initially formed states may eventually result in emission).

Two publications have resulted from work around this porphyrin. Each of the two main sections of this chapter will outline the design, synthesis and properties of a series of **MPP(Pt)** containing polymers. Each section deals with the results from separate published bodies of work that may be found in the appendix.[61-62]

## 2.2 A Platinum Containing Polyfluorene for Phosphorescent Emission: PF MPP(Pt)

*Poly*-9,9-dioctylfluorene-*ran*-5,15-dimesityl-10,20-diphenyl porphyrin(Pt) (**PF MPP(Pt)**) is a polyfluorene based polymer with a red/NIR emitting porphyrin incorporated into the backbone in various weight percentages; **MPP(Pt)**.

The PF backbone was formed by Suzuki cross coupling reaction of dibromo and diboronic ester fluorenes **2.2.1** and **2.2.2** with **MPP(Pt)** added in various ratios so as to form 5 separate polymers with weight percentages (w/w) of incorporated porphyrin; 0.0, 0.5, 1.0, 2.0 and 5.0. ***Figure 2.2.1*** summarises the reterosynthesis.

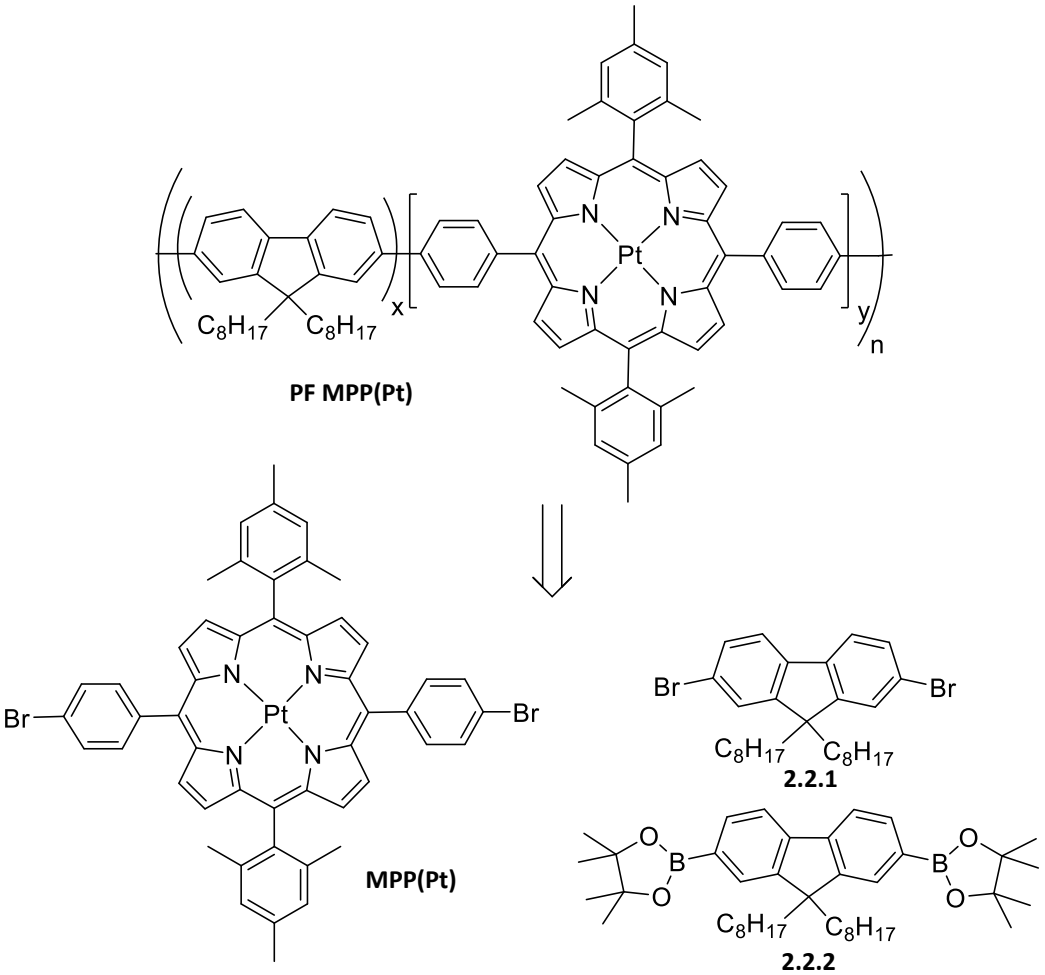


***Figure 2.2.1:*** *Reterosynthesis of* ***PF MPP(Pt)*** *to Suzuki polymerisation monomers.*

The fluorene monomers **2.2.1** and **2.2.2** were synthesised as in ***Scheme 2.2.1***. Fluorene **2.2.3** was dibromonated at the 2 and 7 positions by addition of bromine and catalytic iodine. Dibromofluorene **2.2.4** was subsequently alkylated twice at the 9 position; removing the acidic hydrogen by addition of strong base was followed by dialkylation with 1-bromooctane. The first desired monomer **2.2.1** was formed in an overall yeild of 33% over two steps. The boronic ester monomer **2.2.2** was prepared from dibromide monomer **2.2.1** through lithium-halogen exchange followed by borolation with 2-isopropoxy-4,4,5,5-tetramethyl-1,3,2-dioxaborolane **2.2.5** in 54% yield.

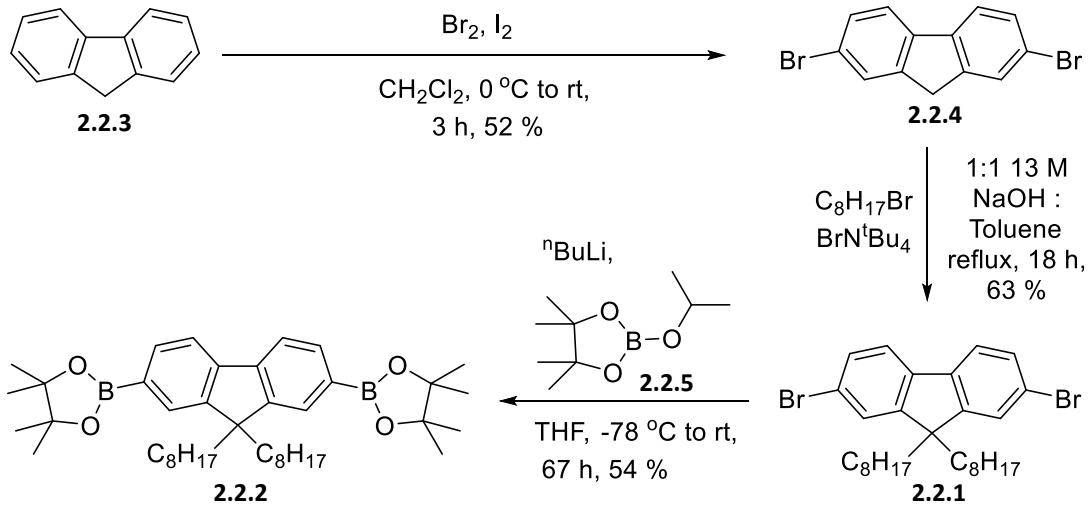


***Scheme 2.2.1:*** *Synthesis of PF monomers **2.2.1** and **2.2.2**.*

**MPP(Pt)** was synthesised in 3 steps from mesitaldehyde and pyrrole using a modified procedure of Lindsey, shown in ***Scheme 2.2.2***.[63] Stirring mesitaldehyde with $MgBr_2$ using pyrrole as solvent resulted in mesityldipyrromethane **2.2.6** being formed in 77% yield. Reaction of mesityldipyrromethane **2.2.6** with a second aldehyde, bromobenzaldehyde, gave **MPP** in 18% yield. Complexation with $PtCl_2$ gave **MPP(Pt)** in 56% yield.

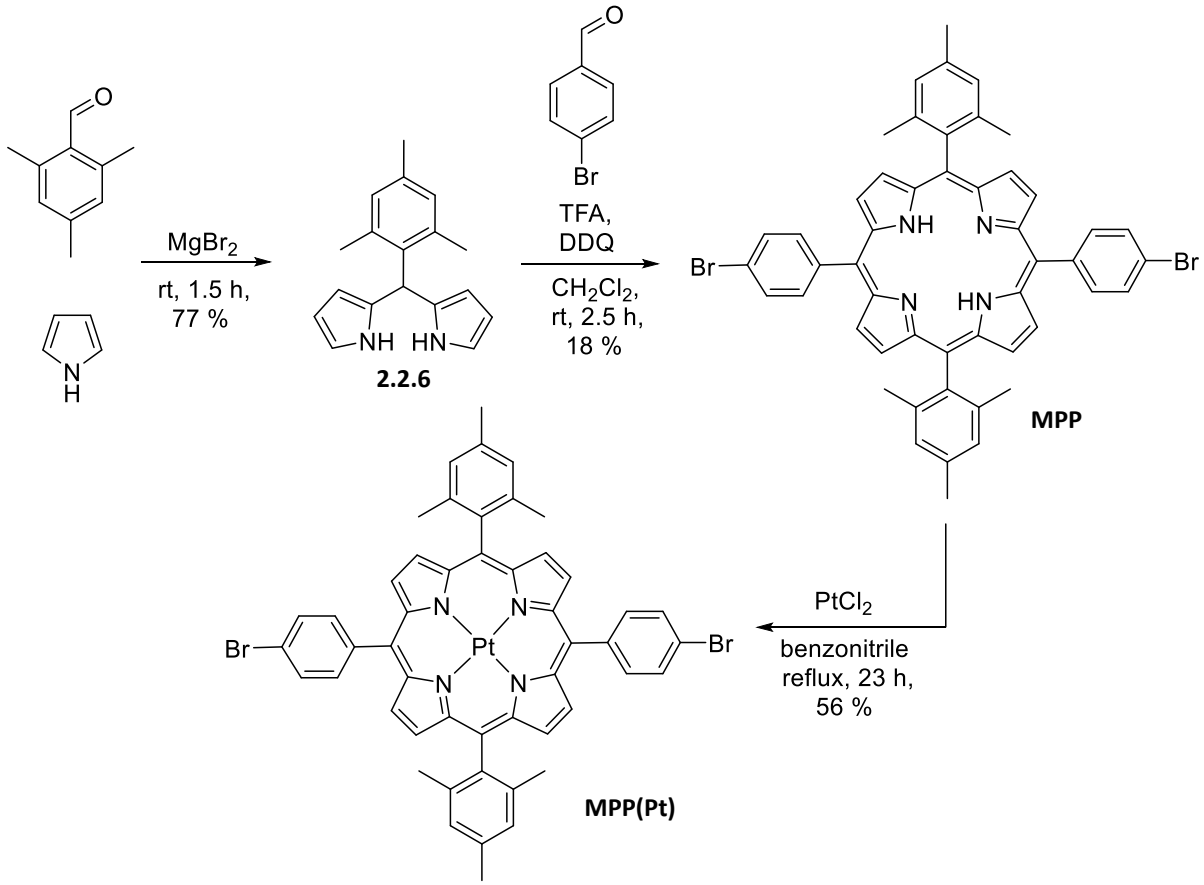


***Scheme 2.2.2:*** *Synthesis of* ***MPP(Pt)****.*

Suzuki polymerisation of the monomers was realised using $Pd(OAc)_2$ with $PPh_3$ as catalyst in the presence of Aliquat 336 and base, ***Scheme 2.2.3***. **PF-MPP(Pt)** was prepared with **MPP(Pt)** in several weight percentages (w/w), controlled by varying the ratio of the monomers. The amount of diboronic ester fluorene **2.2.2** was always constant while the ratio of dibromo fluorene **2.2.1** and **MPP(Pt)** was varied to control the w/w of porphyrin in the final polymer. **MPP(Pt)** was incorporated with w/w of 0.5%, 1.0%, 2.0% and 5.0% into **PF MPP(Pt)**, giving a range of products that were analysed together (**P1**, **P2**, **P3** and **P4** respectively, 0% is labelled as PFO). The novel polymers were isolated as dark red solids and were purified by Soxhlet extraction using acetone, hexane and finally chloroform. Gel permeation chromatography (GPC) of the polymers showed a weight average molecular weight ($M_w$) of 12.0 to 23.0 kDa with PDIs of 1.4 to 1.9 (***Table 2.2.1***).

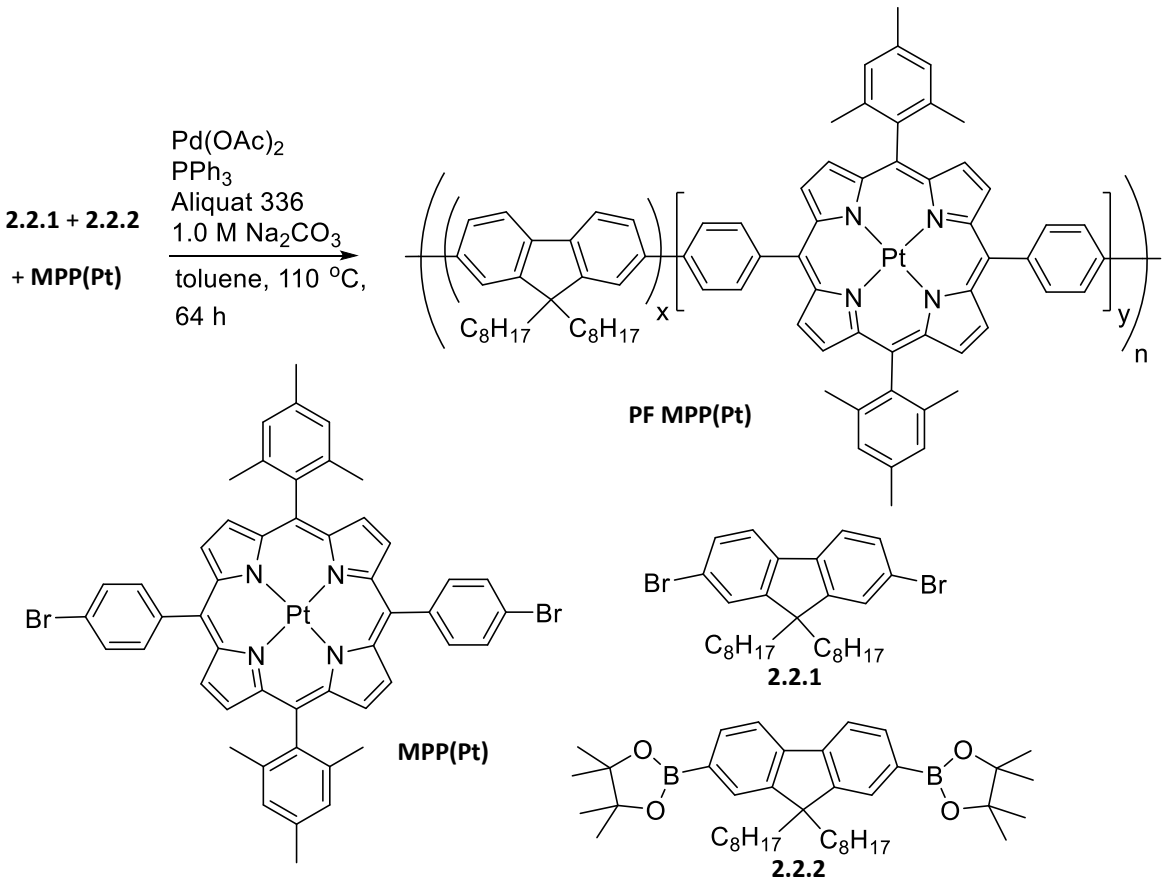


***Scheme 2.2.3:*** *Suzuki polymerisation to form* ***PF MPP(Pt)****. The molar ratio of* ***2.2.2*** *to both* ***2.2.1*** *and* ***MPP(Pt)*** *combined was 1:1, the ratio of* ***MPP(Pt)*** *to* ***2.2.1*** *was varied to create the 5 polymers.*

| | w/w porphyrin /% | | | | |
|---|---|---|---|---|---|
| **Polymer** | **Feed Ratio [a]** | **Incorporation ratio [b]** | **$M_n$ / kDa[c]** | **$M_w$ / kDa[c]** | **PDI[c]** |
| **PFO** | 0.0 | 0.0 | 8.7 | 12 | 1.4 |
| **P1** | 0.5 | 0.2 | 8.0 | 15 | 1.8 |
| **P2** | 1.0 | 0.3 | 11 | 20 | 1.8 |
| **P3** | 2.0 | 0.9 | 11 | 17 | 1.6 |
| **P4** | 5.0 | 2.2 | 12 | 23 | 1.9 |

***Table 2.2.1:*** *Synthetic results of polymerisation. a) Determined by reaction stoichiometery, b) Determined by $^1$H NMR c) Determined by GPC using PhCl eluent.*

The percentage incorporation of **MPP(Pt)** in each of the polymers was measured by $^1$H NMR. ***Figure 2.2.2*** shows how the ratio of pophyrin peaks to PFO peaks changes with increasing porphyrin incorporation. The percentage incorporation of **MPP(Pt)** increases with increased porphyrin feed ratio, and does so in a manner concurrent with the feed ratios. The estimated incorporation values are shown in ***Table 2.2.1*** and are based on the ratio between the alkyl

protons closest to fluorene and the most downfield pyrrolic proton peaks, these being the most isolated. This shows good evidence that the polymers are as expected relative to each other and represent a good range of porphyrin incorporation. The values are lower than the corresponding feed ratio; low incorporation to feed ratios have been shown before on similar systems.[64] It is thought that this discrepancy may be primarily a result of errors associated with analysis of the NMR spectrum (polymers give broader, less defined peaks that are more prone to overlapping with other nearby peaks), rather than lower than expected porphyrin incorporation, due to the good solubility of **MPP(Pt)** in toluene.

By comparing the **MPP(Pt)** peaks in the polymers to monomeric **MPP(Pt)** and **MPP**, the peaks may be tentatively identified in ***Figure 2.2.2***. The four protons *a-d* come at 8.1, 8.4, 8.9 and 9.1 ppm respectively and are visualised as the intensity of the aromatic region is increased. All four shifts are further downfield than **MPP(Pt)** as a monomer. Proton *e* is expected to be under the much larger PFO peaks. The furthest downfield peaks (8.9 and 9.1 ppm) have been assigned as *c* or *d* and the remaining peaks at 8.1 and 8.4 ppm have been assigned as *a* or *b.* These assignments are based on the ordering of peaks of previous compounds (heteroaromatic protons were further downfield than aromatic in all previous **MPP** compounds). As the level of porphyrin incorporation into the polymer is increased from 0.5% to 5.0%, the relative intensities of the proton peaks increases, qualitatively showing that the four porphyrin containing polymers have a good range of w/w.

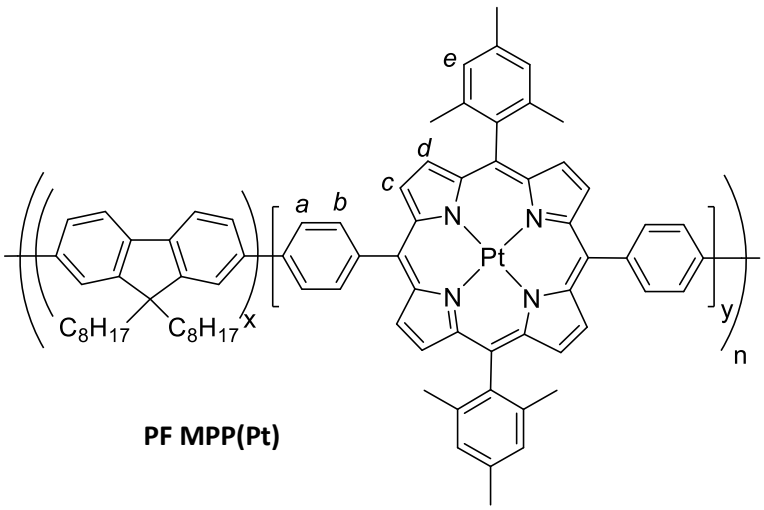


**PF MPP(Pt)**

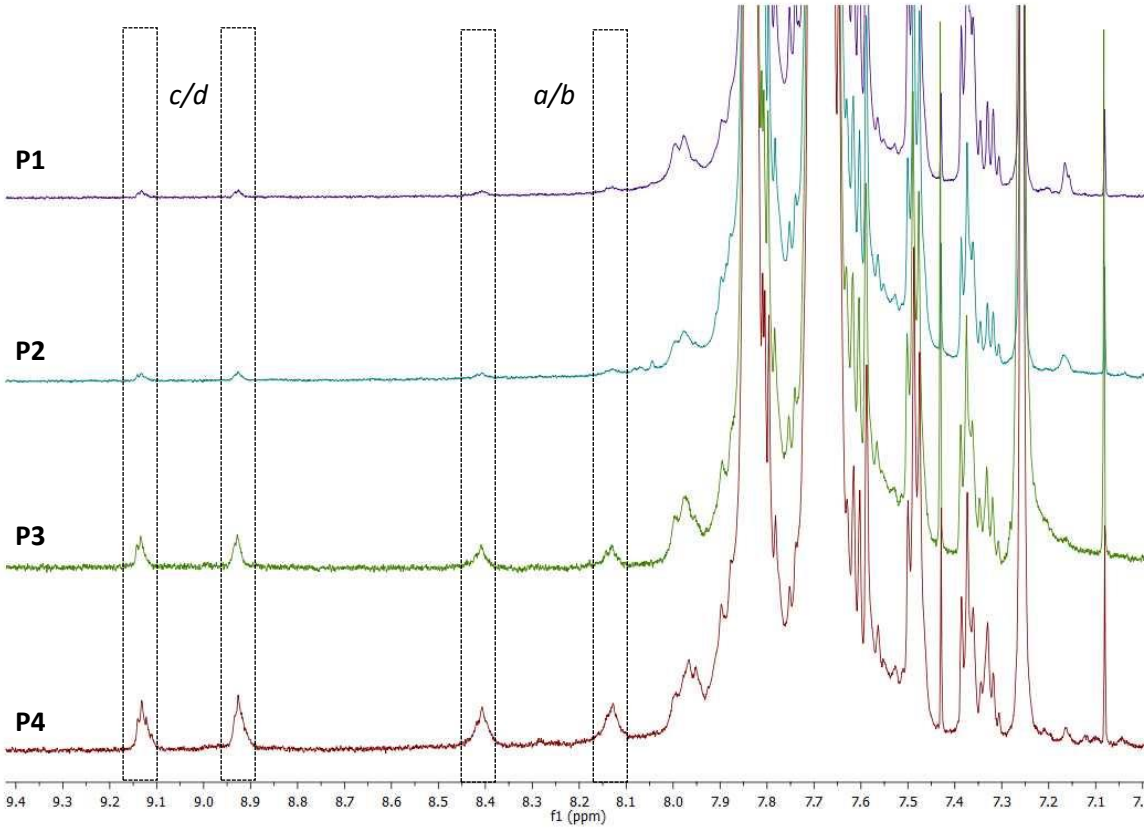


***Figure 2.2.2:*** *$H^1$ NMR spectra of **PF-MPP(Pt)** containing 0.5% (**P1**, purple, top), 1.0% (**P2**, cyan, second from top), 2.0% (**P3**, green, second from bottom) and 5.0% (**P4**, maroon, bottom) w/w of **MPP(Pt)**. PF observed peaks were set to the same level. Peaks corresponding to porphyrin protons are shown in dotted boxes.*

The energy levels and molecular orbitals of **PF MPP(Pt)** were calculated using B3LYP DFT *in silico* using basis set 6-31G* for C, H and N and LanL2DZ for Pt. ***Figure 2.2.3*** shows the HOMO and LUMO levels of an approximation of a porphyrin containing portion of the polymer. To

reduce calculation times the octyl chains of polyfluorene have been replaced with methyl groups.

What is most apparent from the MO calculations is the degree of localisation of the molecular orbitals to either the porphyrin or fluorene portion of the molecule. The twist from porphyrin to phenyl to fluorene is such that conjugation across the entire molecule is broken. While this will have an overall negative impact on the mobilities of the system, it does mean that the basic electronic characteristics of both moieties are likely to be only mildly affected. However the HOMO, and to a smaller degree the LUMO, do both show a mild degree of delocalisation from the porphyrin to the main polymer chain, despite the large twist. It is expected therefore that energy transfer will be more facilitated than the analogous blend of porphyrin and PFO. Significant LUMO contribution from the Pt d-orbitals can be observed indicating that its role not only facilitates inter-system crossing but that the electronic transitions have metal-to-ligand charge transfer characteristics.

***Figure 2.2.4*** shows normalised and averaged absorbance UV spectra for thin films of **P1-P4** and PFO. All polymers clearly show an absorption band for the PFO backbone at 380 nm. **MPP(Pt)** Q-band absorption is seen at 512 nm for all porphyrin containing polymers (and 540 nm as a small second Q band for 5.0% loading) and increases in intensity as the weight ratio of porphyrin is increased. This gradual increase in porphyrin absorption combined with long scan NMR data is excellent evidence that all polymers contain the expected relative weight ratios of porphyrin.

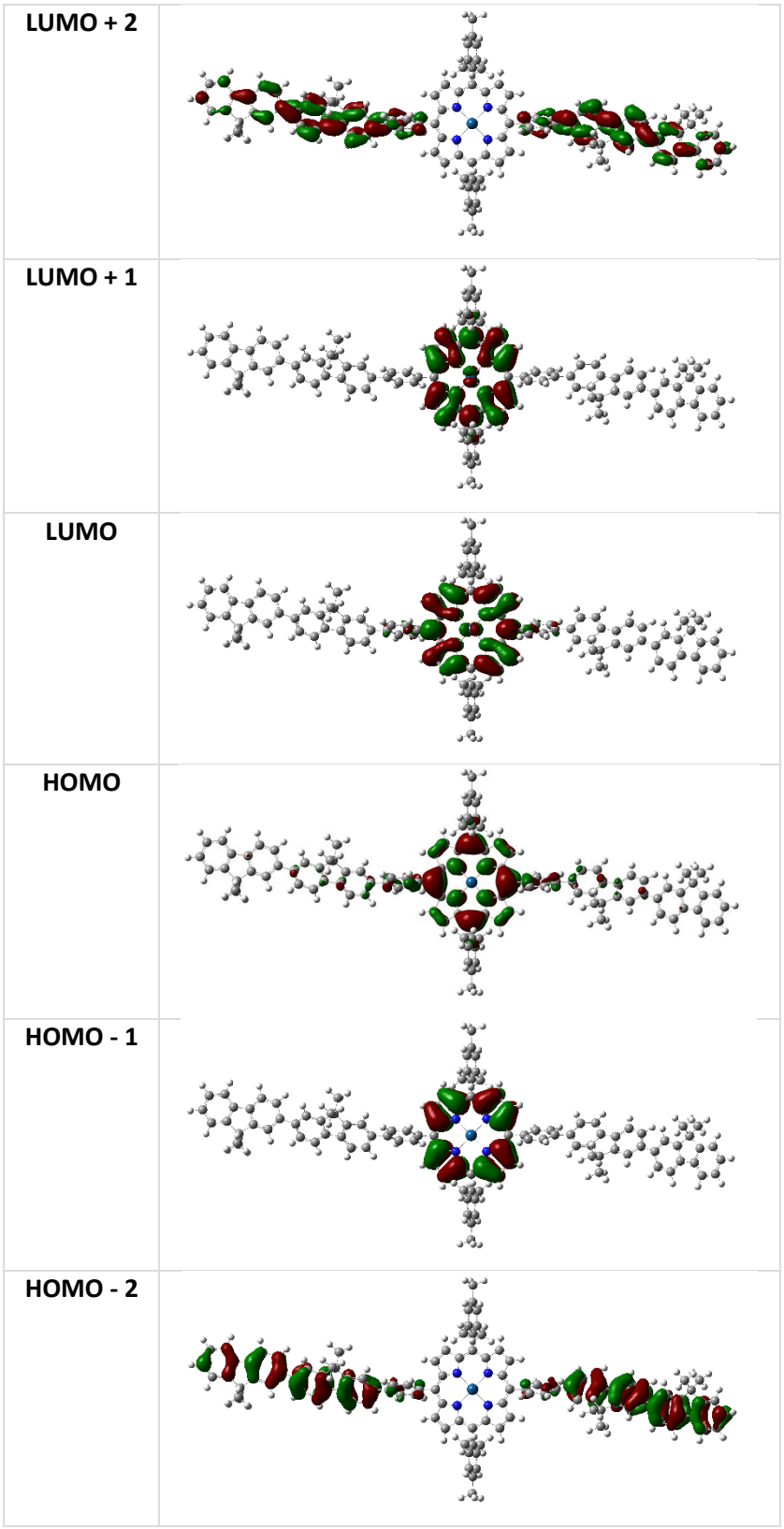


***Figure 2.2.3:*** *Frontier MOs of* ***PF-MPP(Pt)*** *calculated by B3LYP DFT using 6-31G* and LanL2DZ basis sets.*

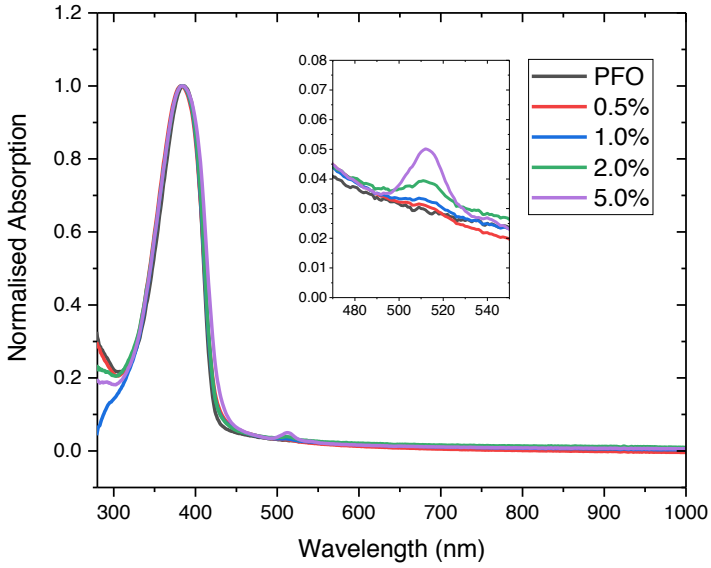


***Figure 2.2.4:*** *Thin film UV data for all* ***PF MPP(Pt)*** *polymers. All data is normalised and is taken as the average of 2 measurements. Inset shows* ***MPP(Pt)*** *Q band absorption features.*

The following data relating to PF-MPP(Pt) was obtained in the UCL physics department by Dr Giulia Tregnago, under the supervision of Prof Franco Cacialli. Device fabrication was also performed by Dr Tregnago, who appears as co-author on the resultant paper from this work.[61]

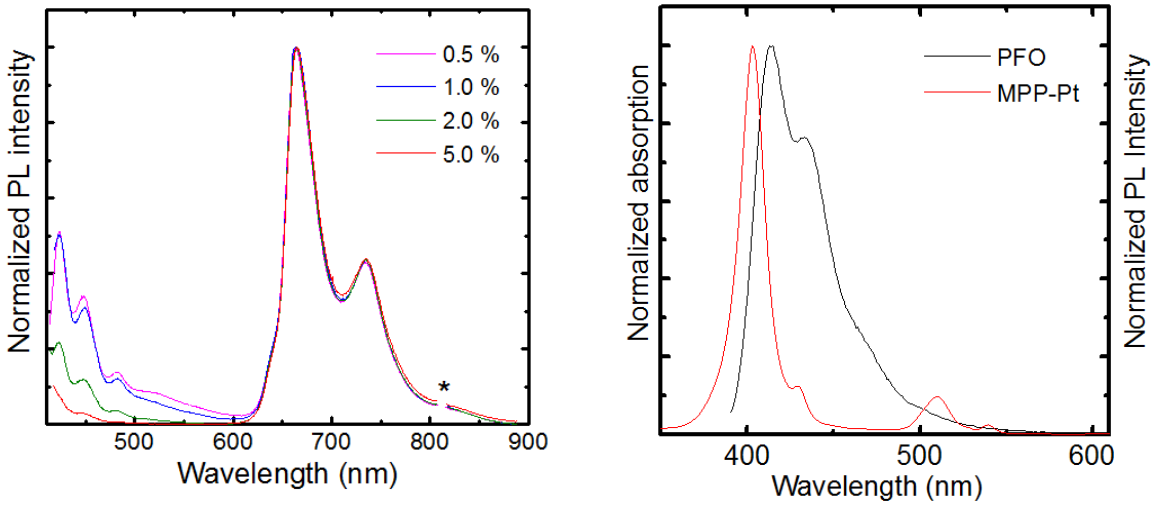


***Figure 2.2.5: i)*** *normalised photoluminescence (PL) spectra of polymers. * indicates monochromator second order transmission of excitation wavelength.* ***ii)*** *Overlaid PFO emission (black) and* ***MPP(Pt)*** *absorption (red) spectra.*

***Figure 2.2.5 i*** shows the photoluminescence spectrum of **PF-MPP(Pt)**. The most notable feature is that for all loadings of porphyrin there are dominant emission peaks at 665 nm and 735 nm, indicating emission primarily from **MPP(Pt)** and good energy transfer from the PFO backbone even at very low porphyrin loadings. The emission shoulder at 645 nm is also assigned to **MPP(Pt)**. As the porphyrin loading is increased, the intensity of the polyfluorene backbone vibronic peaks at 442 nm and 467 nm decreases, again providing good evidence of efficient energy transfer. Efficient energy transfer is achieved when there is good overlap between the PFO emission and MPP(Pt) absorption bands; both the Soret band (402 nm) and Q band (512 nm) of **MPP(Pt)** have significant overlap with PFO emission as can be seen in ***ii***. The PL time decay for all copolymers is on the microsecond time scale (***Figure 2.2.6***), indicating triplet formation with time constants of 9.3 µs, 9.2 µs, 9.2 µs and 8.6 µs for **P1**, **P2**, **P3** and **P4** respectively.

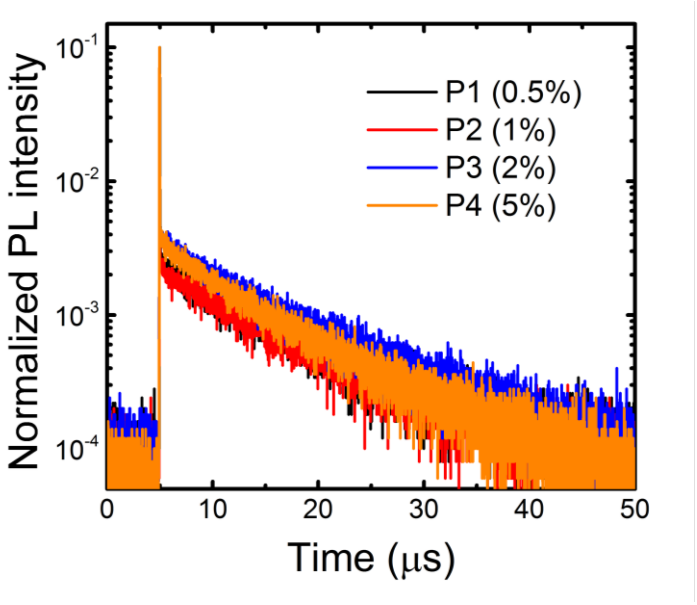


***Figure 2.2.6:*** *PL time decay for MPP(Pt) emission (665 nm) following excitation of PFO backbone (371 nm).*

OLED devices were created from the four porphyrin containing polymers; ***Figure 2.6*** shows the composition of these devices. The OLEDs were fabricated by spin coating PEDOT:PSS (hole conducting layer) onto indium tin oxide coated glass (ITO glass, anode) followed by spin coating of the semiconducting polymer. The Ca/Al cathodes were thermally evaporated under vacuum on top of the active layer. A voltage was then passed through the device and current-voltage-radiance characteristics were measured.

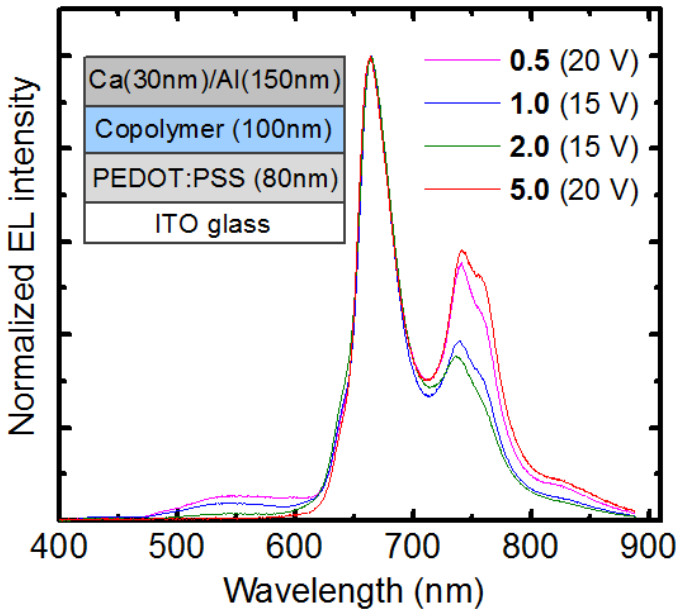


***Figure 2.2.7:*** *Normalized electroluminescence (EL) spectra for the polymers as part of a device. The LED structure is reported. The active layer thickness is ~100 nm and the device area is 3.5 mm$^2$. Key refers to porphyrin feed ratio /%.*

| Polymer | Porphyrin loading /% | EQE[a] /% | $V_{on}$[b] / V | Luminance[a] / Cd/m$^2$ |
|---|---|---|---|---|
| **P1** | 0.5 | 0.17 ± 0.01 | 10.7 ± 0.2 | 14.8 ± 0.7 |
| **P2** | 1.0 | 0.28 ± 0.04 | 7.6 ± 0.2 | 23.8 ± 2.9 |
| **P3** | 2.0 | 0.48 ± 0.01 | 8.3 ± 0.3 | 31.1 ± 0.8 |
| **P4** | 5.0 | 0.28 ± 0.04 | 9.3 ± 0.4 | 9.9 ± 0.4 |

***Table 2.2.2:*** *Summary of LED performance. [a]Measured at 30 mA/cm$^2$. [b]Intercept of the I-V curve with the x-axis in a semi-log plot.*

All polymers display dominant EL peaks at 665 and 736 nm, concurrent with results from the PL specta. **P1** and **P2** both display weak EL below 600 nm that is not present for higher porphyrin w/w. This may be due to emission from a **MPP(Pt)** singlet state (previously reported for similar systems to occur around 580 nm),[65-66] or possibly because of oxidative defects on the polyfluorene backbone.[67] **P3** and **P4** both show pure electrophosphoresence (*i.e.* only emission from a triplet state located on **MPP(Pt)**).

The highest efficiency LED is **P3** (2.0% loading) with an external quantum efficiency (EQE) of 0.48%, a luminance of 23.8 Cd/$m^2$ and the lowest turn-on voltage (8.3 V). This result is very encouraging when compared to similar red/NIR emitting compounds from the literature, especially when taking into account the LEDs are not optimised for charge collection and extraction.[68-69]

A series of conjugated polymers based on polyfluorene have been prepared with various weight percentages of a phosphorescent porphyrin, **MPP(Pt)**, attached *via* the *meso* position. Emission of the polymers was found to be from the triplet state of the porphyrin, as shown by the microsecond lifetime of emission. 0.5% and 1% loadings of porphyrin retained some fluorescence from the polymer backbone. Fluoresence was not observed for higher porphyrin loadings, indicating good energy transfer from polymer to porphyrin.

The triplet state of **MPP(Pt)** has been clearly shown to be readily populated. The second series of polymers synthesised with this porphyrin as comonomer sought to utilise the populated triplet state to back-transfer onto the polymer backbone to facilitate triplet-triplet annihilation (TTA).

## 2.3 Towards a Triplet-triplet Annihilation Polymer: PDPA MPP(Pt)

With a reliable and reproducible synthesis to a polymerisable porphyrin in hand, attention was shifted to other suitable comonomers for interesting polymers. As discussed in chapter 1, a build-up of triplet states in certain materials can lead to triplet-triplet annihilation (TTA) upconversion. The work on **PF MPP(Pt)** has proven that triplets are formed when **MPP(Pt)** is included in the polymer backbone. If a polymer with triplet level close to that of MPP(Pt) and capable of TTA could be found, copolymerisation with **MPP(Pt)** could lead to a single material that may absorb low energy photons (*via* the **MPP(Pt)** moiety) and upconvert to a high energy state (*via* energy transfer to the backbone and TTA).

Triplet-triplet annihilation (TTA) upconversion is the process in which, through the absorption of two photons of lower energy, one excited state of higher energy is formed.[22] In practical terms, this means red/NIR light absorbed into a low lying energy state may be converted into a voltage that is greater in energy than either of the original photons. This allows the fabrication of devices with excellent absorption characteristics and high upconversion quantum yields (20-30%).[70-72] ***Figure 2.3.1*** shows how upconversion can be realised in a semiconductor.

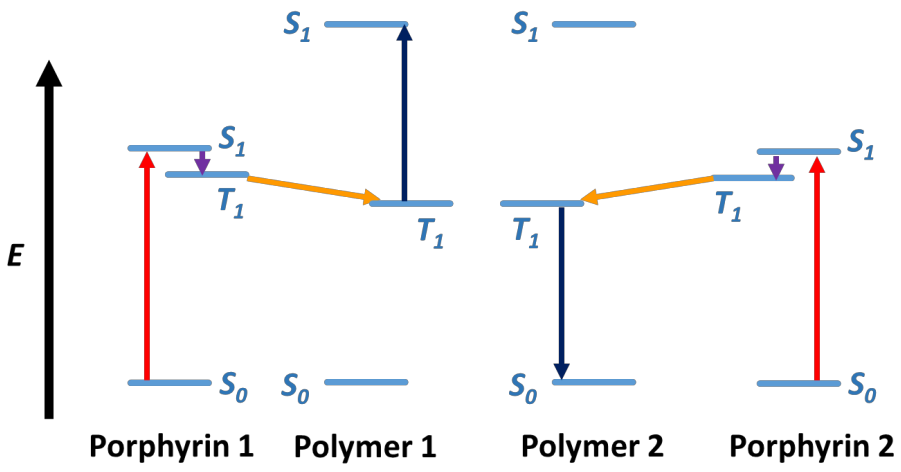


***Figure 2.3.1:*** *TTA upconversion. Low energy light is absorbed by the porphyrin dopant (red arrow) which may then undergo ISC (purple) to $T_1$. TTET to $T_1$ of the polymer backbone (orange) may be followed by TTA upconversion (dark blue) if two excited triplet states are close in space resulting in one high energy exciton that may decay by fluorescence on polymer 1, and one ground state on polymer 2.*

Firstly, an exciton is formed on the porphyrin dopant as an electron is promoted from $S_0$ to $S_1$ (the only allowable transition at low energy excitation) (red). $S_1$ may then decay to $T_1$ (if the dopant contains a heavy metal which promotes spin orbit coupling) through intersystem crossing (ISC) (purple). This triplet state may then undergo the allowable transition to the triplet state of the upconverting polymer (triplet triplet energy transfer (TTET)) (orange). This transition is a Dexter process, and as such the donor and acceptor must be within a close range of each other.[73] By copolymerising the dopant with a known polymer, this contact is controllable and the energy transfer more likely to occur. Once two excitons have been transferred to the main polymer chain and are within a close distance of each other, TTA upconversion can result in a single exciton on $S_1$ (dark blue). This exciton may then decay to release energy, either through emission of low wavelength light or extraction of a higher voltage than was contained within either of the initially absorbed states. When this system is placed in a solar cell, overall efficiency is increased as previously unabsorbed, low energy photons can now be absorbed and utilised.

Acenes are known to efficiently undergo triplet-triplet annihilation when sensitised with triplets.[70] It was our hypothesis that a polymer containing an acene in the backbone with a triplet state close to that of **MPP(Pt)** (ideally, slightly lower in energy) may be able to absorb high wavelength, low energy photons (*via* the porphyrin Soret band) and subsequently upconvert two such excitons to a higher energy state.

Recent examples of TTA upconversion uses a blend of a diphenylanthracene tethered polymer and a simple porphyrin.[74-75] Blends are not ideal for this process as the proximity of donor and acceptor (for TTET) is not guaranteed; porphyrins are known to form aggregates readily.[76-77] By incorporating both donor and acceptor into a single polymer the donor-acceptor distances are much more regimented. If both are incorporated into a conjugated polymer, energy transfer should be even further improved.

A diphenylanthracene that is polymerisable requires some structural changes from plain diphenylanthracene however, primarily to increase solubility. ***Figure 2.3.2*** shows the target for this synthesis, *poly*-4',4''-(2,3,6,7-(octyloxy)-9,10-diphenylanthracene-*alt*-1,4-phenyl)-*ran*-(4',4''-5,15-dimesityl-10,20-diphenylporphyrin(Pt)-*alt*-1,4-phenyl) (**PDPA MPP(Pt)**).

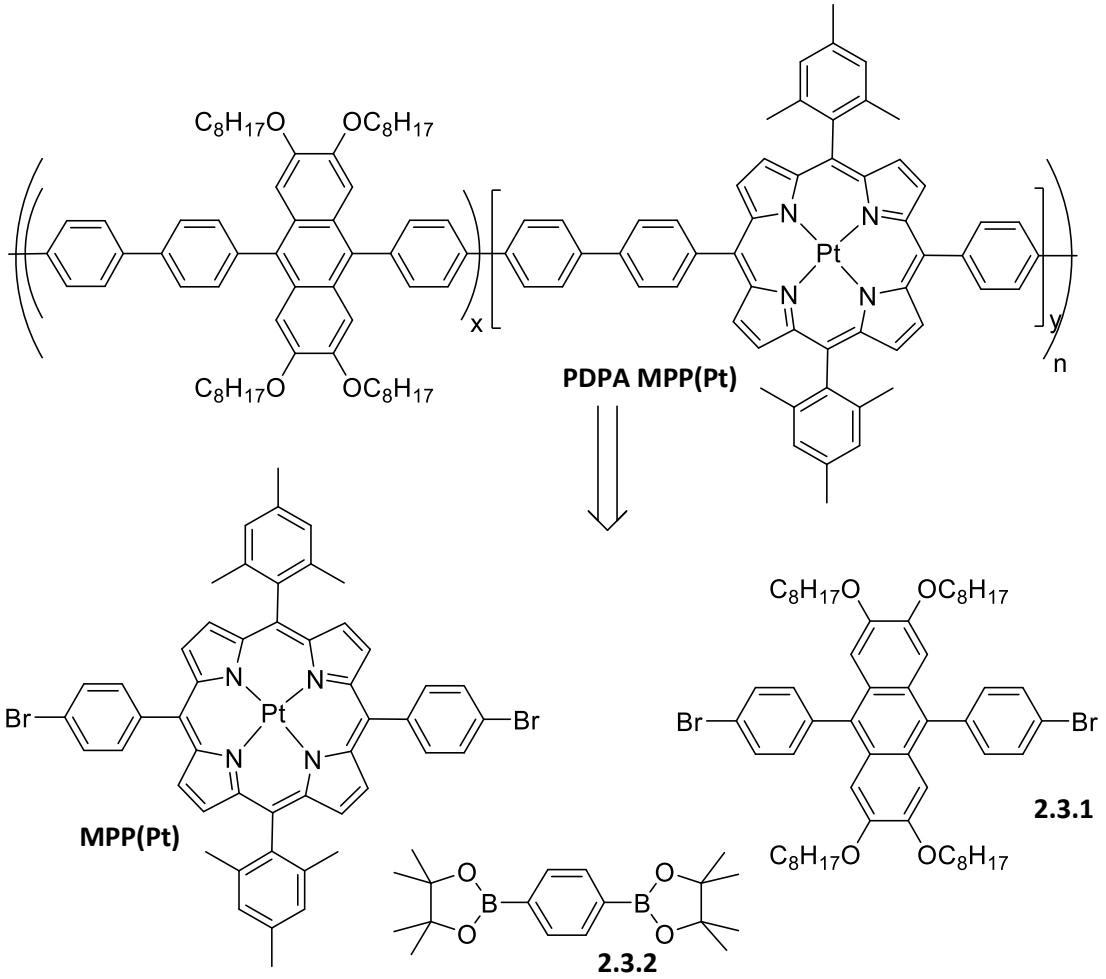


***Figure 2.3.2: PDPA MPP(Pt)*** *(top) and reterosynthesis.*

The energy levels of the constituent parts of the polymer are critical if TTA upconversion is to be achieved. By copolymerising diphenylanthracene monomer **2.3.1** with benzene monomer **2.3.2**, a large twist will be present between the porphyrin and diphenylanthracene moieties. This is normally undesirable; as mentioned above the twist will lessen conjugation across the molecule and lower mobility. In this case however, the twist isolates the two energy systems of the constituent parts, so that the overall energy levels of the polymer are likely to be very similar to those of the monomers in terms of energy, but also be very close together in space, maximising TTET.

It is necessary to modify the diphenylanthracene moiety to aid solubility. This has been done through the addition of alkoxy groups which also aid in the synthesis of the monomer. The effect of these additional groups was estimated through DFT calculations of energy levels. ***Figure 2.3.3*** shows a Jablonski diagram of the energy levels of the various considered parts of **PDPA MPP(Pt)**.

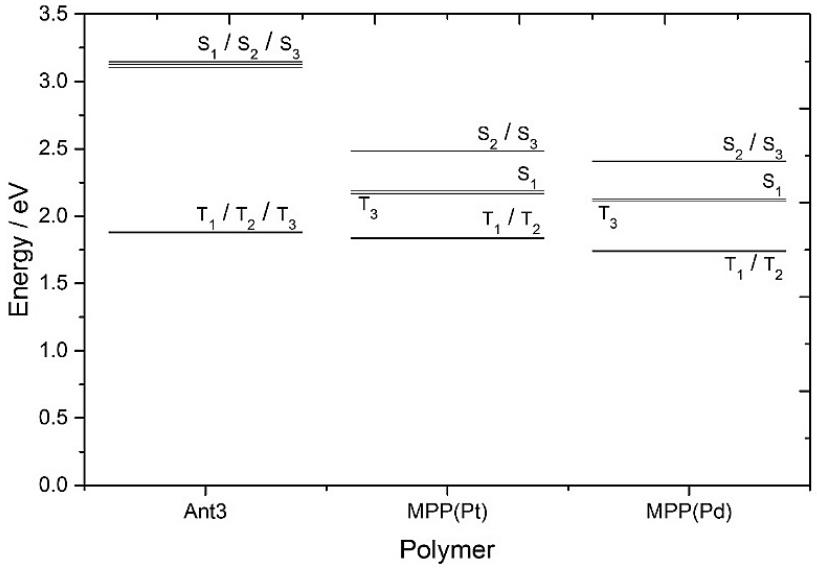


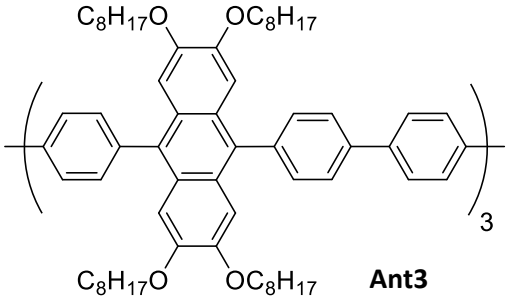


**Ant3**

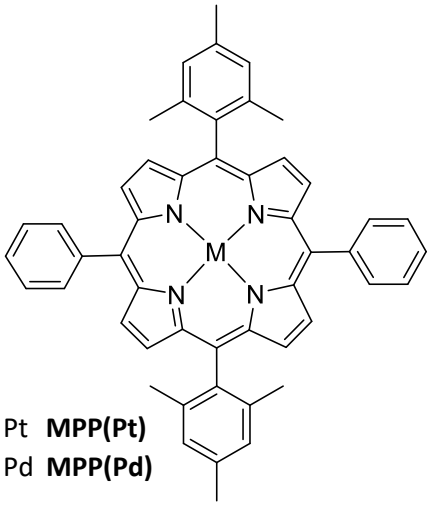


M = Pt **MPP(Pt)**
M = Pd **MPP(Pd)**

| Polymer | $T_1$ / eV | $T_2$ / eV | $T_3$ / eV | $S_1$ / eV | $S_2$ / eV | $S_3$ / eV |
|---|---|---|---|---|---|---|
| **Ant3** | 1.88 | 1.88 | 1.88 | 3.10 | 3.13 | 3.15 |
| **MPP(Pt)** | 1.83 | 1.84 | 2.17 | 2.19 | 2.48 | 2.48 |
| **MPP(Pd)** | 1.74 | 1.75 | 2.11 | 2.13 | 2.41 | 2.41 |

***Figure 2.3.3: :*** *Jablonski diagram of considered monomers for anthracene TTA upconversion polymers (top) with diagrams of calculated structures (middle) and tabulated quantitative data (bottom) calculated by B3LYP DFT using 6-31G* and LanL2DZ basis sets.*

Consideration of the data in ***Figure 2.3.3*** shows that polymerisation of a tetraalkoxy anthracene with **MPP(Pt)** would (if the energy levels remain unaffected) result in a polymer containing a donor with a triplet energy of 1.83 eV and an acceptor with $T_1$ of 1.88 eV. This means the desired transition is energetically unfavourable, however the difference is very small (0.05 eV) and well within the expected differences between DFT and experiment (differences arise from molecules being treated as in the gas phase, estimating triplet state energy levels that are often not well calculated in DFT and limits on the size of the 'polymer' *in silico*). It is thought that the transition would occur with these energy levels, especially considering that energy transfer to $T_1$ of the anthracene may then result in TTA upconversion, thereby lowering the population density of that state. In the platinum porphyrin, phosphorescence is a likely loss mechanism however. This would be mitigated slightly if the metal were changed to palladium (palladium, as a lighter metal, has a lower rate of intersystem crossing from spin-orbit coupling). As can be seen from ***Figure 2.3.3*** however, **MPP(Pd)** has an even lower $T_1$ and is less likely to result in a successful upconverting polymer. The decision therefore was made to create anthracene polymers containing **MPP(Pt)**.

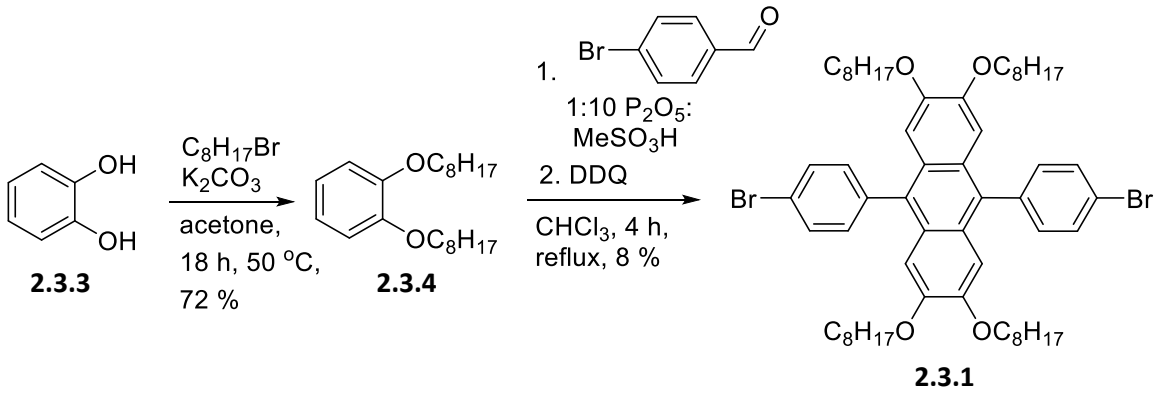


***Scheme 2.3.1:*** *Synthesis of anthracene monomer* ***2.3.1****.*

Diphenylanthracene monomer **2.3.1** was synthesised as in ***Scheme 2.3.1***. A tetramethoxy analogue has been previously synthesised from veratrole by Xia *et al*.[78] Starting from catechol **2.3.3**, dialkylation yields an octyl analogue of veratrole, 1,2-bis(octyloxy)benzene **2.3.4**. Xia's conditions for anthracene formation are similar to Lindsey's porphyrin formation method. 1,2-bis(octyloxy)benzene **2.3.4** is first reacted with an aldehyde in the presence of acid which forms the skeletal ring structure, and an oxidant is then added to oxidise the ring structure

into its aromatic form. This reaction is fairly low yielding (8%) but is nevertheless an elegant way of synthesising a fairly large molecule.

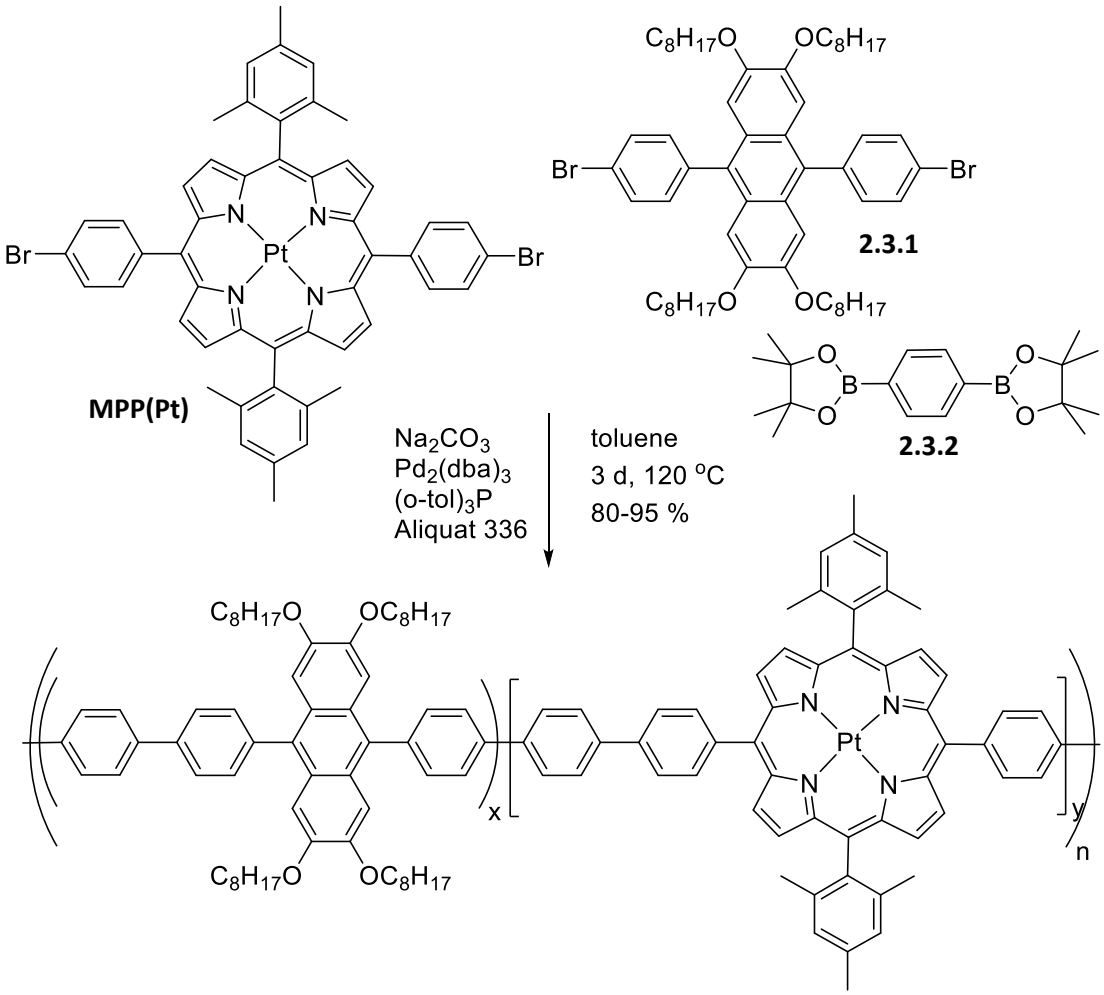


| Polymer | Porphyrin feed / w/w% | $M_n$ / kDa | $M_w$ / kDa | PDI |
|---|---|---|---|---|
| **PDPA** | 0 | 7.8 | 10 | 1.3 |
| **PDPA MPP(Pt) 1** | 1 | 8.8 | 12 | 1.4 |
| **PDPA MPP(Pt) 5** | 5 | 12 | 20 | 1.7 |
| **PDPA MPP(Pt) 10** | 10 | 11 | 21 | 1.8 |

***Scheme 2.3.2:*** *Suzuki polymerisation to form PDPA MPP(Pt) polymers* ***PDPA, PDPA MPP(Pt) 1****,* ***PDPA MPP(Pt) 5*** *and* ***PDPA MPP(Pt) 10*** *with 0, 1, 5 and 10% porphyrin loading respectively.*

4 polymers of various porphyrin loadings were synthesised *via* a Suzuki polymerisation, ***Scheme 2.3.2***. The sizes of all polymers was 7.8 – 12 kDa ($M_n$), which is an acceptable range for physical testing. The absorbance spectra were then obtained for each polymer in chlorobenzene solution.

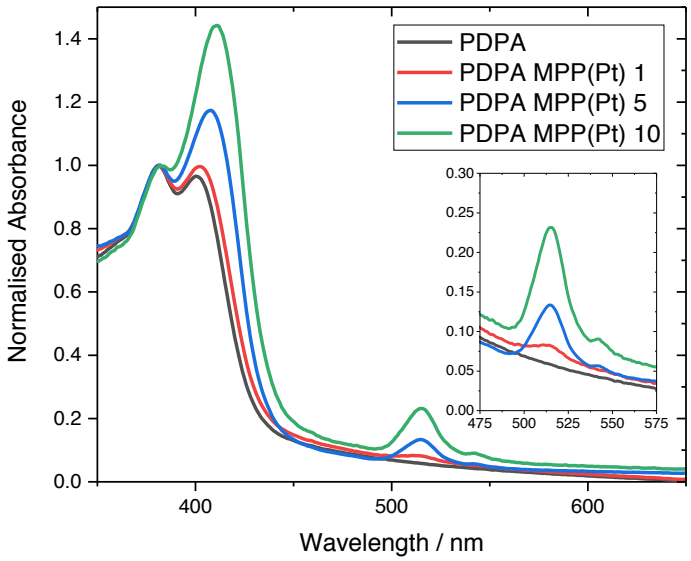


***Figure 2.3.4:*** *Normalised absorption spectrum for* ***PDPA MPP(Pt)*** *polymers in chlorobenzene solution. Inset shows* ***MPP(Pt)*** *Q band absorption.*

All polymers show (predominantly) diphenylanthracene absorption bands at 382 nm and between 400 and 410 nm, ***Figure 2.3.4***. Interestingly, there is a shift to stronger absorption at longer wavelengths as porphyrin loading is increased (*ie*. as porphyrin loading is raised, the peak at 400-410 becomes more dominant and more red-shifted). This is thought to be due to increased contribution from the Soret band of the porphyrin, denoting the $S_2 \leftarrow S_0$ transition. Similar to **PF MPP(Pt)**, the **MPP(Pt)** Q-band absorption peaks are seen at 515 nm (and 543 nm for higher porphyrin loadings) which indicates the $S_1 \leftarrow S_0$ transitions. Q-band absorption is seen to increase with porphyrin loading, indicating the w/w are as expected.

The molecular weights of all polymers was found to be modest (due to solubility resulting in precipitation during the reaction) but similar to each other and therefore comparible. The incorporation ratios of **MPP(Pt)** containing polymers were as expected, ***Table 2.3.1***. An accurate value of the incorporation ratio of **PDPA MPP(Pt) 1** could not be obtained from NMR studies due to the low amounts of porphyrin present, however the presence of Q bands in the absorbance spectra clearly shows porphyrin incorporation. The energy gap was found to be

fairly consistent across the series; the porphyrin containing polymers having slightly red shifted energy gaps as their LUMOs are lower in energy. This is attributed to the increased electron density of the porphyrin moieties.

| Polymer | Feed ratio / w/w% | Inocorp ratio[a] / w/w% | $M_n$[b] / kDa | $M_w$[b] / kDa | PDI[b] | Decomp Temp[c] / °C |
|---|---|---|---|---|---|---|
| **PDPA** | 0 | 0 | 7.8 | 10 | 1.3 | 460 |
| **PDPA MPP(Pt) 1** | 1 | $0 < x \leq 1$ | 8.8 | 12 | 1.4 | 460 |
| **PDPA MPP(Pt) 5** | 5 | 4 | 12 | 20 | 1.7 | 460 |
| **PDPA MPP(Pt) 10** | 10 | 10 | 11 | 21 | 1.8 | 460 |

***Table 2.3.1:*** *Physical properties of PDPA polymers. [a]Determined from $^1$H NMR spectroscopy (as in section 2.2). [b]Determined by GPC using PhCl eluent. [c]Determined from TGA traces.*

The following data relating to PDPA MPP(Pt) was obtained in the UCL physics department by Dr Alessandro Minotto, under the supervision of Prof Franco Cacialli. Device fabrication was also performed by Dr Minotto, who appears as a contributing author on the resultant paper from this work.[62]

***Figure 2.3.5*** shows photoluminescence data for the polymers as thin films. Efficient energy transfer is observed as the **PDPA** backbone emission peaking at 455 nm is quickly quenched and phosphorescence emission bands peaking at 666 nm and 737 nm from the **MPP(Pt)** comonomer begin to dominate.[79-80] These new peaks are attributed to porphyrin Q band triplet state emission.[81-82] Solution photoluminescence was found to be similar to thin film, with the exception of decreased energy transfer. Emission from the polymer backbone dominates for all polymers, with increased contribution from porphyrin Q bands as porphyrin incorporation is increased. This is attributed to intermolecular energy transfer being facilitated only in the solid state.

***Table 2.3.2*** shows the experimental energy level energies and the quantum yield (QY) of each polymer. A high QY of 22% was measured for **PDPA**; anthracene in conjugated polymers has previously been shown to undergo photoluminescence quenching in the solid state.[83-84] Near-IR QYs are reported for the porphyrin containing polymers. NIR emission is problematic to obtain, since the low bandgap excitons have an increased probability of non-radiative, thermal relaxation.[85] The **PDPA MPP(Pt)** polymers also suffer from particularly low stability under laser irradiation, observed as emission quenching under increased irradiation.

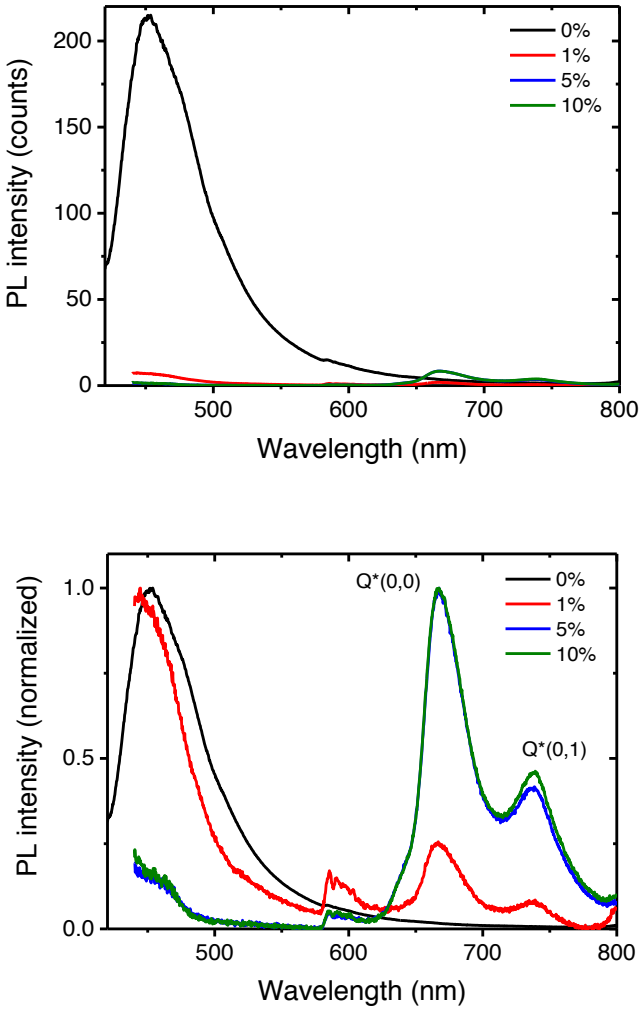


***Figure 2.3.5:*** *PL spectra (top) and normalised PL spectra (bottom) of thin films of polymers spun from chloroform solution. Legend refers to* ***MPP(Pt)*** *incorporation feed ratio. PL spectra were obtained by pumping the films with a 405 nm laser diode (% represents the porphyrin feed of the different polymers). The peak at 595 nm is an artefact.*

| Polymer | HOMO[a] / eV | LUMO[b] / eV | $E_{gap}$[c] / eV | PLQY[d] /% | NIR QY[d] /% |
|---|---|---|---|---|---|
| **PDPA** | -5.5 | -2.6 | 2.9 | 22 | n/a |
| **PDPA MPP(Pt) 1** | -5.5 | -2.9 | 2.6 | n/a | 1 |
| **PDPA MPP(Pt) 5** | -5.5 | -2.9 | 2.6 | n/a | 2 |
| **PDPA MPP(Pt) 10** | -5.4 | -2.8 | 2.6 | n/a | 2 |

***Table 2.3.2:*** *Electronic properties of PDPA polymers. [a]Determined by PESA measurements, ±0.1 eV. [b]Determined from HOMO + optical $E_{gap}$. [c]Determined from thin film UV-Vis onset. [d]Thin film PLQY determined using integrating sphere (NIR measurements were measured in red-NIR region >600 nm).*

The instability of these systems is attributed to a high concentration of triplet states. This again implies energy transfer from polymer backbone (where singlet excitons are formed with 405 nm laser pulse) to porphyrin is an efficient process. It is thought the triplet states result in singlet oxygen generation, or possibly lead to anthracene cyclisation reactions. ***Figure 2.3.6*** shows the PL spectra of the 5 and 10% porphyrin loading polymers when excited with a 532 nm laser pulse.

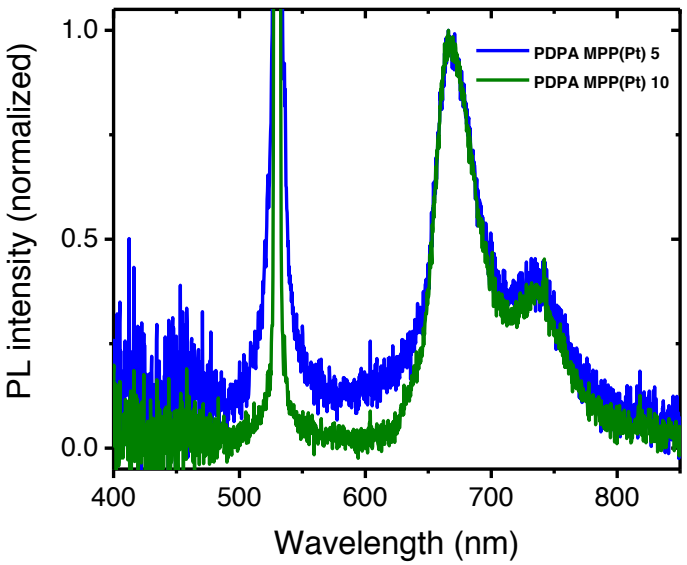


***Figure 2.3.6:*** *PL spectra of* ***PDPA MPP(Pt) 5*** *(blue) and* ***PDPA MPP(Pt) 10*** *(green) thin films excited with 532 nm laser pulse.* ***PDPA MPP(Pt) 1*** *showed similar data, but with high background noise.*

Excitation of the porphyrin was hypothesised to lead to TTA on the anthracene-containing backbone (through ISC and TTET). This would be visualised by emission at 450 nm after an excitation of the porphyrin at 532 nm. From ***Figure 2.3.6***, we observe no emission from the polymer backbone, implying TTA does not significantly occur in these systems. A similar PL trace was obtained for **PDPA MPP(Pt) 1** but has not been included for clarity, as it comprised a high background noise.

Despite no TTA occurring, each polymer was incorporated into an OLED device. The structure of the devices is shown in ***Figure 2.3.7***.

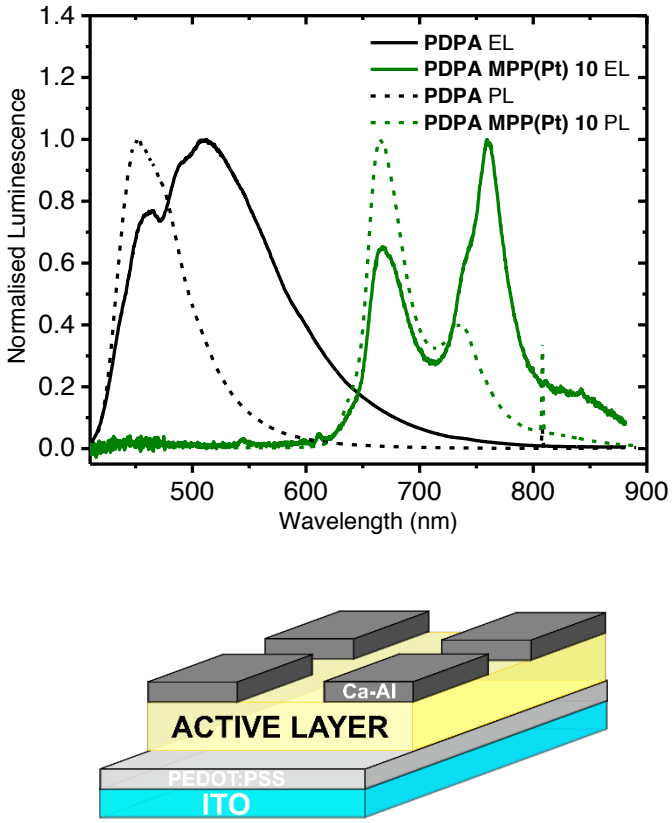


| Polymer | Max EQE /% | PL maxima / nm | EL maxima / nm |
|---|---|---|---|
| **PDPA** | 0.14 | 450 | 460, 510 |
| **PDPA MPP(Pt) 10** | 0.03 | 666, 737 | 666, 760 (shoulder at 737) |

***Figure 2.3.7:*** *Electroluminescence (solid) and photoluminescence (dashed) of* ***PDPA*** *(black) and* ***PDPA MPP(Pt) 10*** *(green) thin films with 405 nm laser pulse (top) and device structure (middle) and luminescent properties (bottom).*

Due to ongoing stability problems, only **PDPA** and **PDPA MPP(Pt)** resulted in successful device fabrication. Both polymers show interesting differences between electroluminescence (EL) and photoluminescence (PL).

PL is observed in **PDPA** to peak at 450 nm. The **PDPA** OLED shows bright green EL at 510, a red shift of 60 nm compared to the PL data. This shift may be attributed to a small number of low lying emissive aggregates. In solid state PL, this aggregation effect is not observed as the number of aggregates is low and excitons radiatively decay close to where they are formed

before they may migrate to aggregate sites. Charges in the EL spectra however are driven from either end of the device and therefore move through the semiconductor, moving through low-energy sites found on the aggregating portions of the device. Excimers are formed and emission from these lower lying states begins to dominate. Some non-aggregate emission is observed in the EL at 460 nm. Aggregation in anthracene is facilitated by its large π system, and solid-state aggregation has been observed in similar systems.[86] The maximum EQE of 0.14% is reasonable for a non-optimised single layer device.

**PDPA MPP(Pt) 10** shows very red emission almost entirely in the NIR (>700 nm) region. The maximum EQE of 0.03% is close to the maximum values reported at the time for NIR light-emitting polymers.[51] A similar, but larger red shift is observed for this polymer. Two Q bands are seen in the PL spectra at 666 nm and 737 nm. The EL spectrum shows a major peak at 760 nm, as well as a minor peak at 666 nm and a shoulder corresponding to the second Q band at 737 nm. This shows the new peak at 760 nm is not simply an increase in intensity of a peak observed in the PL spectrum. The shift is again therefore attributed to excimer/exciplex formation.

Interestingly, the EL emission of **PDPA MPP(Pt) 10** is close to that of the much larger porphyrin **Pt(TPBP)**. By inducing aggregation, either polymer-porphyrin or porphyrin-porphyrin, a simple, small porphyrin may emit at a much lower wavelength than previously expected. The synthesis of larger porphyrins is discussed in chapter 3.

Although the initial aim of creating a polymer capable of TTA was unsuccessful, an interesting aggregation-induced red shift of emission was detected. This observation formed the basis of the resultant paper on this work, as NIR emitters are useful in terms of many applications such as telecommunications and wound-healing.[62]

## 2.4 Conclusions

An $A_2B_2$ porphyrin was synthesised that may be copolymerised with appropriate copolymers to create a polymer with a heavy metal incorporated into a covalently bound portion of the polymer backbone. This has the advantage over blend systems of standardising the distance between porphyrin and polymer, as well as discouraging phase separation and aggregation of porphyrin. **MPP(Pt)** was incorporated into two polymeric systems.

The first polymer series synthesised was **PF MPP(Pt)**. This polymer was synthesised with the aim of increasing internal quantum efficiency by utilising triplet states formed on the polymer backbone through charge injection. This was achieved through energy transfer to the porphyrin moiety (singlets and triplets), where the lowest lying triplet state is populated as higher lying singlets may undergo ISC facilitated by the heavy metal centre. Phosphorescence is then observed. Pure electrophosphorescence is observed for loading of porphyrin of 2% and above.

A second series of diphenylanthracene based polymers was also synthesised with **MPP(Pt)** incorporated in various weight percentages. The initial aim of this synthesis was to create a TTA capable system where low energy triplet excitons would transfer from the porphyrin to the polymer backbone and undergo upconversion. This aim was not successful however, possibly due to TTET not occurring from porphyrin to polymer. By modifying the structure of porphyrin and/or diphenylanthracene monomers, it may be possible to enable TTET in a similar system in the future. The resultant polymer series from this work did show interesting characteristics however, namely an aggregation-induced red shift of emission. The highly aggregating nature of anthracene allowed the formation of an emissive excimer (or possibly exciplex) that is present in polymers with and without porphyrin comonomer. In the porphyrin containing polymers, this red shift results in NIR emitting polymers. Since aggregation is normally associated with loss mechanisms, this type of emission is not well studied in the literature.

# Chapter 3: Low Energy Triplet Formation for TTA Polymers: Extended Porphyrins

## 3.1 Introduction

In the previous chapter, an $A_2B_2$ porphyrin was synthesised and copolymerised to form semiconducting polymers that utilise triplet states. In order to apply this technique to multiple systems, the energy levels of interest on the porphyrin need to be tuneable so as to match any polymer it is copolymerised with. By creating a larger, more conjugated porphyrin, more of the solar spectrum may be absorbed and therefore more polymers may be applicable hosts for TTA applications. This chapter will focus on work towards extended copolymerisable porphyrins that have red shifted $S_1$ and $T_1$ compared to **MPP(Pt)**, with the ultimate aim of the creation of a polymer capable of TTA (thus low energy photons are converted into useful voltages).

One way of extending the conjugated system of porphyrins is through the addition of phenyl groups at the β positions.[10] $A_4$ porphyrins may be synthesised from 1-nitrocyclohexene through 4,5,6,7-tetrahydroisoindole, however this added synthetic complexity is difficult to realise in polymerisable porphyrins. An $A_4$ β-extended porphyrin has been synthesised to be used as a dopant in a blend system, but its application is beyond the scope of this body of work.[87]

As detailed in chapter 2, $A_2B_2$ porphyrins may be incorporated covalently into a polymer backbone. Extended $A_2B_2$ porphyrins have been previously reported as part of a larger polymeric or macrocyclic system. Polyfluorene-*co*-5,15-bis((phenyl)ethynyl)-10,20-dimesitylporphyrinato platinum(II) (**PF PEMP(Pt)**) is an analogous polymer to **PF MPP(Pt)**. ***Figure 3.1.1*** shows how an alkynyl spacer unit between the porphyrin and phenyl moieties can be advantageous in terms of charge transport.

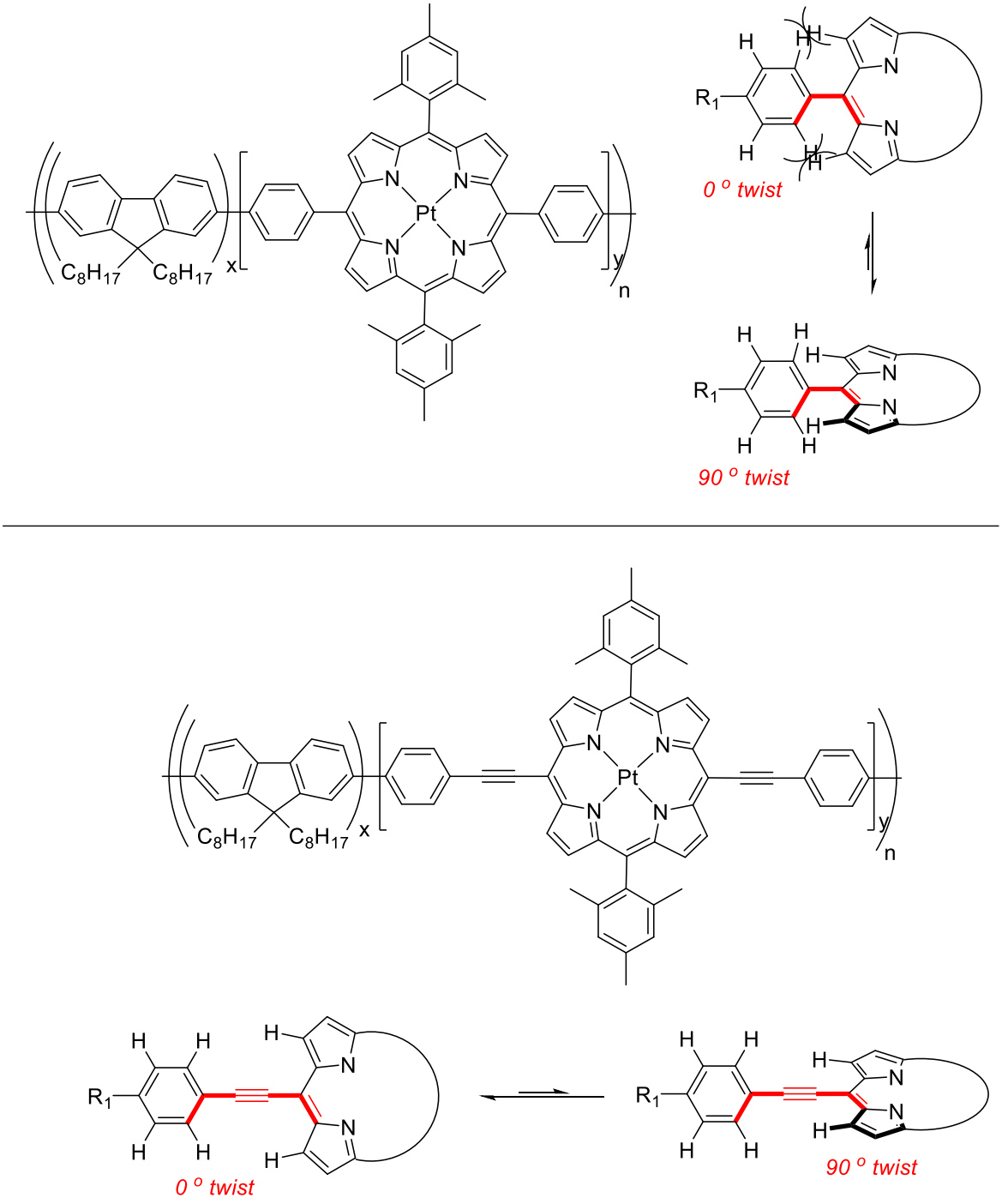


***Figure 3.1.1:*** *Alkynyl spacer unit effect on backbone twisting. Non-planarity of biaryl bond is a problem as conjugation is effectively broken, localising HOMO and LUMO to porphyrin/ flourene and therefore reducing mobility and energy transfer. Addition of alkyne spacer reduces the steric clash of phenyl hydrogens and restores planarity, resulting in greater charge transport, lower energy levels and red-shifted emission.*

In the case of **PF MPP(Pt)**, multiple biaryl bonds are present. Twisting in the polymer backbone reduces charge carrier mobility by limiting conjugation and localising the HOMO and LUMO to specific parts of the polymer as opposed to a large delocalised system across the whole molecule.[88] The twist angle of a biphenyl unit has been computationally shown to be around 42.5°.[89] A much larger effect is seen at the porphyrin-phenyl link however, where typical twist angles are generally above 55°.[90] Because of this larger twist, the first modification of the **PF MPP(Pt)** polymer to be considered was one in which the aryl-porphyrin bond becomes more in plane; an alkynyl extended porphyrin. The planar structure of **PF MPP(Pt)** results in a steric clash between adjacent hydrogen atoms on the pyrrolic positions of the porphyrin and ortho positions of the adjacent phenyl group. In the alkyne extended porphyrin polymer, **PF PEMP(Pt)**, the same hydrogen atoms are spaced out enough to allow the molecule to lay flat and conserve conjugation.

Anderson *et al.* have published multiple interesting and impressive structures that use such a porphyrin to form macrocyclic rings, an example is shown in ***Figure 3.1.2***.[91-93]

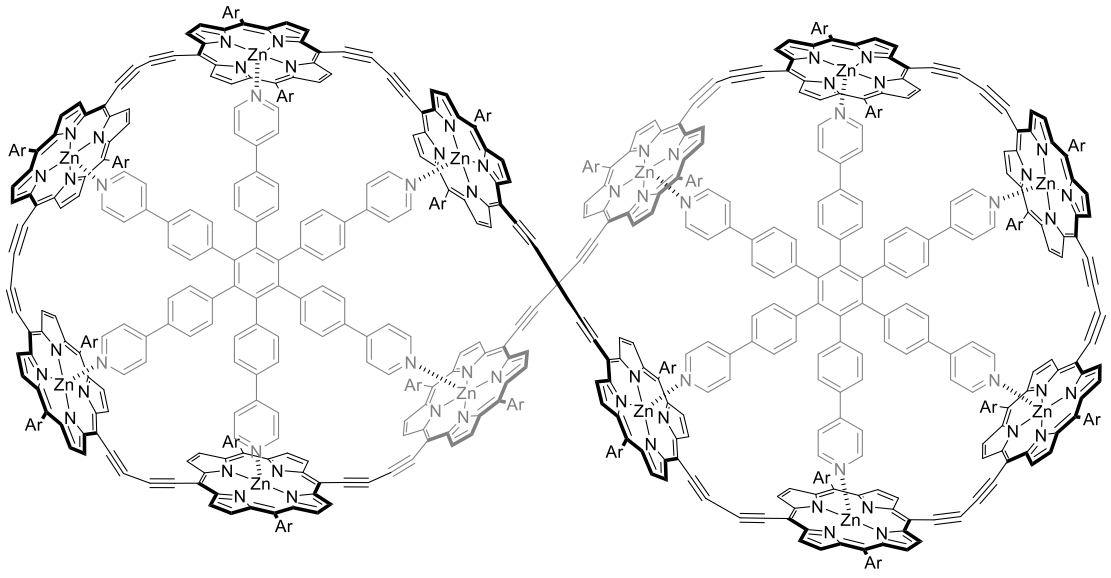

***Figure 3.1.2:*** *12-membered porphyrin macrocycle. Ar = 3,5-tertiarybutylphenyl.*[91]

Linear polymers have also been synthesised using a similarly designed porphyrin. Harvey *et al.* have successfully synthesised polymers containing an alkyne extended porphyrin, ***Figure 3.1.3***.[94-96]

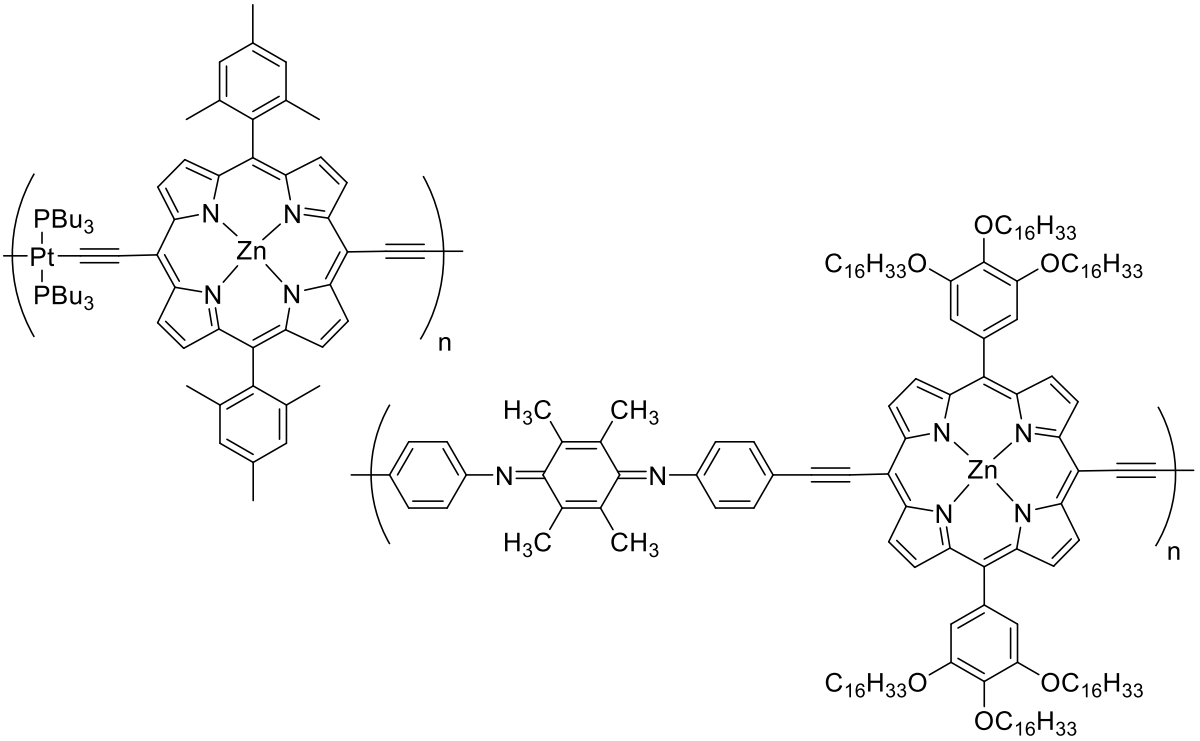


***Figure 3.1.3:*** *Examples of alkyne extended porphyrins in linear conjugated polymers.*[95-96]

The majority of this work focusses on the installation of alkynyl spacer units to the *meso* position of a porphyrin. This proved to be a challenging task and resulted in the development of several different routes before a successful one was found. Physical testing of the resultant polymer from this work is ongoing. This chapter therefore deals with only the synthesis of the polymer and does not go into detail about possible applications and physical processes of the electronically excited polymer.

## 3.2 Synthesis of Extended Porphyrins

The first proposed route to **PEMP** is shown in ***Scheme 3.2.2*** and is analogous to the successful route to **MPP** in chapter 2. The synthesis of the required aldehyde, 3-(4-bromophenyl)propiolaldehyde **3.2.3**, is shown in ***Scheme 3.2.1***. Propargyl alcohol **3.2.1** was initially subjected to Sonogashira conditions in the presence of 1-bromo-4-iodobenzene and the alcoholic product **3.2.2** was subsequently oxidised to the aldehyde using TEMPO and $PhI(OAc)_2$. 3-(4-bromophenyl)propiolaldehyde **3.2.3** was obtained in 53% yield over two steps.

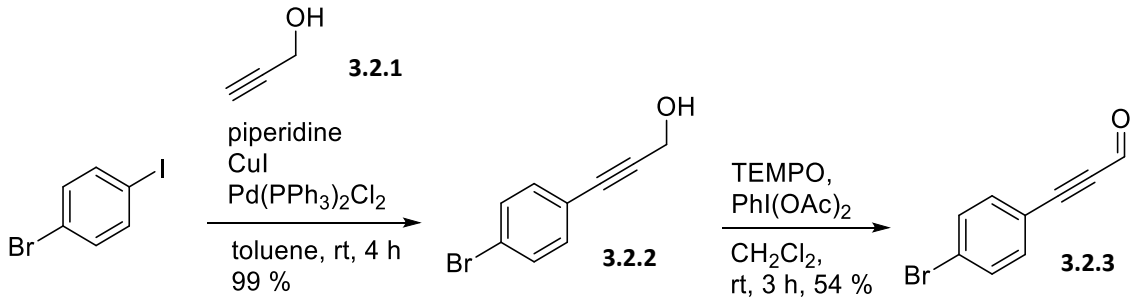


***Scheme 3.2.1:*** *Synthesis of 3-(4-bromophenyl)propiolaldehyde* ***3.2.3****.*

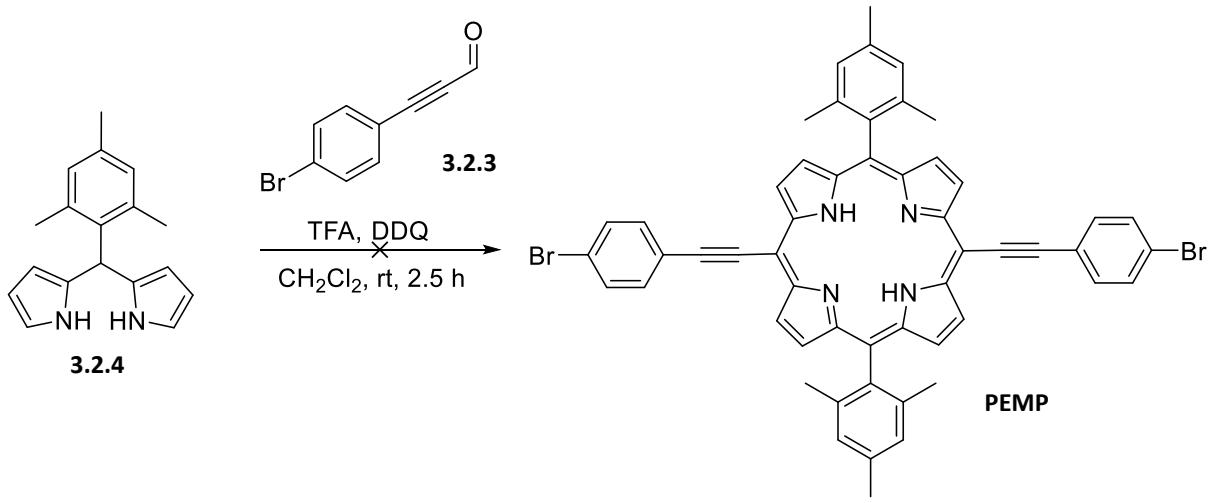


***Scheme 3.2.2:*** *Attempted synthesis of* ***PEMP****.*

The reaction of 3-(4-bromophenyl)propiolaldehyde **3.2.3** with mesityldipyrromethane **3.2.4** to form **PEMP**, ***Scheme 3.2.2***, was then attempted using analogous conditions to the reaction to form **MPP**. $^1$H NMR of the obtained green solid showed a mixture of porphyrins had formed, shown by multiple pyrrolic proton peaks. This is an indication of scrambling in which a pyrrole moiety is inverted during the macrocycle formation, effectively swapping the positions of the *meso* substituents.[36] Separation of the various porphyrins is not facile and this route was

abandoned in favour of an alternative in which the alkyne units are installed onto a pre-existing porphyrin, thereby removing the possibility of scrambling.

***Figure 3.2.1*** shows a reterosynthesis of 5,15-bis((5-bromo-3-hexylthiophen-2-yl)ethynyl)-10,20-dimesitylporphyrinato platinum (II) (**TEMP(Pt)**). By first synthesising dibromo porphyrin **3.2.5***,* a Sonogashira reaction may then be performed with 2-ethynyl-3-hexylthiophene **3.2.6** to create a new C-C bond from the porphyrin to an alkyne. Platinum complexation of the porphyrin and bromination of the thiophene moieties would then result in **TEMP(Pt)**.

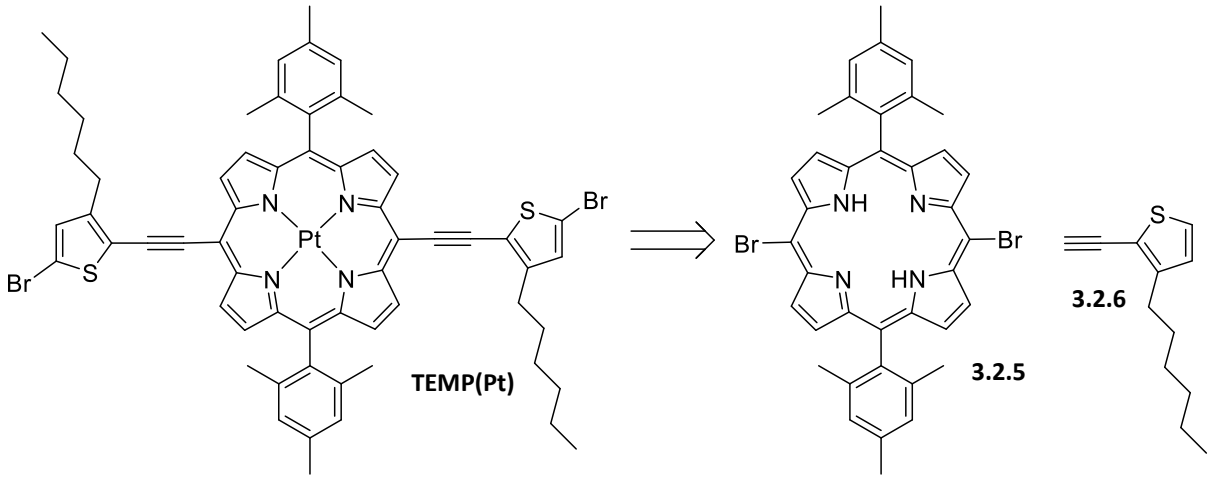


***Figure 3.2.1:*** *Reterosynthesis of* ***TEMP(Pt)****.*

The substitution of thiophene for phenyl of the target molecule from **PEMP(Pt)** to **TEMP(Pt)** was made in an effort to further flatten (increase conjugation) the porphyrin moiety of the resultant polymer. As mentioned above, phenyl linkages cause a twist in the polymer chain which lessens conjugation and charge carrier motilities. Thiophene links are much more planar and so are expected to perform better as semiconducting polymers.[97] It is also fairly facile to synthesise thiophene units with alkyl chains, increasing solubility. A third advantage lies in the final bromination step which may be performed under more mild conditions with thiophene units. By brominating the porphyrin after platinum complexation, there is no chance that during the complexation reaction the platinum will oxidatively insert into the porphyrin-bromine bond. This has been shown to occur to a small degree in various systems and lowers the yield of the final step in the synthesis as well as creating potential defects in the final device.[98]

To synthesise dibromo porphyrin **3.2.5**, dipyrromethane **3.2.7** was reacted with mesitaldehyde, ***Scheme 3.2.3***. This reaction was unsuccessful and did not yield any of the desired product, dimesityl porphyrin **3.2.8**. Crude $^{1}$H NMR of the reaction mixture did show some porphyrin formation however purification was challenging due to its low solubility. To overcome the problems associated with dimesityl porphyrin **3.2.8** insolubility, an alternative porphyrin was synthesised with more solubilising $^{t}$Bu groups.

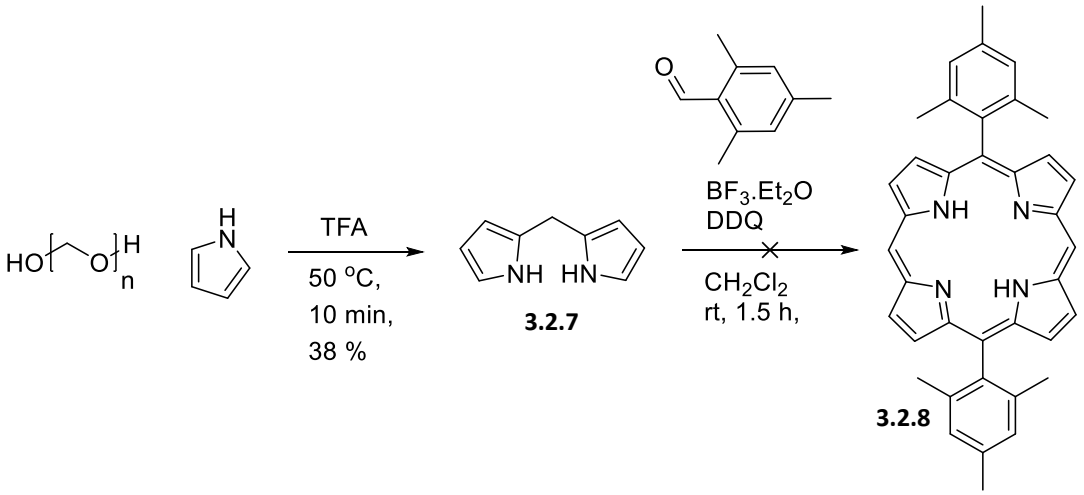


***Scheme 3.2.3:*** *Failed synthesis of dimesityl porphyrin **3.2.8**.*

By substituting bulky $^{t}$Bu groups, porphyrin **3.2.10** was predicted to be more soluble than dimesityl porphyrin **3.2.8**. It was synthesised in a convergent manner from dipyrromethane **3.2.7** and di-tertbutylbenzaldehyde **3.2.9**. This reaction was successful and yielded the desired porphyrin product **3.2.10** in 64% yield.

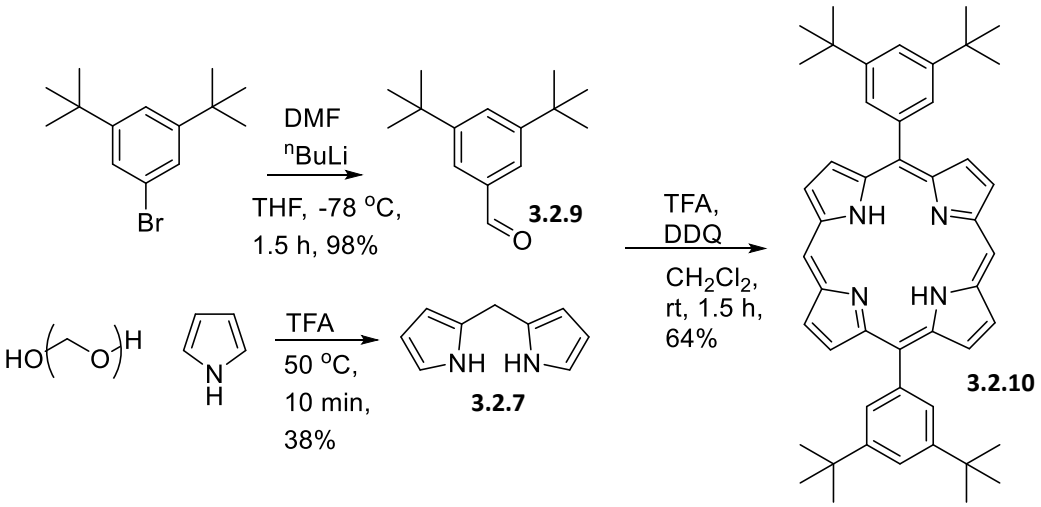


***Scheme 3.2.4:*** *Convergent synthesis to di-bistertbutylphenyl porphyin **3.2.10**.*

Bromination of porphyrin **3.2.10** proceeded as in ***Scheme 3.2.5*** and gave the product, dibromo porphyin **3.2.11** in 81% yield.

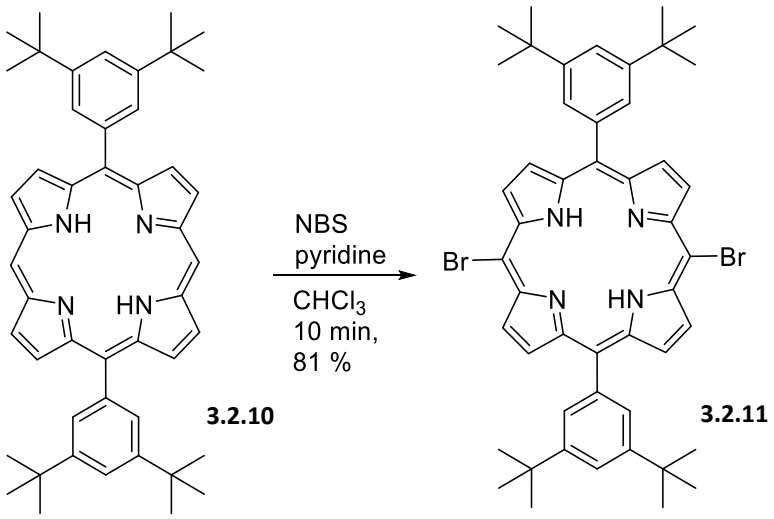


***Scheme 3.2.5:*** *Bromination of porphyin **3.2.10** to dibromo porphyin **3.2.11**.*

Synthesis of alkynyl thiophene **3.2.15** proceeded as in ***Scheme 3.2.6***. Bromination of hexylthiophene **3.2.12** with NBS was achieved with 70% yield and the subsequent Sonogashira reaction with ethynyltrimethylsilane gave TMS protected alkynylhexylthiophene **3.2.14** in 86% yield. Deprotection of the TMS group with base gave the desired alkynylhexylthiophene **3.2.15** in 68% yield, 41% yield over 3 steps from hexylthiophene **3.2.12**.

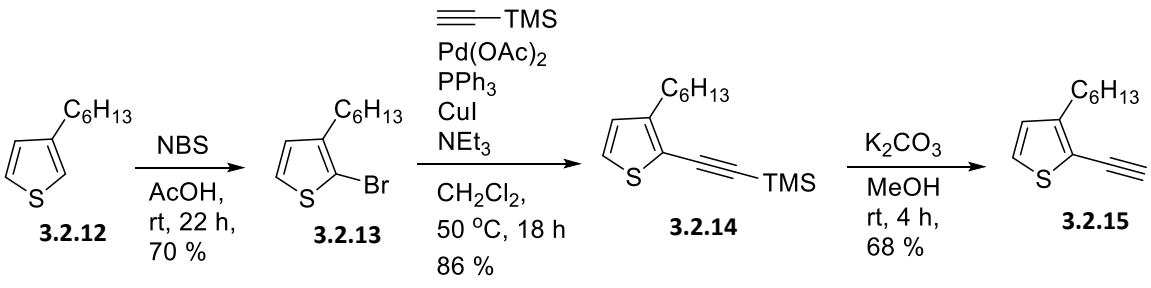


***Scheme 3.2.6:*** *Synthesis of alkynylhexylthiophene **3.2.15**.*

The Sonogashira coupling of dibromo porphyin **3.2.11** and alkynylhexylthiophene **3.2.16** was attempted as in ***Scheme 3.2.7***.

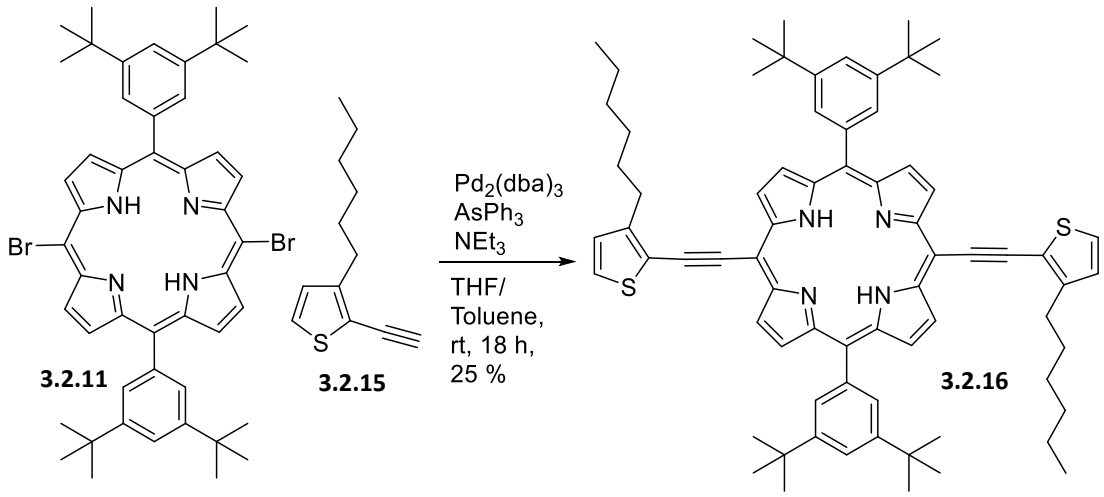


***Scheme 3.2.7:*** *Sonogashira coupling of dibromo porphyin* ***3.2.11*** *and alkynylhexylthiophene* ***3.2.15****.*

The Sonogahira reaction in ***Scheme 3.2.7*** was performed copper free to avoid complexation of the copper into the porphyrin. The reaction gave dithiophenyl porphyin **3.2.16** in 25% yield. It was then attempted to platinate porphyrin **3.2.16** before dibromonation and finally polymerisation. Only small amounts (<40 mg) of porphyrin **3.2.16** were available at this stage. It was expected however that all subsequent reactions should be fairly high yielding and clean. This was not the case; the platinum complexation reaction failed to give any purifiable product. Column chromatography was not possible due to the high $R_f$ of the porphyrin in $CHCl_3$ and its insolubility in less polar systems. Various solvent washes also proved ineffective. The route to thiophene alkynyl extended porphyrins was paused at this point.

A third route to an alkyne extended porphyrin was proposed. A series of Sonogashira reactions would build up the molecule from the porphyrin outwards in a more linear synthesis. For ease of synthesis and to help in the optimisation of the route, the thiophene units were substituted back to phenyl, so that the overall target of the synthesis was 5,15-bis((4-bromophenyl)ethynyl)-10,20-bis(3,5-di-tert-butylphenyl)porphyrin (**PEBPP**), ***Scheme 3.2.8***. Once the route had been shown to be successful, it could be repeated to form the more desirable thiophene analogue if necessary.

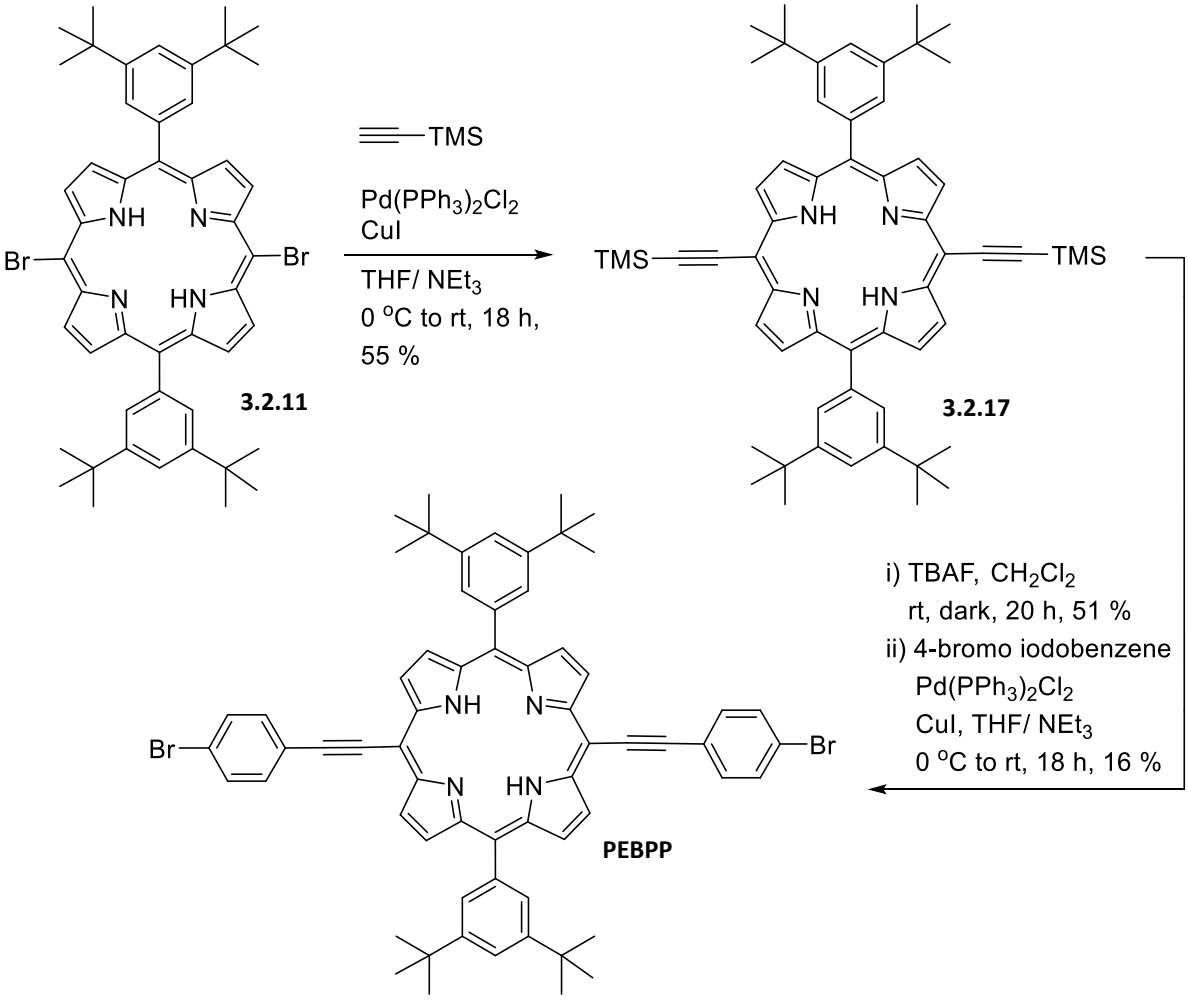


***Scheme 3.2.8:*** *Synthetic route from dibromo porphyrin* ***3.2.11*** *to* ***PEBPP****.*

Dibromo porphyrin **3.2.11** was subjected to Sonogashira coupling conditions in the presence of ethynyltrimethylsilane, ***Scheme 3.2.8***. Copper free conditions were not used for this reaction due to the previously poor yields obtained in the coupling reaction of ***Scheme 3.2.7***. It was found that any copper complexed side product could easily be removed with careful column chromatography and affected the yield in a small enough way so as to be preferable to the copper free alternative. The reaction of porphyrin **3.2.11** to **3.2.17** proceeded in 55% yield. Deprotection of the TMS protecting groups and a second Sonogashira reaction, again using CuI, gave **PEBPP** in a yield of 51% and 16% respectively. Both yields were disappointing, however enough product was isolated to attempt an optimistic platinum complexation, ***Scheme 3.2.9***. With hindsight, it is apparent that the Sonogashira conditions for the second coupling reaction were poorly chosen. The conditions worked well for the first coupling on the relatively electron rich bromoporphyrin and so were used subsequently for the second, more electron poor coupling. It is thought that the poor yield of this coupling may be increased by

changing the conditions, perhaps to those used in ***Scheme 3.2.7***, although this was never trialled.[99]

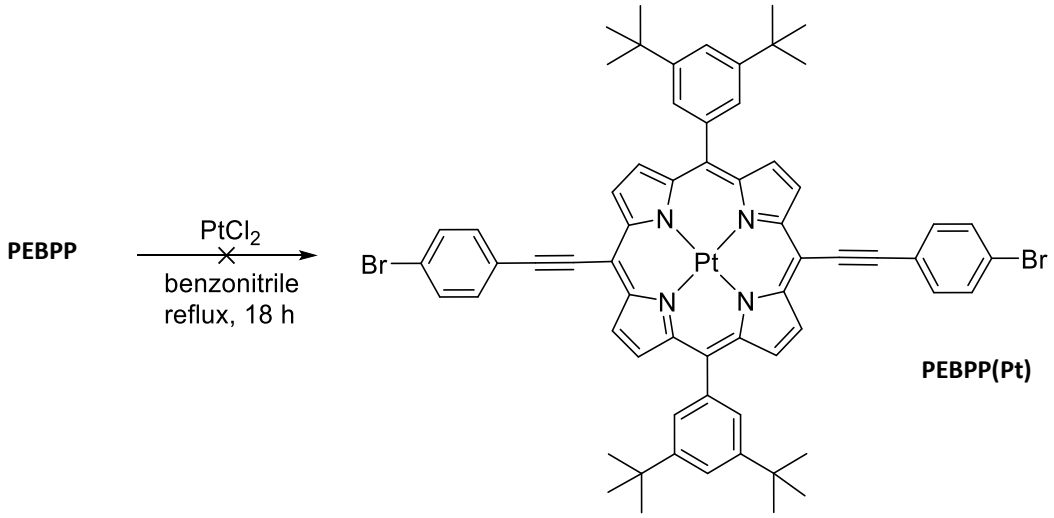


***Scheme 3.2.9:*** *Failed attempt at a platinum complexation of* ***PEBPP****.*

As previously, the platinum complexation reaction did not give any product and consumed all starting material. This reaction was performed on a very small scale and again there were challenges involved with purifying the compound. This reaction and route was abandoned. It was thought that the problems associated with platinum complexation could be solvable with higher heating temperatures (*ie*. more forcing conditions). Separate work conducted within the group has shown that temperature can have a large effect on these reactions. It was also considered that the platinum starting material could be interacting with the alkyne, resulting in several products.

The successful synthesis of **PEBPP** was very encouraging, despite the low quantities obtained. It was planned that the 7-step synthesis would therefore have been attempted a second time, with a concentrated effort on maintaining good yields to provide enough **PEBPP** for a hopefully successful platinum complexation reaction with alternative conditions or possibly an alternative metal halide starting material. A more efficient alternative presented itself however. A newly published paper by Nowak-Król *et al* showed a modified Lindsey procedure for the formation of trans $A_2B_2$ porphyrins from alkynyl aldehydes that had dramatically reduced scrambling.[100] By performing the acid catalysed porphyrinogen formation step in a non-ideal solvent (THF with $H_2O$), the starting aldehyde and dipyrromethane are soluble enough to remain in solution and react while the porphyrinogen is insoluble and forms a

suspension, reducing the likelihood of scrambling. The acid is then removed before the porphyrinogen is oxidised to a porphyrin with DDQ (or another suitable oxidant).

Using this method, **PEMP** was successfully synthesised directly from 4-bromobenzylalkynylaldehyde **3.2.3** and mesityldipyrromethane **3.2.4**, ***Scheme 3.2.10***. The yield was very low (1% isolated yeild), however this is thought to be caused by the purification technique used (long silica column rather than short silica plug) rather than an inherent result of the reaction. Enough product was obtained to attempt a series of different metalation complexation reactions. ***Table 3.2.1*** summarises the results of the metal complexation experiments.

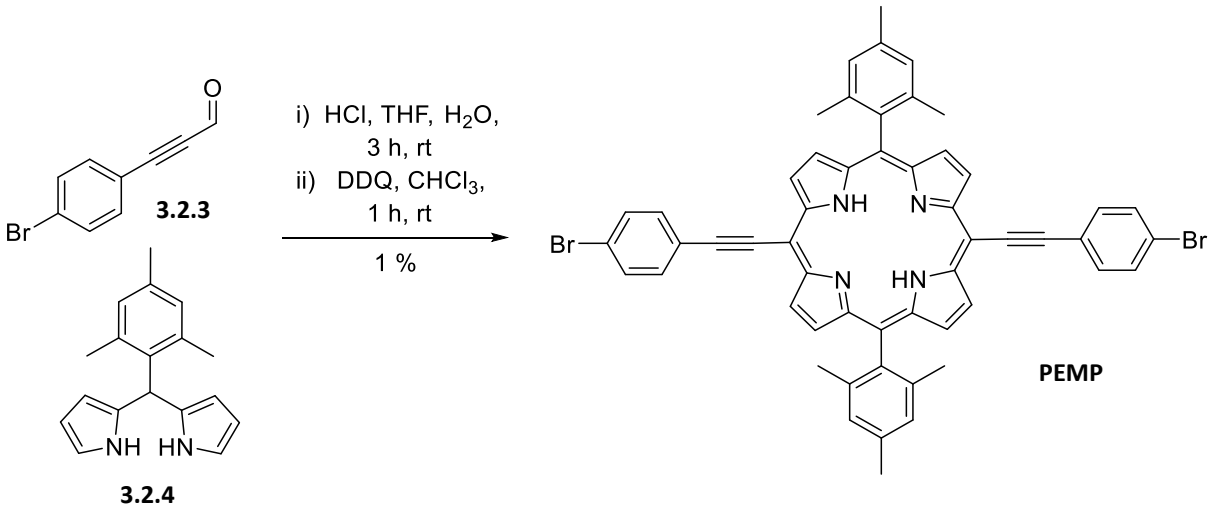


***Scheme 3.2.10:*** *Successful direct synthesis of **PEMP** based on the work of Nowak-Król* et al.[100]

| **Metalation reagent** | **Solvent** | **Temperature / °C** | **Time / h** | **Result** |
|---|---|---|---|---|
| **$PtCl_2$** | Benzonitrile | 220 | 18 | Starting material destroyed |
| **$Pd(OAc)_2$** | $CHCl_3$ | 40 | 72 | No reaction |
| **$Pd(OAc)_2$** | Chlorobenzene | 100 | 72 | Starting material destroyed |
| **$Zn(OAc)_2$** | $CH_2Cl_2$ | 25 | 7 | No reaction |

***Table 3.2.1:*** *Metalation attempts on **PEMP**.*

The same conditions that were used to insert Pt(II) into **MPP(Pt)** were first trialled. It was found that this resulted in a complicated mixture of aromatic compounds. Platinum is the most common metal to be inserted for greatest inter system crossing potential in porphyrins

but is expensive as a reagent. Palladium has relatively similar properties to platinum in terms of its reactivity photophysics in complexes and, while similar in price, is more abundant and allows us to explore different reaction conditions for metalation. If a set of conditions could be found that successfully inserted palladium into the porphyrin in good yield then these conditions could also be used with platinum. This would then give two porphyrins with good intersystem crossing potentials that may be compared.

Using $Pd(OAc)_2$ in 40 °C chloroform failed to affect the porphyrin in any way and starting material was returned. When the solvent was changed to chlorobenzene so that the temperature may be increased to 100 °C, a similar complex mixture of aromatic products was observed to the initial platinum experiment.

The results of these experiments seemed to suggest that interaction with the alkyne moiety of **PEMP** was faster than metal insertion; both metals are known to react with alkyne units.[101] Zinc does not interact with alkynes in the same way and, although much lighter than platinum and palladium, is capable of promoting intersystem crossing.[102] The reaction with Zinc acetate did not give any product by NMR however, and returned starting material unreacted.

To overcome the problems associated with metalation, the order in which the individual reactions of the basic route were performed was changed. Metallation is usually performed at the end of a synthetic route as the reagents are often expensive. However by inserting the metal before the alkynyl units, it was hypothesised that the issues highlighted above may be avoided. As the route was being changed we also changed the target porphyrin so as to increase solubility which had been an additional challenge to experiment design and the acquirement of NMRs.

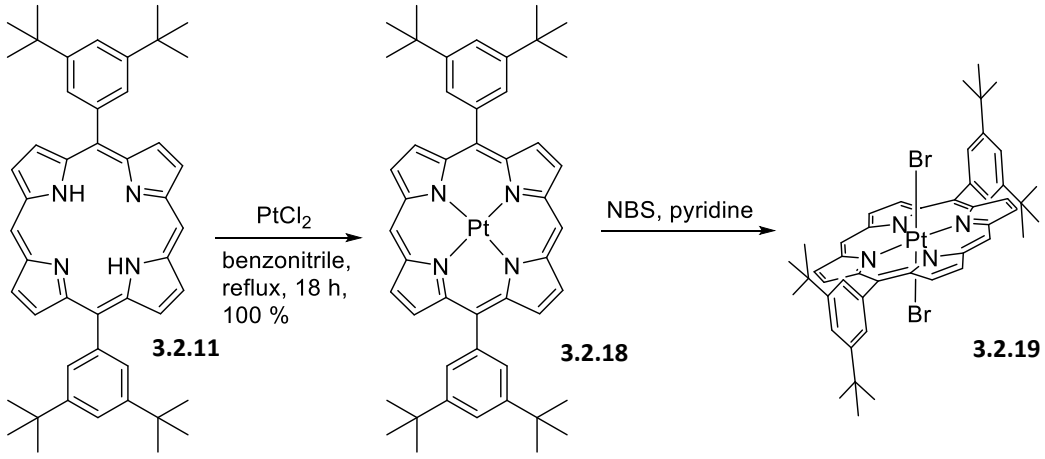


***Scheme 3.2.11:*** *Early metal insertion and subsequent bromination leading to undesired Pt(IV) complex* ***3.2.19****.*

Pt(II) was first inserted into porphyrin **3.2.11** using standard metal insertion conditions and proceeded in excellent yield to yield Pt(II) porphyrin **3.2.18**. The normal bromination conditions however resulted in an interesting Pt(IV) complex **3.2.19**, rather than the expected *meso* brominated porphyrin. Evidence for the formation of this structure is shown in ***Figure 3.2.2***. While the structure was not fully identified (it was clearly not the desired product), the $^{1}$H NMR and mass spec data together show that 2 bromides have been added and that the *meso* protons remain unreacted. This reaction was interesting from a purely scientific view, however it was also problematic as it showed that any bromination reaction (at least one which uses these conditions) after platinum insertion would not give the previously expected product. *Meso* bromination was trialled on Pt(IV) porphyrin **3.2.19**, but was unsuccessful.

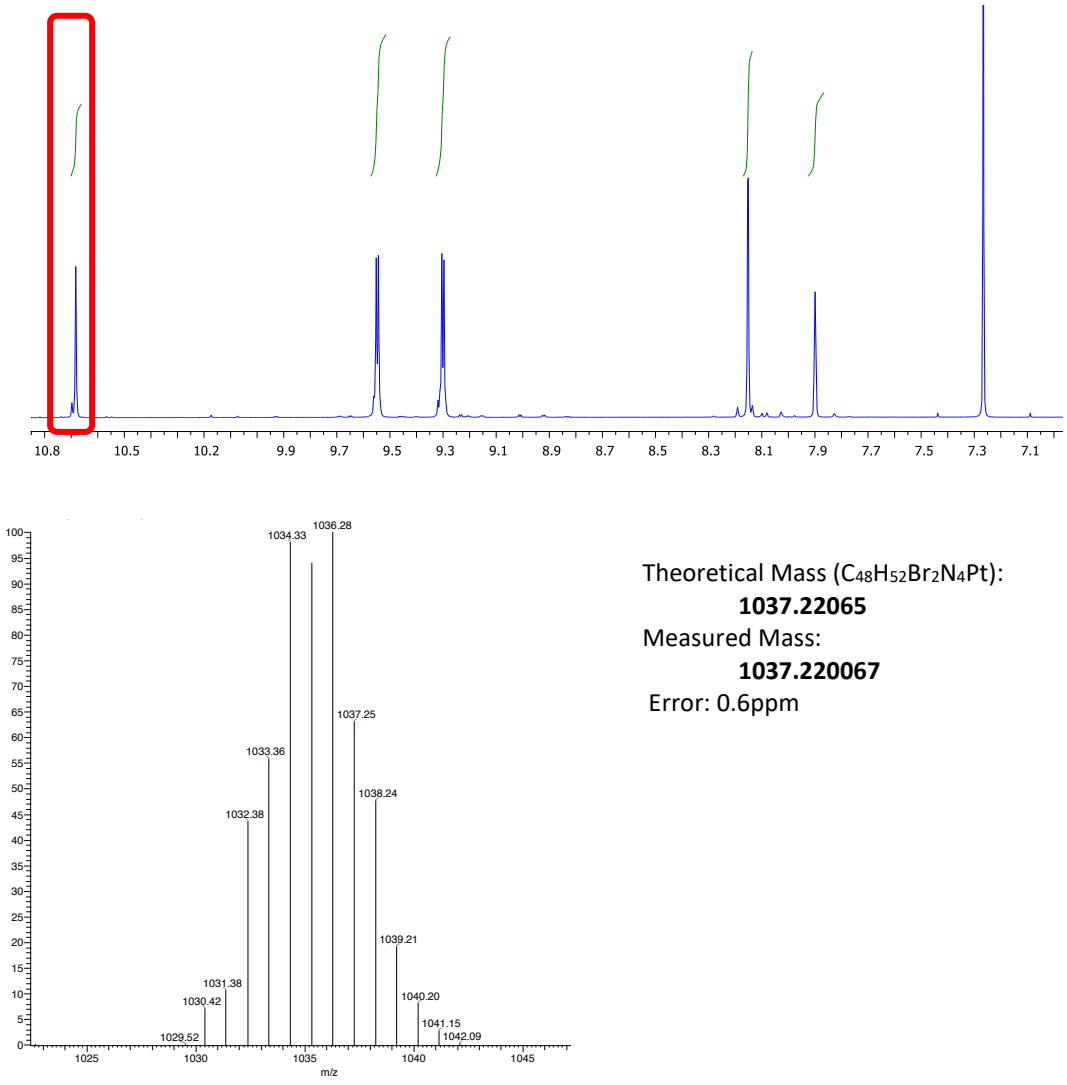


***Figure 3.2.2:*** *Aromatic region $^{1}$H NMR (top) and EI mass spec (bottom left splitting pattern and bottom right numerical data) of Pt(IV) porphyrin* ***3.2.19****.* Meso *protons (red box) are visible in the NMR spectrum but the parent ion found in the mass spectrum shows a weight and splitting pattern of a dibrominated product.*

As discussed briefly above, zinc could solve the potential problems of the metal centre interacting with other reactions as it is less reactive than platinum and palladium and still promotes intersystem crossing. A more soluble porphyrin with incorporated long alkyl chains would also be helpful in terms of synthetic ease and to discourage aggregation in any resultant polymer. The target molecule was therefore switched to a zinc(II) complexed and long-chain alkylated porphyrin.

From the above failed syntheses of an alkyne extended porphyrinato metal complex, we may propose some rules that must be followed for a route to be successful. From ***Scheme 3.2.2***, we infer that an alkynyl aldehyde is unsuitable as it promotes scrambling of the porphyrinogen intermediate. ***Scheme 3.2.3*** and ***Scheme 3.2.4*** show how solubility is important in the initial formation of the porphyrin, as well as being a desirable property in terms of handling of the product as it moves through the route. From ***Table 3.2.1*** we know that the metal insertion conditions will degrade the alkynyl moiety, so the metal must be inserted before the alkyne units. ***Scheme 3.2.11*** however describes a problem with this approach, as Pt(II) is oxidised to Pt(IV) in the presence of NBS. We first set about creating a more soluble porphyrin, through the addition of long alkyl chains.

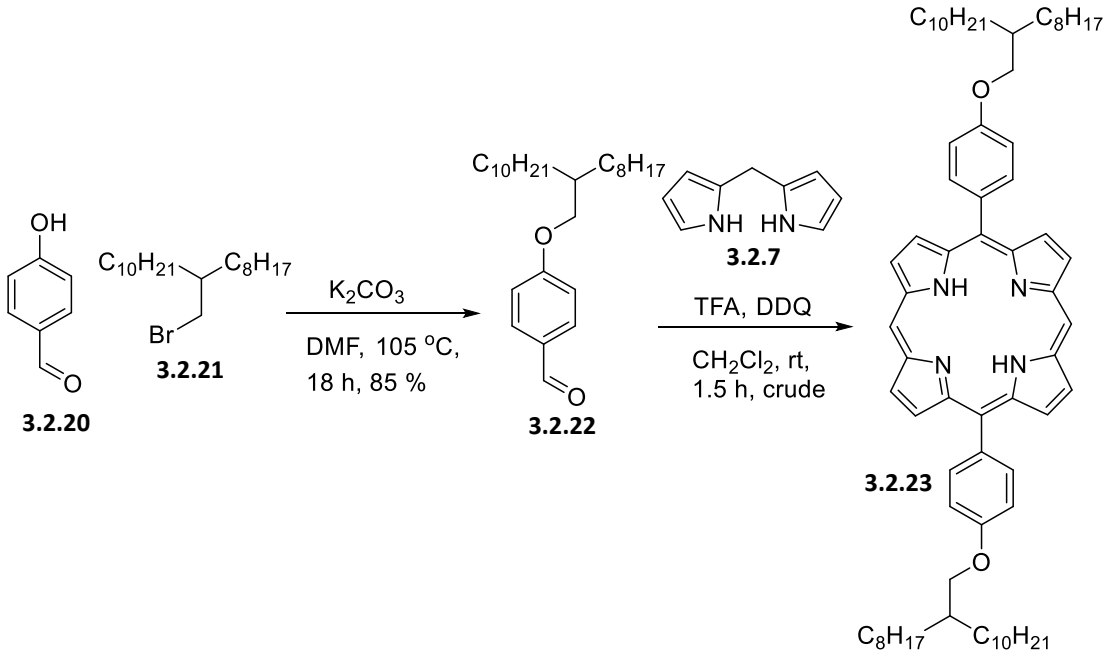


***Scheme 3.2.12:*** *synthetic route to long branched alkyl chain porphyrin* ***3.2.23****. The porphyrin was successfully synthesised in low yield as a complex mixture, but was not purifiable.*

The Lindsey method was again used to synthesise a branched alkyl porphyrin **3.2.23**. It was thought that this branched chain would greatly aid solubility and therefore drastically improve the ease with which these compounds may be handled. Crude $H^1$ NMR of the reaction mixture showed possible scrambling, however due to the increased solubility TLC was feasible with a low polarity solvent system and separated the products of this reaction. Column chromatography proved problematic however, as the products seemed to be only partially soluble in the required solvent systems, resulting in large loading volumes or, if dry loaded, large amounts of streaking. This particular branched alkyl chain system was abandoned.

Rather than a single branched alkyl chain, we then considered multiple straight chains. Trialkoxy benzaldehyde **3.2.25** was formed when 3,4,5-hydroxybenzaldehyde was trialkylated with dodecylbromide **3.2.24**, ***Scheme 3.2.13*** . Further reaction with dipyrromethane **3.2.7**, again using the Lindsey method, resulted in hexalkoxy porphyrin **3.2.26** that was purified by silica plug, ***Scheme 3.2.14***. No scrambling was observed.

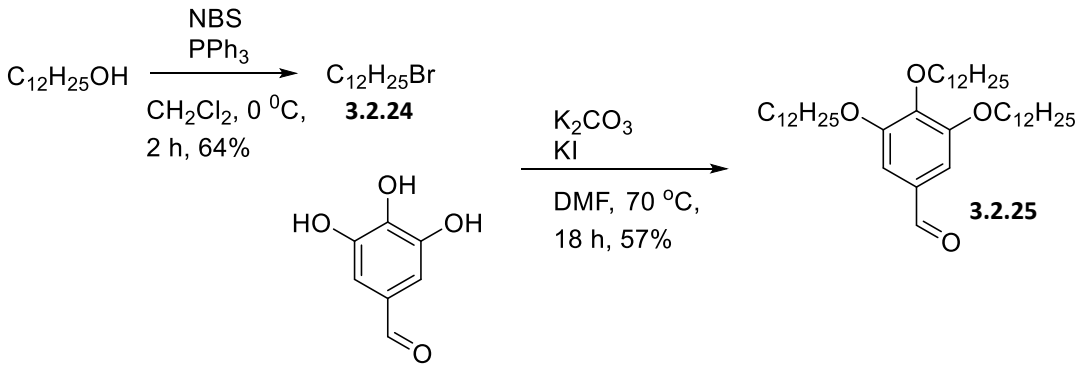


***Scheme 3.2.13:*** *Synthesis of trialkylated bezaldehyde.*

The addition of 6 dodecoxy chains resulted in a highly soluble porphyrin, and enabled column chromatography to be reliably employed throughout the synthesis. The porphyrin **3.2.26** was then brominated at the *meso* positions and zinc(II) was inserted into the complex to yield porphyrinato zinc(II) **3.2.27**. The problems surrounding platinum oxidation and transition metal interference with the alkyne moieties were thus avoided. Sonogashira coupling with trimethylsilylacetylene proceeded in good yield, no transmetalated copper complexed porphyrin was observed. Deprotection of porphyrinato zinc(II) **3.2.28** and a second Sonogashira reaction with 4-iodobromobenzene gave 6.5 mg of the final product, **HAPPAP(Zn)**. A UV-Vis absorbance spectrum is shown in ***Figure 3.2.3***.

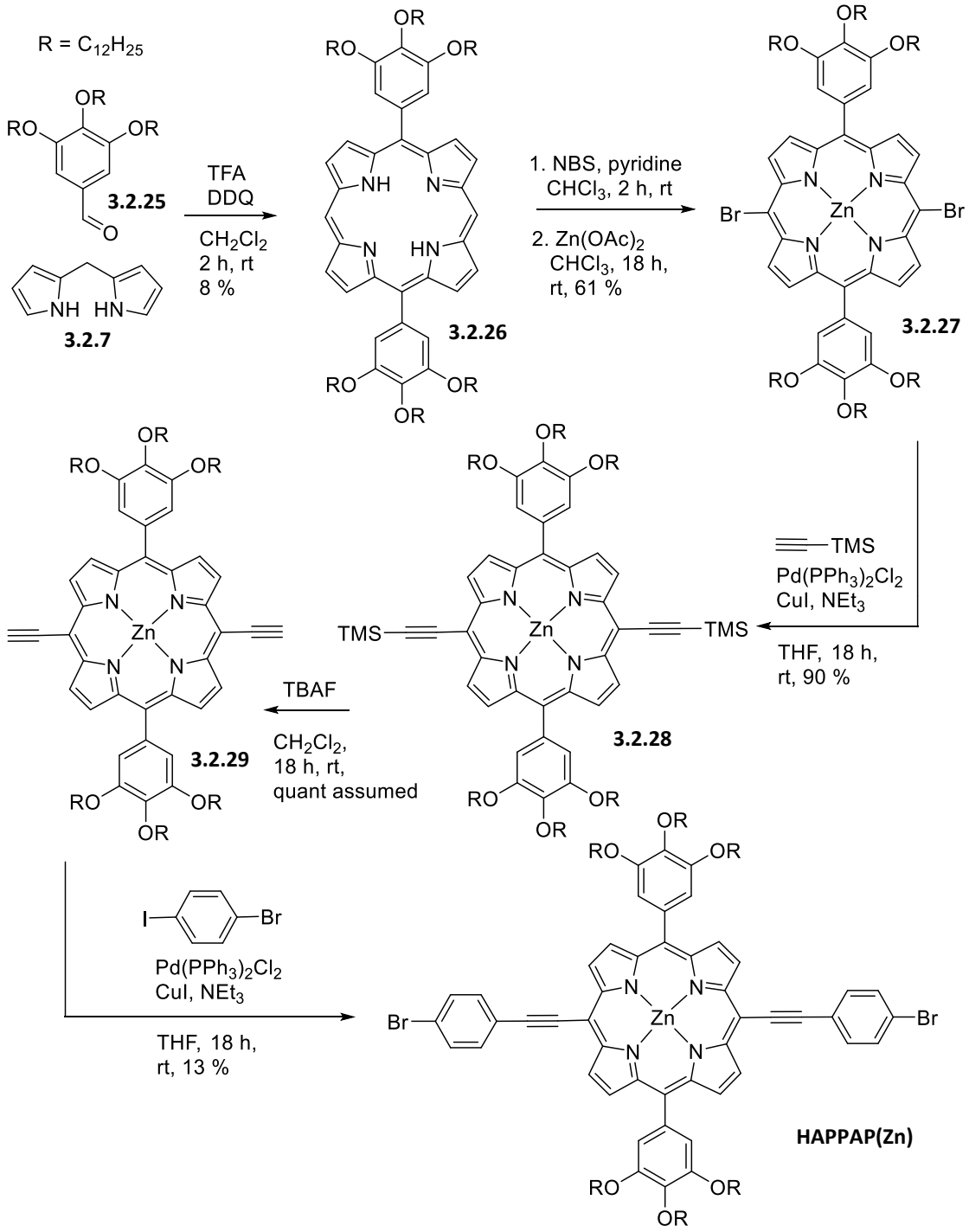


***Scheme 3.2.14:*** *Synthesis of* ***HAPPAP(Zn)****.*

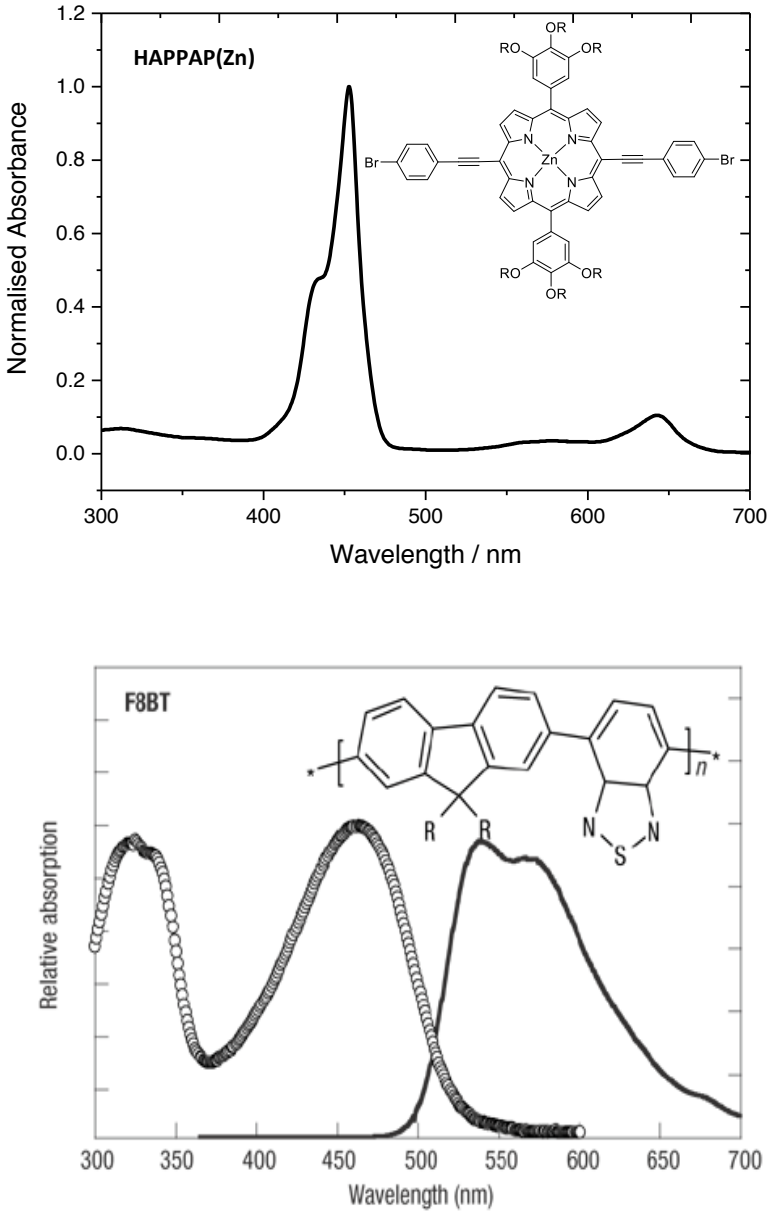


***Figure 3.2.3:*** *Absorbance spectrum of* ***HAPPAP(Zn)*** *(top) and absorbance (circles) and emission (solid) spectra of F8BT. F8BT data taken from Chappell* et al.[103]

For **HAPPAP(Zn)** to be successfully incorporated into a polymer and the system be capable of TTA upconversion the emission and absorbance profiles of both constituent parts must be compatible. The Q band of **HAPPAP(Zn)** is the lowest energy absorbance band of the system; photons with wavelength of 640 nm may be absorbed. For TTA upconversion to occur, the exciton formed from absorption of a 640 nm photon (initially a singlet that then undergoes ISC to a lower lying triplet state on the porphyrin) must be transferred to the polymer

backbone. Two triplet states close together in space on the polymer backbone may then undergo TTA and result in a single excited singlet state, ***Figure 3.2.3***. To stop this singlet state being reabsorbed by the porphyrin (*via* FRET), the emission profile of the polymer should lie in an area of the spectrum that **HAPPAP(Zn)** does not absorb in. In other words, we must choose a polymer that emits only in the area of the spectrum between the Soret and Q bands of **HAPPAP(Zn)** absorption. The emission spectrum of F8BT is also shown in ***Figure 3.2.3***.

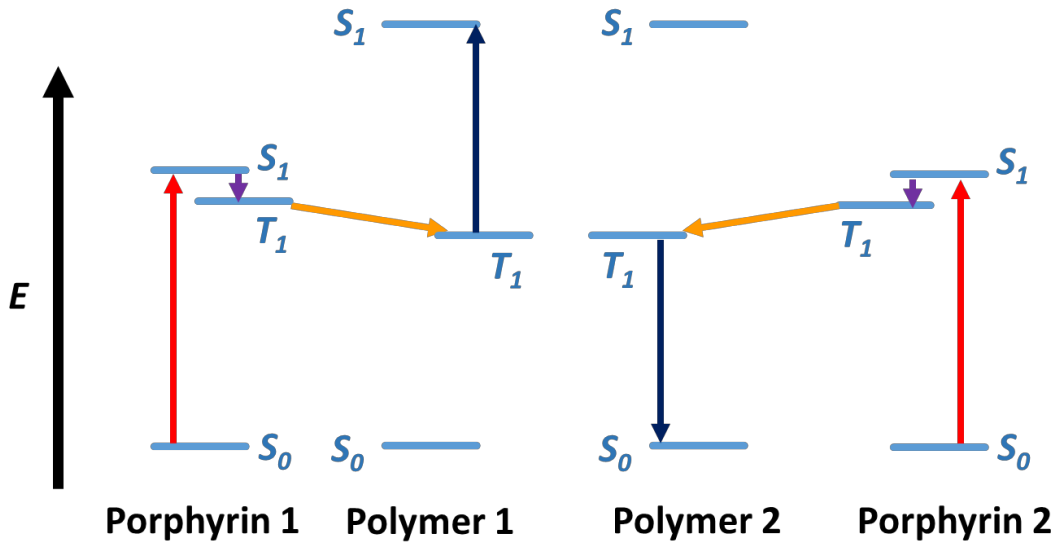


***Figure 3.2.3:*** *Jablonski diagram showing TTA upconversion. Low energy light is absorbed by the porphyrin units and the singlet exciton is converted to a lower energy triplet due to spin-orbit coupling of the metal centre. The excitons migrate to the polymer backbone and when two are in close proximity, they may undergo TTA upconversion to form one ground state and one higher energy singlet excited state.*

**HAPPAP(Zn)** was copolymerised in 5% w/w into a F8BT polymer backbone. This is shown in ***Scheme 3.2.15***.

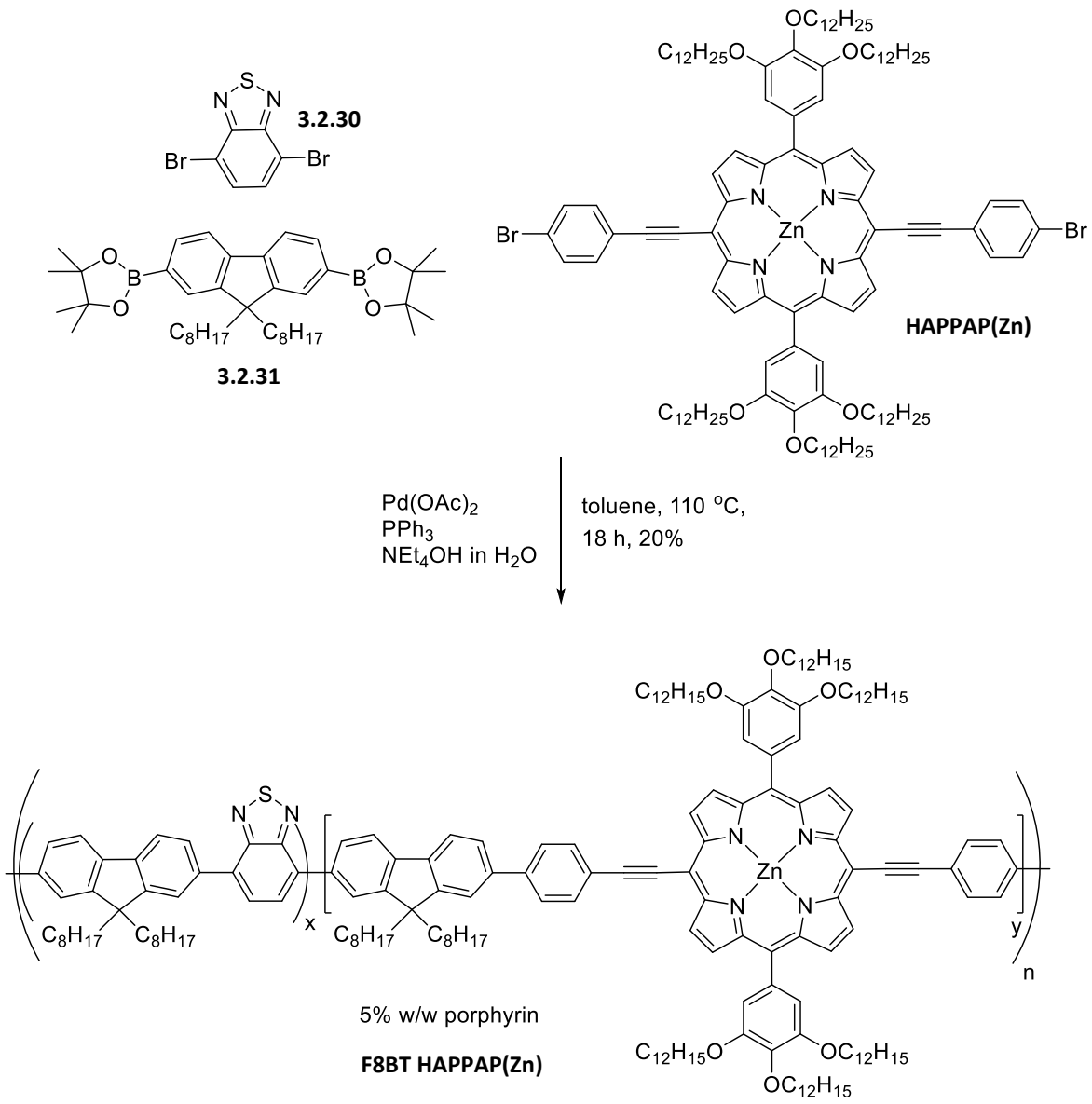


***Scheme 3.2.15:*** *Suzuki polymerisation to form* ***F8BT HAPPAP(Zn)****. Characterisation may be found in the supporting information.*

## 3.3 Conclusions

The synthetic route towards a polymerisable, π-extended porphyrin has undergone many iterations. Each time a route failed, lessons were learned that eventually resulted in the successful synthesis of **HAPPAP(Zn)**. ***Figure 3.3.1*** shows several of the porphyrins synthesised from several different routes.

***Scheme 3.2.2*** shows the first attempt at the synthesis of an alkyne extended porphyrin and is similar to the synthesis of **MPP(Pt)**. The Lindsey method of porphyrin synthesis was unsuccessful in this case, and resulted in porphyrin scrambling. This process is difficult to supress under these conditions and results in a mixture of porphyrins that are challenging to separate. Conditions that use $BF_3$ or no acid catalyst are available, but give low yields.[38] It was decided to synthesise the porphyrin before installing the alkynyl functionality.

Solubility was a known issue from the start. Mesityl groups at the eventual *meso* position of the porphyrin were included to address this; however, as is shown in ***Scheme 3.2.3***, the solubilising power of two mesityl groups is insufficient for these systems. At this point, the mesityl groups were simply switched for ditertiarybutylphenyl groups. At a later stage in the synthesis, the solubilising parts of the porphyrin were again changed to include three dodecoxy solubilising chains.

Work then progressed towards dithiophenyl porphyrin **3.2.16** and diphenyl porphyrin **PEBPP**. Dithiophenyl porphyrin **3.2.16** was synthesised by a convergent synthesis of dibromo porphyrin **3.2.11** and alkynylthiophene **3.2.15**, ***Scheme 3.2.7***. Attempts to palatinate this porphyrin were unsuccessful, and destroyed the starting material. **PEBPP** was synthesised *via* Sonogashira reactions on dibromo porphyrin **3.2.11** to build up functionality from the core unit. Platination was again unsuccessful however.

The work of Nowak-Król *et al.* afforded an expeditious route to **PEMP**, ***Scheme 3.2.10***.[100] This was a very low yielding reaction but gave a reliable source of *trans*-$A_2B_2$ alkynyl porphyrin to test metalation reactions that had caused the previous two routes to fail. ***Table 3.2.1*** describes these experiments. It was learnt from this that under the conditions required to insert Pt(II) into the porphyrin, the metal was interacting with the alkynyl moieties and destroying the porphyrin. Work therefore progressed to a route that installs the metal centre at an earlier point.

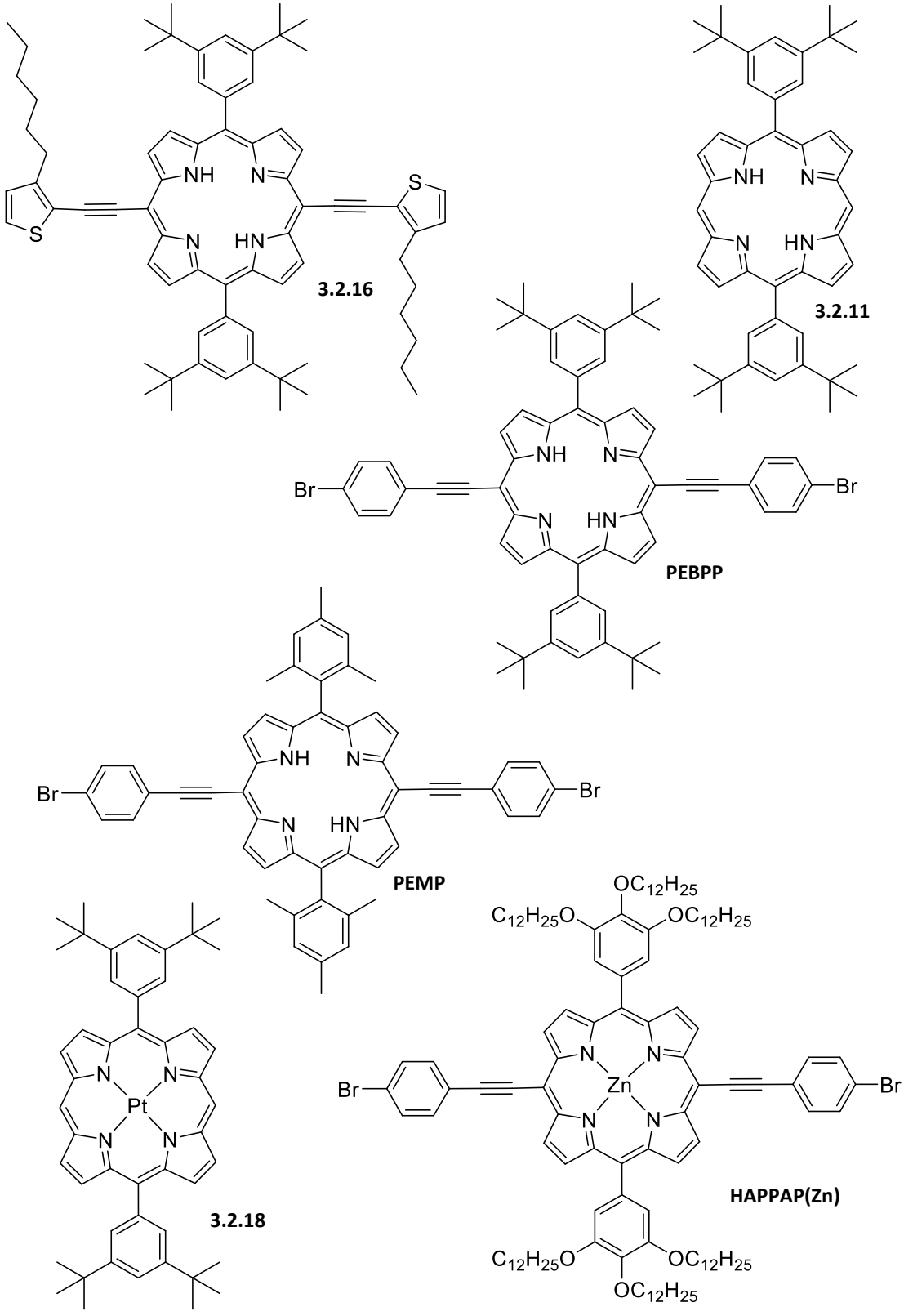


***Figure 3.3.1:*** *Selection of porphyrins synthesised and isolated.*

Pt(II) coordinated porphyrin **3.2.18** was prepared by reaction of $PtCl_2$ and porphyrin **3.2.11**, ***Scheme 3.2.11***. *Meso* bromination using NBS was attempted, but resulted only in bromination of the platinum centre (Pt(II) oxidised to Pt(IV)). This result was not anticipated or desired, but is perhaps interesting from a scientific point of view.

From these unsuccessful routes, four 'rules' may be specified; the aldehyde in the initial porphyrin synthesis cannot be alkyne **3.2.3**; the porphyrin must contain sufficiently solubilising moieties; platinum (and palladium) insertion is not possible on alkyne containing porphyrins; Pt(II) is oxidised to Pt(IV) under standard *meso* bromination conditions. With these rules in mind, a new route was proposed, ***Scheme 3.2.14***. Alkyne units were installed after porphyrin formation to avoid scrambling, and six dodecoxy chains are present on the porphyrin which impart solubility to the system. The problems surrounding platinum insertion and metal-coordinated porphyrin bromination were mitigated by changing the metal to zinc. **HAPPAP(Zn)** was prepared by this route and was successfully copolymerised with F8BT monomers to create a polymer with 5% w/w alkyne-extended porphyrin bound covalently in the main polymer backbone.

**F8BT HAPPAP(Zn) 5** is currently undergoing physical testing. Some interesting results have been obtained, however this is not yet complete and beyond the scope of this body of work.

# Chapter 4: Reducing the Singlet-Triplet Energy Gap: Donor-Orthogonal Acceptor Polymers

## 4.1 Introduction

Fluorene is well known as a monomer in many polymeric systems, as shown in previous chapters. Spirobifluorenes, as they contain a fluorene unit, may be subjected to the same previously studied chemistry with regards to polymerisations and synthesis, and will be comparable in terms of energy levels and mobilities (at least for orbitals that are on the backbone fluorene). The addition of another fluorene unit *via* the crucial spiro linker allows for additional moieties to be introduced orthogonally to the main polymer chain. It is this orthogonality that gives rise to the unique energy level systems that form the basis of this chapter. A comparison of the structures of fluorene and spirobifluorene is shown in ***Figure 4.1.1***.

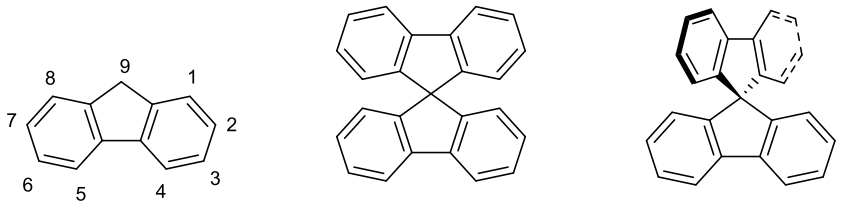


***Figure 4.1.1:*** *Fluorene with selected atom numbers (left) and structure of spirobifluorene (middle) with forced perspective (right). Fluorene is normally polymerised through the 2 and 7 positions and alkylated on the 9 position.*

As discussed in chapter 1, the population of non-emissive triplet states is a huge contributor to the reduction in efficiency of all organic semiconducting devices. Eliminating (or utilising) these loss processes is vital to organic electronic devices becoming competitive in the global marketplace.[104] This requires the careful control of energy levels.

The bandgap of an organic semiconductor has been well studied across many systems and can be manipulated by synthetic design. From ***Figure 4.1.2***, we may visualise this control as moving all levels except the ground state ($S_0$) up (increase bandgap) or down (decrease bandgap) in energy. More subtle control over the individual excited states relative to each other is more challenging however.

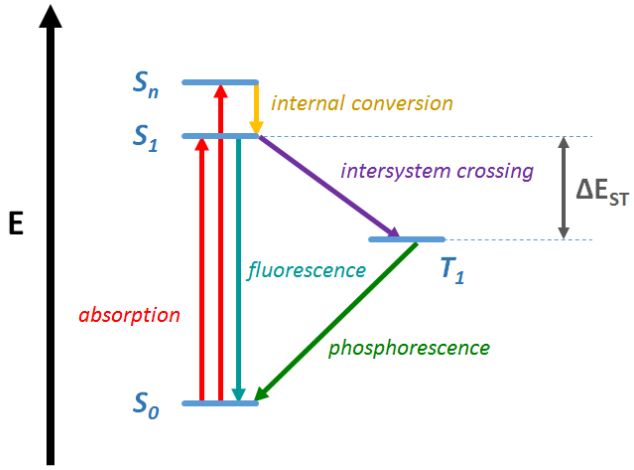


***Figure 4.1.2:*** *Generalised Jablonski diagram of an organic semiconductor.*

One reason this control is especially desirable is for the development of thermally activated delayed fluorescence (TADF) materials. By creating a system in which the first excited singlet and first excited triplet states are the same or close to each other in energy ($0.2 \geq \Delta E_{ST} \geq 0$ eV, from ***Figure 4.1.2***), the previously spin forbidden transition of an exciton moving from singlet to triplet (and *vice versa*) becomes possible. The transition is of course still formally forbidden, however since the levels are so close in energy, the activation energy to surmount this transition becomes comparable to $k_BT$ at 298 K. In other words, by exhibiting control over $\Delta E_{ST}$ so as to make it close to 0, we observe delayed fluorescence that is dependent on temperature.[105-106] For a review of TADF materials, see Yang *et al*.[107]

The key process of a TADF material is reverse intersystem crossing (RISC) from $T_1 \rightarrow S_1$. The rate of RISC is related to $\Delta E_{ST}$ and temperature:

$$k_{RISC} \propto exp \frac{-\Delta E_{ST}}{k_B T}$$

Since $\Delta E_{ST}$ is generally large (0.5 – 1.0 eV) for the majority of organic semiconducting systems, the rate of RISC and therefore TADF is negligible. When we decrease $\Delta E_{ST}$ however, $k_{RISC}$ increases and we eventually reach a point where the population of the first excited singlet is

substantially boosted from the first excited triplet, thereby resulting in a system that may emit from $S_1$ regardless of the original spin of the initially formed exciton.

This degree of energy level control resulting in a high performance device was first reported by Adachi *et al.* in 2011 where a small molecule was incorporated into an OLED that was shown to undergo TADF.[108] This work was expanded upon in 2012 when a high performance OLED was reported by the same group.[105] TADF was achieved by separating the HOMO and LUMO through a twist in the molecular structure, decreasing the exchange energy between the two and thereby decreasing $\Delta E_{ST}$, ***Figure 4.1.3***.

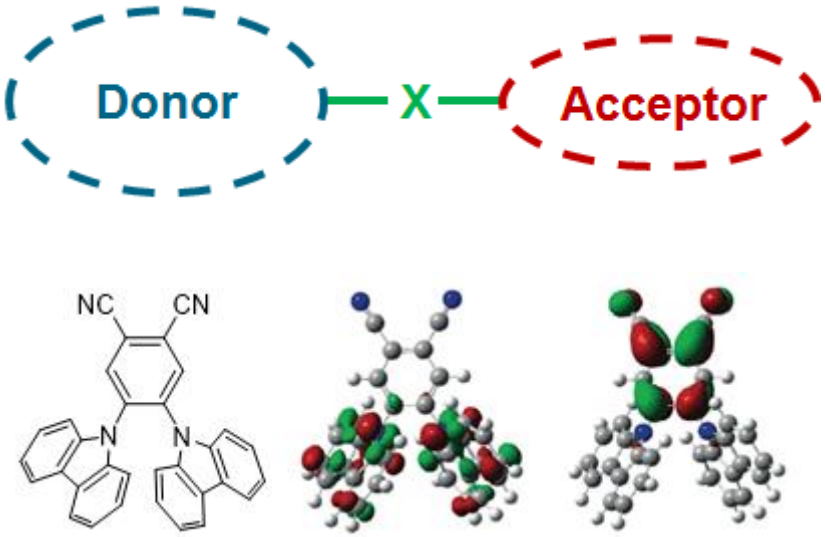


***Figure 4.1.3:*** *Twisted D-A general structure (top) and TADF capable molecule 2CzPn (bottom left) with calculated HOMO (bottom middle) and LUMO (bottom right).*

It has not been more challenging to exhibit this level of control over $\Delta E_{ST}$ in polymers however.[104] In an organic semiconducting system, the frontier molecular orbitals are dominated by π-π* transitions. In polymers both HOMO and LUMO lie on the polymer backbone and separation of the two becomes unfeasible. Köhler *et al.* studied a series of semiconducting polymers and plotted their measured singlet and triplet energy levels, their graph is shown in ***Figure 4.1.4***.[109] As $S_1$ moves further from the ground state $S_0$, it is seen that $T_1$ moves a roughly equivalent amount. This has the result that $\Delta E_{ST}$ is constantly close to 0.7 eV for all polymers. From related papers;

> *"For the all-organic polymers, we find the $T_1$ state to be at a constant separation of 0.7±0.1 eV below the singlet $S_1$ state. It is not possible to change this singlet–*

*triplet splitting by altering the size or the charge-transfer character of the polymer repeat unit or by changing the electron delocalization along the polymer backbone."*[110]

*"For conjugated polymers … the $S_1$-$T_1$ gap is experimentally found to be about 0.7 eV, virtually independent of chemical structure."*[104]

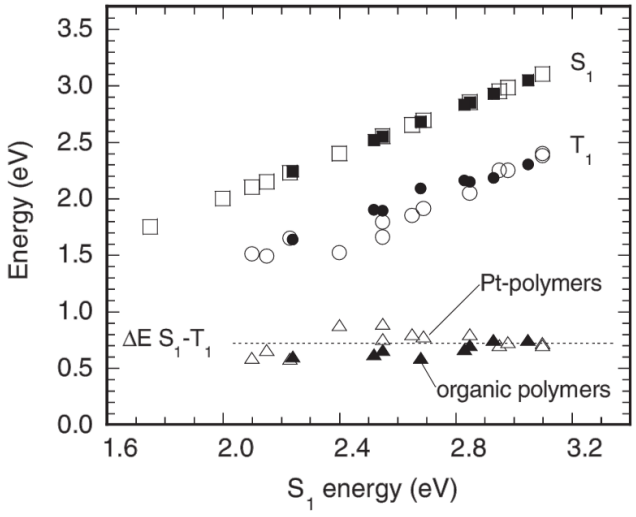


***Figure 4.1.4:*** *Relationship between singlet energy and triplet energy of organic polymers. Reported by Köhler* et al.[109]

Köhler's conclusion that $\Delta E_{ST}$ may not be largely affected in polymers holds true for all standard organic semiconducting polymers, where the HOMO and LUMO must both lie along the backbone because of the extended π-structure. This is true even for donor-acceptor (DA) polymers, where orbitals are somewhat localised to different parts of the polymer backbone.

Polymeric systems that show some degree of TADF have been reported however. In 2015 Fraser *et al.* and Nikolaenko *et al.* separately reported non-conjugated polymers that contain small molecules capable of TADF as end-capping groups or as part of the polymer chain, ***Figure 4.1.5*** and ***Figure 4.1.6***.[111-112]

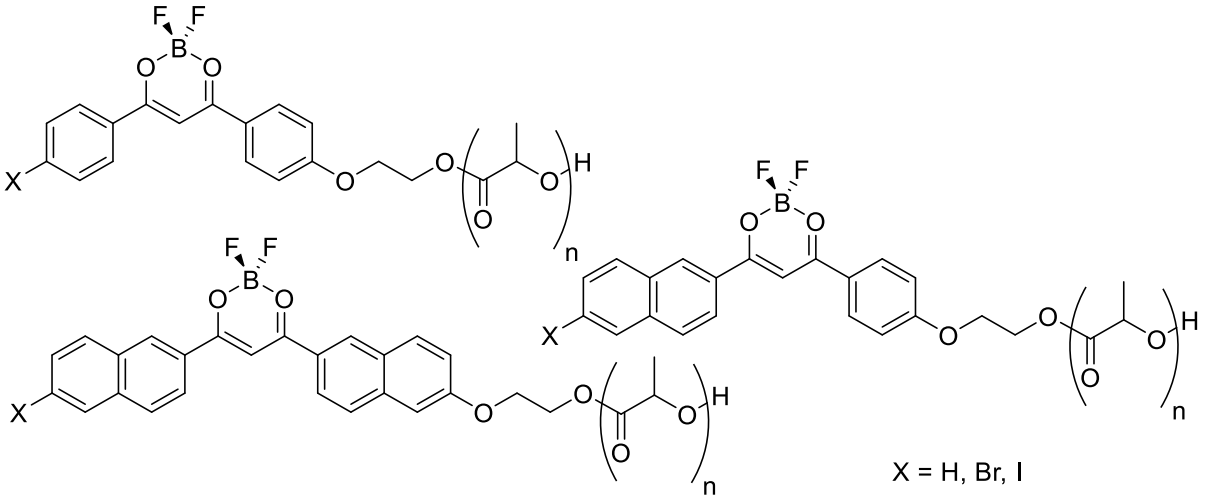


***Figure 4.1.5:*** *Oxygen sensing molecules that exhibit room temperature phosphorescence and TADF.*[111]

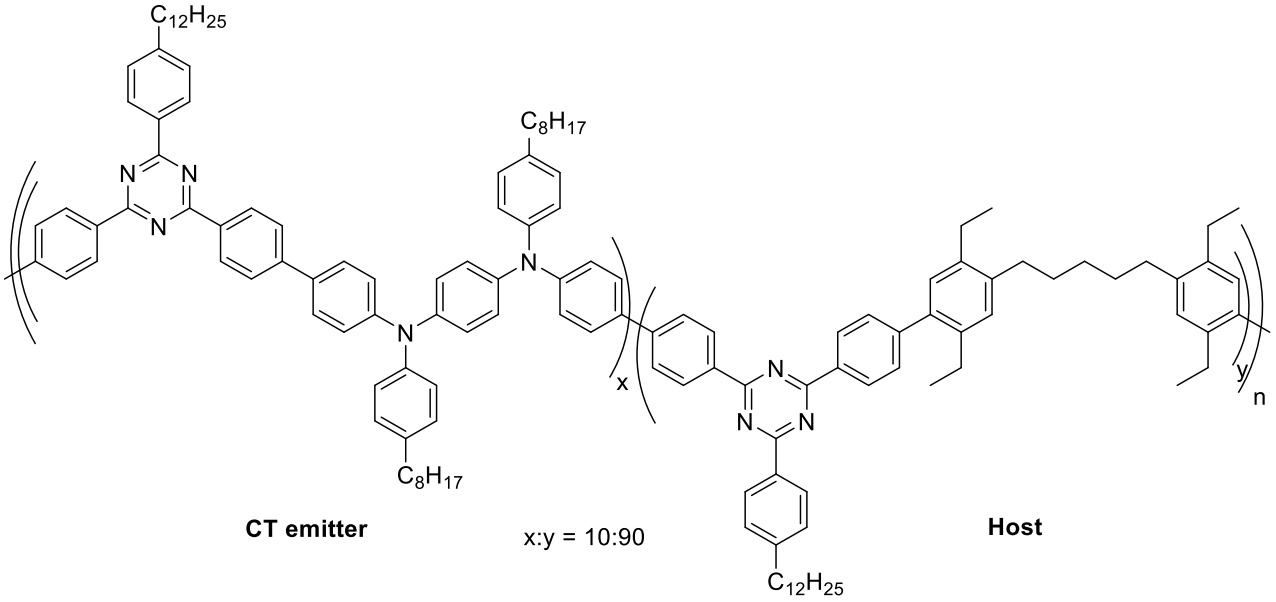


***Figure 4.1.6:*** *"Intermonomer TADF" polymer. The CT emitter portion is doped into a non-conjugated polymer host.*[112]

These approaches provide TADF capable small molecules that have the solution processability and other related advantages of polymers. An alternative approach is to attach small molecule groups as pendants to the main polymer chain, again resulting in a non-conjugated, solution processable polymer with TADF emitting small molecules covalently bound, ***Figure 4.1.7*** and ***Figure 4.1.8***.[113-114]

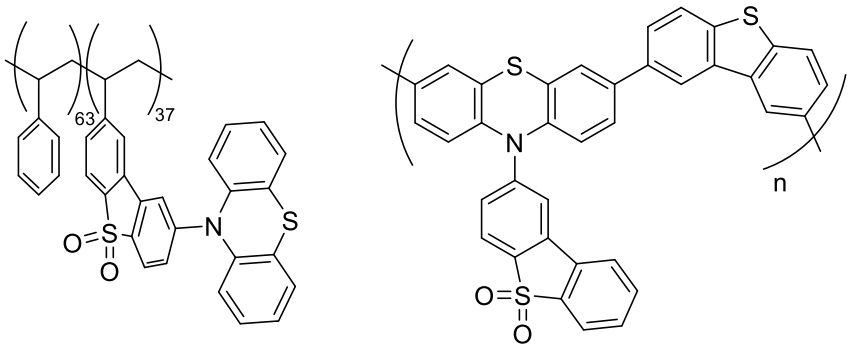

***Figure 4.1.7:*** *TADF and TTA capable pendant groups on polymeric backbone.*[113]

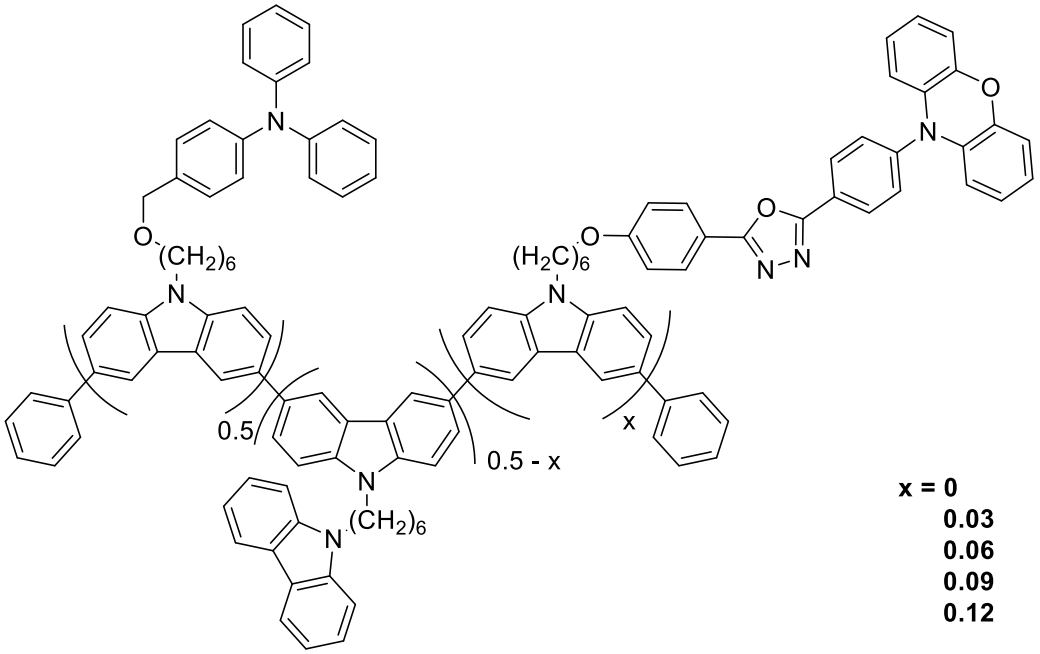


***Figure 4.1.8:*** *TADF emitting side chain on polycarbazole backbone. Other pendant groups, triphenylamine and carbazole, act as hole injection sites.*[114]

An advantage of these systems arises from the increased charge transport across the molecule. This increases the probability of holes and electrons generated at the electrodes (in the case of OLEDs) of reaching a TADF emitting site on a pendant.

Wang and Cheng *et al.* have synthesised a similar polymer that contains an acceptor group as a pendant, ***Figure 4.1.9***.[115] This differs to the previous polymers in that the polymer backbone is directly involved in the emissive state, rather than simply a vehicle for charge transport to a separate emissive site. The backbone acts as a donor and is separated from the acceptor, much like the small molecule systems initially reported by Adachi.

Yasuda and Adachi *et al.* have also reported two polymers that use backbone excited states in TADF emission, ***Figure 4.1.10***.[116] Adachi had previously shown the utility of a benzophenone unit as an acceptor moiety in small molecule TADF emitters.[117] By incorporating this unit into a polymer with an electron rich donor unit, either carbazole or acridine, a polymer was created with HOMO and LUMO separated spatially. This resulted in relatively small $\Delta E_{ST}$ values of 0.18 (carbazole) and 0.10 (acridine) which promoted TADF.

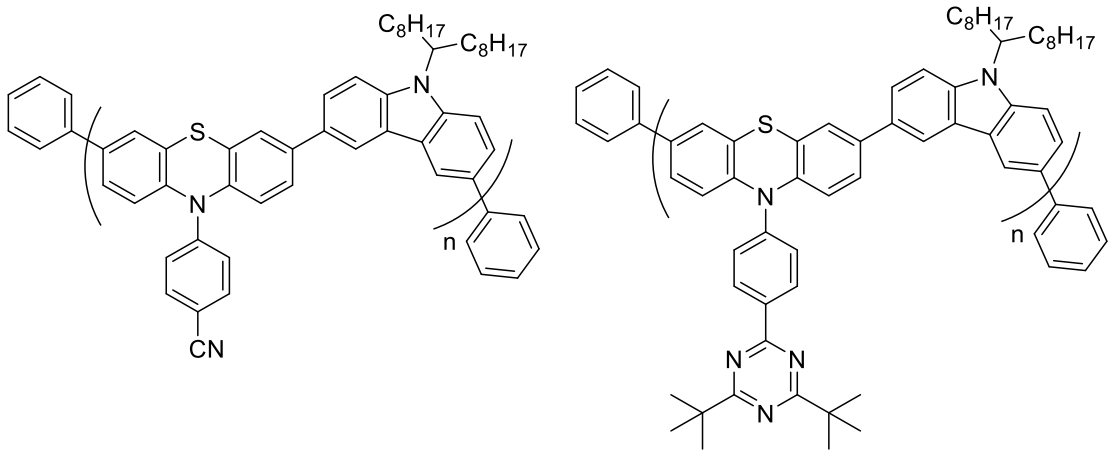


***Figure 4.1.9:*** *Electron rich backbone donor with pendant acceptor.*[115]

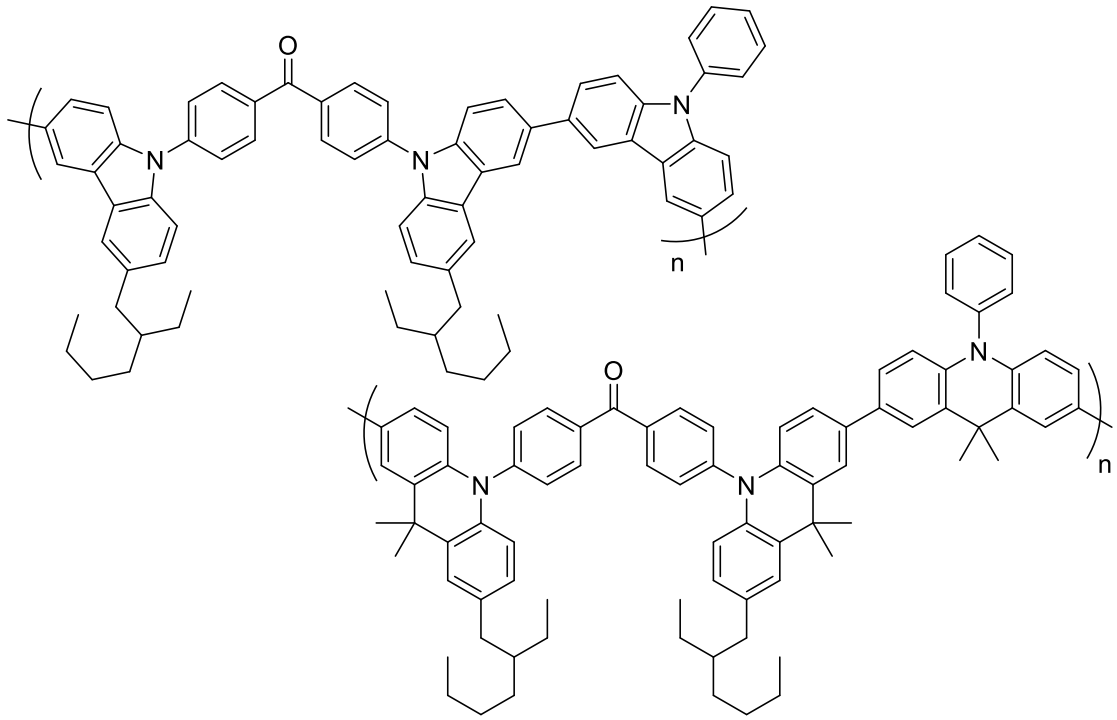


***Figure 4.1.10:*** *Donor and acceptor units both as part of polymer backbone.*[116]

The addition of a ketone moiety in these polymers is an important difference. Where most polymers with aromatic groups have a π→π* transition to create an excited state, the orthogonal electrons in a ketone are not part of an aromatic system and undergo a n→π* transition upon electronic excitation. It is the orthogonality of the ketone ground state electrons relative to the polymer backbone that leads to separation of HOMO and LUMO and therefore a reduction in $\Delta E_{ST}$. This means for this type of system, the ketone is vital. As ketones are often not desirable for semiconducting applications (they act as charge traps), this system has considerable limitations.

Monkman *et al.* and Ding and Wang *et al.* have independently synthesised polymers that separate the HOMO and LUMO *via* a spiro linkage, ***Figure 4.1.11*** and ***Figure 4.1.12***.[118-119] Monkman observes TADF and attributes it to emission from a $^1$CT state that is populated indirectly from TTA upconversion. This is a different version of delayed fluorescence from those based on the minimisation of $\Delta E_{ST}$, known as p-type delayed fluorescence (direct population of the first excited singlet from the first excited triplet using thermal energy is known as e-type delayed fluorescence). The polymers synthesised in this chapter are based on e-type delayed fluorescence, but the manipulation of energy levels is important for both types.

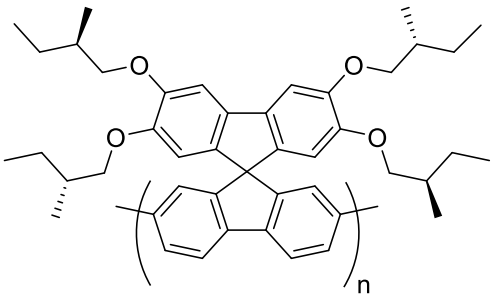


***Figure 4.1.11:*** *Spiro linked TADF polymer. Polyfluorene backbone acts as acceptor and orthogonal fluorene unit acts as donor. TADF occurs in this polymer as a result of population of $^1$CT state from TTA from backbone triplet state.*[120]

The spiro twist separates MOs but also allows enough overlap that energy transfer through the spiro linkage is fast if orbitals are close in energy. These polymers have a very low lying $^3$(π-π*) state (described by Monkman as a $^3$LE state) on the polymer backbone which undergoes TTA to repopulate higher energy states. The spiro link is a good way of introducing orthogonality to a molecule as the two fluorene units are fixed 90° relative to each other.

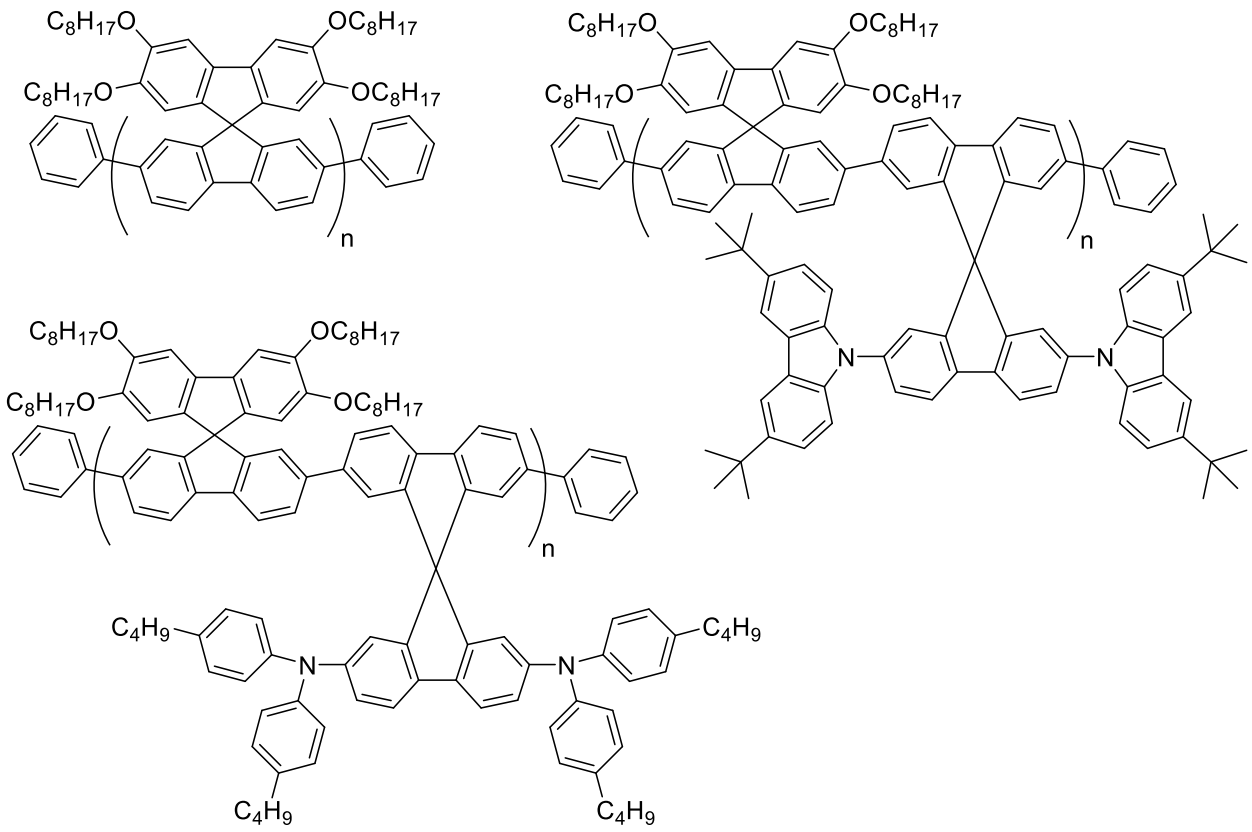


***Figure 4.1.12:*** *Spiro linked polymer. Donor units are linked through a spiro moiety to the polyfluorene backbone which acts as an acceptor. TADF is not reported for these polymers.*[119]

The precedent for TADF in polymers is limited to these cases however, and none show emission as a result of only TADF, but rather observe that RISC is an allowed process. A specific example is also not as useful to the scientific community as a standard tuneable design would be. The scope for new polymeric systems where $\Delta E_{ST}$ may be tuned is therefore large.

We know from Adachi's work on small molecule systems that reduction of $\Delta E_{ST}$ may be achieved through separation of the HOMO and LUMO orbitals.[117] This is also observed in the polymeric systems. In each case, the HOMO and LUMO are separated in space. This is achieved either by using a small molecule covalently attached to the polymer backbone,[111-113] or by creating large twists in the polymer backbone that break conjugation.[114-115]

***Figure 4.1.13*** describes a conjugated polyfluorene with spiro-linked electron poor fluorene groups. An electron poor orthogonal group (as opposed to electron rich seen in ***Figure 4.1.11*** and ***Figure 4.1.12***) creates a classic donor-acceptor copolymer, but one where the acceptor is *orthogonal* to the polymer backbone. ***Figure 4.1.14*** shows how this affects the distributions of the frontier molecular orbitals and relative energy levels.


***Figure 4.1.13:*** *Design of DoA polymer. The polymer backbone acts as the donor unit (HOMO) and an electron poor fluorene acts as the acceptor (LUMO). The two are spatially separated by a spiro 'twist', forcing orthogonality.*

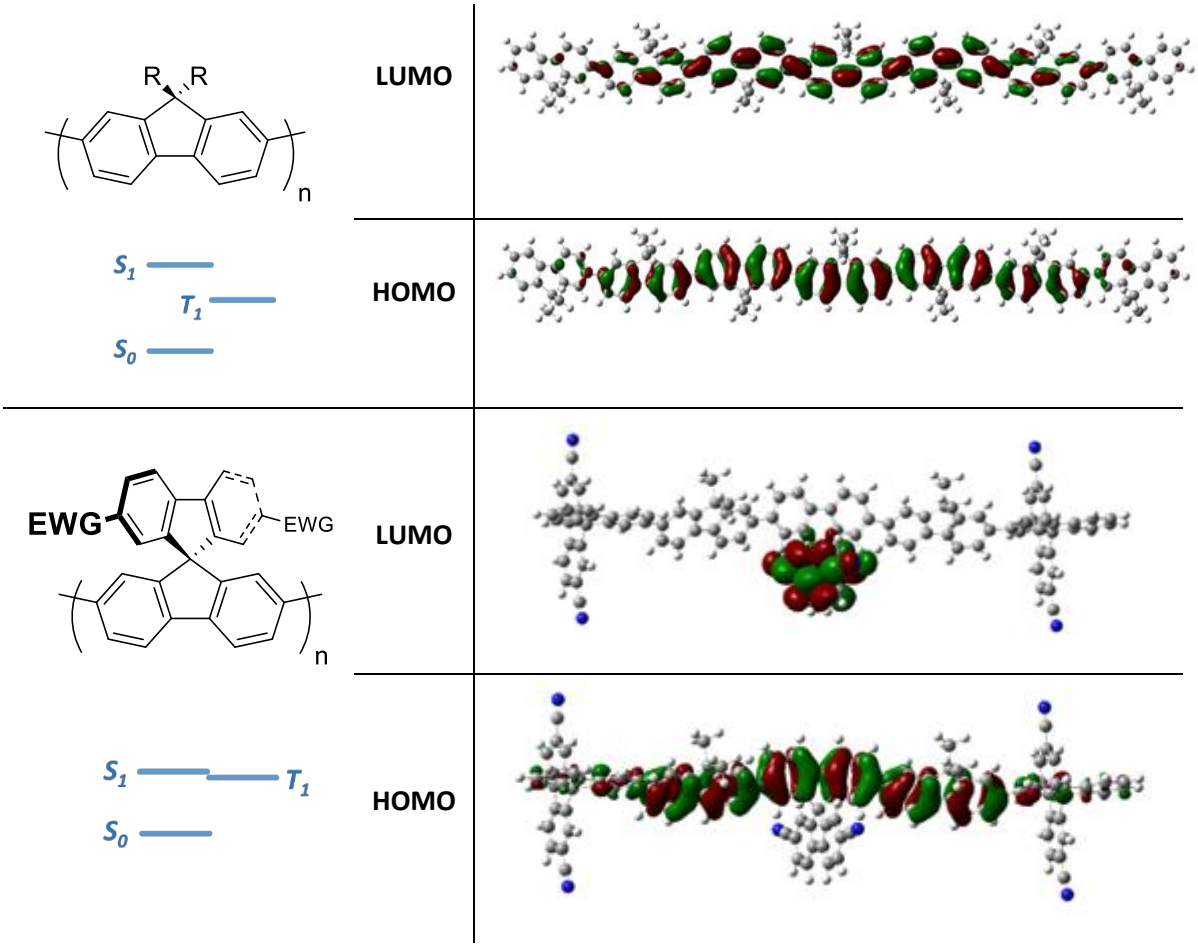


***Figure 4.1.14:*** *Calculated HOMO and LUMO distributaions of polyfluorene (top) and DoA polymer (bottom) using the B3LYP/6-31G* level of theory and accompanying Jablonski diagrams showing relationship between orbital overlap and* $\Delta E_{ST}$.

The LUMO of polyfluorene overlaps the HOMO as both lie across the backbone, as is the case for almost all conjugated polymers. The addition of electron poor orthogonal groups of the donor orthogonal-acceptor (DoA) polymer forces the LUMO onto a spatially distinct part of the polymer. It was hypothesised that this would have the result of a decreased $\Delta E_{ST}$ while maintaining the beneficial properties of polyfluorene, such as processibility and flexibility.

The work described in this chapter has been published.[121]

## 4.2 Synthesis of SFCN and SFH

The initially designed polyspirobifluorene **4.2.1** is shown in ***Figure 4.2.1***. It is worth noting that while there is some precedent for spirobifluorenes exhibiting TADF as small molecules, their exploitation in conjugated polymers is as yet unknown in the literature.[122-123] By adding electron withdrawing groups to the orthogonal fluorene, the LUMO will be forced onto this moiety and be separated from the HOMO which will remain on the (relatively) electron rich backbone. Carbonitrile groups were chosen as electron withdrawing groups on the orthogonal acceptor. The synthesis of the polymer is analogous to previously synthesised fluorene polymers. The boronic ester monomer **4.2.3** synthesis has been discussed above in chapter 2.

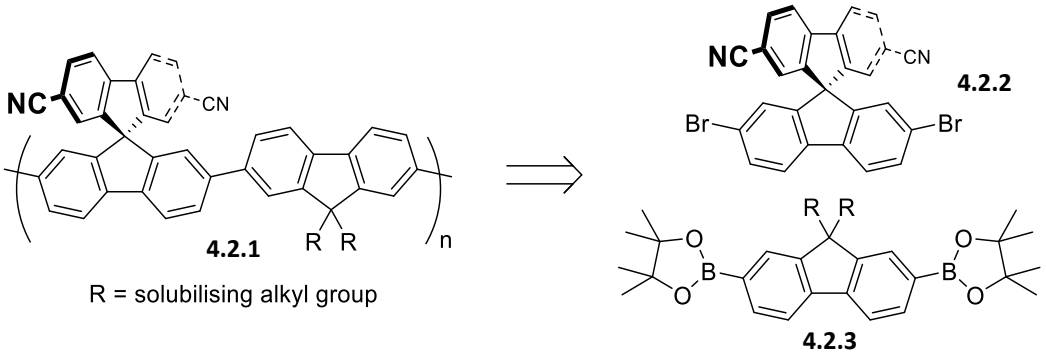


***Figure 4.2.1:*** *Reterosynthesis to Suzuki monomers of poly fluorene spiro bifluorene* ***4.2.1****.*

The first stage in the synthesis of a spirobifluorene is to synthesise dibromofluorenone **4.2.4**.This was achieved *via* two separate routes, as shown in ***Scheme 4.2.1***. The first method trialled was to dibromonate fluorene to produce dibromofluorene **4.2.5**, followed by an oxidation using $CrO_3$. The yield over two steps was 37% and created large amounts of toxic chromium waste upon quenching that made scaling the reaction problematic.

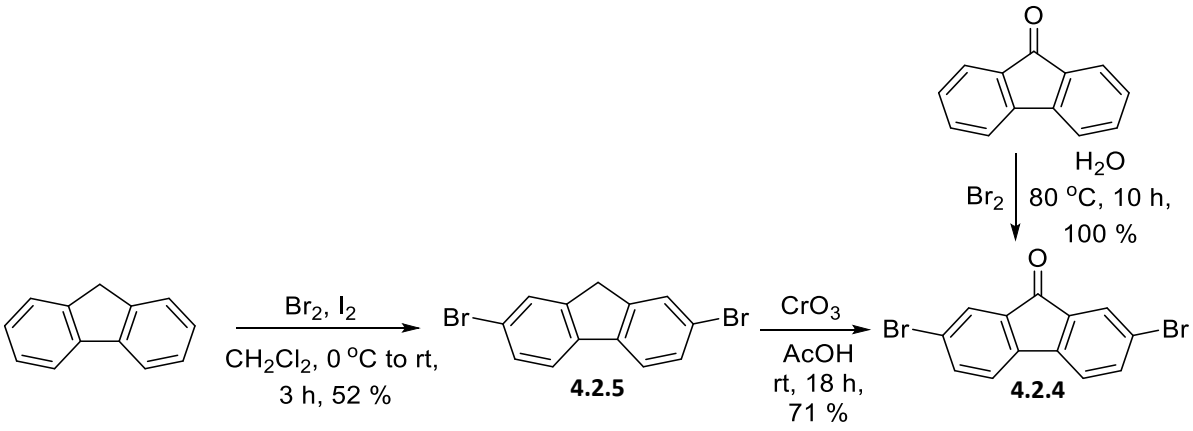


***Scheme 4.2.1:*** *Alternative routes to dibromofluorenone* ***4.2.4****.*

The second route effectively reverses the two reactions of the first. However, while dibromofluorene **4.2.5** must be synthesised, fluorenone is cheap and commercially available in large quantities. Bromination of fluorenone proceeded in quantitative yield when subjected to an excess of bromine and was facile to scale up to multi-gram quantities.

While optimisation of the routes to dibromofluorenone **4.2.4** was ongoing, work progressed on the formation of a spiro centre *via* the formation of a Grignard intermediate, ***Scheme 4.2.2***.

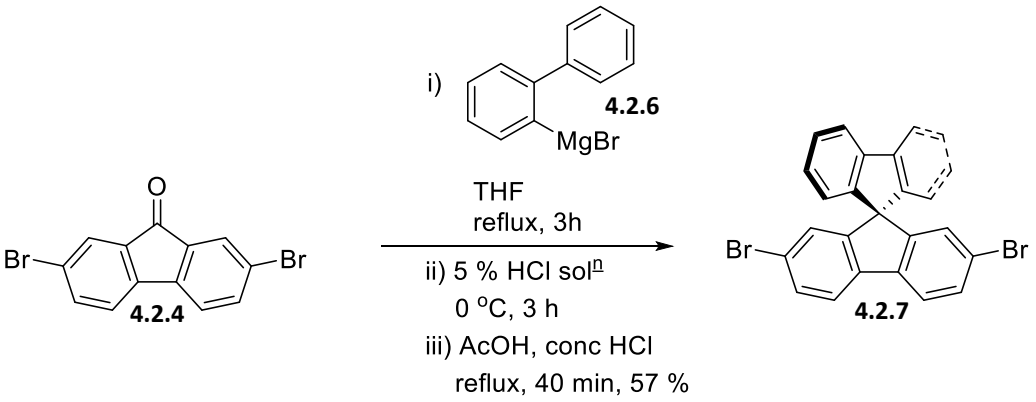


***Scheme 4.2.2:*** *Grignard reaction to form dibromospirodifluorene* ***4.2.7****.*

Following a procedure by Wang *et al*., dibromofluorenone **4.2.4** was reacted first with a Grignard reagent formed from 2-bromobiphenyl; 2-magnesium bromide biphenyl **4.2.6**.[124] The resultant magnesium salt was then converted to the alcohol during work up which was filtered and dissolved in refluxing acetic acid. Protonation of the alcohol and E1 attack forms the spiro centre.[125] Once the spiro centre has been prepared, the product becomes insoluble in the refluxing mixture and may be filtered in 57% yield.

With the spiro centre formed, work began on converting the bromide moieties to cyano groups, ***Scheme 4.2.3***. Initially, the direct reaction with copper cyanide was attempted. This reaction failed to give any product and returned the starting material. The reason for this failure is still unclear (the reaction was tried several times), as a similar reaction has been reported in the literature.[126-127] The route was changed to a more circuitous, but less toxic 3 step synthesis.

An alternative way of forming the cyano groups is to first formylate dibromospirobifluorene **4.2.7** to spirobifluorene dialdehyde **4.2.8**. The formylation reaction was attempted in multiple ways, summarised in ***Table 4.2.1***.

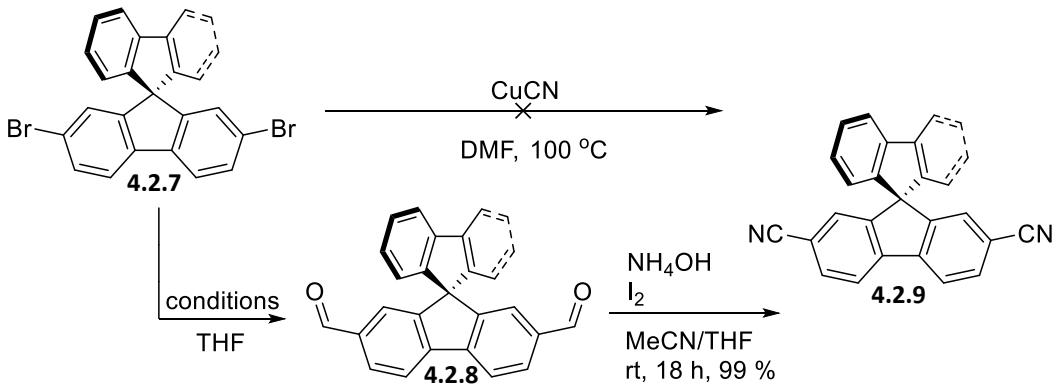


***Scheme 4.2.3:*** *Synthesis of dicyanospirobifluorene* ***4.2.9****.*

| **Carbocation Forming Reagent** | **Formylation Reagent** | **T / °C** | **t / h** | **Result** |
|---|---|---|---|---|
| $^{n}$BuLi | DMF | -78 to rt | 1.5 | No product obtained – debromination observed |
| Mg | DMF | Reflux | 24 | No reaction observed |
| $^{n}$BuLi | N-formyl piperidine | -78 to rt | 1.5 | Product obtained – 39% yield |

***Table 4.2.1:*** *Formylation conditions for dibromospirodifluorene* ***4.2.7****.*

Lithium-halogen exchange followed by addition of DMF was first investigated. No product was obtained and the starting material was completely consumed. Mass spectrometry showed loss of bromine moieties (*i.e.* naked spirobifluorene). Milder conditions were also trialled; formation of a di-Grignard reagent followed by addition of DMF. No reaction was observed in this instance as the Grignard reagent failed to form. $^{n}$BuLi therefore was deemed strong enough to initiate metal-halogen exchange (since starting material had been consumed) whereas Mg was not. By substituting the formylation reagent it was thought that the metal-halogen exchange with $^{n}$BuLi could be more successful. Replacement of DMF as formylation reagent for *N*-formyl piperidine, which has been shown in some cases to give more favourable results, was then attempted.[128] This reaction was successful and gave the desired product in 39% yield. Stirring the product in ammonium hydroxide solution with iodine gave dicyanospirobifluorene **4.2.9** in quantitive yield.

Dibromination then proceeded in an analogous reaction to the dibromination of fluorenone by molecular bromine. The isolated yield of the desired spiro monomer **4.2.2** was low, with the main issue surrounding this final reaction before polymerisation being under-bromination. The monobromide side product is difficult to remove by chromatography and

could act as an end-capping group in the subsequent polymerisation. For this reason the reaction is necessarily low yielding (much is lost in purification).

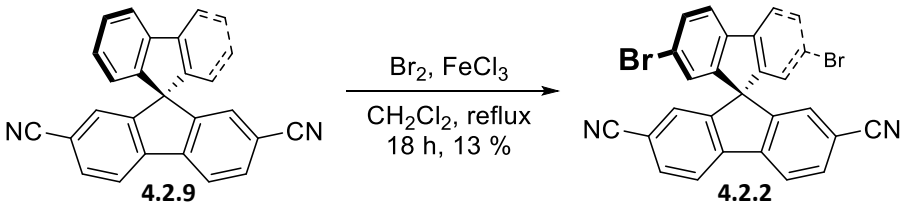


***Scheme 4.2.4:*** *Dibromination of 2,7-dicyanospirobifluorene* ***4.2.9****.*

A Suzuki polymerisation was attempted using dibromo-dicyanospirobifluorene **4.2.2** and dibromofluorene **4.2.10**, ***Scheme 4.2.5***.

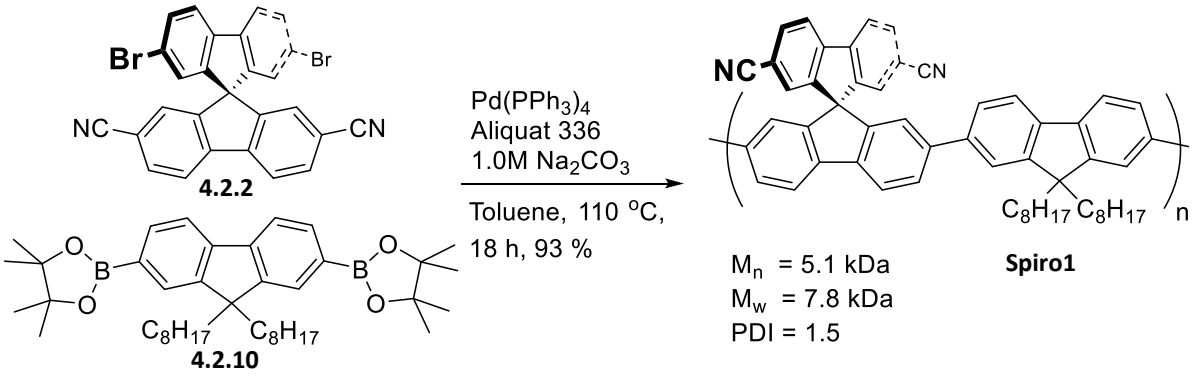


***Scheme 4.2.5:*** *Attempted polymerisation to form* ***Spiro1****. GPC data determined by GPC using PhCl eluent.*

While product was obtained in good yield from the reaction, GPC data showed that the polymer has a low molecular weight ($M_n$ = 5.1 kDa, $M_w$ = 7.8 kDa, n = 7-10). It is believed that this was due to the low solubility of the polymer resulting in its precipitation under the reaction conditions before high molecular weights were obtained. It is possible however, that small amounts of monobromide spiro comonomer were present in the reaction mixture from the final step of the spiro synthesis, acting as end-capping groups and resulting in low molecular weight polymers. Only small amounts are needed to have a large effect on the resultant molecular weights, although none were observed in the $^1$H NMR spectrum of the monomer. Both issues were tackled in the next attempt at polymer synthesis.

To combat the probable solubility issue, the fluorene co-monomer was modified in an effort to increase the solubility of the polymer as it is formed in reaction. This was achieved simply by increasing the length of the alkyl chains, ***Scheme 4.2.6***.

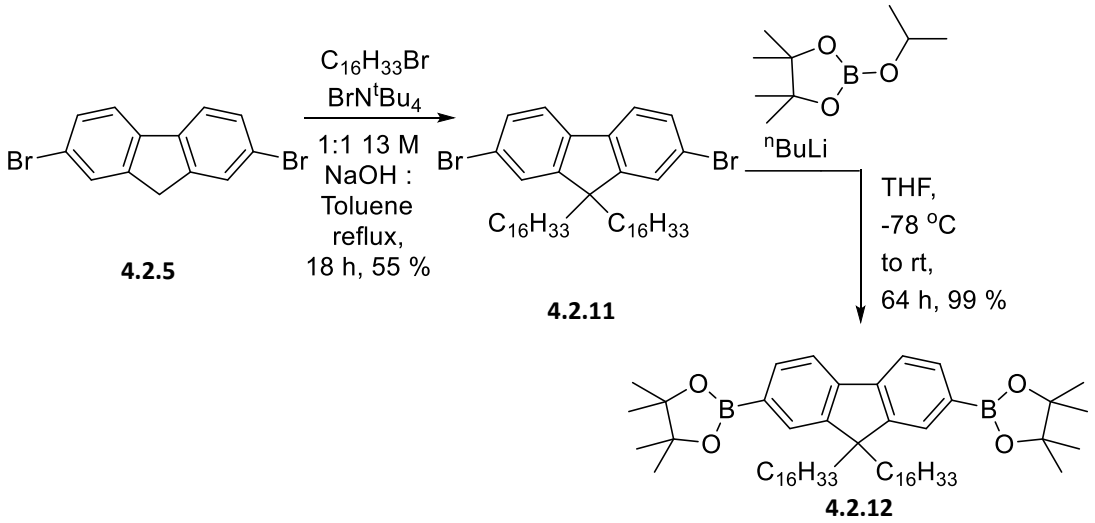


***Scheme 4.2.6:*** *Synthesis of hexadecyl alkylated fluorene boronic ester monomer* ***4.2.12****.*

A new route towards the spiro monomer was proposed that avoided the issue of monobrominated side product in the final material (***Scheme 4.2.7***). Dibromofluoreneone was again used in a Grignard reaction to form the spiro centre but with the modification of a dimethyl biphenyl Grignard reagent. The benzylic moieties were then converted to cyano groups through a three step synthesis.

By converting benzyl (as opposed to aryl bromide) groups to cyano groups the dibromide moiety is installed early and left unchanged. Any monobromide end-capping groups are therefore removed early in the synthesis.

4,4'-Dimethylbiphenyl is firstly monobrominated at the 2-position in quantitative yield to form bromobiphenyl **4.2.13**. An analogous Grignard reaction to ***Scheme 4.2.2*** gave spirobifluorene **4.2.14** in good yield. Conversion of the benzylic positions to carbonitrile groups was achieved through bromination followed by conversion to a dialdehyde and finally the dicyano monomer **4.2.9**.

A downside to this route is the use of toxic $CCl_4$ as solvent in the bromination step; it is employed so as to avoid radical quenching. A similar reaction has since been successful within the group using chloroform as solvent, it is thought this would also be the case here although it was never trialled for this particular route.

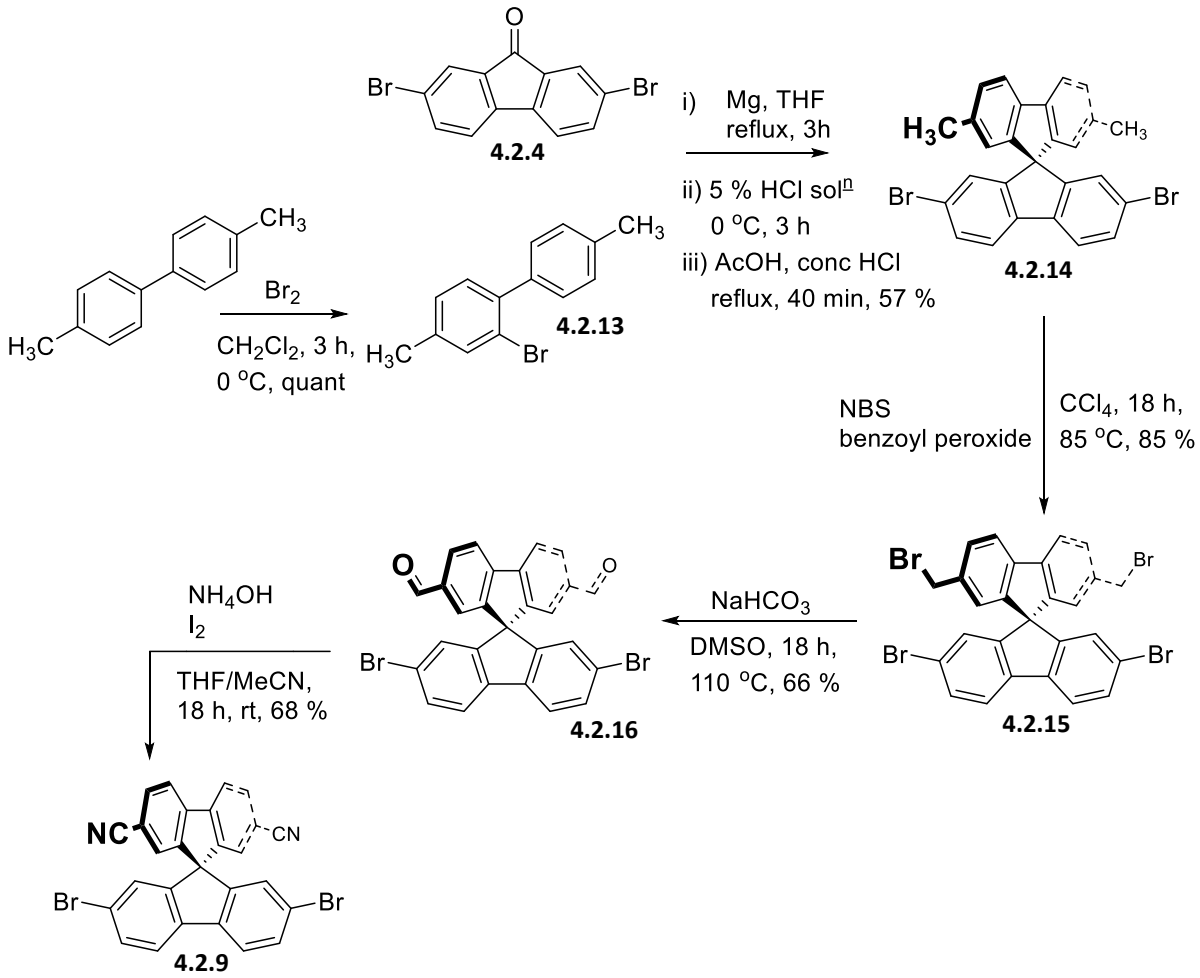


***Scheme 4.2.7:*** *Synthesis of spiro monomer* ***4.2.9*** via *2-bromo-4,4'-dimethylbiphenyl* ***4.2.13****.*

The spiro and hexadecyl monomers **4.2.9** and **4.2.12** were then polymerised as in ***Scheme 4.2.8***.

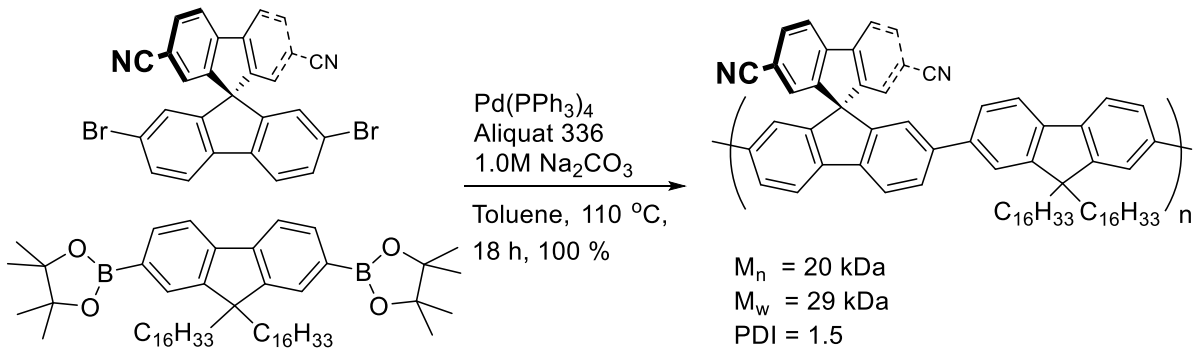


***Scheme 4.2.8:*** *Suzuki polymerisation to form* ***SFCN****.*

The molecular weight of this polymer was much improved compared to the octyl version, **spiro1**. A reference polymer without the electron withdrawing cyano groups was also prepared in order for electrochemical comparisons to be made; **SFH**, ***Scheme 4.2.9***. The synthetic method was identical to the synthesis of **SFCN** with the exception of the spiro monomer (dibromospirobifluorene **4.2.7** was substituted). These two polymers were analysed further at the University of Cambridge by Dr. Andrew Musser to elucidate the complex energy level structure, this work is detailed below in ***section 4.4***. Synthetic efforts at this point moved onto the related polymers **ASFCN** and **ASFH**.

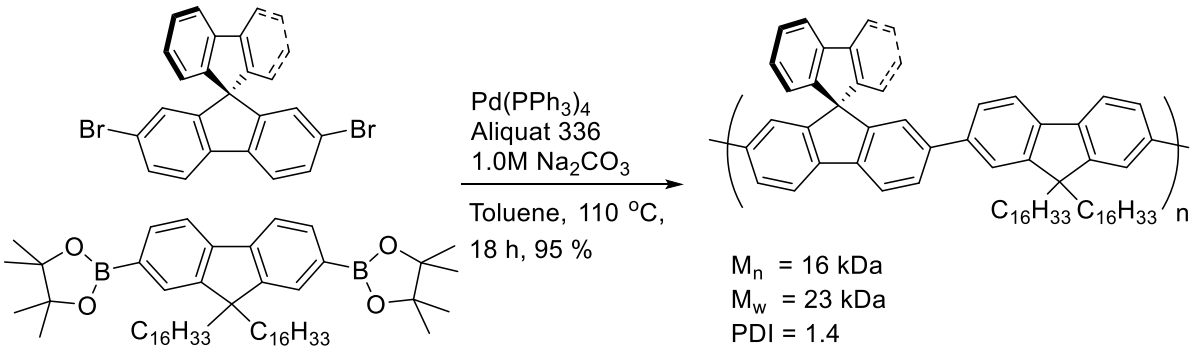


***Scheme 4.2.9:*** *Suzuki polymerisation to form* ***SFH****.*

## 4.3 Synthesis of ASFCN and ASFH

**SFCN** has electron withdrawing groups on an orthogonal (to the backbone) portion of the polymer which 'pulls' electron density (and therefore the LUMO) onto that portion of the molecule. The effect of this is the lowering in energy of the first excited singlet state whilst the first excited triplet state is unaffected; a decrease in $\Delta E_{ST}$. This is achieved through the stabilisation of the π* orbitals on the orthogonal moiety. For a molecule to be capable of TADF, these two states must be extremely close in energy.

The related polymer **ASFCN** was designed with this in mind. By adding an extra 'push' to the system (through the addition of an electron donating amine moiety on the backbone), the LUMO should be even more localised onto the orthogonal portion of the molecule. $S_1$ and $T_1$ should then be even closer and TADF even more likely to occur.

The 'pull' for **ASFCN** was again designed to be the dicyano substituted spiro bifluorene, synthesised as for **SFCN**, and the additional 'push' comes from a tertiary amine containing moiety. Attempts were initially made to form the tertiary amine from secondary amines beginning with ***Scheme 4.3.1***.

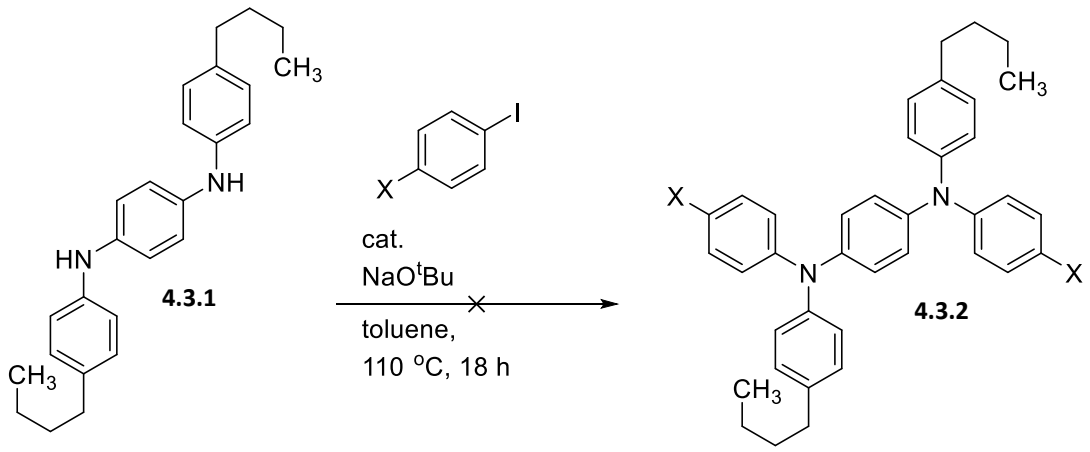


***Scheme 4.3.1:*** *Attempted Buchwald-Hartwig cross coupling of diamine* ***4.3.1****.*

| *X* | *Catalyst system* | *Result* |
|---|---|---|
| *Br* | *$Pd(dppf)Cl_2$* | *No reaction* |
| *Br* | *$Pd(OAc)_2$ + $^tBu_3P$* | *Low yield of mix of several related products isolated. Mix contains **4.3.2** with X = Br,Br and X = Br,I* |
| *I* | *$Pd(OAc)_2$ + $^tBu_3P$* | *Product observed in crude, but could not be isolated* |

***Table 4.3.1:*** *Attempted Buchwald-Hartwig cross coupling of diamine **4.3.1**.*

Bis(4-butylphenyl)benzene-1,4-diamine **4.3.1** was the first choice for the synthesis of a tertiary amine comonomer, as through one reaction it is possible to synthesise a complex diamine with alkyl chains (albeit rather small butyl chains) and dihalide functionality allowing polymerisation. The first set of conditions trialled used $Pd(dppf)Cl_2$ as catalyst, but this failed to react with the starting material.

The failure of the standard Buchwald-Hartwig cross coupling conditions was hypothesised to arise due to the oxidative addition step, as starting material was left unaffected. To address this, the catalyst was changed to $Pd(OAc)_2$ complexed *in situ* with the exceptionally electron donating and bulky ligand $^tBu_3P$. Bulky, electron donating phosphine ligands have been reported to help promote oxidative addition for Buchwald-Hartwig cross coupling reactions on less electron rich aromatic halides.[129]

This reaction produced an interesting, but problematic result. Purification proved to be difficult and it became apparent that multiple products with very similar polarities had been produced. $^1$H NMR showed broad peaks and suggested a complex mixture had formed. Mass spectrometry however showed the expected series of peaks around 682 *m/z* (expected isotopes of dibromo **4.3.2**) as well as a series of peaks around 730 *m/z*, see ***Figure 4.3.1***. The peaks around 730 *m/z* showed only a monobromide rather than a dibromide trace ( *ie.* peaks from $^{79}$Br and $^{81}$Br isotopes. The peak at 682 *m/z* by comparison has 3 major components from $^{79}$Br/$^{79}$Br, $^{79}$Br/$^{81}$Br and $^{81}$Br/$^{81}$Br). 730 *m/z* corresponds to monobromo, monoiodo **4.3.2**. This suggests that the rate of oxidative addition had been increased to the point that the selectivity for aryl halides had become negligible, and that Ar-Br addition had begun to occur at a comparable (though likely still lower) rate.

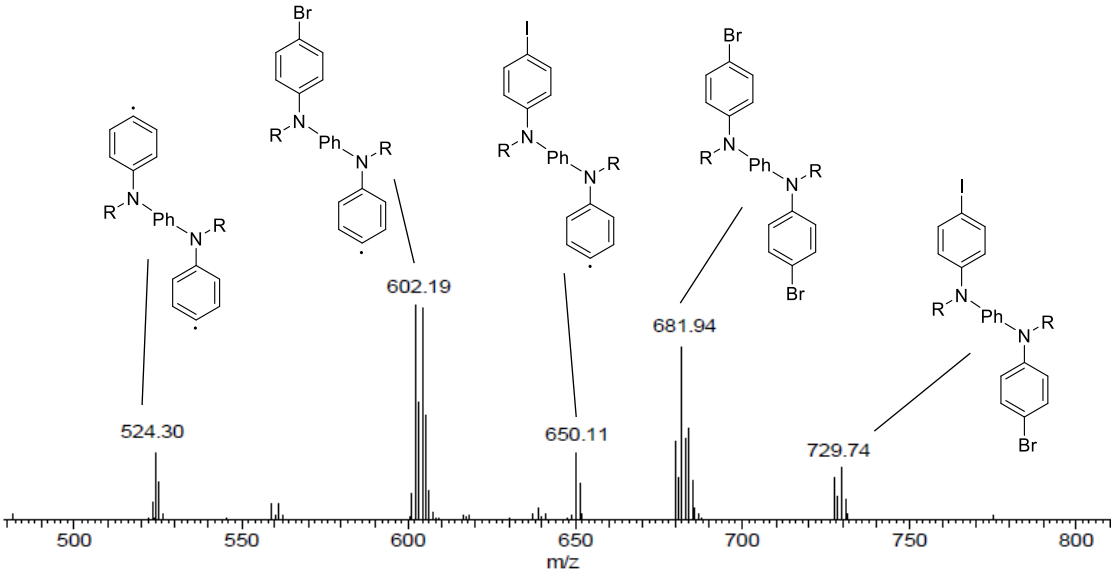


***Figure 4.3.1:*** *$CI^+$ mass spectrum of Buchwald-Hartwig product containing dibromo and monobromo monoiodo diamine* ***4.3.2****. R = 4-n-butylphenyl. Fragments have been shown as radicals for visualisation purposes.*

A Miyaura borylation was attempted on the mixture of products, as both bromo and iodo moieties should react to form the same product, this reaction was done on a very small scale however and didn't give sufficient product to attempt a polymerisation. The Buchwald-Hartwig reaction was repeated, with the exception of using 1,4-diiodobenzene to eliminate the mixture of products obtained previously. It is believed the reaction was successful based on analysis of the crude $^1$H NMR, however purification proved difficult and no pure product was isolated. Due to the problems associated with this route and the fairly high cost of the diamine starting material, focus was shifted to an alternative molecule.

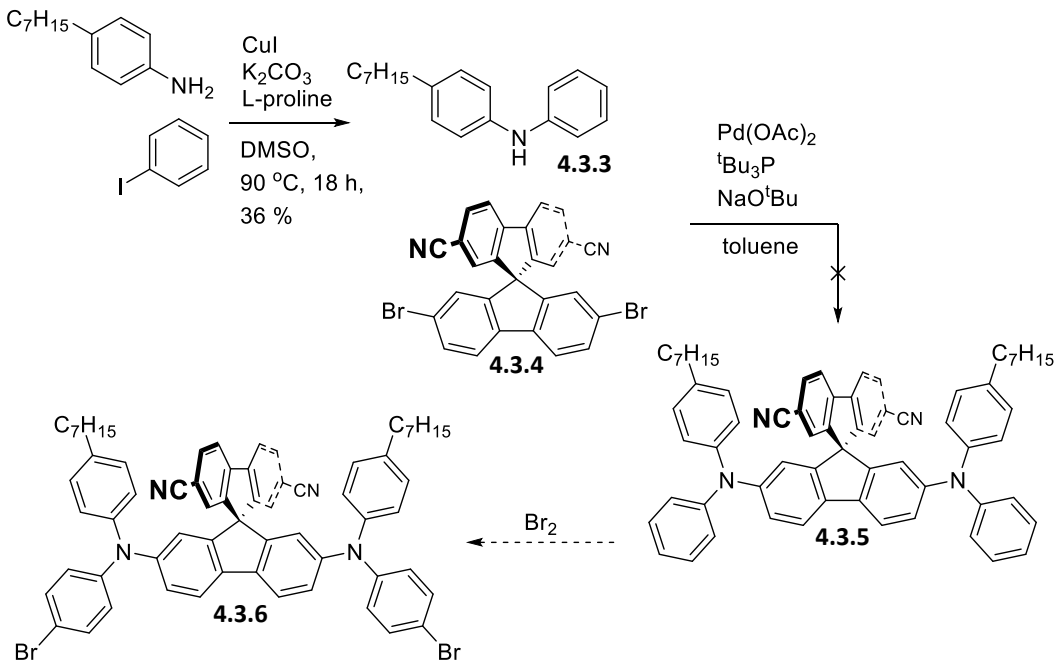


***Scheme 4.3.2:*** *Attempted synthesis of spirobifluorenediamine* ***4.3.6****.*

Installation of a tertiary amine unit into the final polymer backbone can be achieved in two ways; copolymerising a tertiary amine comonomer with the spiro monomer **4.3.4**, or by converting spiro monomer **4.3.4** into a tertiary amine in its own right. This second method has the additional advantages of increased electron density near the orthogonal acceptor as well as the possibility of homopolymerisation using a Yamamoto reaction. This would eliminate the need to synthesise a comonomer, as target spirodiamine **4.3.6** contains an orthogonal acceptor, electron rich tertiary amine moieties and solubilising alkyl chains in a single monomer. Of course, the polymerisation conditions could also be changed to include a comonomer to affect the resultant polymer in various ways if desired.

An Ullmann amine synthesis formed heptylphenylaniline **4.3.3**. This secondary amine and previously formed spiro monomer **4.3.4** were then subjected to the enhanced Buchwald-Hartwig conditions from ***Table 4.3.1*** in an effort to form ditertiary amine **4.3.5**. This reaction was unsuccessful however, and returned both starting materials unreacted.

Due to the difficulties encountered in the synthesis of a bespoke tertiary amine from a secondary amine, focus shifted onto routes that start with a preformed tertiary amine; triphenylamine. ***Scheme 4.3.3*** shows the various routes that were trialled (grey) before the successful route (black) was found. Discussion focusses on the left, middle then right branches.

Monobromination of triphenylamine proceeded in good yield. Bromotriphenylamine **4.3.8** contained a bromide handle which could be used to install the necessary alkyl groups to aid in solubility of the desired polymer. Treatment with $^{n}$BuLi and subsequently with a bromoalkane however yielded only the butylated product, not the desired long alkyl chain triphenylamine **4.3.9**, see ***Table 4.3.2***. This suggests the $S_N2$ step is much faster for the BuBr side product than it is for alkyl bromide **4.3.15**. A more bulky alkyl lithium reagent and a less bulky alkylbromide were therefore substituted: the reaction was tried again with $^{t}$BuLi and $C_{16}H_{33}Br$. This reaction failed to yield significant amounts of product however and returned mostly starting material. This was surprising, as $^{t}$BuLi is a very strong lithiating reagent, it seems likely that the reaction failed due to perhaps water in the reaction vessel or degradation of reagent. The reaction was not retried however, a Kumada coupling was attempted instead.

| ***Reagents*** | ***Conditions*** | ***Result*** |
|---|---|---|
| ***4.3.15***, *$^{n}$BuLi* | *THF, -78 $^{o}$C, 30 min* | *Butylphenyldiphenylamine formed* |
| $C_{16}H_{33}Br$, *$^{t}$BuLi* | *THF, -78 $^{o}$C, 30 min* | *Starting material returned ~ 80%. Green precipitate formed, mixture of products* |
| ***4.3.15***, *Mg, $NiCl_2(dppp)$* | *THF, rt, 18 h* | *Grignard reagent not substantially formed, small (~ 15%) side product in NMR could be product* |
| ***4.3.15***, *Mg, $NiCl_2(dppp)$* | *$Et_2O$, rt, 18 h* | *Grignard reagent not substantially formed* |
| ***4.3.15***, *Mg, $NiCl_2(dppp)$* | *$Et_2O$, rt, 18 h (repeat of above)* | *Grignard reagent formed in low yeild, small (~ 25%) side product in NMR could be product* |

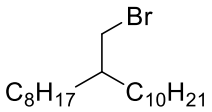


***Table 4.3.2:*** *Conditions trialled for alkylation of monobromotriphenylamine **4.3.8**.*

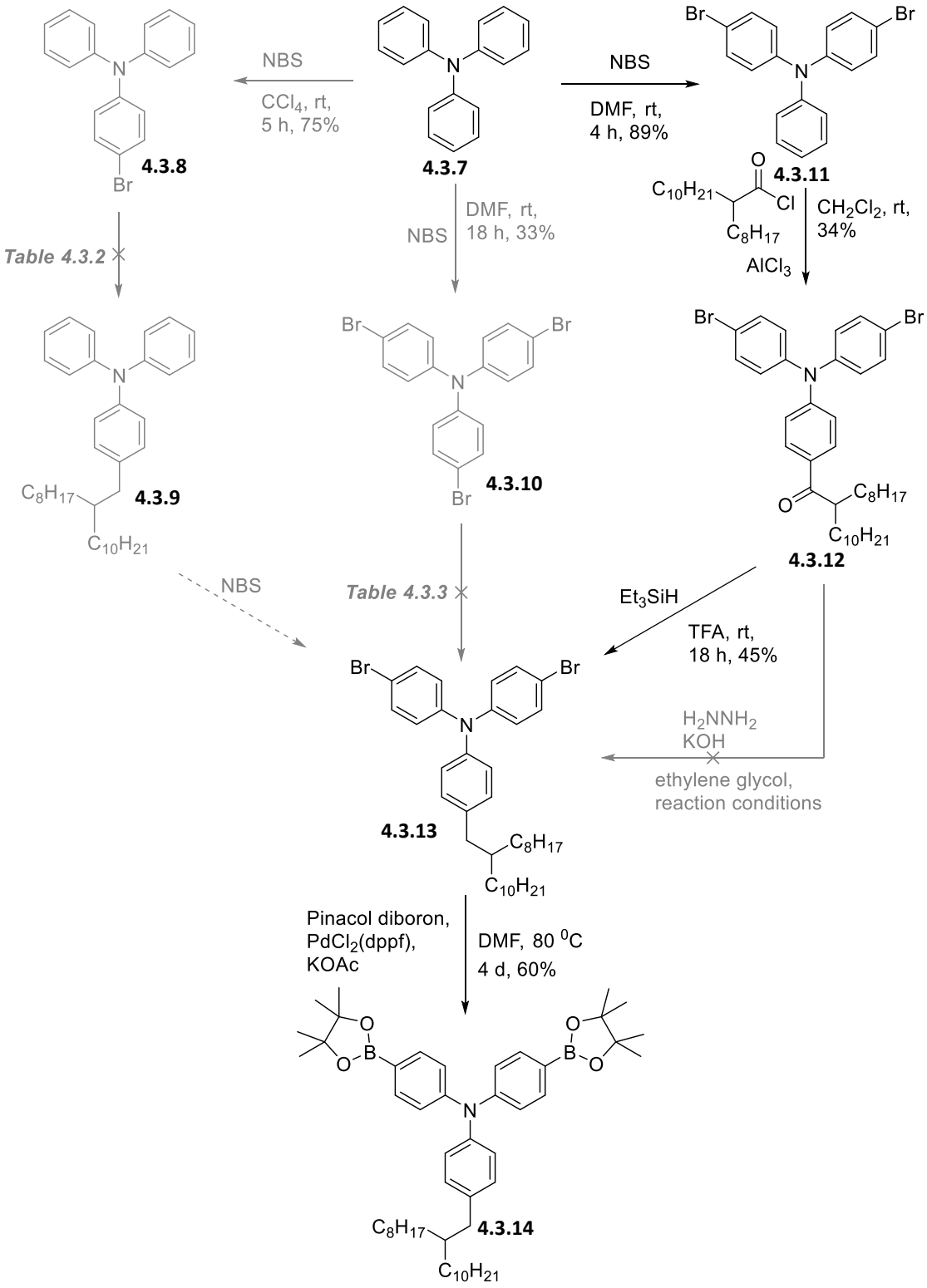


***Scheme 4.3.3:*** *Synthetic attempts and successful route to tertiary amine monomer* ***4.3.14****. Unsuccessful routes are shown in grey.*

The Kumada cross-coupling reaction is useful in the formation of carbon-carbon bonds with normally unreactive aryl halides.[130] As this reactivity seemed to be problematic during the BuLi reactions, this seemed like a good choice of reaction. Three attempts using Kumada conditions were attempted, however each time it became apparent that the initial formation of the Grignard reagent was problematic and proceeded, at best, in low yield.

While this work progressed, tri-4,4',4''-bromophenylamine **4.3.10** was also synthesised using excess NBS on triphenylamine. Treatment of the tribrominated product **4.3.10** with one equivalent of $^{n}$BuLi and alkyl bromide again yielded the butyl product, and the Kumada reaction also had similar results to those of the monobrominated reactions. These reactions are summarised in ***Table 4.3.3***.

| ***Reagents*** | ***Conditions*** | ***Result*** |
|---|---|---|
| ***4.3.15**, $^{n}$BuLi* | *THF, -78 $^{o}$C, 30 min* | *Butylphenyldibromophenylamine formed* |
| ***4.3.15**, Mg, $NiCl_2(dppp)$* | *$Et_2O$, rt, 18 h* | *Grignard reagent not substantially formed* |

***Table 4.3.3:*** *Conditions trialled for alkylation of tribromotriphenylamine **4.3.10**.*

Dibromination was then attempted using 2 equivalents of NBS to 1 of triphenylamine **4.3.7**. This route was not trialled earlier as it was thought that this reaction may produce a mixture of mono, di, and tribrominated products; however the reaction progressed in excellent yield and selectivity. A Friedel-Crafts acylation installed the troublesome alkyl chain as a ketone. A first attempt to reduce the ketone using hydrazine (Wolff-Kishner reduction) was unsuccessful, but alkylketotriphenylamine **4.3.12** was subsequently successfully reduced *via* a reduction with triethylsilane to form alkyltriphenylamine **4.3.13**. A Miyaura borolation then yields the desired amine monomer **4.3.14**.

The amine monomer **4.3.14** was then subjected to Suzuki polymerisation with spiro monomers **4.3.4** and **4.3.16**; ***Scheme 4.3.4*** and ***Scheme 4.3.5***.

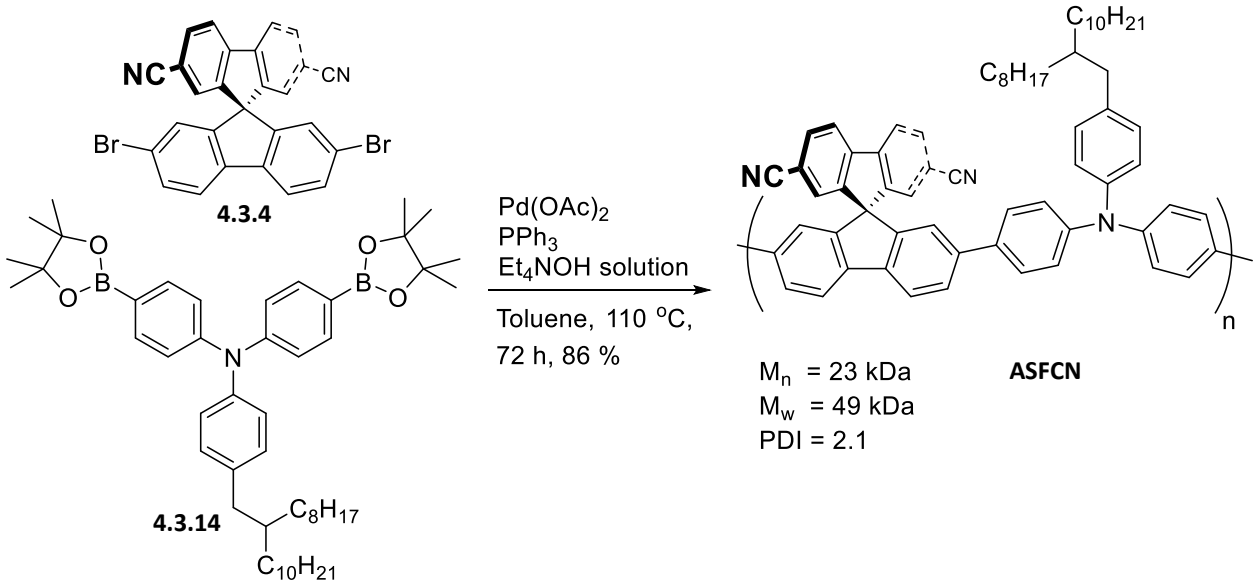


***Scheme 4.3.4:*** *Suzuki polymerisation to form* ***ASFCN****.*

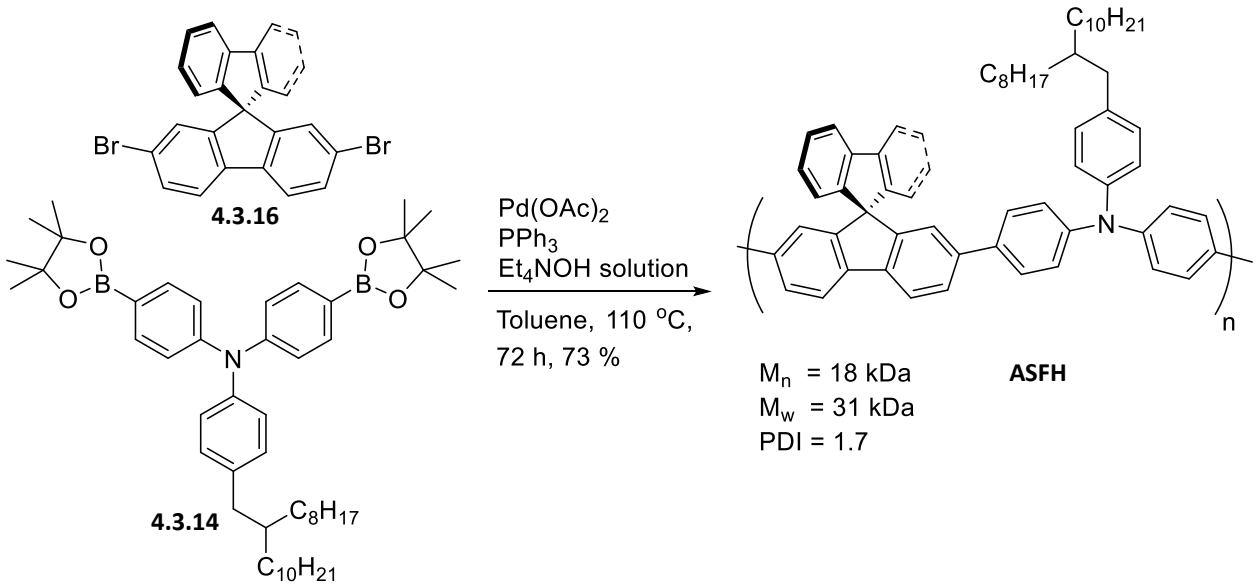


***Scheme 4.3.5:*** *Suzuki polymerisation to form* ***ASFH****.*

## 4.4 Physical and Optical Properties of SFH, SFCN, ASFH and ASFCN

Once synthesised, each polymer was analysed first by GPC, UV-Vis and PL before being sent to the University of Cambridge for more detailed analysis performed by Dr. Andrew Musser, who appears as co-author on the resultant paper.[121] The more advanced computational data for these polymers was obtained by Dr. Jarvist Frost at Imperial College London.

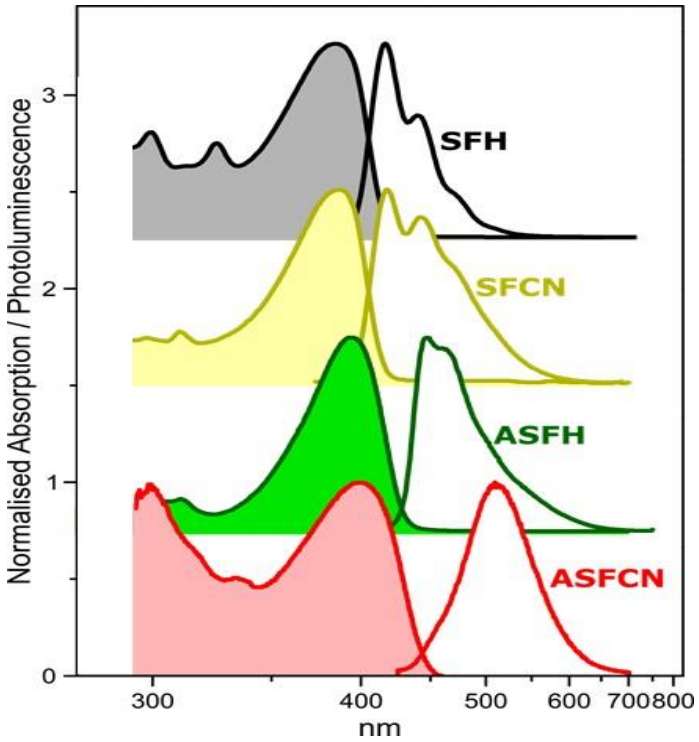


***Figure 4.4.1:*** *UV-Vis absorption (shaded) and photoluminescence (unshaded) of polymer thin films.*

| Polymer | $M_n$[a] / kDa | $M_w$[a] / kDa | PDI[a] | HOMO[b] / eV | $E_{gap}$[c] / eV | $\varepsilon$[d] / $M^{-1}cm^{-1}$ |
|---|---|---|---|---|---|---|
| **SFH** | 16 | 23 | 1.44 | -5.77 | 2.97 | 16104 |
| **SFCN** | 20 | 29 | 1.45 | -5.81 | 2.97 | 18384 |
| **ASFH** | 18 | 31 | 1.72 | -5.37 | 2.89 | 11844 |
| **ASFCN** | 23 | 49 | 2.13 | -5.42 | 2.79 | 7841 |

***Table 4.4.1:*** *Physical properties of polymers. (a) Determined by SEC (PS) using PhCl as eluent. (b) Determined by PESA. (c) Determined from thin film UV-Vis absorption onset. (d) Determined in $CHCl_3$ solution.*

All polymers show good molecular weights and are comparable to each other. The HOMO levels of all polymers are similar to related polymers PFO and TFB (-5.8 eV and -5.3 eV respectively).[131] Addition of orthogonal electron withdrawing groups has a stabilising effect on the HOMO, although this effect is small (< 0.05 eV for both sets of polymers).

***Figure 4.4.1*** shows absorption and photoluminescence spectra for all polymers. **SFH** and **SFCN** show similar absorption bands to PFO (onset at 417 nm); we may infer therefore that photon absorption is a process that is confined to the polymer backbone and is unaffected by the orthogonal groups. The PL spectra shows differences however. **SFH** shows emission similar to PFO and may be attributed to a singlet π* to π transition. **SFCN** has a broader and more red-shifted emission profile. It is therefore emitting from a lower energy state than **SFH**, from a new, lower energy $^1$CT state.[119, 132-135] The addition of an orthogonal acceptor has made available a low energy state that was not accessible before. This effect is small however, the emissive profile of these polymers has only changed slightly with the addition of an orthogonal acceptor, although the emissive state has changed from $^1$(π-π*) to $^1$CT.

Differences are more prominent in **ASFH** and **ASFCN**. The absorption spectra for **ASFH** is similar to TFB (onset at 429 nm), but unlike the previous polymers **ASFCN** shows a broadening and red-shift (onset at 444 nm) of the spectra as well as a decrease in extinction coefficient. This implies that the extra 'push' on the polymer backbone has caused the absorption to take on some charge-transfer character, often seen in linear donor-acceptor copolymers.[136-137] Consideration of the PL spectra shows a huge red shift in **ASFCN** and a reduction in extinction coefficient. This again implies a new low lying charge transfer state.

To elucidate the electronic structure of these polymers, the light absorbing/emitting properties were studied as a function of both time and temperature.

From the decay kinetics of the polymers shown in ***Figure 4.4.2***, we can observe how the addition of an electron poor orthogonal acceptor (black to khaki and green to red) results in emission over a longer period of time. **ASFCN** shows significant emission over several hundred nanoseconds, where triplets are the dominant species. This directly shows that emission from an excited state is dependent on the population of a triplet excited state. This observation could be attributed to triplet-triplet annihilation (TTA), however no change in the shape of the decay kinetics is observed when the laser power is decreased from a 1 kHz amplified to a 2.5 MHz unamplified laser with lower pulse energies. The long lifetime of the emissive species is therefore independent of the excitation density and therefore does not arise from TTA.

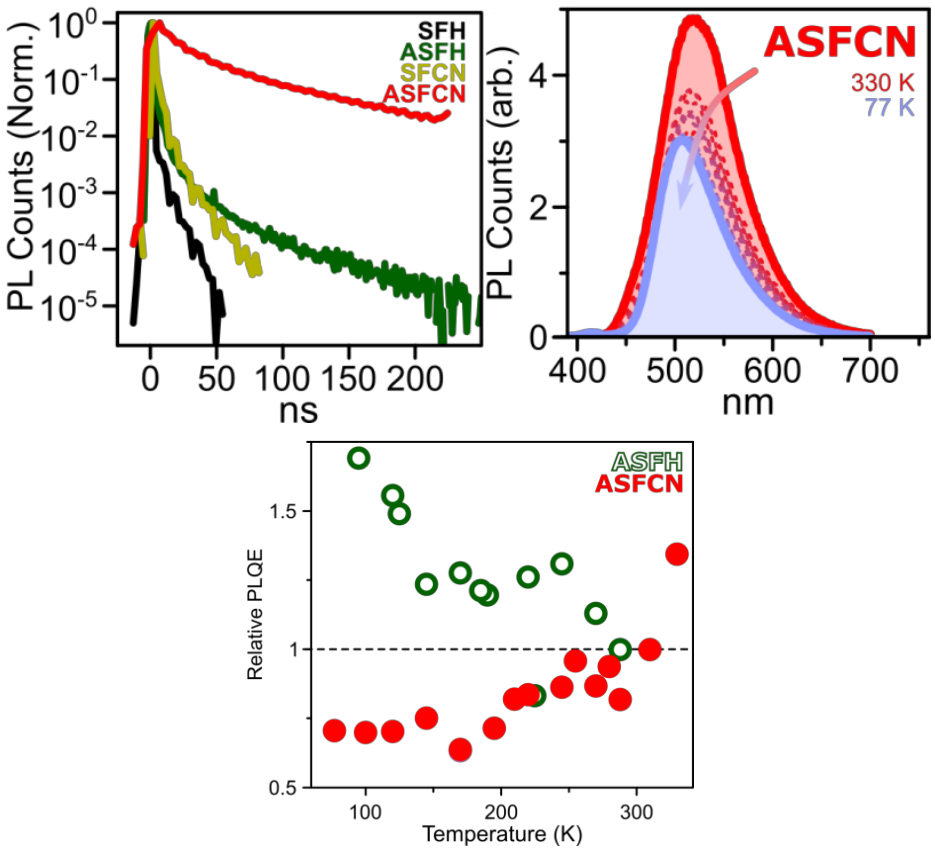


***Figure 4.4.2:*** *Photoluminescence dynamics in $\Delta E_{ST}$-tuned polymer films. PL decay kinetics measured for all polymer films, taken at 450 nm (**SFH** and **SFCN**) and 500 nm (**ASFH** and **ASFCN**) (top left). Steady-state PL spectra of **ASFCN**, from 330 K (red) to 77 K (blue) (top right). Integrated intensity for steady-state temperature-dependent PL measurements for **ASFH** and **ASFCN** (bottom). Measurements were taken during the cooling and warming phases to control for any permanent spectral changes. Data obtained by Andrew Musser.*

**ASFCN** also shows a temperature dependence on PLQY. As the temperature is decreased from 330 K to 77 K, the thin-film PL yield also decreases. We may infer from this that the lowest energy emissive state is populated *via* thermal activation. This temperature dependence is reversed for **ASFH**, where decreasing temperature increases PLQY. This is a typical effect of suppressing non-radiative decay pathways. The opposite behaviour of **ASFCN** is direct proof of the occurrence of TADF.

As further proof of this observation, PLQYs were obtained in solution and as a thin-film for all polymers, ***Table 4.4.2***.

| Polymer | Solution ($CHCl_3$) PLQY /% | Thin Film PLQY /% |
|---|---|---|
| **SFH** | >95 | 57 ± 4 |
| **SFCN** | 28 | 32 ± 4 |
| **ASFH** | 31 | 20 ± 1 |
| **ASFCN** | 5 | 16 ± 4 |

***Table 4.4.2:*** *PLQY measurements of all polymers. Solution PLQYs were calculated using a 9,10-diphenylanthracene standard. Thin film PLQYs were obtained using an integrating sphere by Alexandros Rapidis.*

TADF is a process that is enhanced in the solid state, a consequence of the suppression of collisional and intramolecular rotational quenching in solids.[138-140] This means that a material that is capable of TADF will show a much higher PL quantum yield as a thin film over solution, contrary to a standard light emitting system. As can be seen in ***Table 4.4.2***, **ASFCN** shows a threefold increase upon moving from solution to solid state photoluminescence. This is attributed specifically to non-radiative decay of the $^3(\pi\text{-}\pi^*)$ state in solution, where the backbone is less rigid and the $^3(\pi\text{-}\pi^*)$ state, located on the polymer backbone, is therefore more stable and more able to relax non-radiatively. RISC is therefore less likely; TADF is diminished and non-radiative decay is enhanced from the lower lying $^3(\pi\text{-}\pi^*)$ state. In the solid state where the $^3(\pi\text{-}\pi^*)$ state is closer to the emissive charge transfer state $^1$CT (populated from $^3(\pi\text{-}\pi^*)$ through $^3$CT and emissive through mixing with $^1(\pi\text{-}\pi^*)$), RISC does occur and fluorescence is observed. A Jablonski diagram of this complex system has been tentatively suggested in ***Figure 4.5.1*** based on this evidence, the transient absorption spectroscopy (TAS) studies, ***Figure 4.4.3***, and the DFT calculations, ***Figure 4.4.4***.

TAS is particularly suited to these energetic systems, as it deals with the absorption of excited, often optically dark states. The spectra of each polymer, **SFH**, **SFCN**, **ASFH** and **ASFCN** allow us to elucidate the energetic pathways of excitons in these systems. ***Figure 4.4.3*** shows the two DoA polymers **SFCN** and **ASFCN**. The unsubstituted polymers **SFH** and **ASFH** are not included in this work as their spectra was primarily used only to show the effects observed in the DoA polymers were a result of the addition of carbonitrile groups and to corroborate the assignment of excited states as backbone $^1(\pi\text{-}\pi^*)$ or $^3(\pi\text{-}\pi^*)$.

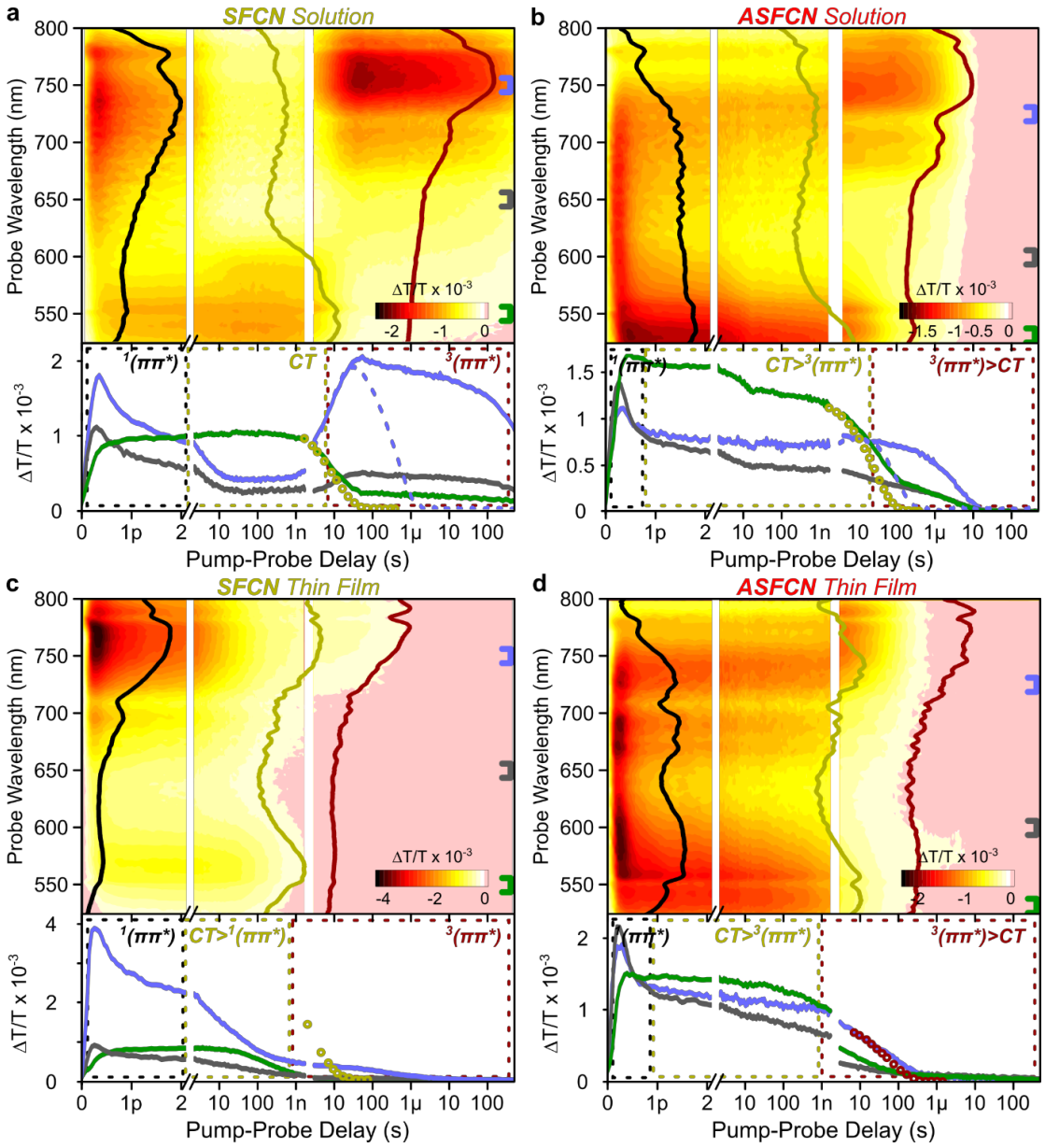


***Figure 4.4.3:*** *TAS spectra of* ***SFCN*** *(a and c) and* ***ASFCN*** *(b and d) in $CHCl_3$ solutions (a and b) and as thin films (c and d). Lower graphs show the population of the bracketed regions over time. Hollow circles show photoluminescence decay.*

Consideration of **SFCN** in solution, ***Figure 4.4.3 a*** shows the initial formation of a photo-induced absorption (PIA) band at 730 nm that corresponds to a backbone $^1(\pi\text{-}\pi^*)$ state. This state then decays to a CT state at 550 nm that eventually cleanly decays to a $^3(\pi\text{-}\pi^*)$ state visualised at 750 nm. The dashed blue line shows how this state relaxes rapidly in the presence of air, indicating triplet quenching by oxygen. Interestingly, the photoluminescence decay (hollow circles) has almost completed at the onset of the formation of the $^3(\pi\text{-}\pi^*)$ state. In other words, a majority of the initially formed $^1(\pi\text{-}\pi^*)$ excitons convert to CT states and

subsequently to a $^3(\pi\text{-}\pi^*)$ state, and the remaining $^1(\pi\text{-}\pi^*)$ states emit. This breaks Kasha's rule; photon emission occurs in appreciable yield only from the lowest excited state of a given multiplicity, as the residual emissive $^1(\pi\text{-}\pi^*)$ states are not the lowest singlet states.[141]

The thin film TAS of **SFCN** is more complex, ***Figure 4.4.3 c***. The initially formed $^1(\pi\text{-}\pi^*)$ state is again observed but the decay pathways are harder to elucidate here, and a much more complex mixture of electronic states is perceived. An important observation we can take from this data however is the existence of excited states after photoluminescence decay has terminated. If RISC could occur, these excited states could convert to emissive ones and PL decay would be seen until these excited states are depleted. From these two transient absorption spectra, we may conclude that **SFCN** has a $\Delta E_{ST}$ that is small, as decay from singlet to charge transfer to triplet is comparatively fast, but also that $\Delta E_{ST}$ is still large enough that RISC is not a substantial contributor to the emissive state.

**ASFCN** in solution shows a singlet state that very quickly decays to a charge transfer state, ***Figure 4.4.3 b***. This shows that the charge transfer states of this system are very close in energy to the initially formed $^1(\pi\text{-}\pi^*)$ states. This $^1$CT state is emissive and continues to emit until around 10 ns, when the only states still present are $^3(\pi\text{-}\pi^*)$ states. These $^3(\pi\text{-}\pi^*)$ states decay non-radiatively, and importantly are not able to undergo RISC to the emissive CT states. Unlike **SFCN**, the system has some $^3(\pi\text{-}\pi^*)$ state character over the entire lifetime of the excited species, CT states also show a similar longevity. This suggests some degree of mixing between the $^3(\pi\text{-}\pi^*)$ and CT states caused by a large decrease in $\Delta E_{ST}$. Small molecule systems have been reported with similar singlet-mixed triplet-pair states.[142-145] On long time scales, RISC becomes unavailable as conformational relaxation stabilises the $^3(\pi\text{-}\pi^*)$ state and quenches emission.

The solid state electronic dynamics of **ASFCN** are similar to those in solution, ***Figure 4.4.3 d***. Prompt $^1(\pi\text{-}\pi^*)$ decay results in the formation of CT and $^3(\pi\text{-}\pi^*)$ states and all three then decay in a similar fashion. After ~ 1 ns, the $^3(\pi\text{-}\pi^*)$ state begins to dominate, however the decay of this state matches directly the decay of photoluminescence (hollow circles). RISC allows the $^3(\pi\text{-}\pi^*)$ state to convert to a CT state and emit. The fact that this is only seen over the entire lifetime of the system in the solid state shows that conformationally locking the $^3(\pi\text{-}\pi^*)$ state is integral to maintaining a small energy gap between it and the emissive CT states.

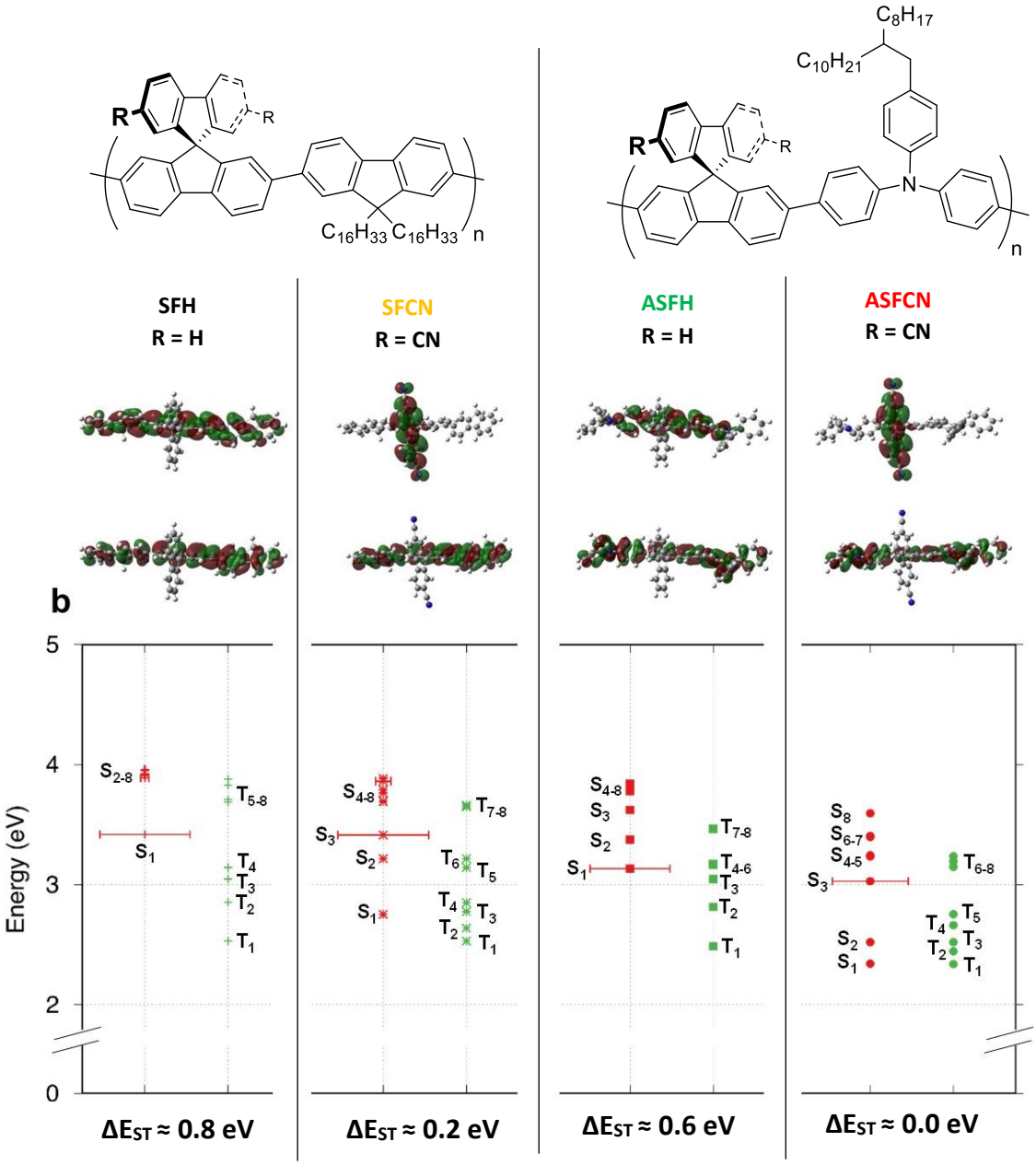


***Figure 4.4.4:*** *DFT calculations of MO distributions of polymer HOMO/LUMO (upper/lower) (a) and Jablonski diagram of singlet (red) and triplet (green) states (b) calculated by LR-TD-DFT at B3LYP/6-31G*. The width of the state indicates the absorption oscillator strength. Polymers are simplified as short chain oligomers for simplicity. Calculations run by Jarvist Frost.*

***Figure 4.4.4*** shows computational calculations of the energy levels of all four polymers calculated using B3LYP/6-31G*. It can be seen from the HOMO/LUMO distributions that upon the addition of electron withdrawing groups to the orthogonal unit, the LUMO is moved from

the polymer backbone of **SFH** and **ASFH** to the orthogonal unit of **SFCN** and **ASFCN**. Thus for the DoA polymers **SFCN** and **ASFCN**, the spatial overlap of the HOMO and LUMO has been dramatically reduced. Some overlap still remains however, as spiro linkages allow a small degree of electronic communication between moieties.[146]

The absorption profile of all polymers remains a π→π* transition from the polymer backbone to the polymer backbone. This has been previously observed in ***Figure 4.4.1***. Emission in the form of fluorescence is then observed from the lowest lying singlet state, $^1$(π-π*), in the case of the reference polymers **SFH** and **ASFH**. The excited $^1$(π-π*) state in the DoA polymers **SFCN** and **ASFCN** however may undergo internal conversion of a lower energy $^1$CT state, located on the orthogonal acceptor. This $^1$CT state has been stabilised through the addition of neighbouring electron withdrawing groups and now lies below the $^1$(π-π*) state of the polymer backbone. The CT states are a mixture of states containing singlet and triplet character localised on the orthogonal moiety and spatially separate from the polymer backbone. The calculated Jablonski diagram clearly shows the DoA polymers have many more states below the initial $^1$(π-π*) exciton that may interact.

In **SFCN** these CT states, mixtures of low lying states on the orthogonal moiety, are around 0.2 eV less stable than the backbone triplet, $^3$(π-π*). The π* portion (as well as the π) of $^3$(π-π*) is calculated to reside on the polymer backbone, and therefore the $\Delta E_{ST}$ of this system is calculated to be the difference between the new CT states and the original $^3$(π-π*) of the naked polymer. Since $^3$(π-π*) is spatially separate and more stable than the CT states, RISC does not occur and **SFCN** exists as a long lived tripletly excited species.

The lowest lying orthogonal excited states of **ASFCN** are very close in energy to the $^3$(π-π*) of the backbone. $\Delta E_{ST}$ of this system is therefore very small and the system is capable of RISC and therfore TADF, as in similar small molecule systems.[147]

## 4.5 Conclusions

The theoretical predictions of ***Figure 4.4.4*** are in agreement with the conclusions of the photoluminescence data of ***Table 4.4.2*** and the transient absorption spectroscopy of ***Figure 4.4.3***. It may be unambiguously concluded that the addition of electron withdrawing groups to an orthogonal moiety in a polymer localises and stabilises the orthogonal π system. This effectively isolates the excited electron of an exciton from the ground state electron, which results in a lessening of $\Delta E_{ST}$.

A polymer with small (≈ 0.2 eV) $\Delta E_{ST}$ that has a long lived non-emissive triplet excited state and a polymer with a negligible (≈ 0.0 eV) $\Delta E_{ST}$ that undergoes TADF have been synthesised. By synthesising related polymers with an orthogonal, but not electron withdrawing moiety, we have proven that the interesting photophysics of these systems is a result of our initial hypothesis of separating energy levels in space.

By analysing these polymers using TAS, the complex system of excited state energy levels has been elucidated for each system. ***Figure 4.5.1*** shows a tentative simplified Jablonski diagram for each polymer, where the orbitals most populated through exciton decay are shown with the electronic transitions that populate them. In the simplest case, **SFH** and **ASFH**, where the frontier orbitals are localised to the polymer backbone, absorption into an excited singlet state decays radiatively *via* fluorescence. The orthogonal groups themselves have no effect on the band structure of these polymers (the same transitions are observed for **PFO** and **TFB**) as the π* orbitals of the orthogonal groups are much higher up within the conduction band of the polymer. Triplet states are not formed in these systems.

Stabilisation of the orthogonal π* orbitals *via* addition of electron withdrawing carbonitrile groups moves the orthogonal molecular orbitals down to an energy lower than that which is absorbed into on the backbone. This allows an exciton in the $^1(\pi\text{-}\pi^*)$ orbital (backbone) to decay to a $^1$CT state (orthogonal), formed as a result of the new lower energy states on the orthogonal moiety. The near equivalency in terms of energy of a $^3$CT state allows electron spin flip. In the case of **SFCN**, the $^3$CT state is close enough in energy, and has enough overlap through the spiro linkage, to populate the $^3(\pi\text{-}\pi^*)$ of the polymer backbone. The $^3(\pi\text{-}\pi^*)$ state is 0.2 eV lower in energy and not capable of RISC however, and as it is non-radiative, acts as an exciton 'trap'. **SFCN** therefore has a very long exciton lifetime, but a very low photoluminescence lifetime. Photoluminescence in this system is observed only from residual

$^1(\pi\text{-}\pi^*)$ states formed from photon absorption and $^1$CT states that have not decayed non-radiatively to the $^3(\pi\text{-}\pi^*)$ state through the $^3$CT. Emission from these two states is what causes the broad emission profile of **SFCN**.

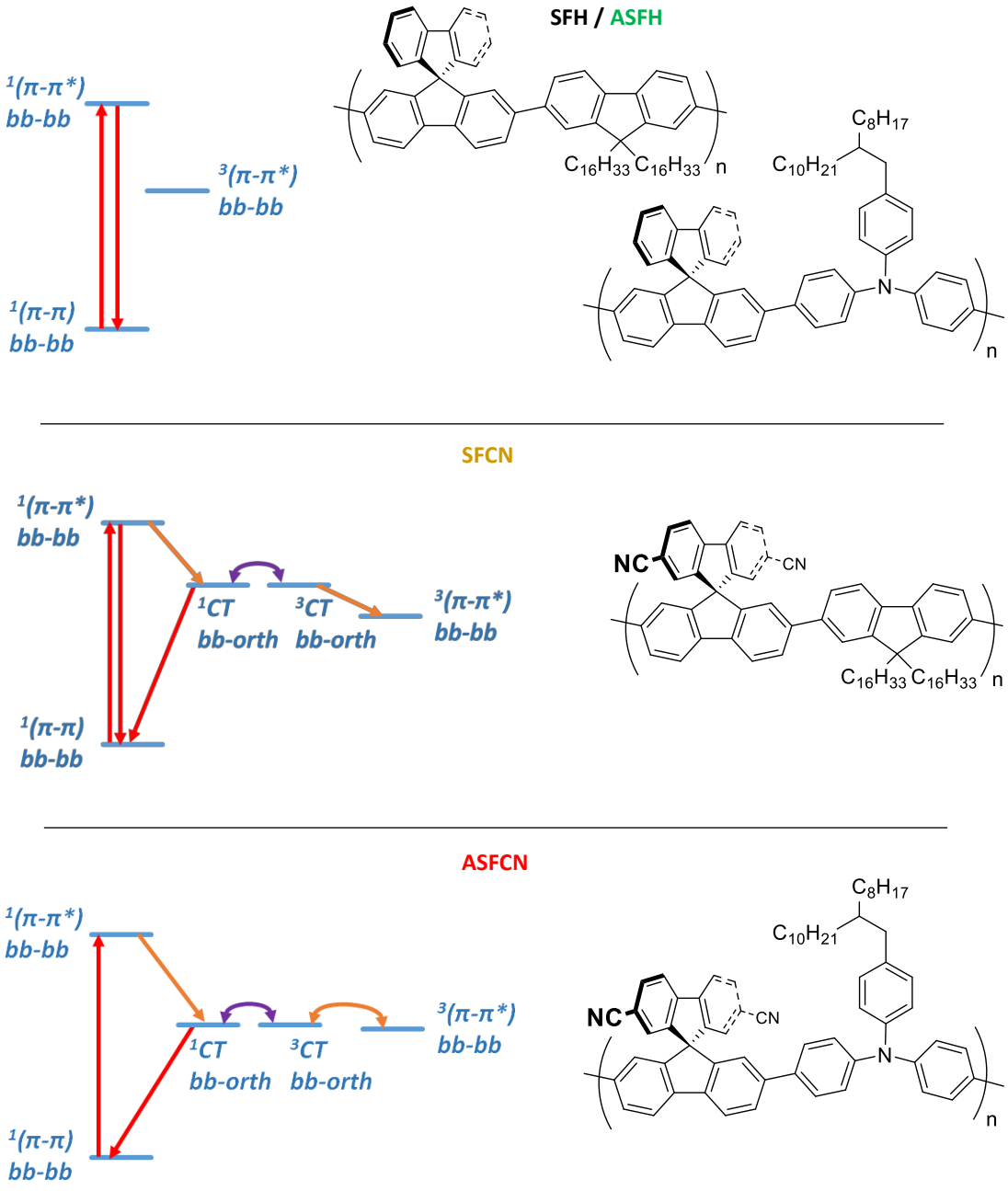


***Figure 4.5.1:*** *Proposed simplified Jablonski diagrams of exciton decay for* ***SFH/ASFH*** *(top),* ***SFCN*** *(middle) and* ***ASFCN*** *(bottom). 'bb' refers to an electron on the polymer backbone, 'orth' refers to an electron on an orthogonal moiety.*

In **ASFCN**, the $^3(\pi\text{-}\pi^*)$ state is very close in energy to the CT states on the orthogonal unit, which have been further stabilised by a more electron rich polymer backbone. The effect of this is excited electrons localised on the polymer backbone, in the lowest excited triplet state $^3(\pi\text{-}\pi^*)$, are able to undergo RISC and excited states are able to emit from the weakly fluorescent $^1$CT state. As with **SFCN**, residual $^1(\pi\text{-}\pi^*)$ may also emit which again causes emission profile broadening. RISC allows all excited electrons to emit over a long period of time. The dynamics of this system are slightly different in solution however, where the additional rotational freedom of the polymer backbone stabilises the $^3(\pi\text{-}\pi^*)$ and the system becomes more like that of **SFCN**. An OLED created from **ASFCN** or a similar material would be in the solid state. Since all excitons may emit from this semiconducting system through RISC to an emissive state, the theoretical internal quantum efficiency is raised to 100%, resulting in highly efficient polymeric light emitting materials.[148]

Although the initial aim of this project was to minimise $\Delta E_{ST}$ to the point where a polymer was capable of TADF, the fact that **SFCN** forms long-lived triplet states is also significant. The generation of long-lived excited states is of great interest in creating semiconductors for solar energy capture applications, as exciton lifetime is intrinsically linked to successful charge separation.[149-151] Triplet generating materials are also of interest for applications such as photocatalysis or singlet-oxygen generation for medicinal purposes.[28, 71, 152]

The applicability of DoA polymers is not limited to the polymers described above. A high proportion of common monomers contain a bridgehead carbon that may conceivably be converted to a spiro linked orthogonal acceptor. The backbone polymer may therefore be substituted for any of a large library of known polymers and is therefore highly tuneable. The ground state physical properties are left unchanged by the addition of an orthogonal acceptor, maintaining the desirable properties of the parent polymer. The orthogonal acceptor is also highly tuneable. The fluorene unit may be substituted at any position for any desired moiety, and may of course be substituted entirely for any other unit containing an aromatic bridgehead carbon. This tuneability and relevance to previous work on conjugated polymers makes the DoA design of organic semiconductors an interesting new approach to energy level design in electronic devices.

# Chapter 5: Circularly Polarised Light Emitting Polymers: Synthesis of Chiral Monomers

## 5.1 Introduction

Circularly polarised light (CPL) refers to an electromagnetic wave that has an electrical field component that has a constant magnitude but rotates around a perpendicular axis relative to the direction of the wave over time. It differs to linear polarised light which has an electrical field that changes in magnitude from n to –n on a plane parallel to the direction of the wave, ***Figure 5.1.1***.

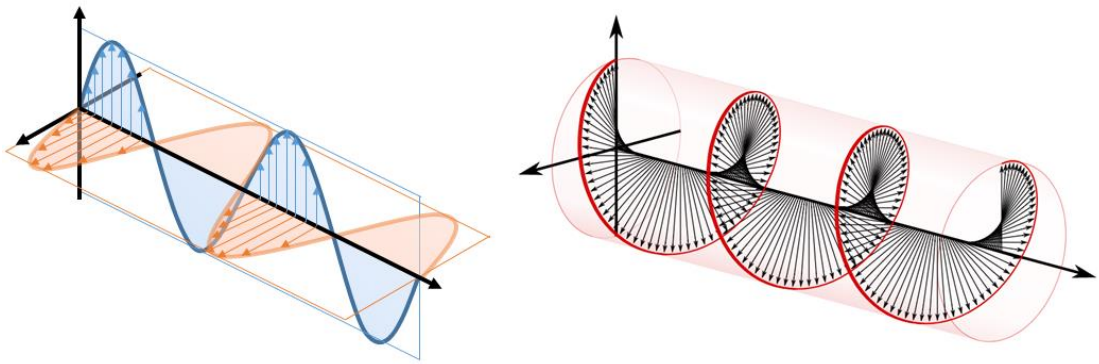

***Figure 5.1.1:*** *Linearly polarised light in yz plane (blue) and xz plane (orange) (left) and right handed circularly polarised light (right). Arrows refer to magnitude and direction of electric field as the wave travels along the z axis.*

Chiral molecules may be utilised to emit CPL in LEDs, or to detect CPL as OFETs.[153-154] Early work used chiral lanthanide complexes,[155] however more recently purely organic systems have been developed for applications in high efficiency display devices,[156-158] optical quantum information processing,[159-160] and optical spintronics.[161]

Helicenes have been shown to be attractive molecules for these types of applications.[154, 162-163] As a series of *ortho*-fused aromatic rings, helicenes have induced chirality as conjoined rings may not occupy the same space. This creates a helical structure that may exist in both right and left handed forms that are fully conjugated. ***Figure 5.1.2*** shows some examples of helicenes used for CPL based applications.

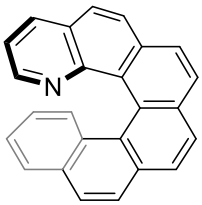


***Figure 5.1.2:*** *Helicene structure used in CPL application devices. Shown to cause emission of CPL when doped into F8BT,[163] and may be used as a single small molecule in the detection of CPL in a transistor.[154]*

Polymers have been also been utilised, although there are fewer examples. Polyfluorene may be synthesised with chiral side chains.[164] This results in emission from the non-chiral polymer chain moderated by the side chains to result in an increase in the polarisation of the emission.

By emitting from a charge transfer state that is itself chiral (electrons are separated across a stereocentre), it is believed that a great increase in the effective polarisation of emission may be observed. The basic motif and synthetic route described in the previous chapter may be used for this application. The spiro centre may be converted to a stereocentre if the rings A and B, and C and D are different, ***Figure 5.1.3***.

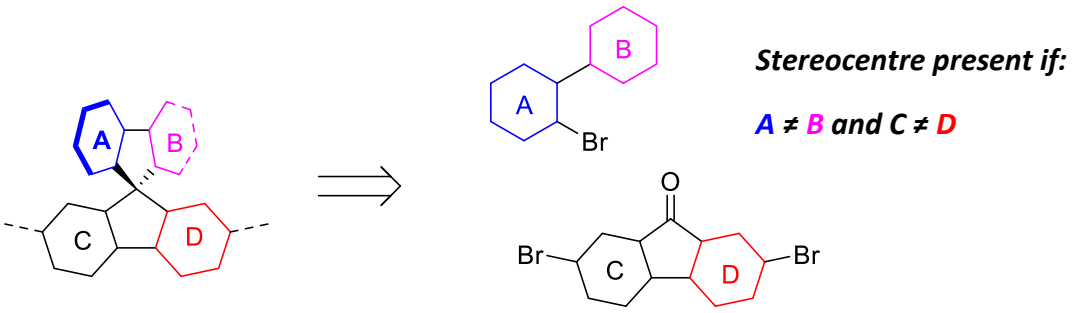


***Figure 5.1.3:*** *Retrosynthesis of chiral spiro monomer.*

Throughout this chapter, the colour scheme used for the ABCD rings in ***Figure 5.1.3*** will be used to distinguish which ring system is being synthesised. Different substitution patterns and ring sizes were trialled for each ring, however the basic spiro structure for the end product

was always the same. Ideally, the synthesis of the spiro monomer would be enantiospecific. A modest *ee* would be acceptable in this case however, as light emission would still be polarised. The extent of polarisation would clearly be reduced, but would be adequate in a proof of concept material.

## 5.2 Synthesis of AB Ring System

Work began with the synthesis of an asymmetric biaryl system with an *ortho* bromide, the AB ring system from ***Figure 5.1.3***.

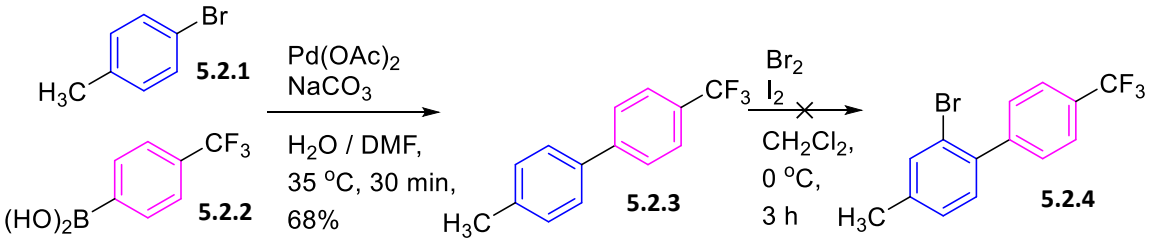


***Scheme 5.2.1:*** *Suzuki coupling to form asymmetrical biphenyl* ***5.2.3*** *and subsequent unsuccessful bromination.*

Asymmetric biphenyl **5.2.3** was synthesised *via* Suzuki cross-coupling of bromotoluene **5.2.1** and trifluorotolueneboronic acid **5.2.2**. In the final product, the benzylic group would be converted to a nitrile group in an analogous fashion to the previous chapter. Biphenyl **5.2.3** was then subjected to analogous bromination conditions to those used in the previous chapter for *ortho*-bromination of 4,4'-dimethylbiphenyl. An initial attempt using 1.2 equivalents of bromine was unsuccessful and returned starting material. The reaction was repeated with 5 equivalents of bromine but again, no reaction was observed. This lack of reactivity is attributed to the electronegativity of the electron withdrawing trifluoromethyl group resulting in a less electron rich ring system that is less nucleophilic towards bromine.

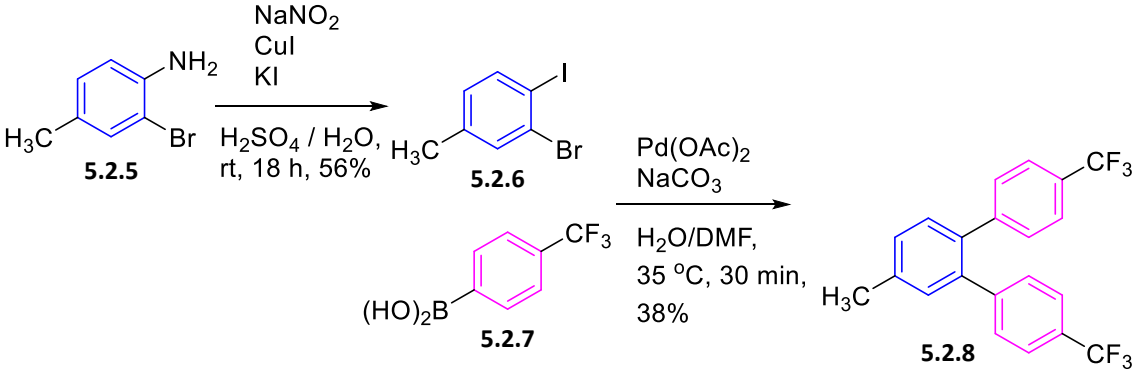


***Scheme 5.2.2:*** *Sandmeyer reaction to form* ortho-*bromoiodotoluene* ***5.2.6*** *and Suzuki reaction giving undesired disubstituted product* ***5.2.8****.*

Bromination of a biphenyl system is avoided if the bromide is installed before the coupling reaction. A Sandmeyer reaction of aniline **5.2.5** proceeded in good yield to give *ortho*-iodobromotoluene **5.2.6**. When subjected to Suzuki conditions, disubstituted product **5.2.8** was observed as the major product. It is thought that the neighbouring bromide of the palladium oxidative addition product **5.2.9** is causing a β-bromide shift of the palladium to yield biphenyl palladium **5.2.10**, which is faster than reductive elimination of the desired product. ***Figure 5.2.1*** shows a contracted Suzuki cycle of this reaction which highlights the β-bromide shift.

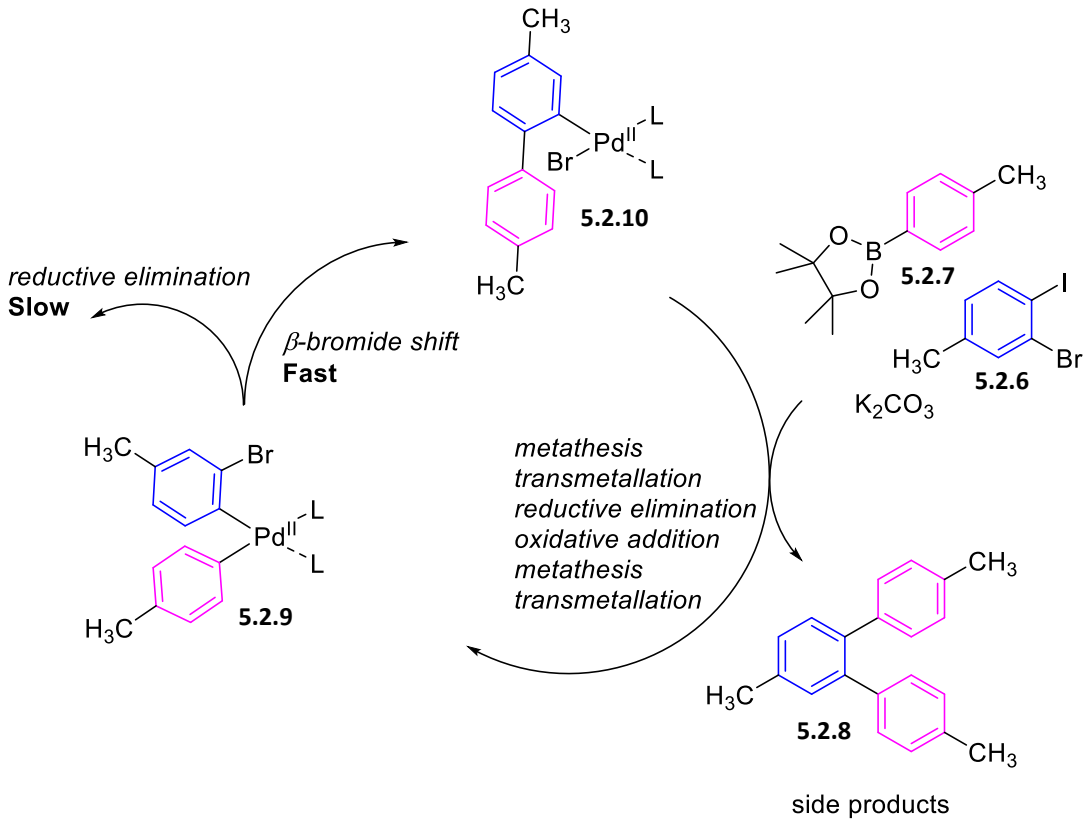


***Figure 5.2.1:*** *Contracted Suzuki cycle showing fast β-bromide shift leading to undesired disubstituted product* ***5.2.8****.*

This type of reaction could be of interest in terms of methodology. *Ortho* substitution without a directing group is not common in the literature, and this type of dual coupling may have applicability to many interesting products. If a second boronic species could be used for the second transmetallation step, the versatility of this reaction is further increased. While scientifically interesting, this type of methodological work is beyond the scope of the aims of this thesis.

The first attempted solution to the undesired bromide shift was to use a protecting group strategy. Trimethylsilyl (TMS) was initially trialled, ***Scheme 5.2.3***.

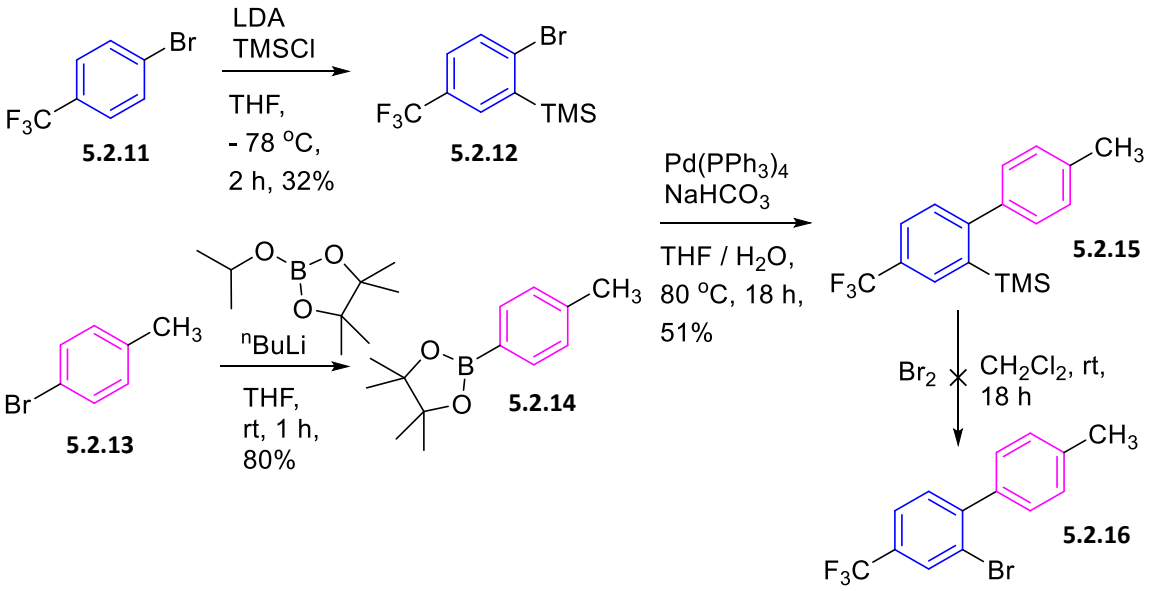


***Scheme 5.2.3:*** *TMS protecting strategy to AB ring system.*

Lithiation *ortho* to the bromide moiety of trifluorotoluene **5.2.11** was followed with silylation using TMSCl to yield trifluorotoluene **5.2.12**. This was coupled to toluene **5.2.14** under Suzuki conditions to give biphenyl **5.2.15**. Reaction with molecular bromine produced a complex mixture that was problematic to purify, possibly the result of overbromination. With greater purification effort, or perhaps more mild conditions, this route may be viable. However at this point it was judged more expedient to change the target molecule to one that does not initially contain an electron withdrawing group.

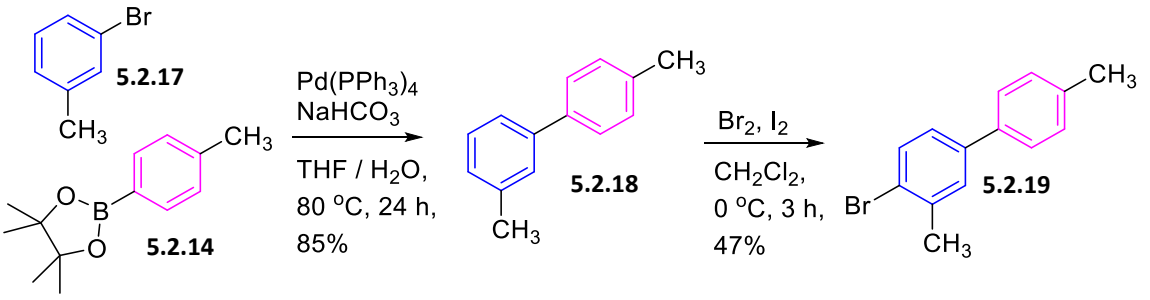


***Scheme 5.2.4:*** *Synthesis of* meta *methyl biphenyl* ***5.2.19*** *and (tentatively assigned)* para*-bromobiphenyl* ***5.2.19***.

Suzuki cross coupling was again utilised to synthesise asymmetric biphenyl **5.2.18**. Bromination gave a single product in good yield. The structure of this product has been tentatively proposed to be *para*-bromobiphenyl **5.2.19**. Bromination (*via* electrophilic bromine) will occur either *ortho* to the phenyl group (2 position), or *ortho* to the methyl group (4 position) on ring system A. This occurs as the *ortho*/*para* directing phenyl and methyl groups on the A ring both direct electrophilic attack to these positions. Sterically, it may seem that the 4 position is more favourable, however this effect seems to be overridden by electronic effects as can be seen from the bromination of 4,4'-dimethylbiphenyl in the previous chapter in which bromide is added *ortho* to the phenyl group (not *ortho* to methyl).

The stronger electronic effect of the phenyl group could direct the bromide to the 2 or the 4 position in this case however. To elucidate which position had been substituted, an NMR study was run. It was thought NOSEY NMR may show interactions between the protons of each ring system that are *ortho* to the other. These interactions would be different in the 2 or 4 substituted product. $^{13}C$, DEPT 135, HMBC and HSQC NMR were also run to unambiguously assign each proton and carbon in the structure. These studies were inconclusive however as complications arose surrounding the similar chemical shifts of multiple aromatic protons. The desired isomer has been previously reported, however the aromatic protons are described only as a 7H multiplet.[165]

A cruder method of assignment was then trialled. The cyclisation reaction to form a spiro bifluorene was attempted, but no product was observed. If this reaction had worked, the biphenyl must have been the desired 2-substituted isomer. However as it failed the absolute structure of biphenyl **5.2.19** is still unclear. The product has tentatively been assigned as the undesired 4-substituted isomer, as it failed to react to form a spirobifluorene.

One possible method of unambiguously assigning the regiochemistry of this molecule could be to use the halide-induced isotopic shift effect.[166-167] With an extremely high resolution $^{13}C$ NMR, the different shifts of $^{35}Cl/^{37}Cl$ (difference of ≈ 5 ppb) or $^{79}Br/^{81}Br$ (≈ 1 ppb) may be observed on a directly attached carbon atom. This is a powerful technique, but requires long scan times and large sample concentrations. If an alternative route to an AB ring system had not been found, more analytical effort would have been made in the assignment of this molecule.

Assignment would also be possible with comparative NMR. ***Scheme 5.2.5*** shows a method designed to unambiguously synthesise the 2-bromobiphenyl isomer.

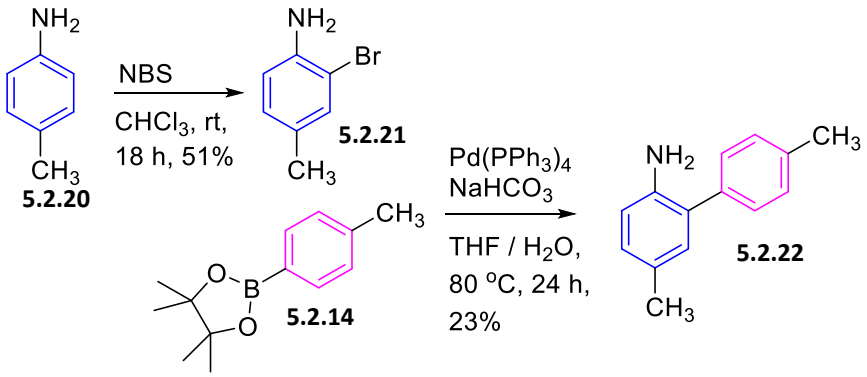


***Scheme 5.2.5:*** *Synthesis of aminobiphenyl* ***5.2.22****.*

The amine group of methylaniline **5.2.20** directs bromination to the *ortho* position to yield methylbromoaniline **5.2.21**. Suzuki coupling was successful and gave biphenyl **5.2.22** in moderate yield. A Sandmeyer reaction was planned as the next step. This was not attempted however, due to the failure of a similar route shown in ***Scheme 5.2.6***.

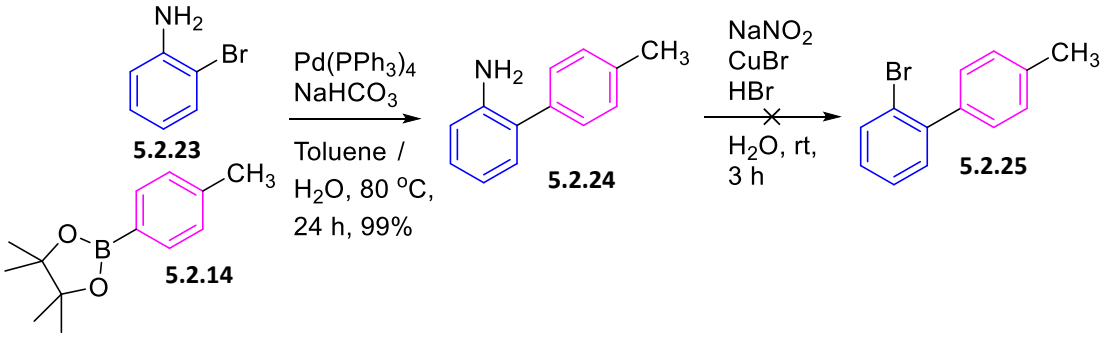


***Scheme 5.2.6:*** *Attempted synthesis of* ortho-*bromobiphenyl* ***5.2.25*** via *Sandmeyer reaction.*

Suzuki coupling proceeded in excellent yield to give biphenyl **5.2.24**. The conversion of amine to halide *via* Sandmeyer reaction was unsuccessful however. The reasons for this failure are unclear, sterically hindered amines have previously been reported to undergo these types of reaction.[168-169]

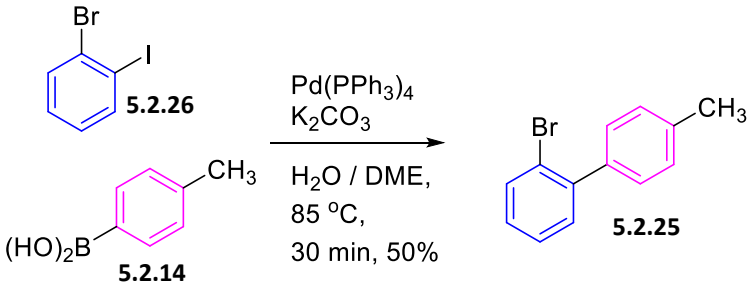


***Scheme 5.2.7:*** *Suzuki coupling using coordinating solvent to form biphenyl* ***5.2.25****.*

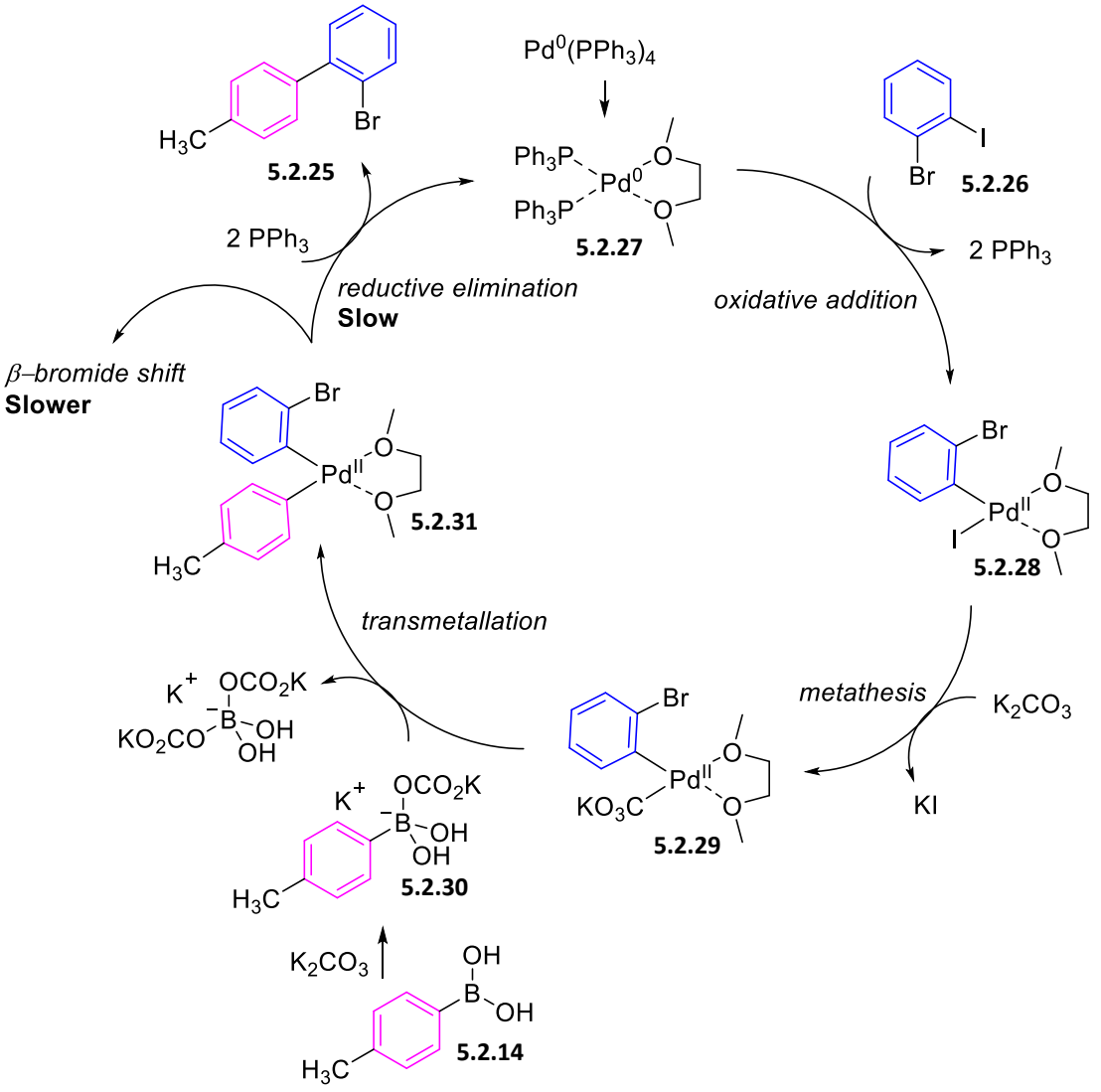


***Figure 5.2.2:*** *Catalytic cycle for Suzuki coupling of* ***5.2.26*** *and* ***5.2.14*** *using coordinating solvent.*

The Suzuki reaction of an *ortho*-bromoiodobenzene was previously unsuccessful as a β-bromide shift resulted in a disubstituted product, ***Scheme 5.2.2*** and ***Figure 5.2.1***. It was hypothesised that this step could be slowed through the addition of bulky ligands, or

coordinating solvents. Dimethoxyethane (DME) is a solvent that may coordinate to a palladium catalyst in a bidentate fashion. By using this solvent, *ortho*-bromobiphenyl **5.2.25** was synthesised in good yield, ***Scheme 5.2.7***. ***Figure 5.2.2*** shows a tentatively proposed catalytic cycle of this reaction, the important difference to ***Figure 5.2.1*** is the fast reductive elimination step. The speed of this step is fast only compared to the alternative β-bromide shift which has been slowed by the more bulky bidentate coordinating solvent DME.

It should be noted that this proposed reaction has been put forward very tentatively. Phosphine ligands are unlikely to be entirely displaced from Pd by the solvent, so the formation of **5.2.28** as it is shown is deemed to be unlikely. A more complicated structure involving phosphine ligands and DME is more likely to be the real complex formed after oxidative addition, but without NMR studies is impossible to define definitively. The proposed cycle should therefore be viewed as a possible explanation of why **5.2.27** is formed with DME as solvent, rather than as the definite mechanism.

By altering the substitution pattern of *ortho*-bromoiodobenzene **5.2.26** and/or phenylboronic acid **5.2.14**, it is believed that many types of 2-bromobiphenyls may be synthesised. With a reliable and fairly facile route to an unsymmetrical AB ring system in hand, the work reported in the next section could progress. Much of this work on both ring systems was completed concurrently.

## 5.3 Synthesis of CD Ring System and Chiral Spiro Monomer

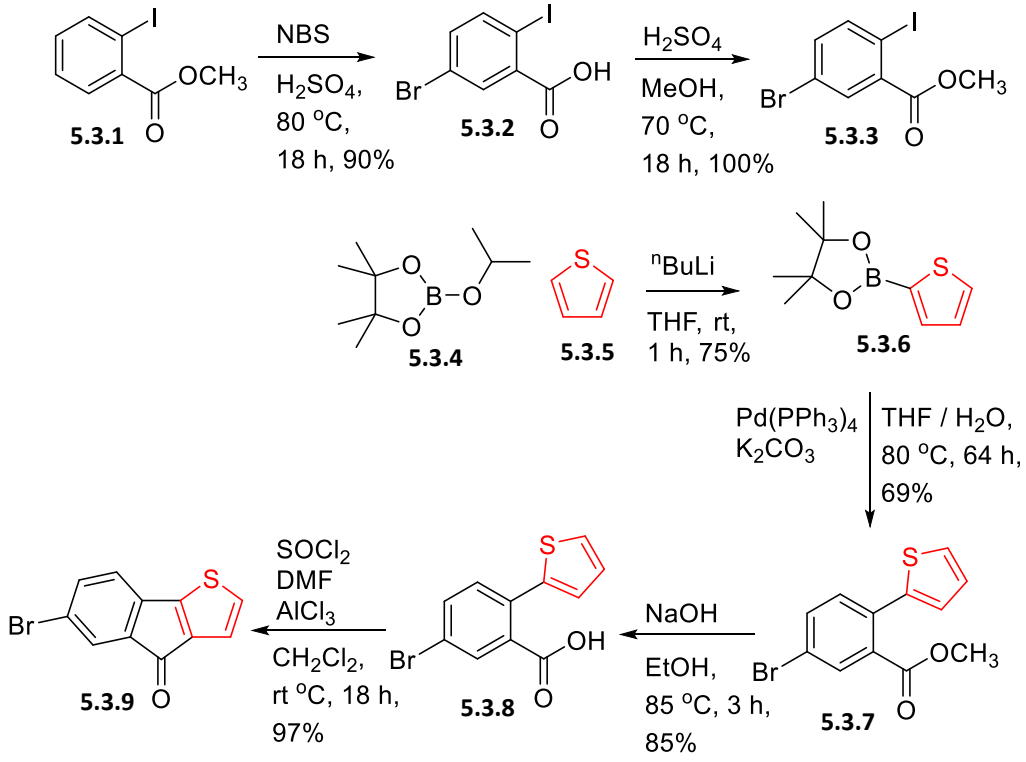


***Scheme 5.3.1:*** *Synthetic route to bromoindenothiophenone* ***5.3.9****.*

The CD ring system requires an unsymmetrical flourenone-like structure. ***Scheme 5.3.1*** shows the route towards bromoindenothiophenone **5.3.9**, a molecule with a cyclic ketone, differing ring systems and (after bromination of the thiophene moiety) two aryl halides. When reacted with a suitable AB ring system, a chiral spiro monomer may be produced.

Bromination of iodobenzoate **5.3.1** occurs *para* to the iodide moiety and *meta* to the ester. No *ortho* (to iodide) bromination was observed, presumably due to steric effects. The methyl ester was converted to a carboxylic acid under the reaction conditions to yield bromoiodobenzylic acid **5.3.2**. The methyl ester was reformed in quantitative yield and bromoiodobenzoate **5.3.3** was subjected to Suzuki conditions with boronic thiophene **5.3.6**. The methyl ester is then again converted to the benzylic acid. Friedel-Crafts conditions allow the 3-position of the thiophene moiety to attack into the acid chloride, ring closing the molecule and forming bromoindenothiophene **5.3.9**.

An interesting observation from this route is the colour of the final product. Bromoindenothiophene **5.3.9** (one phenyl and one thiophene group) is isolated as a bright orange powder. The related fluorenone (two phenyl groups) and cyclopentadithiophenone (two thiophene) exist as bright yellow and deep red solids respectively. It is interesting, but perhaps unsurprising, that the molecule between these two compounds exists as a solid with a colour between yellow and red.

Experimentation was performed on the CD ring system **5.3.9** and the AB ring system **5.2.25**. Grignard conditions were first employed, ***Scheme 5.3.2***, analogous to those used in the previous chapter.

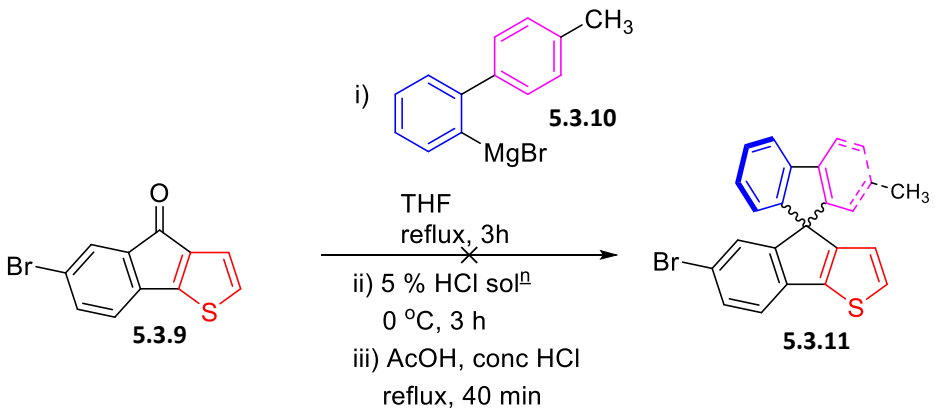


***Scheme 5.3.2:*** *Failed Grignard reaction to form chiral spiro molecule* ***5.3.11****.*

The Grignard reaction between CD ring system **5.3.9** and the Grignard reagent of AB ring system **5.2.25**, Grignard biphenyl **5.3.10** was successful, but only sporadically and was often low yielding. Even with careful purification and drying of starting materials, this reaction continued to be problematic. Rather than focus on solving this issue however, the reaction type was changed. Lithium halogen exchanged is achieved with $^{n}$BuLi, a reaction that proved to be much more facile then Grignard reagent formation, ***Scheme 5.3.3***. HCl in AcOH again promoted ring closure to form the spiro centre.

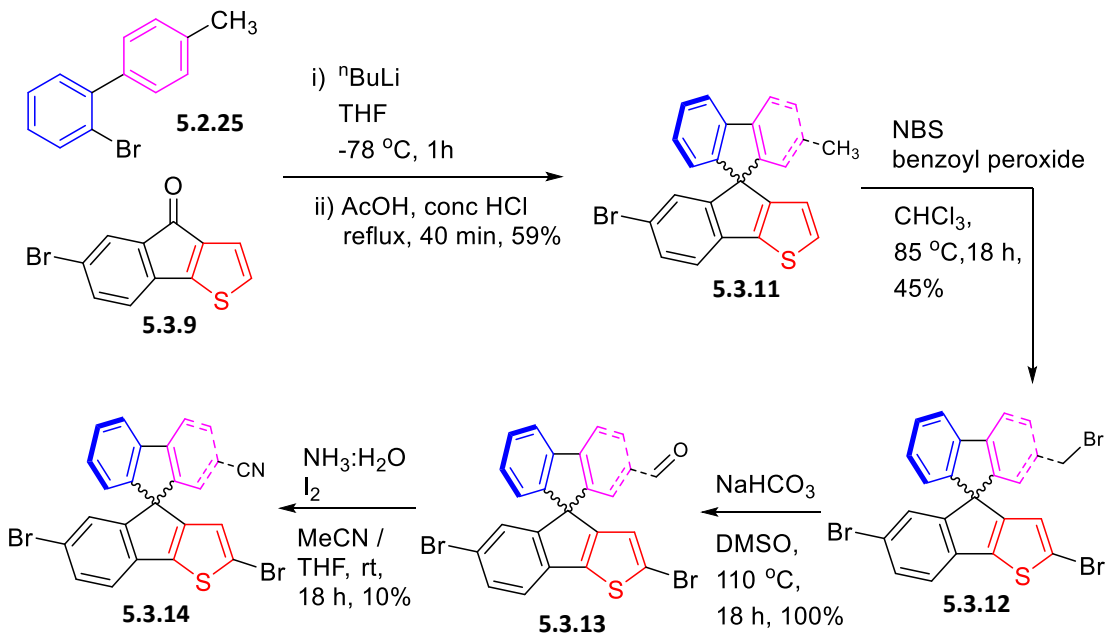


***Scheme 5.3.3:*** *Synthesis of racemic monomer* ***5.3.14****.*

The spirocycle formation was successful with $^{n}$BuLi, and yielded asymmetric, but racemic spiro centre containing molecule **5.3.11**. This was taken through the same steps that were used in the previous chapter to convert a benzylic position to a carbonitrile, and gave racemic monomer **5.3.14** in low yield. $^{1}$H NMR spectrometry suggests that a bromide had added into the 2-position of the thiophene moiety during the NBS reaction. The ≈ 50% yield may therefore be due to insufficient NBS in the reaction mixture. Mass spectrometry was unavailable during the time this synthesis was in progress, so all assignments have been made tentatively by consideration of the $^{1}$H NMR.

The racemic synthesis proves that the previously studied chemistry is still applicable to the new spiro ring system. Work towards an enantiospecific synthesis then progressed. The chirality of the system is created first when an alcohol is created from the nucleophilic attack of the Grignard reagent/lithium salt on the ketone, ***Figure 5.3.1***. The mechanism is understood to be $S_N1$, so this stereochemistry would be destroyed upon protonation of the alcohol and elimination of water.[125] Due to the large *ortho* toluene group however, we believe that rotation around the cyclopentyl-phenyl bond would be restricted, and subsequent ring formation would lead to specific products with matching stereochemistry to the original alcohol.

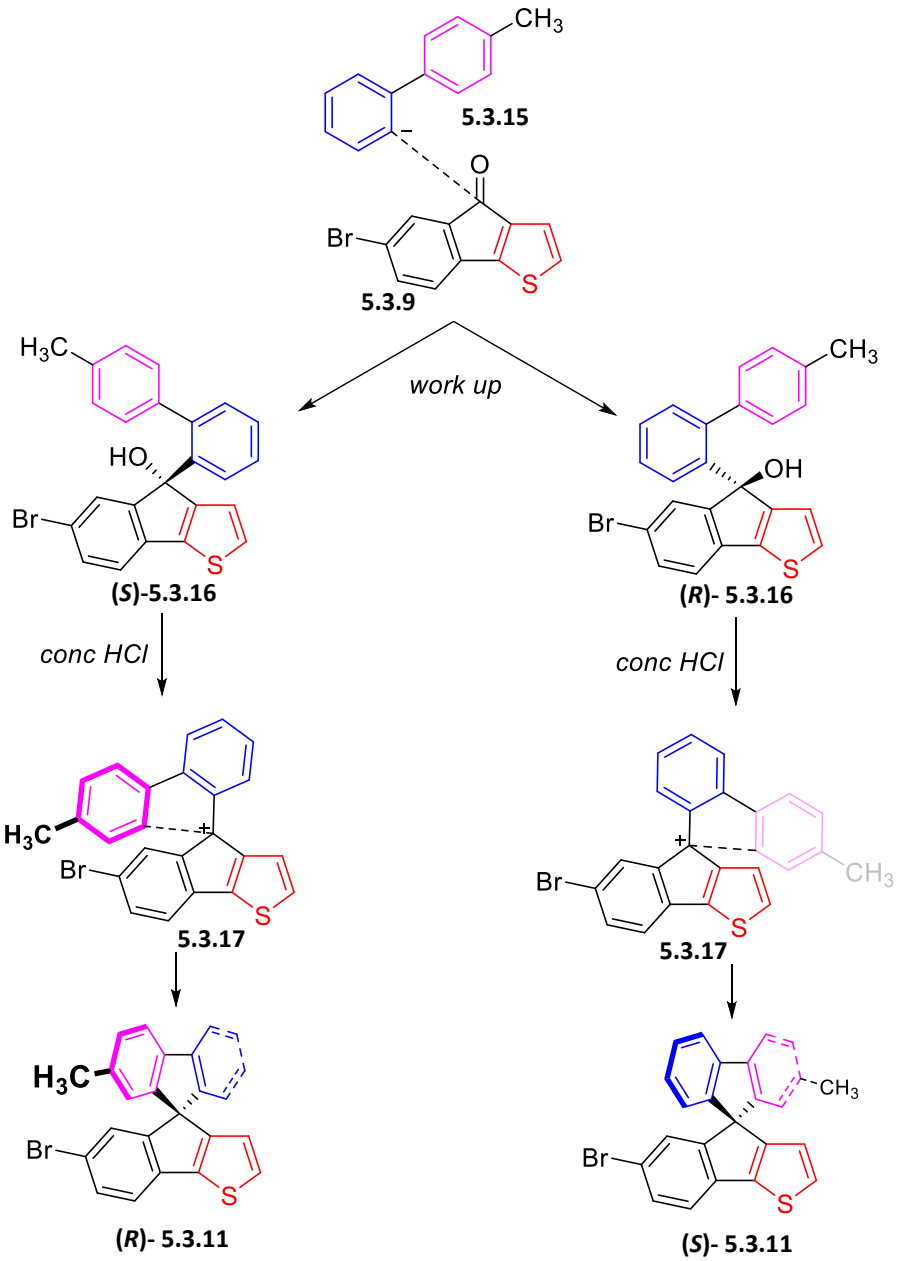


***Figure 5.3.1:*** *Spiro formation steps leading to chiral molecules* ***(S)-5.3.11*** *and* ***(R)-5.3.11****.*

As can be seen in ***Figure 5.3.1***, while carbocation **5.3.17** is not chiral, it is likely to exist in two distinct forms depending on the chirality of alcohol **5.3.16** upon treatment with concentrated acid. This means that separation of the isomers is possible at the alcohol stage, and would still (likely) lead to enantiospecific products. Initial methods of enantiospecific synthesis have therefore focussed around isomer separation at the alcohol stage, rather than inclusion of an enantioselective reaction.

The first attempted isomer separation involved isolation of the alcohol and recrystallization in the presence of brucine, a well-known chiral cocrystallising agent shown in ***Figure 5.3.2***. Brucine is a large and chiral molecule that is used to specifically promote the crystallisation of a single enantiomer of a molecule in solution. Racemic alcohol **5.3.16** was prepared by isolating it from the spiro-centre forming reaction before the addition of concentrated acid, ***Scheme 5.3.4***.

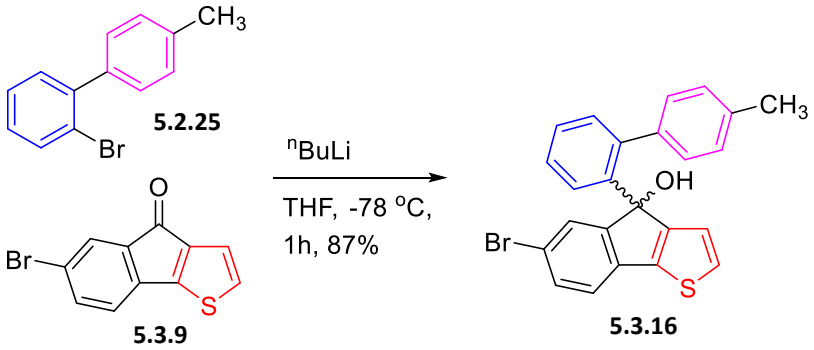


***Scheme 5.3.4:*** *Synthesis of racemic alcohol* ***5.3.16****.*

Attempts at recrystallization were unsuccessful. Multiple solvents were trailled; acetone, chloroform and methanol and ethanol. All failed to give significant amounts of crystallised product, and when an appropriate antisolvent was added slowly, only brucine was observed to precipitate. This implies that brucine was not encouraging precipitation of a single enantiomer. Focus was shifted instead to a chiral derivatising agent based strategy.

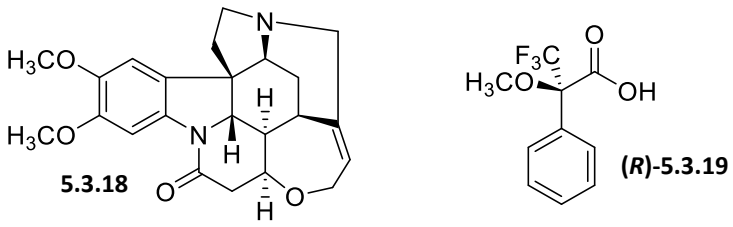


***Figure 5.3.2:*** *Structures of brucine* ***5.3.18*** *and Mosher's acid* ***(R)-5.3.19****.*

By reacting a racemic molecule (*R* and *S*) with an enantiopure derivatising agent (*eg.* only *R*), two diasteriomers are produced as the two steriocentres of the molecule may be in one of two configurations (*R,R* and *S,R*). Since diasteriomers are chemically non-equivalent, standard purification techniques such as column chromatography become viable to separate the two

products. Mosher's acid, ***Figure 5.3.2***, may be reacted with amines or alcohols to enable diasteriomeric separation,[170] or more commonly to determine *ee* of a sample which may be obtained through analysis of the $^{1}H$ and $^{19}F$ NMR spectra.[171-172] Mosher's acid has previously been reacted with a tertiary alcohol to determine its *ee via* a Steglich esterification.[173]

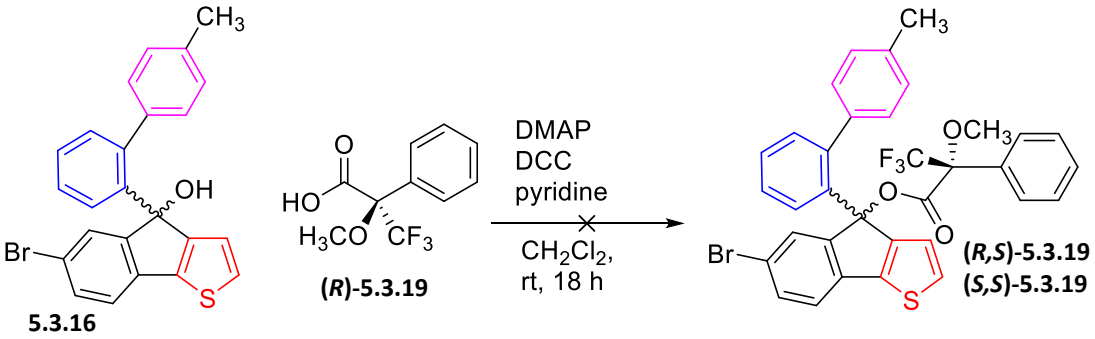


***Scheme 5.3.5:*** *Failed synthesis of diasteriomeric mixture of* **(R,S)-5.3.20** *and* **(S,S)-5.3.20**.

A Steglich esterification was attempted to form diasteriomeric mixture **(*R,S*)-5.3.19 / (*S,S*)-5.3.19** from alcohol **5.3.16** and (*R*)-Mosher's acid **(*R*)-5.3.19**. Note that the formal nomenclature of the Mosher's acid steriocentre is swapped from *R* to *S* upon esterification. Diasteriomers are thought to have formed from analysis of the $^{1}H$ NMR, where two peaks in the methoxide region are observed. $^{19}F$ NMR also shows a shift in the fluoride shift from unreacted Mosher's acid. Two peaks are observed, but the ratio of these peaks is ≈ 7:1 rather than the expected 1:1. If one enantiomer of alcohol **5.3.16** reacted faster (a steric effect) this ratio could be explained. These observations would imply diasteriomer formation.

Purification of the diasteriomers was attempted using a low polarity solvent system. The $R_f$ of the products was therefore low, and separation of the similarly polar diasteriomers more likely. Separation was not achieved however. Separation of diasteriomers with low numbers of hydrogen bond donors and/or acceptors has been shown to be more difficult, as described by Helmchen's postulates.[174-175] Helmchen's postulates are specifically for the separation of diasteriomeric amines using silica gel column chromatography, but may be used as a guide for other systems. Helmchen decribes diasteriomers binding to silica mainly by hydrogen bonding, so that only molecules with sufficient numbers of moieties that may form hydrogen bonds may be separated. Alcohol **5.3.16** contains no hydrogen bond donors/acceptors except the alcohol group itself, so interaction of mixture **5.3.19** with the silica will occur mainly from the Mosher's acid portion of the molecule. As this is the same in both diasteriomers, separation is not observed.

Due to the low availability of alcohol **5.3.19**, work on the enantiospecific synthesis of a chiral light emitting monomer was paused at this point. An applicable next step for this project has been included in the conclusion.

## 5.4 Conclusions

An asymmetric racemic spiro linked monomer has been synthesised. The route towards the monomer was discovered by splitting the molecule into 4 ring systems. Ring system A was designed as an aromatic group with *ortho* bromide and ring system B was designed to have various functionality. Initially, both A and B had benzylic groups that would be converted to electron withdrawing nitrile groups in the final monomer. Various iterations were trialled, but the final system had a single methyl group on the B ring and represents a simple molecule that could be synthesised fairly quickly and allowed further experimentation further down the route. It is thought that different functionality could be introduced by using the same chemistry on alternative starting materials (for example methyl group on the A ring, or in different positions for both).

The CD ring system was designed as a phenyl group for C and a thiophene for D. A five step convergent synthesis yields this system in sufficient amounts to enable experimentation on the spiro cycle formation reaction and subsequent steps. Again, it is thought that different substitution patterns around these ring systems would be possible. The variability is not as high as for the AB ring system however, as bromides must be installed to enable polymerisation.

The Grignard conditions used for spiro cycle formation in the previous chapter were not successful in a first attempt on these reactants. $^{n}$BuLi was substituted, and found to be a more reproducible choice for this reaction. Using similar chemistry to the previous chapter, the methyl group of ring system B was converted to a nitrile group. This created a monomer with a spiro steriocentre.

This monomer was synthesised in a racemic fashion however. First attempts at modifying the route to be enantioselective revolved around the tertiary alcohol created as an intermediate in the spiro cycle formation reaction. Chiral resolution was first attempted through a recrystallization with brucine, however separation of enantiomers failed. Mosher's acid was then employed to create two diasteriomers that would be separated by column chromatography. It is thought that the esterification was successful, however separation on standard silica column was not observed. We attribute this to a lack of hydrogen bond character, as stated in Helmchen's postulates.

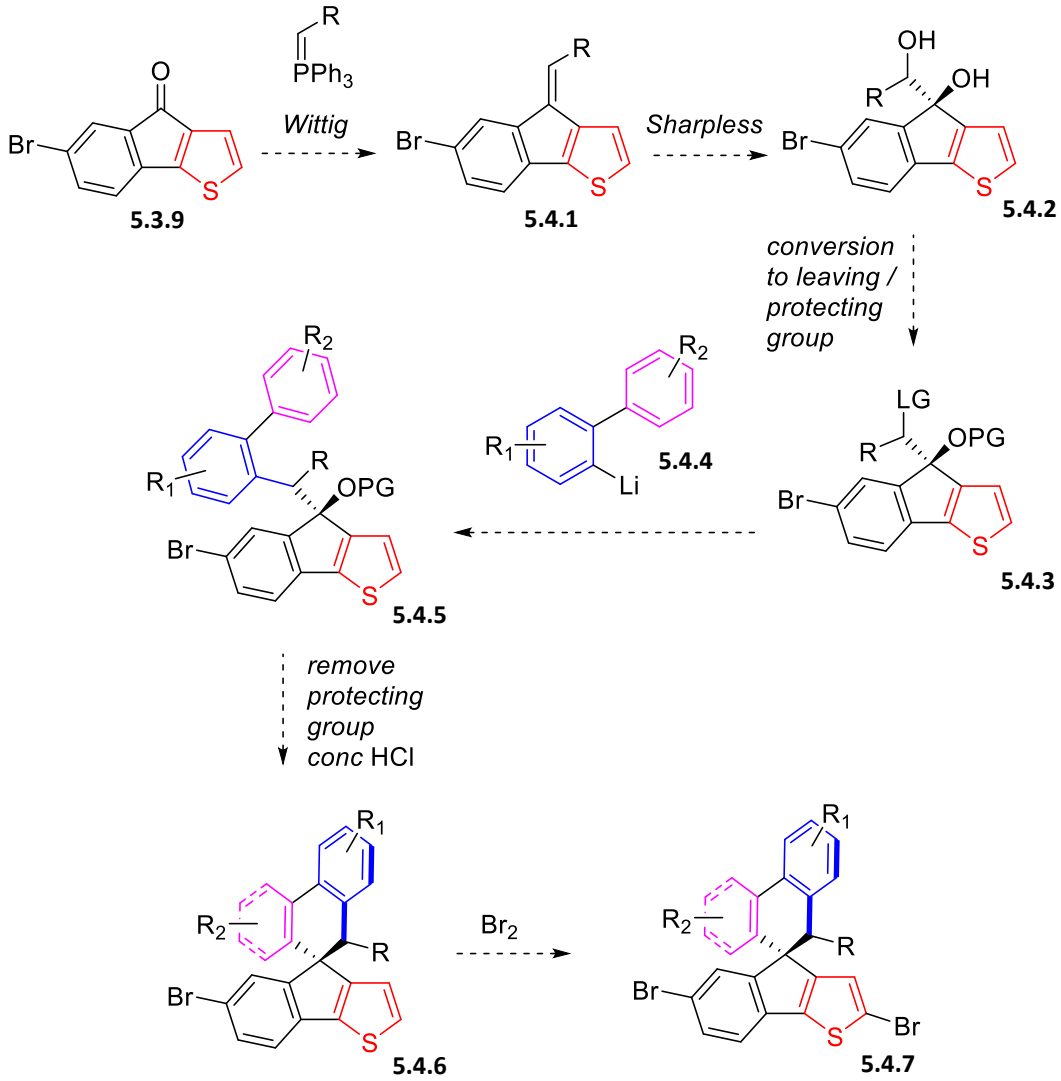


***Figure 5.4.1:*** *Proposed enantioselective route from bromoindenothiophenone* ***5.3.9*** *to chiral monomer* ***5.4.7****.*

A possible future method of synthesising a chiral spiro monomer is described in ***Figure 5.4.1***. A fully enantioselective synthesis is advantageous to simple isomer separation as it avoids the problematic purification of isomers as well as avoids the associated losses in yield.

Beginning with bromoindenothiophene **5.3.9**, Wittig chemistry yields an alkene. To more effectively control which isomer if formed, Horner-Wadsworth-Emmons, Stille-Gennari or Schlosser modifications may be trialled. The formation of a single isomer at this point is important as it will directly affect the *ee* of the subsequent Sharpless reaction. Which isomer is formed is not important however, as the choice of ligand in the Sharpless reaction will allow the eventual spiro centre to be set as either *R* or *S*. A Sharpless dihydroxylation installs the chiral tertiary alcohol.[176] The secondary alcohol may be converted to a leaving group, and the

tertiary may then be protected, indenothiophene **5.4.3**. Reaction of the AB system with $^{n}$BuLi forms the lithium salt **5.4.4** which will preferentially react with the leaving group and yield indenothiophene **5.4.5**. Deprotection of the tertiary alcohol allows the second stage of spiro cycle formation, the same chemistry as previously with the exception of the creation of a six rather than five membered ring. Bromination of the thiophene 2 position yields the monomer **5.4.7**.

A problem with this route has already been discussed. ***Figure 5.3.1*** shows how stereochemistry is maintained even though chirality is destroyed during the $S_N1$ mechanism of this reaction. It should be noted that this attributed mechanism is based on only a single paper, but that the paper in question has a very similar system.[125] With a one-carbon extended structure, rotation may be much more facile. This could racemise the system at this stage. Care must therefore be taken at this stage to ensure *ee* is not overly compromised. As the molecule would exist as diasteriomers (since the stereochemistry of the carbon attached to R has already been set and would not change during the route), $^{1}$H NMR should be sufficient to observe if any racemisation at this stage has taken place.

# Chapter 6: Experimental

## 6.1 General Procedures

**General procedure 1: The Formation of $A_2B_2$-Porphyrins from Relevant Dipyrromethane and Aldehyde**

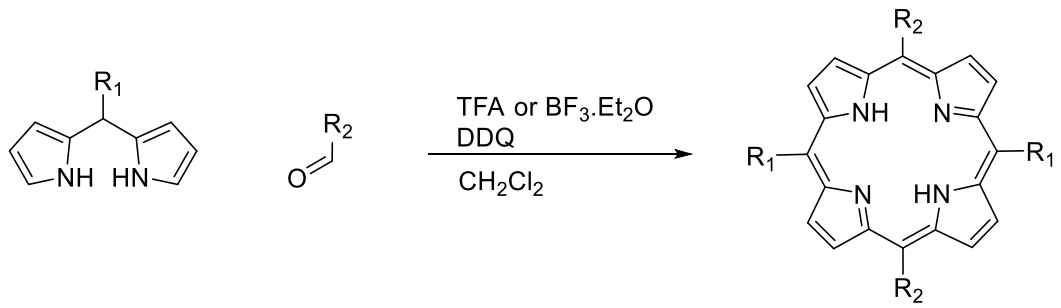


A solution of relevant dipyrromethane (1.0 eq), aldehyde (1.0 eq) and $CH_2Cl_2$ was degassed and either TFA or $BF_3.Et_2O$ (various equivalents used) was added slowly in the dark under an argon atmosphere. The reaction mixture was stirred for 30 min. DDQ (1.2 eq) was added and the reaction mixture was stirred for a further 4 h.

**General procedure 2: Platinum Complexation of Porphyrins with $PtCl_2$**

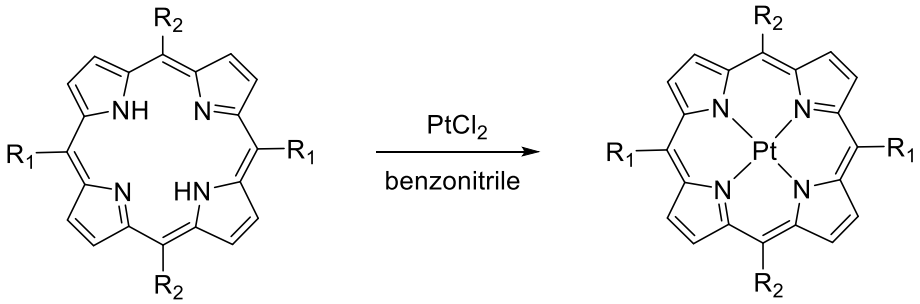


A solution of $PtCl_2$ (2 eq) in benzonitrile was heated to 100 °C. The porphyrin (1.0 eq) was added in one portion and the reaction mixture was heated to reflux and stirred for 18 h. The reaction mixture was then cooled and concentrated *in vacuo*.

**Reagents and Solvents:** All reagents and solvents were used as received. MeOH, $CH_2Cl_2$ and *n*-hexane were HiPerSolv grade. $Et_2O$ and EtOAc were GPR grade. Pet 40-60 refers to BDH AnalaR petroleum spirit 40-60 °C. All other chemicals were used as supplied unless otherwise indicated.

**Experimental techniques:** All reactions were carried out in oven-dried glassware under an argon atmosphere unless otherwise indicated. Air and moisture sensitive reagents were transferred by syringe. Reactions performed at temperatures other than rt were recorded as silicon oil bath temperatures. The phrase "concentrated *in vacuo*" refers to rotary evaporation. Brine refers to an aqueous solution of NaCl. Column chromatography was carried out using BDH (40-60 µm) silica gel and analytical thin layer chromatography was carried out using Merck Keiselgel aluminium-backed plates coated with silica gel. If necessary, components were visualised using combinations of ultra-violet light and potassium permanganate.

**Characterisation:** $^{1}H$ NMR spectra were recorded at 300 MHz on a Bruker AMX300 spectrometer, at 500 MHz on a Bruker Avance 500 spectrometer, or at 600 MHz on a Bruker Avance 600 spectrometer in the stated solvent using residual protic solvent $CHCl_3$ (δ = 7.26 ppm, s), DMSO (δ = 2.56 ppm, qn) or pyridine (δ = 8.74 ppm, s; 7.58 ppm, s; 7.22 ppm, s) as the internal standard. Chemical shifts are quoted in ppm using the following abbre*via*tions: s, singlet; d, doublet; t, triplet; q, quartet; qn, quintet; m, multiplet; br, broad or a combination of these. The coupling constants (*J*) are measured in Hertz. $^{13}C$ NMR spectra were recorded at 75 MHz on a Bruker AMX300 spectrometer, at 125 MHz on a Bruker Avance 500 spectrometer or at 150 MHz on a Bruker Avance 600 spectrometer in the stated solvent using the central reference of $CHCl_3$ (δ = 77.0 ppm, t), DMSO (δ = 39.52 ppm, septet) as the internal standard. Chemical shifts are reported to the nearest 0.1 ppm. UV-visible spectra were recorded, at room temperature, on a Thermo Unicam UV500 spectrometer, in $CH_2Cl_2$ solutions at concentrations of ~$10^{-5}$ M. Thin films of polymers were spin coated from $CH_2Cl_2$ solutions of 10 mg/mL on a Laurell spin coater at 2000 rpm for 30 s. Mass spectra was obtained from the mass spectrometry service at the Department of Chemistry, University College London. Number-average (Mn) and weight-average (Mw) molecular weights were determined against a polystyrene standard using an Agilent Technologies 1200 series GPC in chlorobenzene at 80 °C.

**PF MPP(Pt) optical properties, device fabrication and testing (work carried out by Dr. Guilia Tregnago):**

The optical properties of the copolymers have been investigated in the solid state. We deposited a 100 nm thick film for each compolymer *via* spin coating (1.8 krpm) a 2 wt.% toluene solution over a Spectrosil fused silica substrate. The steady-state photoluminescence (PL) spectra were recorded after exciting the PL with a 405 nm diode laser with an ANDOR Shamrock spectrograph coupled with an ANDOR Newton CCD unit. Time-resolved PL measurements were carried out with a time-correlated single photon counting (TCSPC) spectrometer using a pulsed diode laser (Edinburgh Instruments-EPL-405) at 405 nm as excitation source and a cooled photomultiplier (Becker & Hickl PMC-100-1) coupled to a monochromator and TCSPC electronics (Edinburgh Instrument Lifespec-ps TCC-900 PC card). The PL efficiency was measured using an integrating sphere method.[177] The copolymers were also tested in PLED devices as the active layer. OLEDs were fabricated by spin-coating (4 krpm) a 2.8 wt.% dispersion in water of poly(3,4-ethylenedioxythiophene)-poly(styrenesulfonate)[178] (PEDOT:PSS, Sigma Aldrich) to a thickness of a 80 nm over an ITO-coated glass pre-treated with oxygen plasma[179](10 min at 10.2 W). The substrates were then baked at 150 °C for 10 min in a nitrogen atmosphere to remove residual water. The active layer was deposited by spin-coating (2 krpm) a 2 wt.% toluene solution to obtain a thickness of 100 nm. Ca/Al electrodes (30 nm/150 nm respectively) were thermally evaporated under vacuum $10^{-6}$ mbar) on top of the active layer. Current-voltage-radiance characteristics were measured with a Keithley 2004 source meter and a calibrated Si photodiode (wavelength range of 200-1100 nm) coupled with a Keithley 2000 multimeter, electroluminescence (EL) spectra were taken with the ANDOR spectrometer described above.

**PDPA MPP(Pt) optical properties, device fabrication and testing (work carried out by Dr. Alessandro Minotto):**

Thin films and devices were prepared and analysed as for the **PF MPP(Pt)** polymers above. OLEDs were fabricated by using ITO/PEDOT:PSS anodes, active layer (90 nm) and Ca (30 nm)/Al (150 nm) cathodes.

**ASFCN and related polymers optical properties, device fabrication and testing (work carried out by Dr. Andrew Musser):**

Spectroscopic sample preparation: For solution measurements, polymers were dissolved in chloroform in nitrogen atmosphere to a concentration of 625 µg/mL. The solution was

transferred to a 1 mm path-length quartz cuvette (Hellma Analytics) and tightly sealed prior to removal from the glove box. For oxygen-exposure measurements, the cuvette was opened and the solution was bubbled with air for ~1 minute. Thin films were spun on cleaned quartz substrates from room-temperature chloroform solutions (5 mg/mL) at low speed (1500 rpm) in a nitrogen-filled glove box. They were stored under nitrogen and measured in vacuum or He exchange gas atmosphere. Where oxygen exposure was unavoidable, the films were kept under vacuum or purged with He vapour for >30 minutes prior to measurement. Photoluminescence spectroscopy: PL measurements were acquired on three systems, one equipped with a N2 bath cryostat and the others with a continuous-flow He cryostat. Steadystate photoluminescence spectra were collected on a Fluoromax fluorimeter (Horiba) with excitation at 370 nm, from above room temperature to near liquid-nitrogen temperatures each equipped with a continuous-flow He cryostat. Spectra were also collected down to liquid He temperatures using a pulsed laser at 407 nm (PicoQuant LDH400) run at 2.5 MHz and a 500 mm focal length spectrograph (Princeton Instruments, SpectraPro2500i) with a cooled CCD camera. Single-wavelength dynamics were acquired using the same excitation source and a time-correlated single photon counting system using a monochromator coupled to photomultiplier detectors (Hamamatsu R3809U-50). Simultaneously time- and spectrallyresolved photoluminescence decay was measured with a gated, intensified CCD camera (Andor, iStar) mounted on a 300 mm focal length spectrograph (Andor, Shamrock SR-303i). S4 Solid State Photoluminescence Quantum Yields Spectrosil substrates (UQG) were cleaned in acetone and IPA in ultrasonic bath (10min each step) and dried with N2. In a nitrogen glovebox, 5 mg/ml solutions in anhydrous chloroform were spin-coated at 1500 rpm. Excitation : λ = 405 nm (ThorLabs laser diode). Sample handling in a dark environment with yellow light (spin coating) and a small stylus torch (sample positioning during measurements). Measurements in a nitrogen glovebox. Spectra collected with ANDOR-Shamrock 163 spectrometer coupled with an ANDOR-Newton CCD unit. Solution Photoluminescence Quantum Yields Solution Quantum Yields were measured in dilute chloroform solutions (Amax ~ 0.02-0.05 in order to avoid inner filter effects and ensure linear response on the intensity. Samples were bubbled with Argon for 30 minutes prior to measurement. Quantum Yields are reported relative to Diphenylanthracene in cyclohexane (0.95). Spectra were recorded on a Horiba Fluoromax-4. All spectra are corrected. Transient absorption spectroscopy: Sub-picosecond transient absorption (TA) measurements were performed on a previously reported setup with slight modifications. 2 Narrow-band (~10 nm) excitation pulses at 400 nm were generated in an optical parametric amplifier (TOPAS, Light Conversion Ltd.) coupled to

the output of a 1 kHz regenerative amplifier (Spectra-Physics Solstice). The sample transmission was probed using broadband Top View of the setup S5 pulses generated in two home-built non-collinear optical parametric amplifiers (NOPAs) roughly spanning 500-1125 nm. The probe beam was split to provide a reference signal not affected by the pump to mitigate any laser fluctuation effects, and both were dispersed in a spectrometer (Andor, Shamrock SR-303i) and detected using a pair of linear image sensors (Hamamatsu, G11608) driven and read out at the full laser repetition rate by a custom-built board from Stresing Entwicklungsbüro. The differential transmission (ΔT/T) was then measured as a function of probe wavelength and pump-probe delay, with the pump-probe delay set by a mechanical delay stage (maximum extension ~1700 ps). This setup afforded a temporal resolution of approximately 120 fs. The same setup was employed for subnanosecond TA, using the third-harmonic (355 nm) nanosecond output of a Q-switched Nd:$YVO_4$ laser as the excitation source. The pulse duration and electronic jitter resulted in an instrument response of ~1.5 ns. Data is presented with a break at 1.5-3 ns, which marks the switch from sub-ps to sub-ns excitation setups and a change in excitation wavelength from 400 nm to 355 nm. Where both are presented together, sub-ns-excitation data was scaled to account for differences in excitation density between the two measurements.

## 6.2 Synthetic Techniques for Chapter 2

**2,7-dibromo-9H-fluorene**

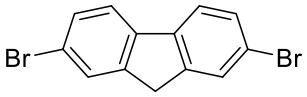


To a solution of fluorene (9.97 g, 60.0 mmol) and $I_2$ (1.52 g, 6.0 mmol) in $CH_2Cl_2$ (120 mL) at 0 $^oC$ in the absence of light was added a solution of $Br_2$ (6.50 mL, 126.0 mmol) in $CH_2Cl_2$ (24 mL) over 10 min. The reaction mixture was stirred at rt for 6 h. The reaction was quenched with $Na_2SO_3$ solution and the organic product was extracted with $CH_2Cl_2$ (100 mL). The combined organic fractions were dried over $MgSO_4$ and concentrated *in vacuo*. The resultant white powder was recrystallised from EtOAc to yield the product as white crystals (10.18 g, 31.4 mmol, 52%). $^1$H NMR (500 MHz, $CDCl_3$) δ 7.67 (s, 2H, $CH_2CCH$), 7.60 (d, *J* = 8.1 Hz, 2H, CBrCHC*H*), 7.50 (d, *J* = 8.1 Hz, 2H, CBrC*H*CH), 3.87 (s, 2H, $CH_2$); MS ($Cl^+$) *m/z* 322, 324 and 326 $(M)^+$. All spectroscopic data is in accordance with literature values.[180]

**2,7-dibromo-9,9-dioctyl-9H-fluorene**

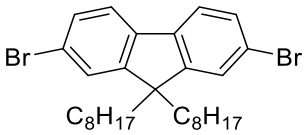


2,7-dibromofluorene (4.0 g, 12.34 mmol) and 1-bromooctane (6.40 mL, 37.04 mmol) in a 1:1 mixture of 13 M NaOH solution and toluene (60 mL) were degassed. Tetrabutylammonium bromide (40 mg, 0.12 mmol) was added and the reaction was heated to reflux for 18 h. The reaction was allowed to cool, the organic layer separated and the aqueous washed with $CH_2Cl_2$ (2 x 50 mL). The combined organic fractions were dried over $MgSO_4$ and concentrated *in vacuo* to yield a yellow solid which was recrystallized from EtOH to give off white crystals (4.24 g, 7.74 mmol, 63%). $^1$H NMR (500 MHz, $CDCl_3$) δ 7.51 (d, *J* = 7.9 Hz, 2H, CBrC*H*CH), 7.45 (m, 4H, $CH_2CCH$ + CBrCHC*H*), 1.95 – 1.86 (m, 4H, $C(CH_2CH_2C_5H_{10}CH_3)_2$), 1.27 – 1.17 (m, 4H, $C(CH_2CH_2C_5H_{10}CH_3)_2$), 1.17 – 1.00 (m, 16H, $C(CH_2CH_2C_5H_{10}CH_3)_2$), 0.83 (t, *J* = 7.2 Hz, 6H, $C(CH_2CH_2C_5H_{10}CH_3)_2$), 0.64 – 0.53 (m, 4H, $C(CH_2CH_2C_5H_{10}CH_3)_2$); MS ($EI^+$) *m/z* 546, 548 and 550 $(M)^+$. All spectroscopic data is in accordance with literature values.[181]

**2,2'-(9,9-dioctyl-9H-fluorene-2,7-diyl)bis(4,4,5,5-tetramethyl-1,3,2-dioxaborolane)**

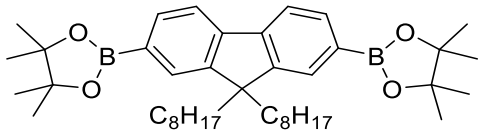


2,7-dibromo-9,9-dioctyl-9H-fluorene (1.0 g, 1.82 mmol) in THF (40 mL) was stirred under argon at -78 °C. 2.5 M n-butyllithium (1.28 mL, 3.82 mmol) was added slowly and the reaction was stirred at -78 °C for a further 2 h. 2-isopropoxy-4,4,5,5-tetramethyl-1,3,2-dioxaborolane (1.11 mL, 5.46 mmol) was added and the reaction mixture was allowed to warm to rt and stirred for 64 h. $H_2O$ (50 mL) was added and the organic product was extracted with $Et_2O$ (2 x 50 mL). The organic fractions were dried over $MgSO_4$, and concentrated *in vacuo* and the product was recrystallized from acetone (631 mg, 0.98 mmol, 54%). $^1$H NMR (600 MHz, $CDCl_3$) δ 7.80 (d, *J* = 7.5 Hz, 2H, CBC*H*CH), 7.74 (s, 2H, C($C_8H_{17}$)$_2$CC*H*), 7.72 (d, *J* = 7.5 Hz, 2H, CBCHC*H*), 2.02 – 1.96 (m, 4H, C($CH_2C_6H_{12}CH_3$)$_2$), 1.38 (s, 24H,OC($CH_3$)$_2$), 1.23 – 0.95 (m, 24H, C($CH_2C_6H_{12}CH_3$)$_2$), 0.80 (t, *J* = 7.3 Hz, 6H, C($CH_2C_6H_{12}CH_3$)$_2$); MS (EI$^+$) *m/z* 640, 642 and 644 (M)$^+$. All spectroscopic data is in accordance with literature values.[182]

**2,2'-(mesitylmethylene)bis(1H-pyrrole)**

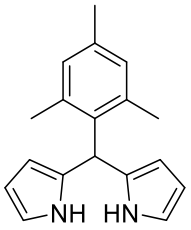


Pyrrole (188 mL) and mesitaldehyde (4.0 mL, 27.2 mmol) were degassed for 10 min. Magnesium bromide (0.5 g, 2.7 mmol) was added and the reaction mixture was stirred at rt for 2 h. NaOH solution was added and the reaction mixture was passed through a plug of silica using $CH_2Cl_2$ as eluent. Concentration *in vacuo* afforded a solid that was washed with pentane (50 mL) to yield the product as a white solid (5.5 g, 20.8 mmol, 77%). $^1$H NMR (500 MHz, $CDCl_3$) δ 7.94 (br s, 2H, N*H*), 6.87 (s, 2H), 6.66 (s, 2H), 6.18 (dd, J = 5.6, 2.8 Hz, 2H), 6.01 (s, 2H), 5.93 (s, 1H), 2.28 (s, 3H), 2.07 (s, 6H); MS (EI$^+$) *m/z* 264 (M)$^+$. All spectroscopic data is in accordance with literature values.[183]

**5,15-bis(4-bromophenyl)-10,20-dimesitylporphyrin (MPP)**

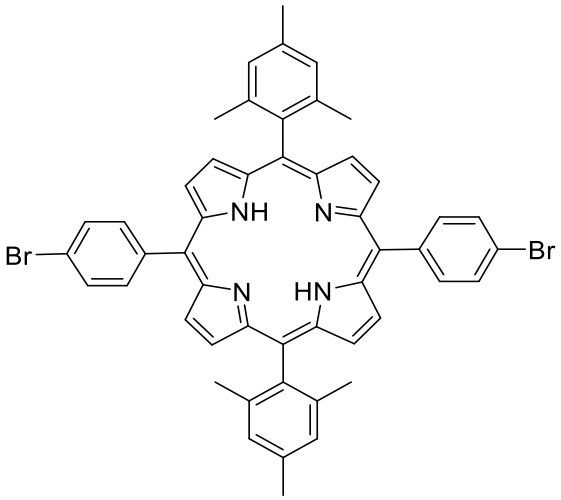


Product was prepared according to general procedure 1 from 2,2'-(mesitylmethylene)bis(1H-pyrrole) (0.54 g, 2.04 mmol) and 4-bromobenzaldehyde (0.38 g, 2.04 mmol) in $CH_2Cl_2$ (250 mL) using TFA (0.28 mL, 3.68 mmol) and DDQ (0.56 g, 2.45 mmol). The reaction mixture was purified by silica plug using $CH_2Cl_2$ as eluent. Concentration *in vacuo* and washing with MeOH (100 mL) yielded the product as purple crystals (156 mg, 0.19 mmol, 18%). $^1$H NMR (500 MHz, $CDCl_3$) δ 8.77 (d, *J* = 4.7 Hz, 4H, NHCC*H*), 8.70 (d, *J* = 4.7 Hz, 4H, NHCC*H*), 8.09 (d, *J* = 8.2 Hz, 4H, CBrC*H*CH), 7.88 (d, *J* = 8.2 Hz, 4H, CBrCHC*H*), 7.29 (s, 4H, NHCCCC($CH_3$)C*H*C$CH_3$), 2.63 (s, 6H, NHCCCC($CH_3$)CHCC*H*$_3$), 1.83 (s, 12H, NHCCCC(C*H*$_3$)CHCC$H_3$), -2.66 (s, 2H, N*H*); $^{13}$C NMR (151 MHz, $CDCl_3$) δ 141.0, 139.5, 138.3, 138.0, 135.9, 132.6, 131.1, 130.0, 127.9, 122.5, 118.8, 118.0, 114.4, 21.8, 21.6; MS (EI$^+$) *m/z* 855, 857 and 859 (M[+H])$^+$; HRMS 855.1698 calculated for $C_{50}H_{41}{}^{79}Br_2N_4$ found 855.1660.

**5,15-bis(4-bromophenyl)-10,20-dimesitylporphyrinato platinum(II) (MPP-Pt)**

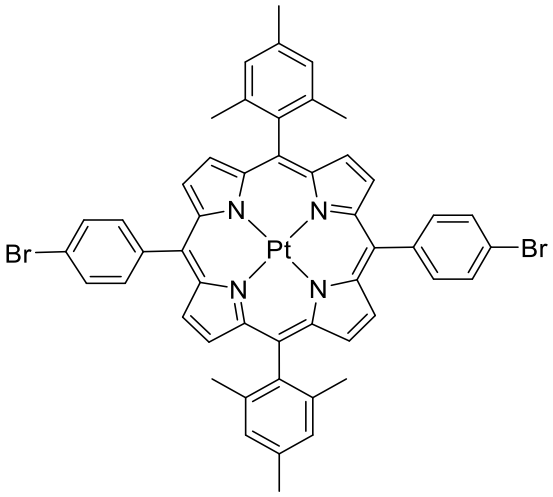


Product was prepared according to general procedure 2 using 5,15-dimesityl-10,20-diparabromophenyl porphyrin (50 mg, 0.058 mmol) and $PtCl_2$ (30 mg, 0.117 mmol) in benzonitrile (10 mL). The crude product was purified by silica plug using $CHCl_3$ as eluent, concentrated *in vacuo* and washed with MeOH (70 mL) to give the product as a red powder (35 mg, 0.033 mmol, 56%). $^1$H NMR (500 MHz, $CDCl_3$) δ 8.68 (d, *J* = 5.0 Hz, 4H, NHCC*H*), 8.61 (d, *J* = 5.0 Hz, 4H, NHCC*H*), 8.04 (d, *J* = 8.3 Hz, 4H, CBrC*H*CH), 7.86 (d, *J* = 8.3 Hz, 4H, CBrCHC*H*), 7.26 (s, 4H, NHCCCC($CH_3$)C*H*C$CH_3$), 2.61 (s, 6H, NHCCCC($CH_3$)CHCC*H*$_3$), 1.83 (s, 12H, NHCCCC(C*H*$_3$)CHC$CH_3$); $^{13}$C NMR (151 MHz, $CDCl_3$) δ 140.8, 140.5, 140.4, 139.2, 138.1, 137.4, 135.3, 131.0, 130.1, 129.9, 128.0, 122.6, 120.9, 120.3, 21.6, 21.5.; MS (TOF ES$^-$) *m/z* 1049 $(M)^-$
.

**PF MPP(Pt) – *Poly*-9,9-dioctylfluorene-*ran*-5,15-dimesityl-10,20-diphenylporphyrinato platinum (II)**

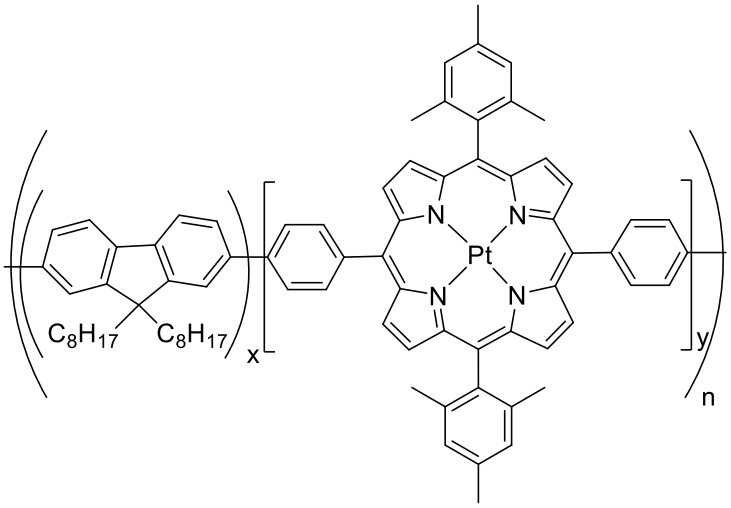


5 polymers were synthesised with varying weight percentages of porphyrin to fluorene; 0.0%, 0.5%, 1.0%, 2.0% and 5.0% (x:y = 1:0, 199:1, 99:1, 48:1 and 19:1 respectively).

A solution of aliquat 336 in toluene and a separate solution of 1.0 M $Na_2CO_3$ were both degassed for 30 min. 2,7-dibromo-9,9-dioctyl-9H-fluorene, 2,2'-(9,9-dioctyl-9H-fluorene-2,7-diyl)bis(4,4,5,5-tetramethyl-1,3,2-dioxaborolane) and 5,15-bis(4-bromophenyl)-10,20-dimesitylporphyrinato platinum(II) were placed in a microwave *via*l and purged with argon. The solution of aliquat 336 in toluene was added and the reaction mixture was degassed for 40 min. $Pd(OAc)_2$ and $PPh_3$ were added and the reaction mixture was degassed for a further 20 min. The 1.0 M $Na_2CO_3$ solution was added and the reaction mixture was heated to 110 $^oC$ and stirred for 64 h. The reaction was allowed to cool and the product was precipitated from MeOH and filtered. The polymer product was then washed with acetone and hexane and extracted with $CHCl_3$.

**PFO - 0.0%:** Reagents and solvents used were 2,7-dibromo-9,9-dioctyl-9H-fluorene (70.6 mg, 0.129 mmol) , 2,2'-(9,9-dioctyl-9H-fluorene-2,7-diyl)bis(4,4,5,5-tetramethyl-1,3,2-dioxaborolane) (82.7 mg, 0.129 mmol), $Pd(OAc)_2$ (3 mg, 0.013 mmol), $PPh_3$ (14 mg, 0.052 mmol), aliquat 336 (1 drop), 1.0 M $Na_2CO_3$ solution (1 mL) and toluene (5 mL). Polymer was obtained as per the above synthesis (10 mg, 10%). $^1$H NMR (600 MHz, $CDCl_3$) δ 7.87 – 7.80 (m, CBrC*H*CH), 7.72 – 7.64 (m, $CH_2$CC*H* + CBrCHC*H*), 2.12 (s, C$H_2$), 1.26 – 1.04 (m, C$H_2$), 0.86 – 0.75 (m, C$H_2$ + C$H_3$); UV ($CHCl_3$) $\lambda_{max}$ 381, (Thin film) $\lambda_{max}$ 385; GPC (PS): $M_n$ = 8700 Da, $M_w$ = 12000 Da, PDI = 1.4.

**P1 - 0.5%:** Reagents and solvents used were 2,7-dibromo-9,9-dioctyl-9H-fluorene (140.5 mg, 0.256 mmol) , 2,2'-(9,9-dioctyl-9H-fluorene-2,7-diyl)bis(4,4,5,5-tetramethyl-1,3,2-dioxaborolane) (165.3 mg, 0.257 mmol), 5,15-bis(4-bromophenyl)-10,20-dimesitylporphyrinato platinum(II) (1.2 mg, 0.001 mmol), $Pd(OAc)_2$ (6 mg, 0.026 mmol), $PPh_3$ (28 mg, 0.104 mmol), aliquat 336 (2 drops), 1.0 M $Na_2CO_3$ solution (2 mL) and toluene (10 mL). Polymer was obtained as per the above synthesis (99 mg, 50%). $^1$H NMR (600 MHz, $CDCl_3$) δ 9.13 (s, MPP*H*), 8.93 (s, MPP*H*), 8.41 (s, MPP*H*), 8.13 (s, MPP*H*), 7.87 – 7.81 (m, CBrC*H*CH), 7.73 – 7.63 (m, $CH_2CCH$ + CBrCHC*H*), 2.23 – 2.01 (m, $CH_2$), 1.25 – 1.03 (m, $CH_2$), 0.90 – 0.72 (m, $CH_2$ + $CH_3$); UV ($CHCl_3$) $\lambda_{max}$ 380, (Thin film) $\lambda_{max}$ 383; GPC (PS): $M_n$ = 8000 Da, $M_w$ = 15000 Da, PDI = 1.8.

**P2 - 1.0%:** Reagents and solvents used were 2,7-dibromo-9,9-dioctyl-9H-fluorene (139.9 mg, 0.255 mmol) , 2,2'-(9,9-dioctyl-9H-fluorene-2,7-diyl)bis(4,4,5,5-tetramethyl-1,3,2-dioxaborolane) (165.3 mg, 0.257 mmol), 5,15-bis(4-bromophenyl)-10,20-dimesitylporphyrinato platinum(II) (2.4 mg, 0.002 mmol), $Pd(OAc)_2$ (6 mg, 0.026 mmol), $PPh_3$ (28 mg, 0.104 mmol), aliquat 336 (2 drops), 1.0 M $Na_2CO_3$ solution (2 mL) and toluene (10 mL). Polymer was obtained as per the above synthesis (198 mg, 99%). $^1$H NMR (600 MHz, $CDCl_3$) δ 9.13 (s, MPP*H*), 8.93 (s, MPP*H*), 8.41 (s, MPP*H*), 8.13 (s, MPP*H*), 7.89 – 7.80 (m, CBrC*H*CH), 7.74 – 7.62 (m, $CH_2CCH$ + CBrCHC*H*), 2.12 (s, $CH_2$), 1.30 – 0.99 (m, $CH_2$), 0.91 – 0.67 (m, $CH_2$ + $CH_3$); UV ($CHCl_3$) $\lambda_{max}$ 381, (Thin film) $\lambda_{max}$ 383; GPC (PS): $M_n$ = 11000 Da, $M_w$ = 20000 Da, PDI = 1.8.

**P3 - 2.0%:** Reagents and solvents used were 2,7-dibromo-9,9-dioctyl-9H-fluorene (69.3 mg, 0.124 mmol) , 2,2'-(9,9-dioctyl-9H-fluorene-2,7-diyl)bis(4,4,5,5-tetramethyl-1,3,2-dioxaborolane) (82.7 mg, 0.129 mmol), 5,15-bis(4-bromophenyl)-10,20-dimesitylporphyrinato platinum(II) (2.4 mg, 0.002 mmol), $Pd(OAc)_2$ (3 mg, 0.013 mmol), $PPh_3$ (14 mg, 0.052 mmol), aliquat 336 (1 drop), 1.0 M $Na_2CO_3$ solution (1 mL) and toluene (5 mL). Polymer was obtained as per the above synthesis (80 mg, 80%). $^1$H NMR (600 MHz, $CDCl_3$) δ 9.13 (s, MPP*H*), 8.64 (s, MPP*H*), 8.36 (s, MPP*H*), 8.11 (s, MPP*H*), 7.88 – 7.80 (m, CBrC*H*CH), 7.75 – 7.63 (m, $CH_2CCH$ + CBrCHC*H*), 2.12 (s, $CH_2$), 1.17 (s, $CH_2$), 0.90 – 0.73 (m, $CH_2$ + $CH_3$); UV ($CHCl_3$) $\lambda_{max}$ 379, (Thin film) $\lambda_{max}$ 385; GPC (PS): $M_n$ = 11000 Da, $M_w$ = 17000 Da, PDI = 1.6.

**P4 - 5.0%:** Reagents and solvents used were 2,7-dibromo-9,9-dioctyl-9H-fluorene (67.5 mg, 0.123 mmol) , 2,2'-(9,9-dioctyl-9H-fluorene-2,7-diyl)bis(4,4,5,5-tetramethyl-1,3,2-dioxaborolane) (82.7 mg, 0.129 mmol), 5,15-bis(4-bromophenyl)-10,20-dimesitylporphyrinato platinum(II) (5.9 mg, 0.006 mmol), $Pd(OAc)_2$ (3 mg, 0.013 mmol), $PPh_3$ (14 mg, 0.052 mmol), aliquat 336 (1 drop), 1.0 M $Na_2CO_3$ solution (1 mL) and toluene (5 mL).

Polymer was obtained as per the above synthesis (54 mg, 54%). $^1$H NMR (600 MHz, $CDCl_3$) δ 9.13 (s, MPP*H*), 8.93 (s, MPP*H*), 8.41 (s, MPP*H*), 8.13 (s, MPP*H*), 7.87 – 7.81 (m, CBrC*H*CH), 7.73 – 7.64 (m, $CH_2CCH$ + CBrCHC*H*), 2.12 (s, $CH_2$), 1.27 – 1.03 (m, $CH_2$), 0.90 – 0.74 (m, $CH_2$ + $CH_3$); UV ($CHCl_3$) $\lambda_{max}$ 381, (Thin film) $\lambda_{max}$ 383; GPC (PS): $M_n$ = 12000 Da, $M_w$ = 23000 Da, PDI = 1.9.

**1,2-bis(octyloxy)benzene**

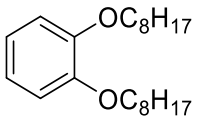


1-bromooctane (25.0 mL, 145.30 mmol) was added slowly to a solution of catechol (2.0 g, 18.18 mmol) and $K_2CO_3$ (10.0 g, 72.65 mmol) in acetone (100 mL) at 50 °C. The reaction mixture was stirred at reflux for 18 h. The reaction mixture was concentrated *in vacuo* and extracted with $CH_2Cl_2$ (2 x 50 mL) from brine (50 mL). The crude product was purified *via* column chromatography ($SiO_2$, Eluent Hexane) to give white crystals (4.39 g, 13.12 mmol, 72%). $^1$H NMR (300 MHz, $CDCl_3$) δ 6.89 (s, *J* = 2.6 Hz, 4H, Ph*H*), 3.99 (t, *J* = 6.7 Hz, 4H, PhOC$H_2$$CH_2C_5H_{10}CH_3$), 1.88 – 1.73 (m, 4H, $PhOCH_2CH_2C_5H_{10}CH_3$), 1.54 – 1.20 (m, 20H, $PhOCH_2CH_2C_5H_{10}CH_3$), 0.95 – 0.82 (t, *J* = 8.8 Hz, 6H, $PhOCH_2CH_2C_5H_{10}CH_3$); MS ($EI^+$) *m/z* 334 $(M)^+$. All spectroscopic data is in accordance with literature values.[184]

**9,10-bis(4-bromophenyl)-2,3,6,7-tetra(octyloxy)anthracene**

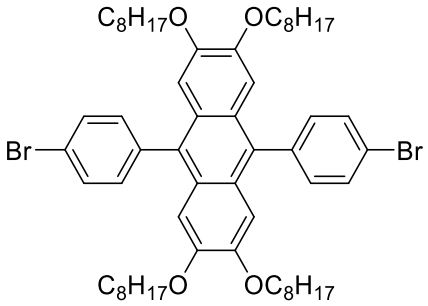


Following a modified procedure by Xia,[78] 1,2-bis(octyloxy)benzene (3.0 g, 8.97 mmol), 4-bromobenzaldehyde (2.5 g, 13.44 mmol) and $CHCl_3$ (30 mL) were added slowly to a 1:10 w/w solution of $P_2O_5$ (0.42 g) in $MeSO_3H$ (3.0 mL) at 0 °C under an atmosphere of argon. The reaction mixture was heated to reflux and stirred for 2 h. 2,3-Dichloro-5,6-dicyano-1,4-benzoquinone (2.0 g, 8.97 mmol) was added and the reaction was cooled to 40 °C and stirred for 2 h. The reaction mixture was washed with brine (2 x 30 mL) and the aqueous fractions

were further extracted with $CHCl_3$ (2 x 50 mL). The organic fractions were dried over $MgSO_4$ and concentrated *in vacuo*. The crude product was purified *via* column chromatography ($SiO_2$, Eluent $Et_2O$:Hexane (1:19)) and recrystallization from $CHCl_3$ and MeOH (716 mg, 0.72 mmol, 8%). $^1$H NMR (300 MHz, $CDCl_3$) δ 7.73 (d, *J* = 8.3 Hz, 4H, Ph*H*), 7.33 (d, *J* = 8.3 Hz, 4H, Ph*H*), 6.72 (s, 4H, $C_8H_{17}OCC\mathit{H}$), 3.85 (t, *J* = 6.5 Hz, 8H, $OC\mathit{H}_2CH_2C_5H_{10}CH_3$), 1.83 – 1.69 (m, 8H, $OCH_2C\mathit{H}_2C_5H_{10}CH_3$), 1.48 – 1.19 (m, 40H, $OCH_2CH_2C_5\mathit{H}_{10}CH_3$), 0.88 (t, *J* = 6.7 Hz, 12H, $OCH_2CH_2C_5H_{10}C\mathit{H}_3$); $^{13}$C NMR (151 MHz, $CDCl_3$) δ 149.0, 139.0, 133.0, 132.0, 131.5, 125.7, 121.6, 105.1, 68.7, 32.0, 29.5, 29.4, 29.0, 26.2, 22.8, 14.3; MS ($ES^+$) *m/z* 998, 1000, 1002 $(M)^+$; HRMS 998.4424 calculated for $C_{58}H_{80}{}^{79}Br_2O_4$ found 998.5254.

**PDPA MPP(Pt) – *Poly*-4',4''-(2,3,6,7-(octyloxy)-9,10-diphenylanthracene-*alt*-1,4-phenyl)-*ran*-(4',4''-5,15-dimesityl-10,20-diphenylporphyrin(Pt)-*alt*-1,4-phenyl)**

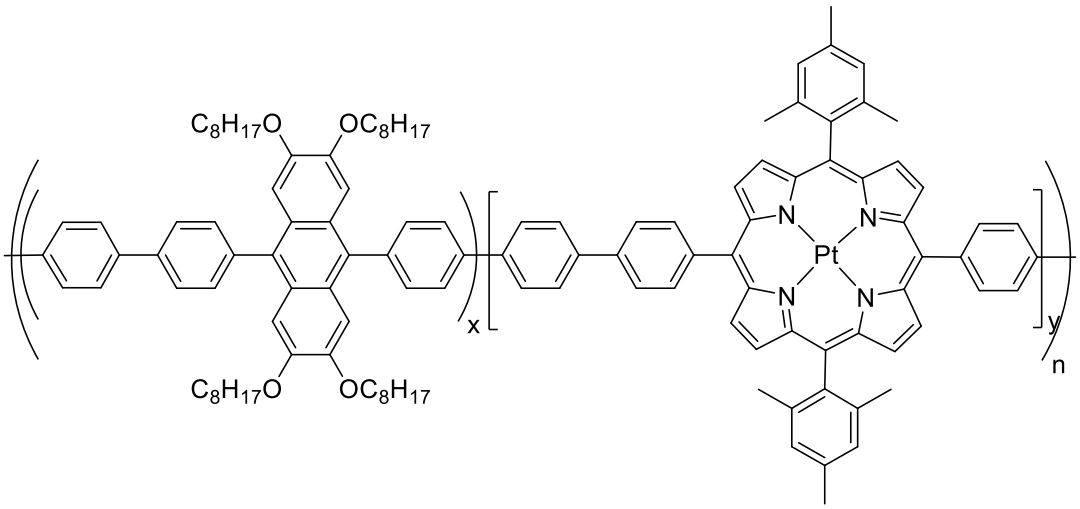


4 polymers were synthesised with varying weight percentages of porphyrin to diphenylanthracene moiety; 0.0%, 1.0%, 5.0% and 10.0% (x:y = 1:0, 99:1, 19:1 and 9:1).

A mixture of 9,10-bis(4-bromophenyl)-2,3,6,7-tetrakis(octyloxy)anthracene, 1,4-bis(4,4,5,5-tetramethyl-1,3,2-dioxaborolan-2-yl)benzene, 5,15-bis(4-bromophenyl)-10,20-dimesitylporphyrinato platinum(II), $Pd_2(dba)_3$, $(o\text{-}tol)_3P$, aliquat 336, and toluene was degassed in a microwave *via*l for 30 min. A degassed 1.0 M solution of $Na_2CO_3$ was added and the reaction mixture was stirred for 3 d at 120 °C. The reaction was allowed to cool and the product was precipitated from MeOH and filtered. The polymer product was then washed with acetone and hexane and extracted with $CHCl_3$.

**PDPA:** Reagents and solvents used were 9,10-bis(4-bromophenyl)-2,3,6,7-tetrakis(octyloxy)anthracene (108.9 mg, 0.109 mmol), 1,4-bis(4,4,5,5-tetramethyl-1,3,2-dioxaborolan-2-yl)benzene (35.9 mg, 0.109 mmol), $Pd_2(dba)_3$ (2.0 mg, 0.002 mmol), $(o\text{-}tol)_3P$ (2.6 mg, 0.009 mmol), aliquat 336 (1 drop), 1.0 M $Na_2CO_3$ (1.0 mL), and toluene (4.0 mL). Polymer was obtained as per the above synthesis (79 mg, 79%). UV (chlorobenzene) $\lambda_{max}$ 381; GPC (PS): $M_n$ = 7800 Da, $M_w$ = 10000 Da, PDI = 1.3.

**PDPA MPP(Pt) 1:** Reagents and solvents used were 9,10-bis(4-bromophenyl)-2,3,6,7-tetrakis(octyloxy)anthracene (216.1 mg, 0.216 mmol), 1,4-bis(4,4,5,5-tetramethyl-1,3,2-dioxaborolan-2-yl)benzene (71.8 mg, 0.218 mmol), 5,15-bis(4-bromophenyl)-10,20-dimesitylporphyrinato platinum(II) (2.2 mg, 0.002 mmol), $Pd_2(dba)_3$ (4.0 mg, 0.004 mmol), $(o\text{-}tol)_3P$ (5.2 mg, 0.017 mmol), aliquat 336 (1 drop), 1.0 M $Na_2CO_3$ (2.0 mL), and toluene (8.0 mL). Polymer was obtained as per the above synthesis (120 mg, 60%). UV (chlorobenzene) $\lambda_{max}$ 382; GPC (PS): $M_n$ = 8800 Da, $M_w$ = 12000 Da, PDI = 1.4.

**PDPA MPP(Pt) 5:** Reagents and solvents used were 9,10-bis(4-bromophenyl)-2,3,6,7-tetrakis(octyloxy)anthracene (103.7 mg, 0.104 mmol), 1,4-bis(4,4,5,5-tetramethyl-1,3,2-dioxaborolan-2-yl)benzene (35.9 mg, 0.109 mmol), 5,15-bis(4-bromophenyl)-10,20-dimesitylporphyrinato platinum(II) (5.4 mg, 0.005 mmol), $Pd_2(dba)_3$ (2.0 mg, 0.002 mmol), $(o\text{-}tol)_3P$ (2.6 mg, 0.009 mmol), aliquat 336 (1 drop), 1.0 M $Na_2CO_3$ (1.0 mL), and toluene (4.0 mL). Polymer was obtained as per the above synthesis (80 mg, 80%). UV (chlorobenzene) $\lambda_{max}$ 408; GPC (PS): $M_n$ = 12000 Da, $M_w$ = 20000 Da, PDI = 1.7.

**PDPA MPP(Pt) 10:** Reagents and solvents used were 9,10-bis(4-bromophenyl)-2,3,6,7-tetrakis(octyloxy)anthracene (98.2 mg, 0.098 mmol), 1,4-bis(4,4,5,5-tetramethyl-1,3,2-dioxaborolan-2-yl)benzene (35.9 mg, 0.109 mmol), 5,15-bis(4-bromophenyl)-10,20-dimesitylporphyrinato platinum(II) (10.9 mg, 0.010 mmol), $Pd_2(dba)_3$ (2.0 mg, 0.002 mmol), $(o\text{-}tol)_3P$ (2.6 mg, 0.009 mmol), aliquat 336 (1 drop), 1.0 M $Na_2CO_3$ (1.0 mL), and toluene (4.0 mL). Polymer was obtained as per the above synthesis (42 mg, 42%). UV (chlorobenzene) $\lambda_{max}$ 411; GPC (PS): $M_n$ = 11000 Da, $M_w$ = 21000 Da, PDI = 1.8.

## 6.3 Synthetic Techniques for Chapter 3

**3-(4-bromophenyl)propynol**

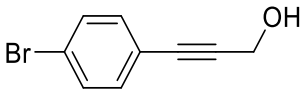


1-iodo-4-bromobenzene (1.0 g, 3.54 mmol) and copper iodide (42 mg, 0.22 mmol) in toluene (20 mL) were degassed for 10 min. Propargyl alcohol (0.26 mL, 3.54 mmol) and piperidine (0.70 mL, 7.03 mmol) were added, resulting in a yellow solution. Bis(triphenylphosphine)palladium(II) dichloride (70 mg, 0.10 mmol) was added and the reaction was stirred at 35 °C for 2 h. The reaction mixture was passed through a silica plug using $CHCl_3$ as eluent and concentrated *in vacuo*. The crude solid off-white product (744 mg, 3.52 mmol, 99%) was taken into the next reaction without further purification. $^1$H NMR (500 MHz, $CDCl_3$) δ 7.45 (d, *J* = 8.4 Hz, 2H, CBrC*H*CH), 7.29 (d, *J* = 8.4 Hz, 2H, CBrCHC*H*), 4.48 (s, 2H, CCC*H*OH). All spectroscopic data is in accordance with literature values.[185]

**3-(4-bromophenyl)propiolaldehyde**

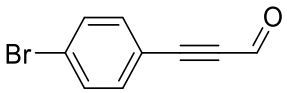


Crude 3-(4-bromophenyl)propynol (1.60 g, 7.58 mmol), TEMPO (119 mg, 0.76 mmol), (Diacetoxyiodo)benzene (2.90 g, 9.10 mmol) and $CH_2Cl_2$ (100 mL) were stirred under argon at rt for 3 h. $Na_2SO_3$ solution (150 mL) and $CH_2Cl_2$ (100 mL) were added and the organic layer was separated. The aqueous layer was washed with $CH_2Cl_2$ (2 x 100mL) and the combined organic fractions were dried over $MgSO_4$ and concentrated *in vacuo*. The crude product was purified *via* column chromatography ($SiO_2$, Eluent Hexane:$Et_2O$ (9:1)) to give the desired product as an off white solid (862 mg, 4.13 mmol, 54%). $^1$H NMR (500 MHz, CDCl3) δ 9.41 (s, 1H, CCC*H*O), 7.56 (d, *J* = 8.7 Hz, 2H, CBrC*H*CH), 7.46 (d, *J* = 8.7 Hz, 2H, CBrCHC*H*); MS ($CI^+$) *m/z* 209 and 211 $(M[+H])^+$. All spectroscopic data is in accordance with literature values.[186]

**Dipyrromethane**

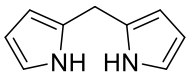


Pyrrole (60 mL, 832.50 mmol) and paraformaldehyde (1.0 g, 32.50 mmol) were degassed and heated to 50 °C. After 20 min, triflouroacetic acid (0.24 mL, 3.25 mmol) was added and the reaction was stirred for a further 10 min. 0.1 M NaOH solution (25 mL) was added and the layers were separated. The organic layer was washed with a saturated brine solution (2 x 25 mL). The product was dried over $MgSO_4$ and concentrated *in vacuo*. The product was purified *via* column chromatography ($SiO_2$, Eluent $CHCl_3$:Hexane (2:1)). The off white crystalline product (1.80 g, 38%) solidified upon standing in a fridge and further dried under high vacuum for 30 min. $^1$H NMR (500 MHz, CDCl3) δ 7.90 (br s, 2H, N*H*), 6.67 (br m, 2H, NHC*H*), 6.15 (d, J = 2.5 Hz, 2H, NHCHC*H*), 6.04 (br m, 2H, $CH_2$CC*H*), 3.99 (s, 2H, C$H_2$); MS (EI$^+$) *m/z* 146 (M)$^+$. All spectroscopic data is in accordance with literature values.[187]

**3,5-di-tert-butylbenzaldehyde**

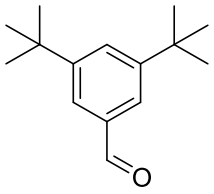


3,5-di-tert-butylbromobenzene (2.5 g, 9.30 mmol) and THF (30 mL) were stirred at -78 °C under an argon atmosphere. 2.5 M n-butyllithium (4.46 mL, 11.15 mmol) was added slowly over 10 min and the reaction mixture was allowed to stir for a further 20 min. DMF (1.07 mL, 13.00 mmol) was added and the reaction mixture was allowed to warm to rt with stirring over 1 h. $H_2O$ (25 mL) was added to quench the reaction, the layers were separated and the aqueous layer was further extracted with $Et_2O$ (2 x 25 mL). The combined organic fractions were dried over $MgSO_4$ and concentrated *in vacuo* to yield the product as a white solid (1.99 g, 98%). $^1$H NMR (500 MHz, $CDCl_3$) δ 10.01 (s, 1H, C*H*O), 7.73 (d, *J* = 1.9 Hz, 2H, CHOCC*H*), 7.71 (t, *J* = 1.9 Hz, 1H, CHOCCHCC*H*), 1.37 (s, 18H, C(C$H_3$)$_3$); MS (EI$^+$) *m/z* 218 (M)$^+$. All spectroscopic data is in accordance with literature values.[188]

**5,15-bis(3,5-di-tert-butylphenyl)porphyrin**

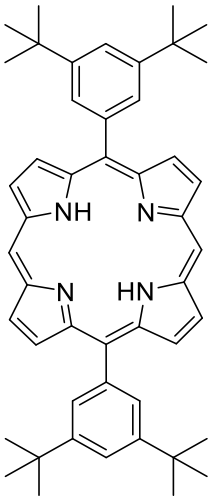


Product was prepared according to general procedure 1 from dipyrromethane (0.99 g, 6.78 mmol) and 3,5-di-tert-butylbenzaldehyde (1.48 g, 6.78 mmol) in $CH_2Cl_2$ (1200 mL) using TFA (0.16 mL, 2.03 mmol) and DDQ (2.31 g, 10.17 mmol). The reaction was quenched with $NEt_3$ (5 mL). The reaction mixture was concentrated *in vacuo* to approximately 250 mL and purified by silica plug using $CH_2Cl_2$ with 1% $NEt_3$ as eluent. Concentration *in vacuo* and washing with MeOH (300 mL) yielded the product as purple crystals (1.50 g, 2.18 mmol, 64%). $^1$H NMR (600 MHz, $CDCl_3$) δ 10.32 (s, 2H, NHCC*H*CN), 9.40 (d, *J* = 4.5 Hz, 4H, NHCC*H*CH), 9.14 (d, *J* = 4.5 Hz, 4H, NHCCHC*H*), 8.15 (d, *J* = 1.8 Hz, 4H, NHCCCC*H*CCH), 7.84 (t, *J* = 1.8 Hz, 2H, NHCCCCHCC*H*), 1.57 (s, 36H, C(C*H*$_3$)$_3$), -3.03 (s, 2H, N*H*); MS (EI$^+$) *m/z* 687 (M)$^+$. All spectroscopic data is in accordance with literature values.[189]

**5,15-dibromo-10,20-bis(3,5-di-tert-butylphenyl)porphyrin**

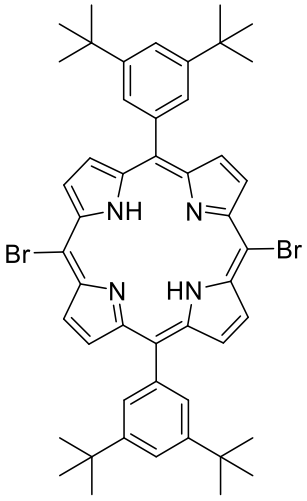

To a solution of 5,15-H-10,20-di(bismetatertbutylbenzene) pophyrin (225 mg, 0.33 mmol) in $CHCl_3$ (20 mL) was added NBS (123 mg, 0.689 mmol) and pyridine (0.3 mL), the reaction mixture was stirred at rt for 10 min. The reaction was quenched with acetone (10 mL), concentrated *in vacuo* and washed with MeOH (100 mL) to yield purple crystals (225 mg, 0.266 mmol, 81%). $^1$H NMR (500 MHz, $CDCl_3$) δ 9.63 (d, *J* = 4.4 Hz, 4H, NHCC*H*), 8.88 (d, *J* = 4.4 Hz, 4H, NHCC*H*), 8.02 (s, 4H, NHCCCC*H*CCH), 7.83 (s, 2H, NHCCCCHCC*H*), 1.54 (d, *J* = 3.6 Hz, 36H, C(C*H*$_3$)$_3$), -2.67 (s, 2H, N*H*); *m/z* 842, 844 and 846 $(M)^+$; HRMS 843.2637 calculated for $C_{48}H_{53}{}^{79}Br_2N_4$ found 843.2615. All spectroscopic data is in accordance with literature values.[190]

**2-bromo7hexylthiophene**

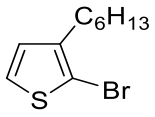


3-hexylthiophene (1.07 mL, 5.94 mmol), NBS (1.06 g, 5.94 mmol) and AcOH (5 mL) were stirred at rt under an argon atmosphere for 18 h. The reaction mixture was then poured into a saturated $NaHCO_3$ solution (20 mL) and extracted with $Et_2O$ (2 x 30 mL). The combined organic fractions were washed with saturated $NaHCO_3$ solution (2 x 20mL), dried over $MgSO_4$ and concentrated *in vacuo* to afford the product (1.03 g, 4.17 mmol, 70%). $^1$H NMR (500 MHz, $CDCl_3$) δ 7.18 (d, *J* = 5.6 Hz, 1H, SC*H*CH), 6.79 (d, *J* = 5.6 Hz, 1H, SCHC*H*), 2.57 (t, *J* = 7.6 Hz, 2H, SCBrC(C*H*$_2$CH$_2$C$_3$H$_6$CH$_3$)), 1.62 – 1.52 (m, 2H, SCBrC(CH$_2$C*H*$_2$C$_3$H$_6$CH$_3$)), 1.38 – 1.26 (m, 6H, SCBrC(CH$_2$CH$_2$C$_3$*H*$_6$CH$_3$)), 0.89 (t, *J* = 6.9 Hz, 3H, SCBrC(CH$_2$CH$_2$C$_3$H$_6$C*H*$_3$)). All spectroscopic data is in accordance with literature values.[191]

**((3-hexylthiophen6yl)ethynyl)trimethylsilane**

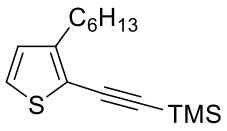


An anhydrous solution of 2-bromo7hexylthiophene (1.03 g, 4.17 mmol), ethynyltrimethylsilane (0.88 mL, 6.26 mmol), $Pd(OAc)_2$ (29 mg, 0.13 mmol), $PPh_3$ (100 mg, 0.38 mmol), CuI (40 mg, 0.21 mmol), $NEt_3$ (10 mL) and $CH_2Cl_2$ (10 mL) were degassed in a dry flask and stirred at 50 °C for 18 h under an argon atmosphere. The reaction mixture was filtered and concentrated *in vacuo* and the product was purified *via* column chromatography ($SiO_2$,

Eluent pentane) (953 mg, 3.60 mmol, 86%). $^1$H NMR (500 MHz, $CDCl_3$) δ 7.11 (d, *J* = 5.1 Hz, 1H, SC*H*CH), 6.82 (d, *J* = 5.1 Hz, 1H, SCHC*H*), 2.69 (t, *J* = 7.6 Hz, 2H, SCC($C\mathit{H}_2CH_2C_3H_6CH_3$)), 1.66 – 1.56 (m, 2H, SCC($CH_2C\mathit{H}_2C_3H_6CH_3$)), 1.39 – 1.25 (m, 6H, SCC($CH_2CH_2C_3\mathit{H}_6CH_3$)), 0.93 – 0.81 (m, 3H, SCC($CH_2CH_2C_3H_6C\mathit{H}_3$)), 0.25 (s, *J* = 5.9 Hz, 9H, CCSi($C\mathit{H}_3$)$_3$). All spectroscopic data is in accordance with literature values.[192]

**2-ethynyl7hexylthiophene**

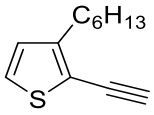


$K_2CO_3$ (96 mg, 0.69 mmol) was added to a solution of ((3-hexylthiophen6yl)ethynyl)trimethylsilane (168 mg, 0.63 mmol) in MeOH (3 mL) and was stirred at rt in the dark for 4 h. $H_2O$ (10 mL) was added and the product was extracted with pet 40-60 (2 x 10 mL). The organic fractions were dried over $MgSO_4$ and concentrated *in vacuo* to afford the product (82 mg, 0.43 mmol, 68%). $^1$H NMR (500 MHz, $CDCl_3$) δ 7.15 (d, *J* = 5.1 Hz, 1H, SC*H*CH), 6.85 (d, *J* = 5.1 Hz, 1H, SCHC*H*), 3.43 (s, 1H, SCCC*H*), 2.71 (t, *J* = 7.6 Hz, 2H, SCC($C\mathit{H}_2CH_2C_3H_6CH_3$)), 1.67 – 1.56 (m, 2H, SCC($CH_2C\mathit{H}_2C_3H_6CH_3$)), 1.39 – 1.23 (m, 6H, SCC($CH_2CH_2C_3\mathit{H}_6CH_3$)), 0.94 – 0.83 (m, 3H, SCC($CH_2CH_2C_3H_6C\mathit{H}_3$)). All spectroscopic data is in accordance with literature values.[192]

**5,15-bis(3,5-di-tert-butylphenyl)-10,20-bis((3-hexylthiophen6yl)ethynyl)porphyrin**

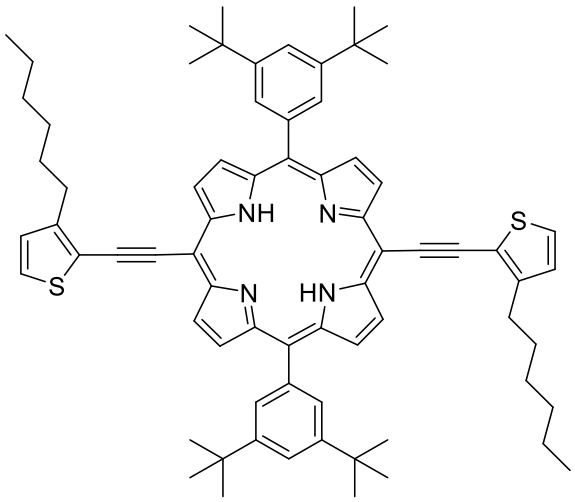

A solution of 5,15-bromo-10,20-di(bismetatertbutylbenzene) pophyrin (120 mg, 0.142 mmol), 2-ethynyl7hexylthiophene (82 mg, 0.426 mmol), $NEt_3$ (4.2 mL), THF (21.0 mL) and toluene (2.1 mL) was degassed. $Pd_2(dba)_3$ (98 mg, 0.107 mmol) and $AsPh_3$ (22 mg, 0.071 mmol) were added and the reaction mixture was stirred at rt $^oC$ for 18 h. The reaction mixture was concentrated *in vacuo*. The product was purified *via* column chromatography ($SiO_2$, Eluent $CHCl_3$:Hexane (1:8 to 1:4)), the organic fractions collected and concentrated *in vacuo* and washed with MeOH to yield a green powder (37 mg, 0.035 mmol, 25%). $^1H$ NMR (500 MHz, $CDCl_3$) δ 9.63 (d, *J* = 4.6 Hz, 4H, NHCC*H*), 8.86 (d, *J* = 4.6 Hz, 4H, NHCC*H*), 8.06 (d, *J* = 1.8 Hz, 4H, NHCCCC*H*CCH), 7.83 (t, *J* = 1.8 Hz, 2H, NHCCCCHCC*H*), 7.39 (d, *J* = 5.1 Hz, 2H, SC*H*CH), 7.09 (d, *J* = 5.1 Hz, 2H, SCHC*H*), 3.25 – 3.16 (m, 4H, SCCC$H_2$$CH_2CH_2CH_2CH_2CH_3$), 2.00 – 1.90 (m, 4H, $SCCCH_2CH_2CH_2CH_2CH_2CH_3$), 1.63 – 1.51 (m, 40H, $C(CH_3)_3$ and $SCCCH_2CH_2CH_2CH_2CH_2CH_3$), 1.47 – 1.39 (m, 4H, $SCCCH_2CH_2CH_2CH_2CH_2CH_3$), 1.39 – 1.30 (m, 4H, $SCCCH_2CH_2CH_2CH_2CH_2CH_3$), 0.84 (t, *J* = 7.3 Hz, 6H, $SCCCH_2CH_2CH_2CH_2CH_2CH_3$), -1.77 (s, 2H, N*H*); $^{13}C$ NMR (151 MHz, $CDCl_3$) δ 149.1, 148.6, 140.5, 130.0, 129.9, 128.9, 126.8, 123.5, 121.5, 119.3, 101.3, 98.3, 90.5, 35.2, 31.9, 31.9, 31.0, 30.5, 29.5, 22.8, 14.2; MS (TOF $ES^+$) *m/z* 1068 $(M[+H])^+$.

**5,15-bis(3,5-di-tert-butylphenyl)-10,20-bis((trimethylsilyl)ethynyl)porphyrin**

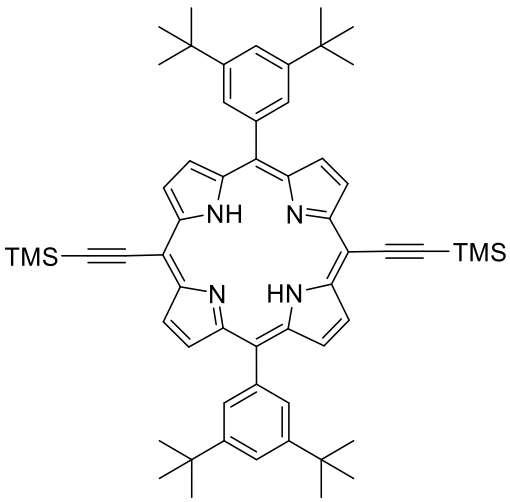


THF (10 mL) and $NEt_3$ (30 mL) were degassed and 5,15-bromo-10,20-di(bismetatertbutylbenzene) pophyrin (105 mg, 0.124 mmol), ethynyltrimethylsilane (19 µL, 0.136 mmol), $Pd(PPh_3)_2Cl_2$ (8 mg, 0.012 mmol) and CuI (6 mg, 0.031 mmol) were added at 0 $^oC$. The reaction mixture was allowed to warm to rt and stirred for 18 h under an argon atmosphere. The reaction mixture was passed through a silica plug using $CHCl_3$ as eluent and concentrated *in vacuo*. The free base product was purified and separated from the copper

complexed side product *via* column chromatography ($SiO_2$, Eluent $CHCl_3$:Hexane (1:4)) and was obtained as a purple powder (60 mg, 0.068 mmol, 55%). $^1$H NMR (600 MHz, $CDCl_3$) δ 9.61 (d, *J* = 4.6 Hz, 4H, NHCC*H*), 8.87 (d, *J* = 4.6 Hz, 4H, NHCC*H*), 8.04 (d, *J* = 1.8 Hz, 4H, NHCCCC*H*CCH), 7.82 (t, *J* = 1.8 Hz, 2H, NHCCCCHCC*H*), 1.55 (s, *J* = 7.3 Hz, 36H, C(C*H*$_3$)$_3$), 0.60 (s, *J* = 3.5 Hz, 18H, Si(C*H*$_3$)$_3$), -2.14 (s, 2H, N*H*); MS ($Cl^+$) *m/z* 878 $(M)^+$.

**5,15-bis(3,5-di-tert-butylphenyl)-10,20-diethynylporphyrin**

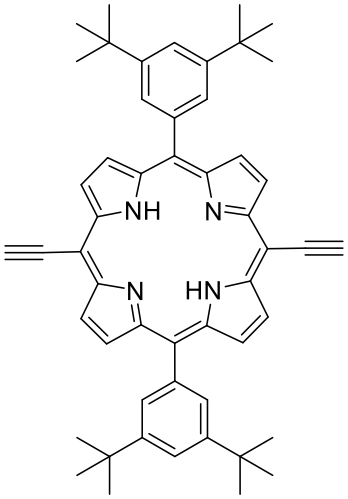


A solution of 5,15-bis(3,5-di-tert-butylphenyl)-10,20-bis((trimethylsilyl)ethynyl)porphyrin (60 mg, 0.068 mmol) in $CH_2Cl_2$ (20 mL) was purged with argon and treated with 1.0 M TBAF in THF (0.34 mL, 0.341 mmol). The reaction mixture was stirred under argon in the dark for 20 h. The reaction mixture was passed through a silica plug using $CHCl_3$ as eluent, concentrated *in vacuo* and washed with MeOH (20 mL) to yield the product (26 mg, 0.035 mmol, 51%) which was taken immediately into the next reaction. $^1$H NMR (600 MHz, $CDCl_3$) δ 9.66 (d, *J* = 4.6 Hz, 4H, NHCC*H*), 8.91 (d, *J* = 4.6 Hz, 4H, NHCC*H*), 8.05 (d, *J* = 1.7 Hz, 4H, NHCCCC*H*CCH), 7.83 (t, *J* = 1.7 Hz, 2H, NHCCCCHCC*H*), 4.20 (s, 2H, NHCC(CN)CC*H*), 1.55 (s, 36H, C(C*H*$_3$)$_3$), -2.26 (s, 2H, N*H*).

**5,15-bis((4-bromophenyl)ethynyl)-10,20-bis(3,5-di-tert-butylphenyl)porphyrin (TBAPP)**

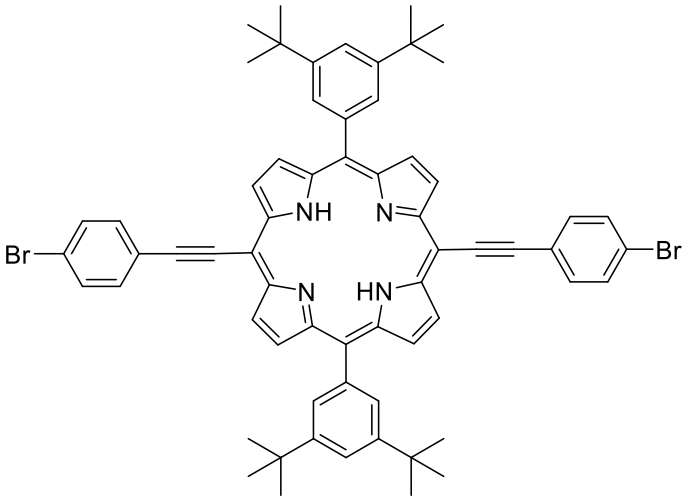


THF (5 mL) and $NEt_3$ (15 mL) were degassed and 5,15-bis(3,5-di-tert-butylphenyl)-10,20-diethynylporphyrin (26 mg, 0.036 mmol), 1-bromo8iodobenzene (21 mg, 0.073 mmol), $Pd(PPh_3)_2Cl_2$ (3 mg, 0.004 mmol) and CuI (2 mg, 0.008 mmol) were added at 0 °C. The reaction mixture was allowed to warm to rt and stirred for 18 h in the dark under an argon atmosphere. The reaction mixture was passed through a silica plug using $CHCl_3$ as eluent and concentrated *in vacuo*. The free base product was purified and separated from the copper complexed side product *via* column chromatography ($SiO_2$, Eluent $CHCl_3$:Hexane (1:9 to 1:6)) and was obtained as a green powder (6 mg, 0.006 mmol, 16%). $^1$H NMR (600 MHz, $CDCl_3$) δ 9.66 (d, *J* = 4.6 Hz, 4H, NHCC*H*), 8.90 (d, *J* = 4.4 Hz, 4H, NHCC*H*), 8.07 (d, *J* = 1.8 Hz, 4H, NHCCCC*H*CCH), 7.88 (d, *J* = 8.4 Hz, 4H, CBrC*H*CH), 7.84 (t, *J* = 1.8 Hz, 2H, NHCCCCHCC*H*), 7.70 (d, *J* = 8.4 Hz, 4H, CBrCHC*H*), 1.56 (s, 36H, C(C*H*$_3$)$_3$), -1.93 (s, 2H, N*H*); $^{13}$C NMR (151 MHz, $CDCl_3$) δ 149.2, 140.3, 133.2, 132.1, 130.1, 123.7, 123.0, 123.0, 121.5, 100.6, 96.1, 93.4, 35.2, 31.9; MS (TOF ES$^+$) *m/z* 1045 (M[+H])$^+$; HRMS 1043.3185 calculated for $C_{64}H_{61}{}^{79}Br_2N_4$ found 1043.3434.

**5,15-bis((4-bromophenyl)ethynyl)-10,20-dimesitylporphyrin (PEMP)**

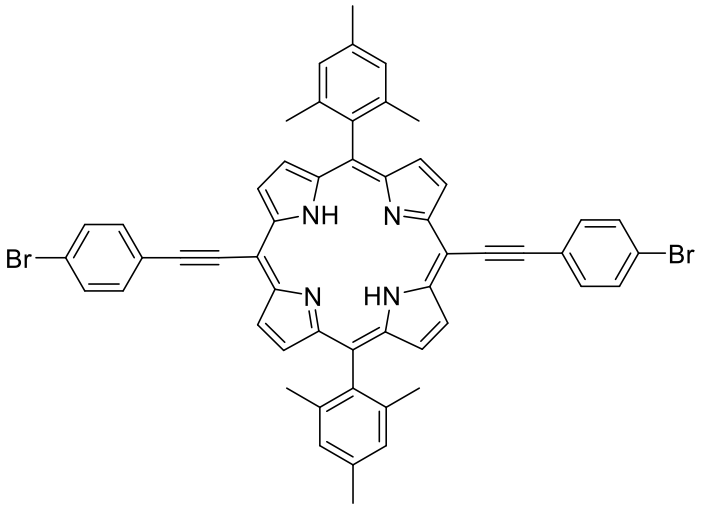


According to a modified procedure by Nowak-Król *et al*, 3-(4-bromophenyl)propiolaldehyde (418 mg, 2.0 mmol) and 2,2'-(mesitylmethylene)bis(1H-pyrrole) (529 mg, 2.0 mmol) were dissolved in THF (100 mL).[100] 37% HCl (2.0 mL, 23.0 mmol) in $H_2O$ (50 mL) was subsequently added and the reaction mixture was stirred for 3 h. The reaction mixture was diluted with brine (100 mL) and the intermediate porphyrinogen product was extracted with $CHCl_3$ (3 x 100 mL). The organic fractions were dried over $Mg(SO_4)$, filtered and diluted with $CHCl_3$ to a volume of 500 mL. DDQ (700 mg, 3.1 mmol) was added and the reaction mixture was stirred for 1 h. The reaction mixture was concentrated *in vacuo* and purified *via* column chromatography ($SiO_2$, Eluent $CHCl_3$). The relevant fractions were combined, concentrated *in vacuo* and washed with MeOH and hexane to yield a shiny, dark green powder (2 mg, 0.02 mmol, 1%). $^1$H NMR (300 MHz, $CDCl_3$) δ 9.58 (d, *J* = 4.7 Hz, 4H, NHCC*H*), 8.68 (d, *J* = 4.9 Hz, 4H, NHCC*H*), 7.86 (d, *J* = 8.4 Hz, 4H, CBrC*H*CH), 7.70 (d, *J* = 8.4 Hz, 4H, CBrCHC*H*), 7.31 (s, 4H, NHCCCC($CH_3$)C*H*C$CH_3$), 2.65 (s, 6H, NHCCCC($CH_3$)CHCC*H*$_3$), 1.86 (s, 12H, NHCCCC(C*H*$_3$)CHC$CH_3$), -1.85 (s, 2H, N*H*); MS (TOF ES$^+$) *m/z* 903.17, 905.18, 907.19 (M[+H])$^+$; HRMS 903.1698 calculated for $C_{54}H_{41}{}^{79}Br_2N_4$ found 903.1664.

**5,15-bis(3,5-di-tert-butylphenyl)porphyrinato platinum(II)**

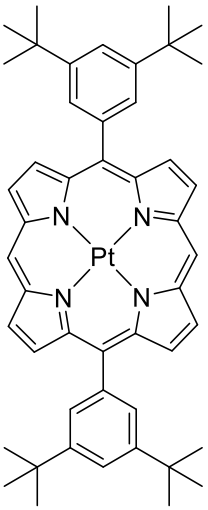


Product was prepared according to general procedure 2 using 5,15-bis(3,5-di-tert-butylphenyl)porphyrin (200 mg, 0.29 mmol) and $PtCl_2$ (154 mg, 0.58 mmol) in benzonitrile (40 mL). The crude product was purified by silica plug using $CHCl_3$ as eluent, concentrated *in vacuo* and washed with MeOH (300 mL) to give the product as a red powder (255 mg, 0.29 mmol, 100%). $^1$H NMR (600 MHz, $CDCl_3$) δ 10.17 (s, 2H, NCC*H*CN), 9.23 (d, *J* = 4.7 Hz, 4H, NCC*H*CH), 9.01 (d, *J* = 4.7 Hz, 4H, NCCHC*H*), 8.08 (d, *J* = 1.4 Hz, 4H, NCCCC*H*CCH), 7.85 – 7.80 (m, 2H, NCCCCHCC*H*), 1.56 (s, 36H, C(C*H*$_3$)$_3$); MS (MALDI micro) *m/z* 881 (M[+H])$^+$.

**5,15-bis(3,5-di-tert-butylphenyl)porphyrinato platinum(IV) dibromide**

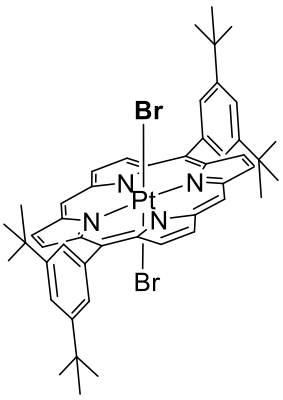


NBS (109 mg, 0.61 mmol) and pyridine (0.3 mL) were added to a solution of 5,15-bis(3,5-di-tert-butylphenyl)porphyrinato platinum(II) (255 mg, 0.29 mmol) in $CHCl_3$ (20 mL). The reaction mixture was stirred at rt 10 min in the dark under argon. The reaction mixture was quenched with acetone (15 mL), passed through a silica plug using $CHCl_3$ as eluent, concentrated *in vacuo* and washed with MeOH (200 mL) to yield the product (168 mg, 0.16 mmol, 55%). $^1$H NMR

(600 MHz, $CDCl_3$) δ 10.68 (s, 2H, NCC*H*CN), 9.55 (d, *J* = 4.9 Hz, 4H, NCC*H*CH), 9.30 (d, *J* = 4.8 Hz, 4H, NCCHC*H*), 8.15 (d, *J* = 1.5 Hz, 4H, NCCCC*H*CCH), 7.90 (s, 2H, NCCCCHCC*H*), 1.58 (s, *J* = 5.6 Hz, 36H, C($CH_3$)$_3$); $^{13}$C NMR (151 MHz, $CDCl_3$) δ 149.5, 139.5, 138.6, 137.9, 133.2, 132.3, 130.0, 122.3, 122.0, 106.7, 35.3, 31.9; MS ($EI^-$) *m/z* 1034, 1036 $(M[-3H])^+$; HRMS 1037.2207 calculated for $C_{48}H_{52}{}^{79}Br_2N_4Pt$ found 1037.2201.

**4-((2-Octyldodecyl)oxy)benzaldehyde**

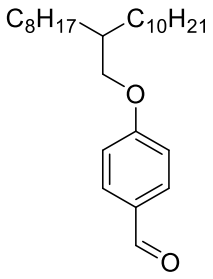


4-Hydroxybenzaldehyde (1.0 g, 8.19 mmol), 9-(bromomethyl)nonadecane (2.8 g, 8.19 mmol), $K_2CO_3$ (5.7 g, 40.94 mmol) and DMF (30 mL) were stirred under argon at 105 $^0$C for 18 h. The reaction mixture was allowed to cool and diluted with brine (50mL). The product was extracted with $Et_2O$ (3 x 50 mL), washed with brine (5 x 50 mL) and concentrated *in vacuo* to give a yellow oil (2.4 g, 6.93 mmol, 85%). $^1$H NMR (600 MHz, $CDCl_3$) δ 9.88 (s, 1H, C*H*O), 7.83 (d, *J* = 8.6 Hz, 2H, CHC*H*CCHO), 7.00 (d, *J* = 8.6 Hz, 2H, C*H*CHCCHO), 3.92 (d, *J* = 5.7 Hz, 2H, OC$H_2$), 1.84 -1.76 (m, 1H, $OCH_2CH$), 1.49 – 1.21 (m, 30H, CH($C_6H_{12}$)$CH_3$ and CH($C_9H_{18}$)$CH_3$), 0.88 (t, *J* = 7.0 Hz, 6H, C$H_3$); MS ($EI^-$) *m/z* 402 $(M)^-$; HRMS 402.3492 calculated for $C_{27}H_{46}O_2$ found 402.3491.

**1-Bromododecane**

$C_{12}H_{25}Br$

NBS (28.7 g, 161.00 mmol) was added in portions to 1-Dodecanol (20.0 g, 107.34 mmol) and $PPh_3$ (42.2 g, 161.00 mmol) in $CH_2Cl_2$ (500 mL) at 0 $^o$C. The reaction mixture was stirred for 2 h. The reaction mixture was quenched with saturated $Na_2SO_3$ solution (300 mL), the product was extracted with $CH_2Cl_2$ (3 x 250 mL), dried over $MgSO_4$ and concentrated *in vacuo*. The crude product was purified *via* column chromatography ($SiO_2$, Eluent hexane) and was isolated as a colourless liquid (23.39 g, 101.87 mmol, 95%). $^1$H NMR (600 MHz, $CDCl_3$) δ 3.41 (t, *J* = 6.9 Hz, 2H, $BrCH_2CH_2CH_2C_8H_{16}CH_3$), 1.90 – 1.82 (m, 2H, $BrCH_2CH_2CH_2C_8H_{16}CH_3$), 1.46 – 1.38 (m, 2H,

$BrCH_2CH_2CH_2C_8H_{16}CH_3$), 1.35 – 1.21 (m, 16H, $BrCH_2CH_2CH_2C_8H_{16}CH_3$), 0.88 (t, *J* = 7.1 Hz, 3H, $BrCH_2CH_2CH_2C_8H_{16}CH_3$); MS ($EI^+$) *m/z* 248, 250 $(M)^+$. All spectroscopic data is in accordance with literature values.[193]

**3,4,5-tris(dodecyloxy)benzaldehyde**

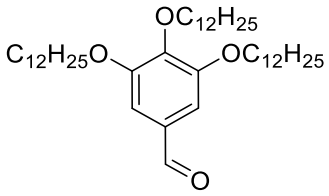


1-bromododecane (5.0 g, 20.15 mmol), 3,4,5-Trihydroxybenzaldehyde monohydrate (578 mg, 3.36 mmol), $K_2CO_3$ (1.39 g, 10.06 mmol) and KI (33 mg, 0.20 mmol) were dissolved in DMF (20 mL). The reaction mixture was heated at 70 °C for 18 h. The product was extracted with $CHCl_3$ (40 mL) from brine (40 mL) and the organic layer was further washed with brine (3 x 40 mL). The organic layer was dried over $MgSO_4$, concentrated *in vacuo* and the product was recystallised from $CHCl_3$/MeOH (1.27 g, 1.93 mmol, 57%). $^1H$ NMR (600 MHz, $CDCl_3$) δ 9.83 (s, 1H, CO*H*), 7.08 (s, 2H, C*H*CCOH), 4.07 – 4.02 (m, 6H, $OCH_2CH_2CH_2(C_7H_{14})CH_3$), 1.86 – 1.80 (m, 4H, *meta*$OCH_2CH_2CH_2(C_7H_{14})CH_3$), 1.78 – 1.72 (m, 2H, *para*$OCH_2CH_2CH_2(C_7H_{14})CH_3$), 1.51 – 1.45 (m, 6H, $OCH_2CH_2CH_2(C_7H_{14})CH_3$), 1.39 – 1.22 (m, 42H, $OCH_2CH_2CH_2(C_7H_{14})CH_3$), 0.88 (t, *J* = 7.0 Hz, 9H, $OCH_2CH_2CH_2(C_7H_{14})CH_3$); MS ($Cl^+$) *m/z* 659 $(M[+H])^+$. All spectroscopic data is in accordance with literature values.[194]

**3,4,5-tris(hexadecyloxy)benzaldehyde**

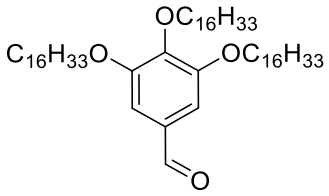


1-Bromohexadecane (4.58 g, 15.0 mmol), 3,4,5-trihydroxybenzaldehyde monohydrate (430 mg, 2.5 mmol), $K_2CO_3$ (1.04 g, 7.5 mmol) and KI (25 mg, 0.15 mmol) were dissolved in DMF (15 mL). The reaction mixture was heated at 70 °C for 64 h. The product was extracted with $CHCl_3$ (40 mL) from brine (40 mL) and the organic layer was further washed with brine (3 x 40 mL). The organic layer was dried over $MgSO_4$, concentrated *in vacuo* and the product was

recystallised from $CHCl_3$/MeOH (1.73 g, 2.09 mmol, 84%). $^1$H NMR (600 MHz, $CDCl_3$) δ 9.83 (s, 1H, C*H*O), 7.08 (s, 2H, OCHCC*H*), 4.08 – 4.01 (m, 6H, CHCOC*H*$_2$ and CHCCOC*H*$_2$), 1.86 – 1.79 (m, 4H, CHCOCH$_2$C*H*$_2$), 1.79 – 1.72 (m, 2H, CHCCOCH$_2$C*H*$_2$), 1.52 – 1.44 (m, 6H, CHCOCH$_2$CH$_2$C*H*$_2$ and CHCCOCH$_2$CH$_2$C*H*$_2$), 1.39 – 1.21 (m, 48H, CHCOCH$_2$CH$_2$CH$_2$C$_8$*H*$_{16}$CH$_3$ and CHCOCH$_2$CH$_2$CH$_2$C$_8$*H*$_{16}$CH$_3$), 0.88 (t, *J* = 7.0 Hz, 9H, C*H*$_3$). All spectroscopic data is in accordance with literature values.[195]

**5,15-bis(3,4,5-tris(dodecyloxy)phenyl)porphyrin**

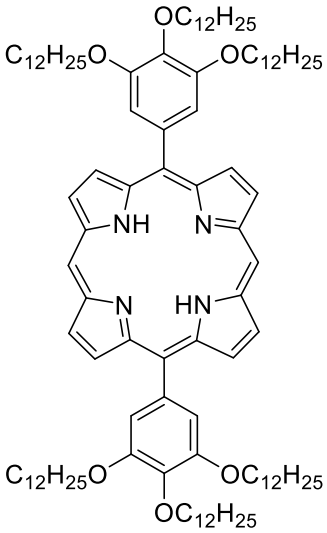


3,4,5-tris(dodecyloxy)benzaldehyde (742 mg, 1.13 mmol), dipyrromethane (165 mg, 1.13 mmol) and $CH_2Cl_2$ (400 mL) were degassed with argon for 10 min. Trifluoroacetic acid (0.03 mL, 0.34 mmol) was added and the reaction mixture was stirred at rt under argon in the dark for 2 h. DDQ (385 mg, 1.70 mmol) was added and the reaction mixture was stirred for a further 1 h. The reaction mixture was passed through a plug of silica using $CH_2Cl_2$ as eluent and concentrated *in vacuo*. The crude product was further purified *via* column chromatography ($SiO_2$, Eluent Hexane:$CHCl_3$ (9:1 to 1:4)) and washed with MeOH and acetone to yield a thick oil (150 mg, 0.096 mmol, 8%). $^1$H NMR (600 MHz, $CDCl_3$) δ 10.31 (s, 2H, NHCC*H*), 9.39 (d, *J* = 4.5 Hz, 4H, NCC*H*CH), 9.19 (d, *J* = 4.5 Hz, 4H, NCCHC*H*), 7.48 (s, 4H, OCC*H*), 4.32 (t, *J* = 6.5 Hz, 4H, NCCCCHC(OC$_{12}$H$_{25}$)COC*H*$_2$C$_{11}$H$_{23}$), 4.14 (t, *J* = 6.4 Hz, 8H, NCCCCHC(OC*H*$_2$C$_{11}$H$_{23}$)COC$_{12}$H$_{25}$), 2.03 – 1.96 (m, 4H, NCCCCHC(OC$_{12}$H$_{25}$)COCH$_2$C*H*$_2$C$_{10}$H$_{21}$), 1.93 – 1.87 (m, 8H, NCCCCHC(OCH$_2$C*H*$_2$C$_{10}$H$_{21}$)COC$_{12}$H$_{25}$), 1.72 – 1.65 (m, 4H, NCCCCHC(OC$_{12}$H$_{25}$)COC$_2$H$_4$C*H*$_2$C$_9$H$_{19}$), 1.55 – 1.18 (m, 104H, NCCCCHC(OC$_{12}$H$_{25}$)COC$_3$H$_6$C$_8$*H*$_{16}$CH$_3$ and NCCCCHC(OC$_2$H$_4$C$_9$*H*$_{18}$CH$_3$)COC$_{12}$H$_{25}$), 0.91 (t, *J* = 7.0 Hz, 6H, NCCCCHC(OC$_{12}$H$_{25}$)COC$_{11}$H$_{22}$C*H*$_3$),

0.85 (t, *J* = 7.0 Hz, 12H, NCCCCHC($OC_{11}H_{22}CH_3$)$COC_{12}H_{25}$), -3.12 (s, 2H, N*H*); MS (TOF $LD^+$) *m/z* 1568 $(M)^+$.

**5,15-dibromo-10,20-bis(3,4,5-tris(dodecyloxy)phenyl)porphyrin**

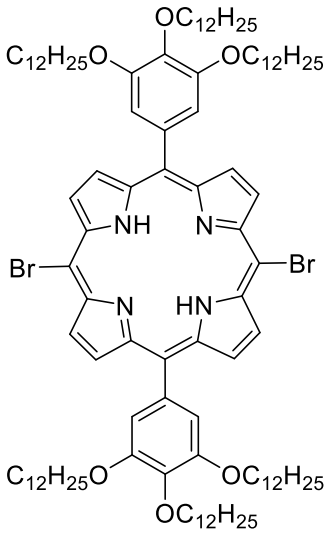


To a solution of 5,15-bis(3,4,5-tris(dodecyloxy)phenyl)porphyrin (150 mg, 0.10 mmol) in $CHCl_3$ (15 mL) was added NBS (43 mg, 0.24 mmol) and pyridine (0.1 mL) and the reaction mixture was stirred for 2 h at rt under argon in the dark. The reaction mixture was concentrated *in vacuo* and purified *via* column chromatography ($SiO_2$, Eluent Hexane:$CHCl_3$ (8:1 to 0:1)) to yield the product as a thick oil (165 mg, 0.10 mmol, quant) which was taken into the next reaction without further purification. $^1$H NMR (300 MHz, $CDCl_3$) δ 9.61 (d, *J* = 4.6 Hz, 4H, NCC*H*CH), 8.95 (d, *J* = 4.7 Hz, 4H, NCCHC*H*), 7.37 (s, 4H, OCC*H*), 4.30 (t, *J* = 6.5 Hz, 4H, NCCCCHC($OC_{12}H_{25}$)$COCH_2C_{11}H_{23}$), 4.10 (t, *J* = 6.2 Hz, 8H, NCCCCHC($OCH_2C_{11}H_{23}$)$COC_{12}H_{25}$), 2.02 – 1.85 (m, 12H, NCCCCHC($OC_{12}H_{25}$)$COCH_2CH_2C_{10}H_{21}$ and NCCCCHC($OCH_2CH_2C_{10}H_{21}$)$COC_{12}H_{25}$), 1.53 – 1.18 (m, 108H, NCCCCHC($OC_{12}H_{25}$)$COC_2H_4C_9H_{18}CH_3$ and NCCCCHC($OC_2H_4C_9H_{18}CH_3$)$COC_{12}H_{25}$), 0.95 – 0.80 (m, 18H, $CH_3$), -2.72 (s, 2H, N*H*); MS (TOF $LD^+$) *m/z* 1726 $(M)^+$.

**5,15-dibromo-10,20-bis(3,4,5-tris(dodecyloxy)phenyl)porphyrinato zinc (II)**

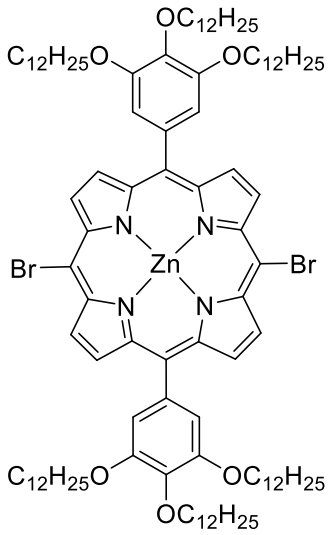


5,15-dibromo-10,20-bis(3,4,5-tris(dodecyloxy)phenyl)porphyrin (165 mg, 0.10 mmol) and $Zn(OAc)_2$ (351 mg, 1.912 mmol) were stirred in $CH_2Cl_2$ (30 mL) for 18 h at rt in the dark. The reaction mixture was concentrated *in vacuo* and purified *via* column chromatography ($SiO_2$, Eluent Hexane:$CHCl_3$ (8:1 to 0:1)) to yield the product as a thick oil (100 mg, 0.06 mmol, 58%). $^1$H NMR (600 MHz, $CDCl_3$) δ 9.74 (d, *J* = 4.6 Hz, 4H, NCC*H*CH), 9.07 (d, *J* = 4.6 Hz, 4H, NCCHC*H*), 7.38 (s, 4H, OCC*H*), 4.31 (t, *J* = 6.6 Hz, 4H, NCCCCHC($OC_{12}H_{25}$)COC$H_2C_{11}H_{23}$), 4.10 (t, *J* = 6.6 Hz, 8H, NCCCCHC(OC$H_2C_{11}H_{23}$)C$OC_{12}H_{25}$), 2.02 – 1.96 (m, 4H, NCCCCHC($OC_{12}H_{25}$)COCH$_2$C$H_2C_{10}H_{21}$), 1.91 – 1.85 (m, 8H, NCCCCHC(OCH$_2$C$H_2C_{10}H_{21}$)C$OC_{12}H_{25}$), 1.71 – 1.65 (m, 4H, NCCCCHC($OC_{12}H_{25}$)COC$_2$H$_4$C$H_2C_9H_{19}$), 1.53 – 1.46 (m, 8H, NCCCCHC($OC_2H_4CH_2C_9H_{19}$)C$OC_{12}H_{25}$), 1.45 – 1.17 (m, 96H, NCCCCHC($OC_{12}H_{25}$)COC$_3$H$_6$C$_8H_{16}$CH$_3$ and NCCCCHC(OC$_3$H$_6$C$_8H_{16}$CH$_3$)C$OC_{12}H_{25}$), 0.91 (t, *J* = 7.1 Hz, 6H, NCCCCHC($OC_{12}H_{25}$)COC$_{11}$H$_{22}$C$H_3$), 0.85 (t, *J* = 7.0 Hz, 12H, NCCCCHC(OC$_{11}$H$_{22}$C$H_3$)C$OC_{12}H_{25}$); MS (TOF LD$^+$) *m/z* 1790 $(M)^+$.

**5,15-bis((trimethylsilyl)ethynyl)-10,20-bis(3,4,5-tris(dodecyloxy)phenyl)porphyrinato zinc (II)**

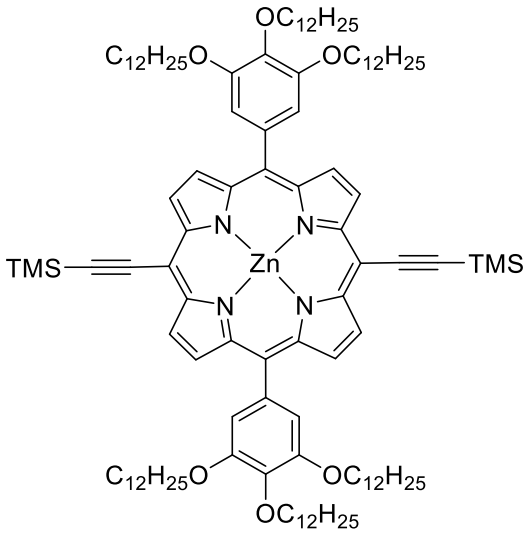


A mixture of triethylamine (30 mL) and THF (10 mL) was degassed with argon for 30 min before the addition of 5,15-dibromo-10,20-bis(3,4,5-tris(dodecyloxy)phenyl)porphyrinato zinc (II) (100 mg, 0.06 mmol). Trimethylsilylacetylene (17 µL, 0.12 mmol), $Pd(PPh_3)_2Cl_2$ (4 mg, 0.006 mmol) and CuI (2 mg, 0.011 mmol) were added, the reaction mixture was further degassed for 10 min at 0 °C and then allowed to warm to rt and stirred for 18 h under argon in the dark. The reaction mixture was concentrated *in vacuo* and purified *via* column chromatography ($SiO_2$, Eluent Hexane:$CHCl_3$ (8:1 to 0:1)) to yield the product as a thick oil (92 mg, 0.05 mmol, 90%). $^1$H NMR (600 MHz, $CDCl_3$) δ 9.70 (d, *J* = 4.5 Hz, 4H, NCC*H*CH), 9.03 (d, *J* = 4.5 Hz, 4H, NCCHC*H*), 7.39 (s, 4H, OCC*H*), 4.31 (t, *J* = 6.5 Hz, 4H, NCCCCHC($OC_{12}H_{25}$)COC$H_2C_{11}H_{23}$), 4.11 (t, *J* = 6.4 Hz, 8H, NCCCCHC(OC$H_2C_{11}H_{23}$)C$OC_{12}H_{25}$), 2.02 – 1.95 (m, 4H, NCCCCHC($OC_{12}H_{25}$)COC$H_2$C$H_2C_{10}H_{21}$), 1.92 – 1.85 (m, 8H, NCCCCHC(OC$H_2$C$H_2C_{10}H_{21}$)C$OC_{12}H_{25}$), 1.72 – 1.64 (m, 4H, NCCCCHC($OC_{12}H_{25}$)C$OC_2H_4$C$H_2C_9H_{19}$), 1.52 – 1.46 (m, 8H, NCCCCHC($OC_2H_4$C$H_2C_9H_{19}$)C$OC_{12}H_{25}$), 1.46 – 1.17 (m, 96H, NCCCCHC($OC_{12}H_{25}$)C$OC_3H_6C_8H_{16}CH_3$ and NCCCCHC($OC_3H_6C_8H_{16}CH_3$)C$OC_{12}H_{25}$), 0.90 (t, *J* = 6.9 Hz, 6H, NCCCCHC($OC_{12}H_{25}$)C$OC_{11}H_{22}CH_3$), 0.84 (t, *J* = 7.0 Hz, 12H, NCCCCHC($OC_{11}H_{22}CH_3$)C$OC_{12}H_{25}$), 0.61 (s, *J* = 5.8 Hz, 18H, Si$CH_3$); MS (TOF $LD^+$) *m/z* 1824 $(M)^+$.

**5,15-diethynyl-10,20-bis(3,4,5-tris(dodecyloxy)phenyl)porphyrinato zinc (II)**

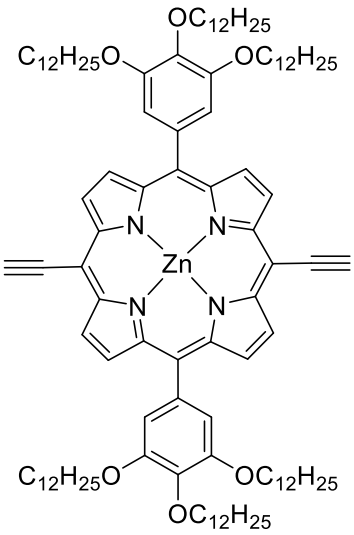


5,15-bis((trimethylsilyl)ethynyl)-10,20-bis(3,4,5-tris(dodecyloxy)phenyl)porphyrinato zinc (II) (46 mg, 0.025 mmol) was dissolved in $CH_2Cl_2$ (20 mL), a 1.0 M solution of TBAF in THF was added (0.1 mL, 0.1 mmol) was added and the reaction mixture was stirred for 18 h at rt under argon in the dark. The reaction mixture was concentrated *in vacuo* and purified *via* column chromatography ($SiO_2$, Eluent Hexane:$CH_2Cl_2$ (8:1 to 0:1)) to yield the product as a thick oil (42 mg, 0.025 mmol, quant). $^1$H NMR (600 MHz, $CDCl_3$) δ 9.75 (d, *J* = 4.6 Hz, 4H, NCC*H*CH), 9.07 (d, *J* = 4.6 Hz, 4H, NCCHC*H*), 7.40 (s, 4H, OCC*H*), 4.31 (t, *J* = 6.7 Hz, 4H, NCCCCHC($OC_{12}H_{25}$)COC*H*$_2$$C_{11}H_{23}$), 4.20 (s, 2H, C≡C*H*), 4.11 (t, *J* = 6.5 Hz, 8H, NCCCCHC(OC*H*$_2$$C_{11}H_{23}$)$COC_{12}H_{25}$), 2.02 – 1.96 (m, 4H, NCCCCHC($OC_{12}H_{25}$)$COCH_2CH_2C_{10}H_{21}$), 1.92 – 1.85 (m, 8H, NCCCCHC($OCH_2CH_2C_{10}H_{21}$)$COC_{12}H_{25}$), 1.72 – 1.65 (m, 4H, NCCCCHC($OC_{12}H_{25}$)$COC_2H_4CH_2C_9H_{19}$), 1.53 – 1.46 (m, 8H, NCCCCHC($OC_2H_4CH_2C_9H_{19}$)$COC_{12}H_{25}$), 1.46 – 1.18 (m, 96H, NCCCCHC($OC_{12}H_{25}$)$COC_3H_6C_8H_{16}CH_3$ and NCCCCHC($OC_3H_6C_8H_{16}CH_3$)$COC_{12}H_{25}$), 0.91 (t, *J* = 7.0 Hz, 6H, NCCCCHC($OC_{12}H_{25}$)$COC_{11}H_{22}CH_3$), 0.85 (t, *J* = 7.1 Hz, 12H, NCCCCHC($OC_{11}H_{22}CH_3$)$COC_{12}H_{25}$).

**HAPPAP - 5,15-bis((4-bromophenyl)ethynyl)-10,20-bis(3,4,5-tris(dodecyloxy)phenyl) porphyrinato zinc(II)**

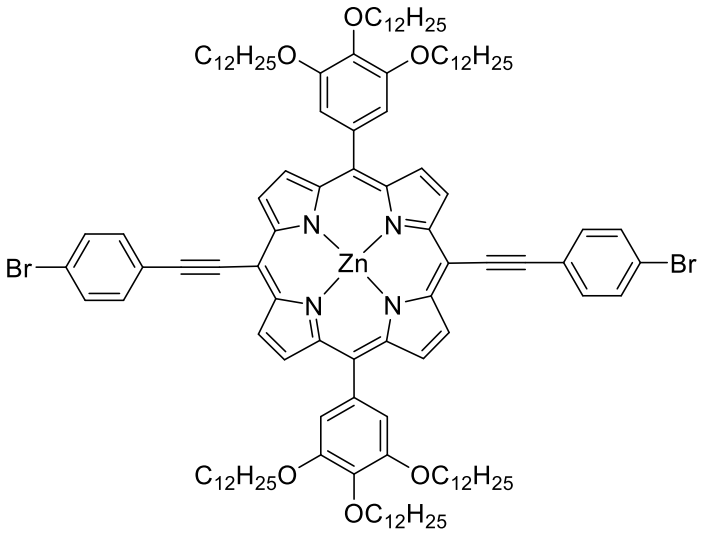


5,15-diethynyl-10,20-bis(3,4,5-tris(dodecyloxy)phenyl)porphyrinato zinc (II) (53 mg, 0.032 mmol), triethylamine (30 mL) and THF (10 mL) were degassed with argon for 30 min. 1-bromo-4-iodobenzene (20 mg, 0.070 mmol), $Pd(PPh_3)_2Cl_2$ (2 mg, 0.003 mmol) and CuI (1 mg, 0.005 mmol) were added and the reaction mixture was stirred for 18 h at rt under argon in the dark. The reaction mixture was concentrated *in vacuo* and purified *via* column chromatography ($SiO_2$, Eluent Hexane:$Et_2O$ (1:0 to 9:1)) to yield the product as a thick oil (13 mg, 0.007 mmol, 20%). $^1$H NMR (600 MHz, $CDCl_3$) δ 9.75 (d, *J* = 4.6 Hz, 4H, NCC*H*CH), 9.07 (d, *J* = 4.6 Hz, 4H, NCCHC*H*), 7.90 (d, *J* = 8.3 Hz, 4H, BrCC*H*CH), 7.72 (d, *J* = 8.3 Hz, 4H, BrCCHC*H*), 7.42 (s, 4H, OCC*H*), 4.32 (t, *J* = 6.6 Hz, 4H, NCCCCHC($OC_{12}H_{25}$)CO$CH_2C_{11}H_{23}$), 4.12 (t, *J* = 6.5 Hz, 8H, NCCCCHC(O$CH_2C_{11}H_{23}$)CO$C_{12}H_{25}$), 2.03 – 1.96 (m, 4H, NCCCCHC($OC_{12}H_{25}$)CO$CH_2CH_2C_{10}H_{21}$), 1.93 – 1.86 (m, 8H, NCCCCHC(O$CH_2CH_2C_{10}H_{21}$)CO$C_{12}H_{25}$), 1.74 – 1.66 (m, 4H, NCCCCHC($OC_{12}H_{25}$)CO$C_2H_4CH_2C_9H_{19}$), 1.53 – 1.47 (m, 8H, NCCCCHC(O$C_2H_4CH_2C_9H_{19}$)CO$C_{12}H_{25}$), 1.41 – 1.18 (m, 96H, NCCCCHC($OC_{12}H_{25}$)CO$C_3H_6C_8H_{16}CH_3$ and NCCCCHC(O$C_3H_6C_8H_{16}CH_3$)CO$C_{12}H_{25}$), 0.91 – 0.82 (m, 18H, NCCCCHC($OC_{12}H_{25}$)CO$C_{11}H_{22}CH_3$ and NCCCCHC(O$C_{11}H_{22}CH_3$)CO$C_{12}H_{25}$); $^{13}$C NMR (151 MHz, $CDCl_3$) δ 151.3, 151.0, 150.3, 133.1, 132.1, 114.4, 69.5, 50.7, 32.1, 32.0, 30.7, 30.0, 29.9, 29.8, 29.6, 29.5, 26.5, 26.3, 22.9, 22.8, 14.3, 14.2; UV (chlorobenzene) $\lambda_{max}$ 453; MS (TOF $LD^+$) *m/z* 1988 $(M)^+$.

**F8BT-HAPAPP5 – *Poly*-2,7-(9,9-dioctylfluorene-*alt*-4,7-2,1,3-benzothiadiazole)-*ran*-2,7-(9,9-dioctylfluorene-*alt*-4',4''-5,15-bis(phenylethynyl)-10,20-bis(3,4,5-tris(dodecyloxy)phenyl)porphyrinato Zinc (II))**

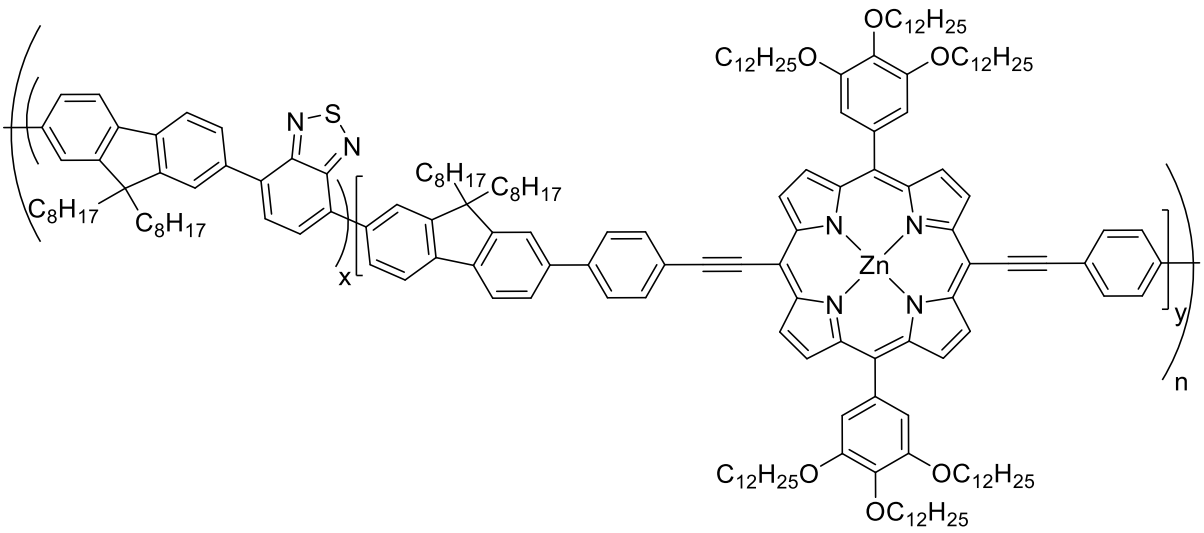


A polymer was synthesised with a weight percentage of 5% porphyrin to benzothiadiazole moiety (x:y = 19:1).

A solution of 4,7-dibromo-2,1,3-benzothiadiazole (53 mg, 0.181 mmol), 9,9-Dioctyl-9*H*-fluorene-2,7-diboronic acid bis(pinacol) ester (118 mg, 0.183 mmol) and 5,15-bis((4-bromophenyl)ethynyl)-10,20-bis(3,4,5-tris(dodecyloxy)phenyl)porphyrinato zinc (II) (4.5 mg, 0.002 mmol) in toluene (4 mL) and a separate solution of 20% tetraethylammonium hydroxide in water (3 mL) were degassed for 30 min. $Pd(OAc)_2$ (1 mg, 0.005 mmol) and $PPh_3$ (5 mg, 0.019 mmol) were added to the organic solution which was again degassed for 30 min. The aqueous solution was added to the organic and the reaction mixture was stirred under argon at 110 $^oC$ for 18 h. The reaction was allowed to cool and the product was precipitated from MeOH and filtered. The polymer product was then washed with acetone and hexane and extracted with $CHCl_3$. The polymer was then concentrated *in vacuo* to a small volume and precipitated from MeOH (20 mg, 20%). UV (chlorobenzene) $\lambda_{max}$ 469; GPC (PS): $M_n$ = 10000 Da, $M_w$ = 15000 Da , PDI = 1.5.

## 6.4 Synthetic Techniques for Chapter 4

**2,7-dibromo-9H-fluoren-9-one**

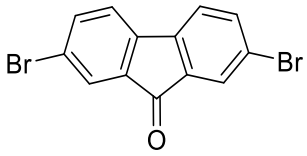


**Method 1**

To a solution of 2,7-dibromo-9H-fluorene (1.0 g, 3.09 mmol) in AcOH (10 mL) was added $CrO_3$ (1.5 g, 15.0 mmol) in AcOH (10 mL). The reaction mixture was stirred open to air for 42 h at rt. The reaction was quenched with saturated $NaHCO_3$ solution and the solid yellow product was filtered and recrystallized twice from a 1:1 mixture of EtOH: toluene (745 mg, 2.2 mmol, 71%). $^1$H NMR (500 MHz, $CDCl_3$) δ 7.77 (d, *J* = 1.8 Hz, 2H, COCC*H*), 7.63 (dd, J = 7.9, 1.8 Hz, 2H, CBrC*H*CH), 7.39 (d, J = 7.9 Hz, 2H, CBrCHC*H*).; MS ($Cl^+$) *m/z* 336, 338 and 340 $(M)^+$. All spectroscopic data is in accordance with literature values.[196]

**Method 2**

Fluorenone (5.00 g, 27.70 mmol) in $H_2O$ (70 mL) was heated to 80 °C. Neat $Br_2$ (7.15 mL, 138.70 mmol) was added over 10 min and the reaction mixture was stirred for 10 h. The reaction was cooled to rt and additional $H_2O$ (150 mL) was added followed by saturated $Na_2SO_3$ solution (150 mL). The crude product was filtered and washed with $H_2O$ to yield a solid yellow product (9.25 g, 27.7 mmol, quant) was isolated. All spectra in accordance with previously reported data.

**2,7-dibromo-9,9'-spirobi[fluorene]**

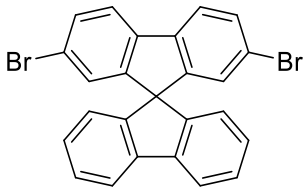


Mg (306 mg, 12.6 mmol) and a crystal of $I_2$ were stirred anhydrously with the slow addition of 2-bromobiphenyl (2.2 mL, 12.6 mmol) in THF (15 mL) over 10 min. The reaction was heated to reflux and stirred for 2 h. The reaction mixture was then cooled to -78 °C and 2,7-dibromo-

9H-fluoren-9-one (3.55 gg, 10.5 mmol) in THF (50 mL) was added slowly over 10 min and the reaction mixture was then stirred at reflux for 18 h. The reaction mixture was concentrated *in vacuo* and the magnesium salt was collected as an orange powder which was stirred in 5% HCl solution (100 mL) at 0 $^{o}$C for 3 h. The alcohol intermediate was filtered as an orange solid and was then dissolved in refluxing AcOH (120 mL) before concentrated HCl (5 mL) was added. After 40 min, the off-white product (2.84 g, 5.99 mmol, 57%) was filtered and washed with AcOH (30 mL). $^{1}$H NMR (600 MHz, $CDCl_3$) δ 7.85 (d, *J* = 7.6 Hz, 2H, Ar*H*), 7.67 (d, *J* = 8.2 Hz, 2H, BrCCHC*H*), 7.49 (dd, *J* = 8.2, 1.8 Hz, 2H, BrCC*H*CH), 7.40 (ddd, *J* = 7.6, 7.6, 1.0 Hz, 2H, Ar*H*), 7.15 (ddd, *J* = 7.6, 7.6, 1.0 Hz, 2H, Ar*H*), 6.83 (d, *J* = 1.8 Hz, 2H, CCC*H*CBr), 6.72 (d, *J* = 7.6 Hz, 2H, Ar*H*); MS ($EI^+$) *m/z* 472, 474 and 476 $(M)^+$. All spectroscopic data is in accordance with literature values.[124]

**9,9'-spirobi[fluorene]-2,7-dicarbaldehyde**

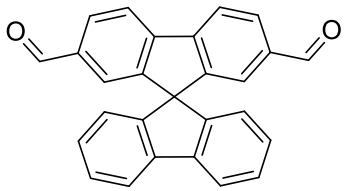


2,7-dibromo-9,9'-spirobi[fluorene] (200 mg, 0.42 mmol) and THF (5 mL) were degassed at -78 $^{o}$C and 2.5 M n-butyllithium (0.42 mL, 1.05 mmol) was added dropwise over 10 min. The reaction mixture was stirred for 20 min and formyl piperidine (0.14 mL, 1.26 mmol) was added. The reaction mixture was allowed to warm to rt and was stirred under argon for 1 h. $H_2O$ (20 mL) was added and the product was extracted with $Et_2O$ (2 x 30 mL), dried over $MgSO_4$ and concentrated *in vacuo*. The crude product was purified *via* column chromatography ($SiO_2$, Eluent $CHCl_3$:Hexane (1:1)) to give an off white powder (61 mg, 0.16 mmol, 39%). $^{1}$H NMR (600 MHz, $CDCl_3$) δ 9.86 (s, 2H, C*H*O), 8.07 (d, *J* = 8.0 Hz, 2H, CHOCCHC*H*), 7.96 (d, *J* = 8.0 Hz, 2H, CHOCC*H*CH), 7.90 (d, *J* = 7.6 Hz, 2H, Ar*H*), 7.42 (dd, *J* = 7.6, 7.6 Hz, 2H, Ar*H*), 7.30 (s, 2H, CC*H*CCHO), 7.12 (dd, *J* = 7.6, 7.6 Hz, 2H, Ar*H*), 6.68 (d, *J* = 7.6 Hz, 2H, Ar*H*); MS ($ES^+$) *m/z* 373 $(M[+H])^+$. All spectroscopic data is in accordance with literature values.[197]

**9,9'-spirobi[fluorene]-2,7-dicarbonitrile**

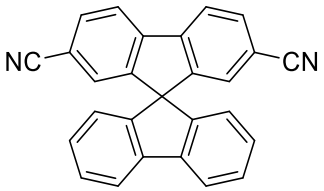


28% ammonium hydroxide solution (0.4 mL) and $I_2$ (89 mg, 0.36 mmol) were added to a solution of 9,9'-spirobi[fluorene]-2,7-dicarbaldehyde (61 mg, 0.16 mmol) in acetonitrile (2 mL) and THF (0.5 mL). The reaction mixture was allowed to stir for 64 h. The reaction was quenched with saturated $Na_2SO_3$ solution (20 mL) and the product was extracted with $Et_2O$ (2 x 30mL), dried over $MgSO_4$ and concentrated *in vacuo* to give an off white powder (59 mg, 0.36 mmol, 99%). $^1$H NMR (500 MHz, $CDCl_3$) δ 7.98 (d, *J* = 8.0 Hz, 2H, NCCCHC*H*), 7.89 (d, *J* = 7.6 Hz, 2H, Ar*H*), 7.72 (dd, *J* = 8.0, 1.4 Hz, 2H, NCCC*H*CH), 7.45 (ddd, *J* = 7.6, 7.6, 1.0 Hz, 2H, Ar*H*), 7.16 (ddd, *J* = 7.6, 7.6, 1.0 Hz, 2H, Ar*H*), 7.05 (d, *J* = 1.4 Hz, 2H, CC*H*CCN), 6.65 (d, *J* = 7.6 Hz, 2H, Ar*H*); MS (EI$^+$) *m/z* 366 (M)$^+$. All spectroscopic data is in accordance with literature values.[198]

**2',7'-dibromo-9,9'-spirobi[fluorene]-2,7-dicarbonitrile**

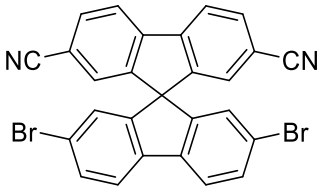


**Method 1**

9,9'-spirobi[fluorene]-2,7-dicarbonitrile (485 mg, 1.32 mmol), $FeCl_3$ (11 mg, 0.07 mmol) and $CH_2Cl_2$ (40 mL) were heated to reflux under anhydrous conditions under an atmosphere of argon. A solution of $Br_2$ (0.27 mL, 5.28 mmol) in $CH_2Cl_2$ (8 mL) was added slowly and the reaction mixture was stirred at reflux for 7 h. The reaction was quenched with saturated $Na_2SO_3$ solution (70 mL) and the product was extracted with $CH_2Cl_2$ (2 x 50 mL), dried over $MgSO_4$ and concentrated *in vacuo*. The crude product was purified *via* column chromatography ($SiO_2$, Eluent $CHCl_3$:Hexane (1:1)) to give an off white powder that was further purified by recrystallization from $CHCl_3$ and hexane (88 mg, 0.17 mmol, 13%). $^1$H NMR (600 MHz, $CDCl_3$) δ 8.00 (d, *J* = 8.0 Hz, 2H, NCCCHC*H*), 7.78 (d, *J* = 8.0, 2H, NCCC*H*CH), 7.73 (d, *J* = 8.2 Hz, 2H, BrCCHC*H*), 7.59 (dd, *J* = 8.2, 1.6 Hz, 2H, BrCC*H*CH), 7.06 (s, 2H, CC*H*CCN), 6.77

(d, *J* = 1.6 Hz, 2H, CC*H*CBr); $^{13}$C NMR (151 MHz, $CDCl_3$) δ 148.8, 147.2, 143.9, 139.8, 133.1, 132.5, 128.3, 127.2, 122.6, 122.2, 122.1, 118.3, 113.3, 65.2; MS ($EI^+$) *m/z* 522, 524 and 526 $(M)^+$; HRMS 521.9367 calculated for $C_{27}H_{12}{}^{79}BrN_2$ found 521.9362. All spectroscopic data is in accordance with literature values.[198]

**Method 2**

28% ammonium hydroxide solution (6.0 mL) and $I_2$ (765 mg, 3.01 mmol) were added to a solution of 2',7'-dibromo-9,9'-spirobi[fluorene]-2,7-dicarbaldehyde (729 mg, 1.37 mmol) in acetonitrile (30 mL) and THF (8 mL). The reaction mixture was allowed to stir for 18 h. The reaction was quenched with saturated $Na_2SO_3$ solution (50 mL) and the product was extracted with $Et_2O$ (2 x 50mL), dried over $MgSO_4$ and concentrated *in vacuo* to give an off white powder (489 mg, 0.93 mmol, 68%). All spectra in accordance with previously reported data.

***Poly*-9,9-dioctyl-9H-fluorene-*alt*-9,9'-spirobi[fluorene]-2,7-dicarbonitrile**

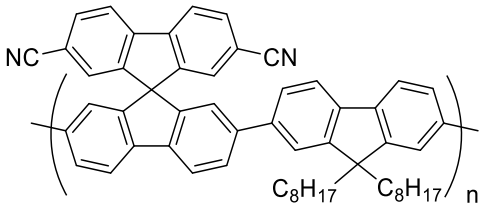


A solution of aliquat 336 (1 drop) in toluene (5 mL) and a separate solution of 1.0 M $Na_2CO_3$ (1 mL) were both degassed for 30 min. 2',7'-dibromo-9,9'-spirobi[fluorene]-2,7-dicarbonitrile (67 mg, 0.127 mmol) and 2,2'-(9,9-dioctyl-9H-fluorene-2,7-diyl)bis(4,4,5,5-tetramethyl-1,3,2-dioxaborolane) (82 mg, 0.127 mmol) were placed in a microwave *via*l and purged with argon. The solution of aliquat 336 in toluene was added and the reaction mixture was degassed for 40 min. $Pd(PPh_3)_4$ (15 mg, 0.013 mmol) was added and the reaction mixture was degassed for a further 20 min. The 1.0 M $Na_2CO_3$ solution (1 mL) was added and the reaction mixture was heated to 110 $^oC$ and stirred for 18 h. The reaction was allowed to cool and the product was precipitated from MeOH and filtered. The polymer product was then washed with acetone and hexane and extracted with $CHCl_3$ (89 mg, 93%). GPC (PS): $M_n$ = 5100 Da, $M_w$ = 7800 Da, PDI = 1.5.

**2,7-dibromo-9,9-dihexadecyl-9H-fluorene**

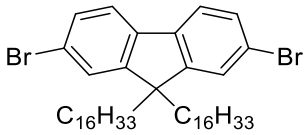


2,7-dibromofluorene (1.44 g, 4.44 mmol) and 1-bromohexadecane (4.07 mL, 13.33 mmol) in a 1:1 mixture of 13 M NaOH solution and toluene (30 mL) were degassed for 30 min. Tetrabutylammonium bromide (13 mg, 0.04 mmol) was added and the reaction was heated to reflux for 18 h. The reaction was allowed to cool, the organic layer separated and the aqueous washed with $CH_2Cl_2$ (2 x 25 mL). The combined organic fractions were dried over $MgSO_4$ and concentrated *in vacuo* to yield a yellow solid which was recrystallized from EtOH to give off white crystals (1.90 g, 2.46 mmol, 55%). $^1$H NMR (300 MHz, $CDCl_3$) δ 7.54 – 7.48 (m, 2H, CBrC*H*CH), 7.47 – 7.41 (m, 4H, $CH_2CCC$*H* + CBrCHC*H*), 1.95 – 1.85 (m, 4H, $C(CH_2C_{14}H_{28}CH_3)_2$), 1.34 – 0.99 (m, 56H, $C(CH_2C_{14}H_{28}CH_3)_2$), 0.87 (t, *J* = 6.7 Hz, 6H, $C(CH_2C_{14}H_{28}CH_3)_2$); $^{13}$C NMR (151 MHz, $CDCl_3$) δ 152.7, 139.2, 130.3, 126.3, 121.6, 121.3, 55.8, 40.3, 32.1, 30.00, 29.8, 29.8, 29.8, 29.8, 29.7, 29.7, 29.7, 29.5, 29.3, 23.7, 22.8, 14.3; MS (EI$^+$) *m/z* 769, 771 and 773 $(M)^+$; HRMS 770.4001 calculated for $C_{45}H_{72}{}^{79}Br_2$ found 770.4005.

**2,7-dibromo-9,9-dihexadecyl-9H-fluorene**

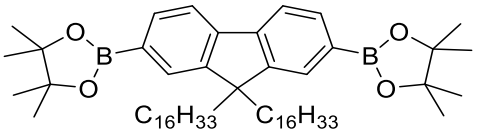


2,7-dibromo-9,9-dihexadecyl-9H-fluorene (900 mg, 1.16 mmol), bis(pinacolato)diboron (886 mg, 3.49 mmol), [1,1'-Bis(diphenylphosphino)ferrocene]dichloropalladium(II), complex with dichloromethane (65 mg, 0.08 mmol), potassium acetate (457 mg, 4.66 mmol) and DMF (50 mL) were degassed with argon for 10 min and then stirred at 80 °C for 64 h. The reaction mixture was poured into $H_2O$ (150 mL) and the product was extracted with $CH_2Cl_2$ (2 x 100 mL). The organic fraction was washed with brine (4 x 150 mL), dried over $MgSO_4$ and concentrated *in vacuo*. The crude product was purified *via* column chromatography ($SiO_2$, Eluent $CHCl_3$:Hexane (1:3)) to give a clear liquid that solidified to white crystals upon standing (1.00 g, 1.15 mmol, 99%). $^1$H NMR (600 MHz, $CDCl_3$) δ 7.81 (d, *J* = 7.6 Hz, 2H, CBrCHC*H*), 7.75 (s, 2H, $CH_2CCC$*H*), 7.72 (d, *J* = 7.6 Hz, 2H, CBrC*H*CH), 2.03 – 1.97 (m, 4H, $C(CH_2C_{14}H_{28}CH_3)_2$), 1.39 (s, 24H, BOCC*H*$_3$), 1.34 – 1.17 (m, 56H, $C(CH_2C_{14}H_{28}CH_3)_2$), 0.89 (t, *J* = 7.0 Hz, 6H,

$C(CH_2C_{14}H_{28}CH_3)_2$); $^{13}C$ NMR (151 MHz, $CDCl_3$) δ 150.6, 144.0, 133.8, 129.0, 119.5, 83.8, 55.3, 40.3, 32.1, 31.7, 30.1, 29.8, 29.7, 29.5, 29.4, 25.0, 22.8, 14.3; MS ($EI^+$) *m/z* 890 $(M+Na)^+$; HRMS 889.7392 calculated for $C_{57}H_{96}B_2NaO_4$ found 889.8323.

**2-bromo-4,4'-dimethyl-1,1'-biphenyl**

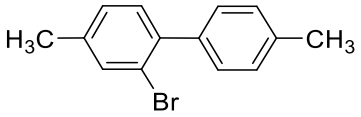


4,4'-Dimethylbiphenyl (4.0 g, 21.9 mmol), a crystal of $I_2$ and dry $CH_2Cl_2$ (40 mL) were stirred anhydrously for 30 min at 0 °C. $Br_2$ (1.36 mL, 26.3 mmol) was added and the reaction mixture was stirred at 0 °C for 3 h. $Na_2SO_3$ solution (50 mL) was added and the organic layer was separated and extracted with further $Na_2SO_3$ solution (2 x 50 mL). The organic layer was dried over $MgSO_4$ and concentrated *in vacuo*. Product (5.73 g, 21.9 mmol, 100%) was taken into the next reaction without further purification. $^1H$ NMR (600 MHz, $CDCl_3$) δ 7.51 (d, *J* = 0.8 Hz, 1H, BrCC*H*), 7.31 (d, *J* = 8.1 Hz, 2H, MeCC*H*CH), 7.24 (d, *J* = 8.1 Hz, 2H, MeCCHC*H*), 7.22 (d, *J* = 7.7 Hz, 1H, BrCCHC(Me)CHC*H*), 7.16 (dd, *J* = 7.7 Hz, 0.8 Hz, 1H, BrCCHC(Me)C*H*); MS ($ES^+$) *m/z* 260, 262 $(M)^+$; HRMS 260.0201 calculated for $C_{14}H_{13}{}^{79}Br$ found 260.0199. All spectroscopic data is in accordance with literature values.[199]

**2,7-dibromo-2',7'-dimethyl-9,9'-spirobi[fluorene]**

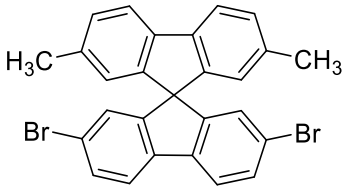


Mg (537 mg, 22.1 mmol) and a crystal of $I_2$ were placed under argon and 2-bromo-4,4'-dimethyl-1,1'-biphenyl (5.77 g, 22.1 mmol) in THF (40 mL) was added slowly at rt. The solution was heated to 85 °C for 1 h and was then cooled to -78 °C and 2,7-dibromo-9H-fluoren-9-one (3.40 g, 10.1 mmol) in THF (100 mL) was added slowly. The reaction was heated to 85 °C and stirred for 18 h. The reaction mixture was then concentrated *in vacuo* and 5% HCl solution was added and stirred for 2 h. The HCl solution was then decanted off and the remaining solid was dissolved in AcOH (100 mL) at 120 °C. Concentrated HCl (2 drops) was added and the solution was allowed to cool to rt. The product was filtered off as a white powder (4.26 g, 8.47 mmol,

84%). $^1$H NMR (600 MHz, $CDCl_3$) δ 7.69 – 7.66 (m, 4H, $CH_3CCHCH$ and $BrCCHCH$), 7.50 (dd, *J* = 8.2, 1.8 Hz, 2H, $BrCCHCH$), 7.19 (dd, *J* = 7.8, 0.7 Hz, 2H, $CH_3CCHCH$), 6.85 (d, *J* = 1.8 Hz, 2H, $BrCCHC$), 6.48 (d, *J* = 0.7 Hz, 2H, $CH_3CCHC$), 2.23 (s, 6H, $CH_3$); MS ($EI^+$) *m/z* 502 $(M)^+$; HRMS 499.9770 calculated for $C_{27}H_{18}{}^{79}Br_2$ found 499.9790. All spectroscopic data is in accordance with literature values.[200]

**2,7-dibromo-2',7'-bis(bromomethyl)-9,9'-spirobi[fluorene]**

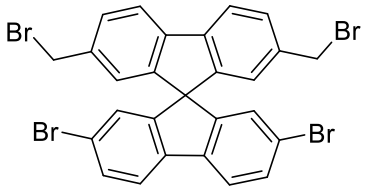


2,7-dibromo-2',7'-dimethyl-9,9'-spirobi[fluorene] (283 mg, 0.56 mmol), NBS (219 mg, 1.23 mmol), benzoyl peroxide (75:25 with $H_2O$) (25 mg, 0.14 mmol) and $CCl_4$ (4 mL) were stirred at 85 °C under argon for 18 h. The solvent was then allowed to evaporate. The brown solid was purified *via* column chromatography ($SiO_2$, Eluent 3:1 hexane:$CHCl_3$) to give a white powder (315 mg, 0.48 mmol, 85%). $^1$H NMR (600 MHz, $CDCl_3$) δ 7.81 (d, *J* = 8.1 Hz, 2H, $BrCH_2CCHCH$), 7.70 (d, *J* = 7.9 Hz, 2H, $BrCCHCH$), 7.53 (d, *J* = 8.1 Hz, 2H, $BrCH_2CCHCH$), 7.48 (d, *J* = 7.9 Hz, 2H, $BrCCHCH$), 6.83 (s, 2H, $BrCCHC$), 6.70 (s, 2H $BrCH_2CCHC$), 4.38 (s, 4H, $CH_2$); MS ($ES^+$) *m/z* 660 $(M)^+$. All spectroscopic data is in accordance with literature values.[200]

**2',7'-dibromo-9,9'-spirobi[fluorene]-2,7-dicarbaldehyde**

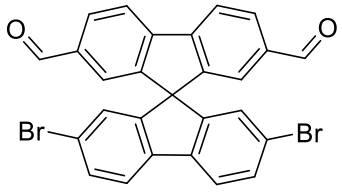


2,7-dibromo-2',7'-bis(bromomethyl)-9,9'-spirobi[fluorene] (315 mg, 0.48 mmol), $NaHCo_3$ (1.2 g) and DMSO (5 mL) were stirred at 110 °C under argon for 18 h. The reaction mixture was poured into $H_2O$ and the precipitate was filtered and placed in a vacuum desiccator overnight. The product was purified *via* column chromatography ($SiO_2$, Eluent $CHCl_3$) to give a white solid (167 mg, 0.31 mmol, 66%). $^1$H NMR (600 MHz, $CDCl_3$) δ 9.91 (s, 2H, $CHO$), 8.10 (d, *J* = 7.9 Hz, 2H, $OCHCCHCH$), 8.01 (dd, *J* = 7.9, 1.4 Hz, 2H, $OCHCCHCH$), 7.73 (d, *J* = 8.2 Hz, 2H, $BrCCHCH$),

7.56 (dd, *J* = 8.2, 1.8 Hz, 2H, BrCC*H*CH), 7.31 (d, *J* = 1.4 Hz, 2H, OCHCC*H*C), 6.79 (d, *J* = 1.8 Hz, 2H, BrCC*H*C); MS ($EI^+$) *m/z* 530 $(M)^+$; HRMS 529.9335 calculated for $C_{27}H_{14}{}^{79}Br_2O_2$ found 529.9338. All spectroscopic data is in accordance with literature values.[200]

**SFCN – *Poly*-2,7-(9,9-dihexadecyl-9H-fluoren-2-yl)-*alt*-2,7-(9,9'-spirobi[fluorene]-2',7'-dicarbonitrile)**

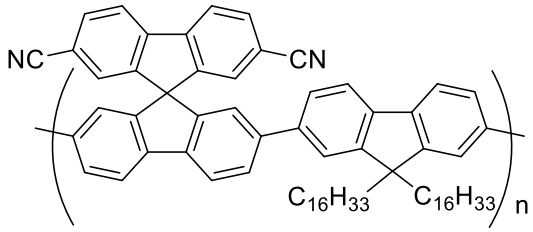


A solution of 2',7'-dibromo-9,9'-spirobi[fluorene]-2,7-dicarbonitrile (132 mg, 0.253 mmol) and 2,2'-(9,9-dihexadecyl-9H-fluorene-2,7-diyl)bis(4,4,5,5-tetramethyl-1,3,2-dioxaborolane) (219 mg, 0.253 mmol) in toluene (4 mL) and a separate solution of 20% tetraethylammonium hydroxide in water (3 mL) were degassed for 30 min. $Pd(OAc)_2$ (1 mg, 0.005 mmol) and $PPh_3$ (7 mg, 0.025 mmol) were added to the organic solution which was again degassed for 30 min. The aqueous solution was added to the organic and the reaction mixture was stirred under argon at 110 °C for 18 h. The reaction was allowed to cool and the product was precipitated from MeOH and filtered. The polymer product was then washed with acetone and hexane and extracted with $CHCl_3$ (253 mg, 100%). UV (chlorobenzene) $\lambda_{max}$ 385, (Thin film) $\lambda_{max}$ 385; GPC (PS): $M_n$ = 20000 Da, $M_w$ = 29000 Da, PDI = 1.5.

**SFH – *Poly*-2,7-(9,9-dihexadecyl-9H-fluoren-2-yl)-*alt*-2,7-(9,9'-spirobi[fluorene])**

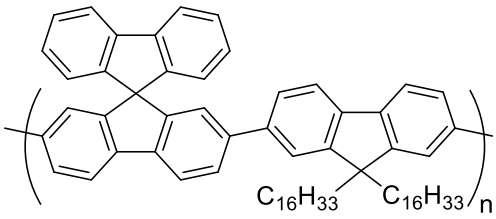


A solution of 2',7'-dibromo-9,9'-spirobi[fluorene] (55 mg, 0.117 mmol) and 2,2'-(9,9-dihexadecyl-9H-fluorene-2,7-diyl)bis(4,4,5,5-tetramethyl-1,3,2-dioxaborolane) (101 mg, 0.117 mmol) in toluene (4 mL) and a separate solution of 20% tetraethylammonium hydroxide in water (3 mL) were degassed for 30 min. $Pd(OAc)_2$ (1 mg, 0.005 mmol) and $PPh_3$ (7 mg, 0.025

mmol) were added to the organic solution which was again degassed for 30 min. The aqueous solution was added to the organic and the reaction mixture was stirred under argon at 110 °C for 18 h. The reaction was allowed to cool and the product was precipitated from MeOH and filtered. The polymer product was then washed with acetone and hexane and extracted with $CHCl_3$ (103 mg, 95%). UV (chlorobenzene) $\lambda_{max}$ 390, (Thin film) $\lambda_{max}$ 387; GPC (PS): $M_n$ = 16000 Da, $M_w$ = 23000 Da, PDI = 1.4.

**$N^1$,$N^4$-bis(4-bromophenyl)-$N$1,$N$4-bis(4-butylphenyl)benzene-1,4-diamine / $N^1$-(4-bromophenyl)-$N^1$,$N^4$-bis(4-butylphenyl)-$N^4$-(4-iodophenyl)benzene-1,4-diamine**

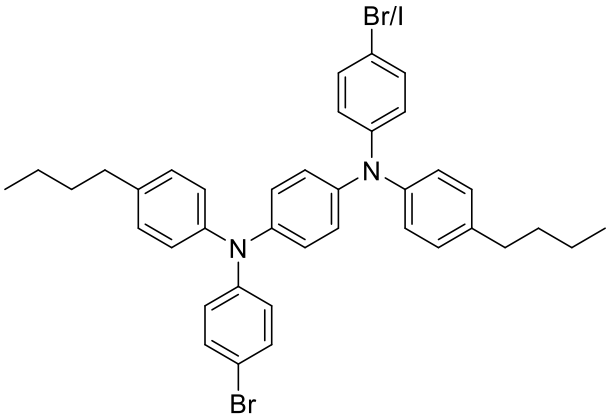


$N^1$,$N^4$-bis(4-butylphenyl)benzene-1,4-diamine (200 mg, 0.54 mmol), 4-bromoiodobenzene (758 mg, 2.68 mmol) and $NaO^tBu$ (73 mg, 0.76 mmol) were added to $Pd(OAc)_2$ (11 mg, 0.05 mmol) in toluene (5 mL) under argon. A 0.2 M solution of $^tBu_3P$ in toluene was added (0.4 mL, 0.08 mmol) and the reaction mixture was stirred at rt under argon for 18 h. The reaction mixture was quenched with $H_2O$ (20 mL) and the product was extracted with EtOAc (3 x 20 mL), dried over $MgSO_4$ and concentrated *in vacuo*. The product was purified *via* column chromatography (eluent hexane) to give a mixture of the bromo and iodo products (31 mg, 0.04 mmol, 8%). $^1$H NMR shows a complex mixture and is not reported. MS ($CI^+$) *m/z* 680, 682, 684 $(C_{38}H_{38}Br_2N_2)^+$, 728, 730 $(C_{38}H_{38}BrIN_2)^+$.

**4-heptyl-*N*-phenylaniline**

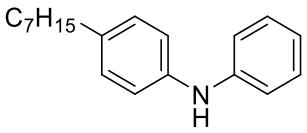


CuI (27 mg, 0.14 mmol), $K_2CO_3$ (193 mg, 1.40 mmol) and L-proline (16 mg, 0.14 mmol) were dissolved in DMSO (5 mL) and degassed with argon. 4-heptylaniline (200 mg, 1.05 mmol) and iodobenzene (142 mg, 0.70 mmol) were added and the reaction mixture was stirred at 90 °C under argon for 18 h. The reaction mixture was poured into brine (15 mL) and extracted with EtOAc (2 x 20 mL). The combined organic fractions were dried over $MgSO_4$ and concentrated *in vacuo*. The product was purified *via* column chromatography (eluent 3:1 hexane:$CHCl_3$) to give a clear oil (100 mg, 0.37 mmol, 36%). $^1$H NMR (600 MHz, $CDCl_3$) δ 7.25 (d, *J* = 8.3 Hz, 2H, NC*H*CHC$C_7H_{15}$), 7.10 (d, *J* = 8.3 Hz, 2H, NCHC*H*C$C_7H_{15}$), 7.08 – 7.03 (m, 4H, NCC*H*CHCH and NCCHC*H*CH), 6.92 (t, *J* = 6.9 Hz, 1H, NCCHCHC*H*), 2.59 – 2.53 (t, *J* = 7.8 Hz, 2H, $CH_3C_4H_8CH_2CH_2$), 1.59 (m, 2H, $CH_3C_4H_8CH_2CH_2$), 1.36 – 1.23 (m, 8H, $CH_3C_4H_8CH_2CH_2$), 0.89 (t, *J* = 7.1 Hz, 3H, $CH_3$).

**4-bromo-*N*,*N*-diphenylaniline**

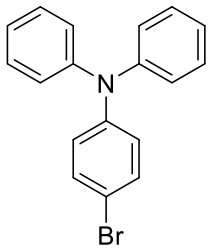


Triphenylamine (1.0 g, 4.08 mmol), NBS (726 mg, 4.08 mmol) and $CCl_4$ (10 mL) were stirred under argon at 80 °C for 5 h. The succinimide side product was filtered and the solvent was allowed to evaporate in an isolated fume hood. The grey solid was recrystallized from EtOH to give white crystals (762 mg, 2.35 mmol, 58%). $^1$H NMR (600 MHz, DMSO) δ 7.43 (d, *J* = 8.9 Hz, 2H, BrCC*H*), 7.32 (dd, *J* = 8.5, 7.4 Hz, 4H, NCCHC*H*CH), 7.08 (t, *J* = 7.4 Hz, 2H, NCCHCHC*H*), 7.02 (d, *J* = 8.5, 4H, NCC*H*CHCH), 6.89 (d, *J* = 8.9 Hz, 2H, BrCCHC*H*).

**Tris(4-bromophenyl)amine**

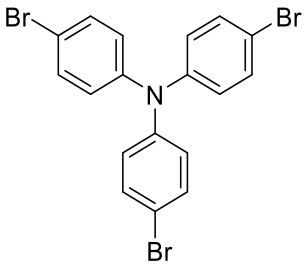


NBS (2.4 g, 13.45 mmol) was added to Triphenylamine (1.0 g, 4.08 mmol) in dry DMF (15 mL) at 0 °C and was then allowed to warm to rt and stirred for 18 h. The product was extracted with $Et_2O$ and brine and the organic fractions were dried over $MgSO_4$ and concentrated *in vacuo*. The obtained brown oil was left for 64 h, and white crystals appeared and were filtered (656 mg, 1.36 mmol, 33%). $^1$H NMR (600 MHz, $CDCl_3$) δ 7.36 (d, *J* = 8.8 Hz, 6H, BrCC*H*), 6.93 (d, *J* = 8.8 Hz, 6H, BrCCHC*H*); MS (ES$^+$) *m/z* 479, 481, 483, 485 $(M)^+$; HRMS 478.8514 calculated for $C_{18}H_{12}{}^{79}Br_3N$ found 478.8513. All spectroscopic data is in accordance with literature values.[201]

**4-bromo-*N*-(4-bromophenyl)-*N*-phenylaniline**

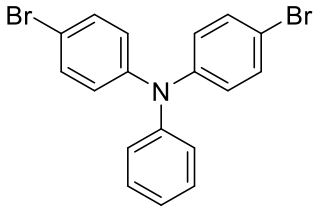


To a solution of triphenylamine (5.0 g, 20.35 mmol) in DMF (60 mL) was added NBS (7.26 g, 40.70 mmol) in DMF (80 mL) at 0 °C. The reaction mixture was stirred for 4 h and then concentrated *in vacuo*. The product was purified *via* column chromatography ($SiO_2$, Eluent Hexane) to yield a waxy colourless solid (7.30 g, 18.11 mmol, 89%). $^1$H NMR (600 MHz, DMSO) δ 7.45 (d, *J* = 8.7 Hz, 4H, BrCC*H*), 7.35 – 7.32 (m, 2H, NCCHC*H*CH), 7.11 (t, *J* = 7.4 Hz, 1H, NCCHCHC*H*), 7.04 (d, *J* = 8.5 Hz, 2H, NCC*H*CHCH), 6.93 (d, *J* = 8.9 Hz, 4H, BrCCHC*H*); MS (EI$^+$) *m/z* 401, 403, 405 $(M)^+$; HRMS 400.9409 calculated for $C_{18}H_{13}N^{79}Br_2$ found 400.9409. All spectroscopic data is in accordance with literature values.[201]

**2-octyldodecanoic acid**

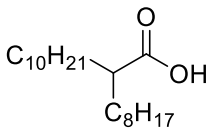


To a solution of periodic acid (7.56 g, 33.16 mmol) in acetonitrile (45 mL) was added 2-octyldodecan-1-ol (4.5 g, 15.07 mmol) at 0 °C. The mixture was stirred for 15 minutes before the slow addition of a solution of pyridinium chlorochromate (65 mg) in acetonitrile (8 mL). The reaction mixture was allowed to warm to rt and stirred for 18 h. The reaction mixture was quenched with $NaHCO_3$ solution (100 mL) and the product was extracted with EtOAc (3 x 100 mL), dried over $MgSO_4$ and concentrated *in vacuo*. The product was placed in a vacuum desiccator for 2 h to give a white powder (4.35 g, 13.92 mmol, 92%). $^1$H NMR (600 MHz, $CDCl_3$) δ 2.35 (m, 1H, C*H*COOH), 1.67 – 1.58 (m, 2H, C*H*$_2$CHCOOH), 1.50 – 1.43 (m, 2H, C*H*$_2$CHCOOH), 1.35 – 1.21 (m, 28H, $CH_3C_8$*H*$_{16}$$CH_2CH(COOH)CH_2C_6$*H*$_{12}$$CH_3$), 0.88 (t, *J* = 7.0 Hz, 6H, C*H*$_3$); MS (EI$^+$) *m/z* 312 (M)$^+$; HRMS 312.3023 calculated for $C_{20}H_{40}O_2$ found 312.3022. All spectroscopic data is in accordance with literature values.[202]

**2-octyldodecanoyl chloride**

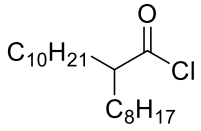


2-octyldodecanoic acid (4.00 g, 12.80 mmol) in $CH_2Cl_2$ (12 mL) was treated with $SOCl_2$ (2.80 mL, 38.40 mmol) then DMF (0.2 mL) under an atmosphere of argon at rt. The reaction mixture was stirred for 18 h. The reaction mixture was then concentrated *in vacuo* and used directly in the next reaction without further purification or analysis.

**1-(4-(bis(4-bromophenyl)amino)phenyl)-2-octyldodecan-1-one**

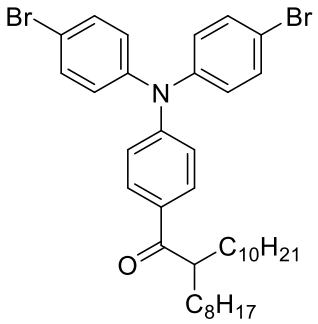


2-octyldodecanoyl chloride (4.34 g, 13.12 mmol) was added to 4-bromo-N-(4-bromophenyl)-N-phenylaniline (3.7 g, 7.99 mmol) in $CH_2Cl_2$ (30 mL) under an atmosphere of argon at 0 °C. $AlCl_3$ (1.75 g, 13.12 mmol) was added in portions over 15 min. the reaction mixture was allowed to warm to rt and stirred for 18 h. The reaction mixture was poured slowly into $H_2O$ (75 mL) and the product was extracted with $CH_2Cl_2$ (3 x 50 mL), dried over $MgSO_4$ and concentrated *in vacuo*. The product was purified *via* column chromatography ($SiO_2$, Eluent $CHCl_3$:Hexane (0:1 to 1:1)), the organic fractions collected and concentrated *in vacuo* to yield the product as a yellow oil which was placed in a vacuum desiccator for 30 min (5.24 g, 7.51 mmol, 94%). $^1$H NMR (600 MHz, $CDCl_3$) δ 7.83 (d, *J* = 8.8 Hz, 2H, C(O)CC*H*CHCN), 7.42 (d, *J* = 8.7 Hz, 4H, BrCC*H*CHCN), 7.03 – 6.99 (m, 6H, C(O)CCHC*H*CN and BrCCHC*H*CN), 3.34 – 3.28 (m, 1H, C(O)C*H*), 1.77 – 1.68 (m, 2H, CHC$H_2$), 1.50 – 1.42 (m, 2H, CHC$H_2$), 1.33 – 1.18 (m, 28H, $CHCH_2(CH_2)_{5/7}CH_3$), 0.91 – 0.84 (m, 6H, C$H_3$); MS (EI$^+$) *m/z* 695, 697, 699 $(M)^+$; HRMS 695.2332 calculated for $C_{38}H_{51}N^{79}Br_2O$ found 695.2333.

**4-bromo-*N*-(4-bromophenyl)-*N*-(4-(2-octyldodecyl)phenyl)aniline**

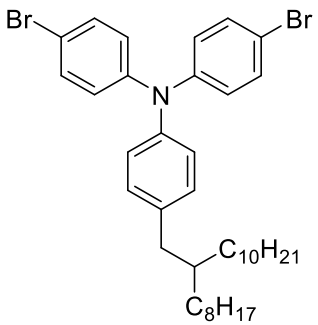


To a solution of 1-(4-(bis(4-bromophenyl)amino)phenyl)-2-octyldodecan-1-one (1.0 g, 1.43 mmol) in trifluoroacetic acid (10 mL) was added triethylsilane (1.14 mL, 7.17 mmol) slowly at rt. The reaction mixture was stirred for 4 d. The reaction mixture was poured into 1 M $NaHCO_3$

solution (100 mL) and the product was extracted with $Et_2O$ (3 x 100 mL), dried over $MgSO_4$ and concentrated *in vacuo*. The product was purified *via* column chromatography ($SiO_2$, Eluent Hexane) and the organic fractions collected and concentrated *in vacuo* to yield the product as a clear waxy solid which was placed in a vacuum desiccator for 30 min (410 mg, 0.60 mmol, 42%). $^1$H NMR (600 MHz, $CDCl_3$) δ 7.32 (d, *J* = 8.9 Hz, 4H, BrCC*H*), 7.04 (d, *J* = 8.4 Hz, 2H, NCC*H*CHC(Alk)), 6.96 (d, *J* = 8.4 Hz, 2H, NCCHC*H*C(Alk)), 6.92 (d, *J* = 8.9 Hz, 4H, BrCCHC*H*), 2.48 (d, *J* = 7.0 Hz, 2H, C*H*$_2$CH($C_8H_{17}$)($C_{10}H_{21}$)), 1.61 – 1.56 (m, 1H, $CH_2$C*H*($C_8H_{17}$)($C_{10}H_{21}$)), 1.33 – 1.20 (m, 32H, $CH_3C_7H_{14}CHC_9H_{18}CH_3$), 0.90 – 0.86 (m, 6H, C*H*$_3$); MS (EI$^+$) *m/z* 681, 683, 685 $(M)^+$; HRMS 681.2539 calculated for $C_{38}H_{53}N^{79}Br_2$ found 681.2534.

**4-(2-octyldodecyl)-*N*,*N*-bis(4-(4,4,5,5-tetramethyl-1,3,2-dioxaborolan-2-yl)phenyl)aniline**

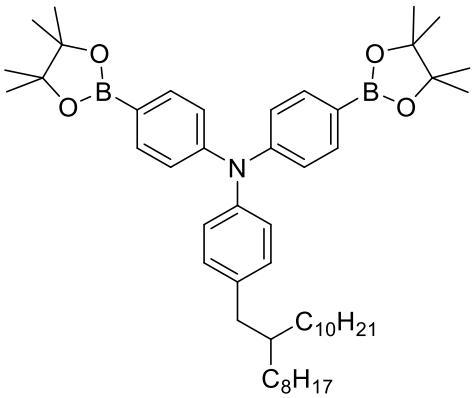


Bis(pinacolato)diboron (1.23 g, 4.83 mmol), $PdCl_2$(dppf) (82 mg, 0.11 mmol) and KOAc (606 mg, 6.44 mmol) were placed in an argon filled flask. 4-bromo-N-(4-bromophenyl)-N-(4-(2-octyldodecyl)phenyl)aniline (1.10 g, 1.61 mmol) in DMF (70 mL) was added, the reaction mixture was degassed for 30 min and then heated under argon to 80 $^o$C for 18 h. The reaction mixture was concentrated *in vacuo*, dissolved in $CHCl_3$ and passed through a plug of silica using $CHCl_3$ as eluent. The product was concentrated *in vacuo* and placed in a vacuum dessicator for 30 min, yielding a clear, waxy solid (750 mg, 0.96 mmol, 60%). $^1$H NMR (400 MHz, $CDCl_3$) δ 7.69 – 7.64 (m, 4H, BCC*H*), 7.07 – 6.98 (m, 8H, BCCHC*H* and $CH_2$CC*H*CHCN and $CH_2$CCHC*H*CN), 2.49 (d, J = 7.0 Hz, 2H, C*H*$_2$CH($C_8H_{17}$)($C_{10}H_{21}$)), 1.62 – 1.59 (m, 1H, $CH_2$C*H*($C_8H_{17}$)($C_{10}H_{21}$)), 1.36 – 1.20 (m, 56H, $CH_3C_7H_{14}CHC_9H_{18}CH_3$ and BOCC*H*$_3$), 0.92 – 0.84 (m, 6H, C*H*$_3$); $^{13}$C NMR (151 MHz, $CDCl_3$) δ 150.37, 144.50, 138.11, 135.96, 130.25, 122.47, 83.70, 40.19, 39.71, 33.33, 32.05, 30.14, 29.77, 29.50, 26.71, 25.15, 24.98, 22.83, 14.29; MS (EI$^+$) m/z 777 $(M)^+$ ; HRMS 775.6107 calculated for $C_{50}H_{77}N^{79}Br_2O^4$ found 775.6106.

**ASFCN – *Poly*-4',4''-(4-(2-octyldodecyl)-*N*,*N*-diphenylaniline)-*alt*-2,7-(9,9'-spirobi[fluorene]-2',7'-dicarbonitrile)**

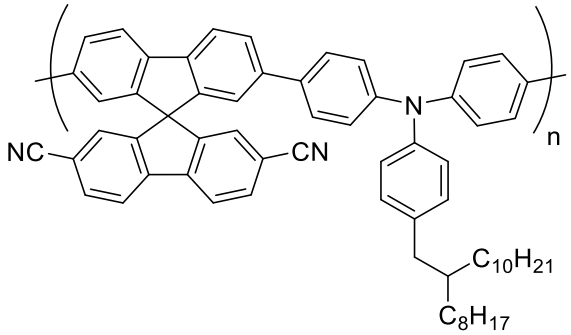


A solution of 2',7'-dibromo-9,9'-spirobi[fluorene]-2,7-dicarbonitrile (191 mg, 0.365 mmol) and 4-(2-octyldodecyl)-N,N-bis(4-(4,4,5,5-tetramethyl-1,3,2-dioxaborolan-2-yl)phenyl)aniline (284 mg, 0.365 mmol) in toluene (8 mL) and a separate solution of 20% tetraethylammonium hydroxide in water (7 mL) were degassed for 30 min. $Pd(OAc)_2$ (2 mg, 0.007 mmol) and $PPh_3$ (10 mg, 0.038 mmol) were added to the organic solution which was again degassed for 30 min. The aqueous solution was added to the organic and the reaction mixture was stirred under argon at 110 °C for 3 d. The reaction was allowed to cool and the product was precipitated from MeOH and filtered. The polymer product was then washed with acetone and hexane and extracted with $CHCl_3$ (280 mg, 86%). UV (chlorobenzene) $\lambda_{max}$ 396, (Thin film) $\lambda_{max}$ 400; GPC (PS): $M_n$ = 23000 Da, $M_w$ = 49000 Da, PDI = 2.1.

**ASFH - *Poly*-4',4''-(4-(2-octyldodecyl)-*N*,*N*-diphenylaniline)-*alt*-2,7-(9,9'-spirobi[fluorene])**

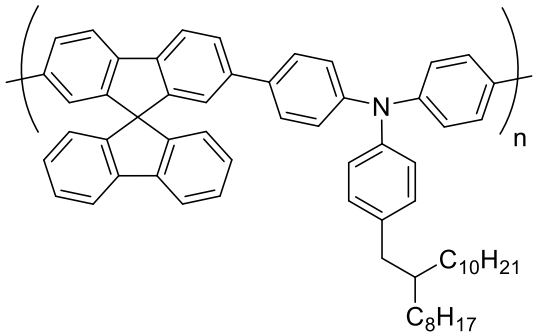


A solution of 2',7'-dibromo-9,9'-spirobi[fluorene] (169 mg, 0.357 mmol) and 4-(2-octyldodecyl)-N,N-bis(4-(4,4,5,5-tetramethyl-1,3,2-dioxaborolan-2-yl)phenyl)aniline (278 mg, 0.357 mmol) in toluene (8 mL) and a separate solution of 20% tetraethylammonium hydroxide in water (7 mL) were degassed for 30 min. $Pd(OAc)_2$ (2 mg, 0.007 mmol) and $PPh_3$ (9 mg, 0.036 mmol) were added to the organic solution which was again degassed for 30 min. The aqueous

solution was added to the organic and the reaction mixture was stirred under argon at 110 °C for 3 d. The reaction was allowed to cool and the product was precipitated from MeOH and filtered. The polymer product was then washed with acetone and hexane and extracted with $CHCl_3$ (220 mg, 73%). UV (chlorobenzene) $\lambda_{max}$ 387, (Thin film) $\lambda_{max}$ 394; GPC (PS): $M_n$ = 18000 Da, $M_w$ = 31000 Da, PDI = 1.7.

## 6.5 Synthetic Techniques for Chapter 5

**4-methyl-4'-(trifluoromethyl)-1,1'-biphenyl**

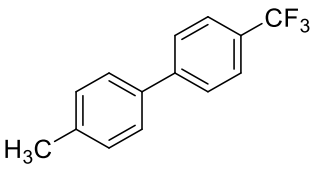


1-bromo-4-methylbenzene (597 mg, 3.51 mmol), (4-(trifluoromethyl)phenyl)boronic acid (1.0 g, 5.27 mmol), $Pd(OAc)_2$ (9 mg, 0.04 mmol) and $Na_2CO_3$ (744 mg, 7.02 mmol) in $H_2O$ (12 mL) and DMF (10 mL) were stirred in air at 35 °C for 30 min. The reaction mixture was extracted with $Et_2O$ (3 x 20 mL), dried over $MgSO_4$ and concentrated *in vacuo*. The product was purified *via* column chromatography ($SiO_2$, eluent $CH_2Cl_2$) and the relevant organic fractions collected and concentrated *in vacuo* to yield the product (565 mg, 2.39 mmol, 68%). $^1$H NMR (600 MHz, DMSO) δ 7.86 (d, *J* = 8.2 Hz, 2H, $CF_3CC$*H*), 7.79 (d, *J* = 8.2 Hz, 2H, $CF_3CCHC$*H*), 7.63 (d, *J* = 8.0 Hz, 2H, $CH_3CCHC$*H*), 7.32 (d, *J* = 8.0 Hz, 2H, $CH_3CC$*H*), 2.35 (s, 3H, C*H*$_3$). All spectroscopic data is in accordance with literature values.[203]

**2-bromo-1-iodo-4-methylbenzene**

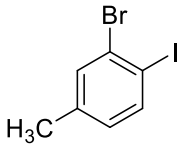


2-bromo-4-methylaniline (1.0 g, 5.37 mmol) was suspended in a solution of concentrated $H_2SO_4$ (2 mL) in $H_2O$ (4 mL) at 0 °C. 2M $NaNO_2$ in $H_2O$ (2.82 mL, 5.64 mmol) was added followed by CuI (51 mg, 0.27 mmol) and 2M KI in $H_2O$ (2.96 mL, 5.92 mmol). The reaction mixture was stirred at rt for 18 h under argon. The product was extracted with $CH_2Cl_2$ (3 x 20 mL) and brine (30 mL), dried over $MgSO_4$ and concentrated *in vacuo*. The product was purified *via* column chromatography ($SiO_2$, eluent hexane) and the relevant organic fractions collected and concentrated *in vacuo* to yield the product (899 mg, 3.03 mmol, 56%). $^1$H NMR (600 MHz, $CDCl_3$) δ 7.71 (d, *J* = 8.1 Hz, 1H, ICC*H*), 7.47 (d, *J* = 2.0 Hz, 1H, BrCC*H*), 6.82 (dd, *J* = 8.1, 2.0 Hz, 1H, ICCHC*H*), 2.29 (s, 3H, C*H*$_3$); MS (EI$^+$ ) m/z 296, 298 (M)$^+$. All spectroscopic data is in accordance with literature values.[204]

**4'-methyl-4,4''-bis(trifluoromethyl)-1,1':2',1''-terphenyl**

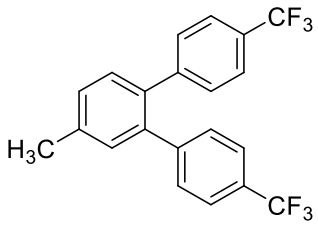


2-bromo-1-iodo-4-methylbenzene (899 mg, 3.03 mmol), (4-(trifluoromethyl)phenyl)boronic acid (575 mg, 3.03 mmol), $Pd(OAc)_2$ (7 mg, 0.03 mmol) and $Na_2CO_3$ (642 mg, 6.06 mmol) in $H_2O$ (12 mL) and DMF (10 mL) were stirred in air at 35 °C for 30 min. The reaction mixture was extracted with $Et_2O$ (3 x 20 mL), dried over $MgSO_4$ and concentrated *in vacuo*. The product was purified *via* column chromatography ($SiO_2$, eluent hexane) and the relevant organic fractions collected and concentrated *in vacuo* to yield the product (216 mg, 0.57 mmol, 38%). $^1$H NMR (600 MHz, $CDCl_3$) δ 7.49 (m, 4H, $CF_3CC\mathit{H}$), 7.34 (d, *J* = 7.8 Hz, 1H, $CH_3CCHC\mathit{H}$), 7.31 (d, *J* = 7.8 Hz, 1H, $CH_3CC\mathit{H}CH$), 7.26 (s, 1H, $CH_3CC\mathit{H}C$), 7.24 (d, *J* = 8.0 Hz, 2H, $CF_3CCHC\mathit{H}$), 7.22 (d, *J* = 8.0 Hz, 2H, $CF_3CCHC\mathit{H}$), 2.47 (s, 3H, $C\mathit{H_3}$); MS ($EI^+$ ) m/z 380 $(M)^+$.

**(2-bromo-5-(trifluoromethyl)phenyl)trimethylsilane**

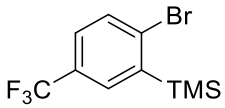


1-bromo-4-(trifluoromethyl)benzene (1.0 g, 4.44 mmol), TMSCl (531 mg, 4.89 mmol) and THF (10 mL) were stired under argon at -78 °C. 2M LDA in THF (2.45 mL, 4.89 mmol) was added slowly and the reaction mixture was stirred for 2 h at -78 °C under argon. The reaction was quenched by slow addition of dilute $H_2SO_4$, and the product was extracted with $Et_2O$ (3 x 30 mL), dried over $MgSO_4$ and concentrated *in vacuo*. The product was purified *via* column chromatography ($SiO_2$, eluent hexane) and the relevant organic fractions collected and concentrated *in vacuo* to yield the product (425 mg, 1.43 mmol, 32%). $^1$H NMR (600 MHz, $CDCl_3$) δ 7.67 – 7.63 (m, 2H, $CF_3CCHC\mathit{H}$ and $TMSCC\mathit{H}$), 7.44 (dd, *J* = 8.2, 2.4 Hz, 1H, $CF_3CC\mathit{H}CH$), 0.43 (s, *J* = 3.4 Hz, 9H, $SiCH_3$).

**4,4,5,5-tetramethyl-2-(*p*-tolyl)-1,3,2-dioxaborolane**

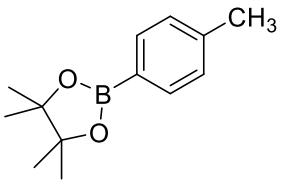


4-bromotouene (5.0 g, 29.2 mmol) in THF (50 mL) was stirred under argon at -78 °C. 1.6 M n-butyllithium (51.5 mL, 32.2 mmol) was added slowly and the reaction was stirred at -78 °C for a further 30 min. 2-isopropoxy-4,4,5,5-tetramethyl-1,3,2-dioxaborolane (5.96 mL, 29.2 mmol) in THF (80 mL) was added and the reaction mixture was allowed to warm to rt and stirred for 1 h. Brine (100 mL) was added and the organic product was extracted with $Et_2O$ (3 x 100 mL). The organic fractions were dried over $MgSO_4$ and concentrated *in vacuo*. The product was purified *via* column chromatography ($SiO_2$, eluent $CH_2Cl_2$) and the relevant organic fractions collected and concentrated *in vacuo* to yield the product (5.1 g, 23.38 mmol, 80%). $^1$H NMR (600 MHz, $CDCl_3$) δ 7.71 (d, *J* = 7.8 Hz, 2H, BCC*H*), 7.19 (d, *J* = 7.5 Hz, 2H, $CH_3$CC*H*), 2.37 (s, 3H, CCHCHCC*H*$_3$), 1.34 (s, 12H, BOCC*H*$_3$). All spectroscopic data is in accordance with literature values.[205]

**Trimethyl(4'-methyl-4-(trifluoromethyl)-[1,1'-biphenyl]-2-yl)silane**

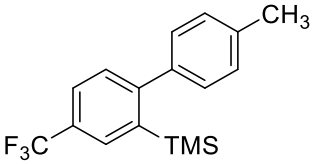


A solution of (2-bromo-5-(trifluoromethyl)phenyl)trimethylsilane (425 mg, 1.43 mmol) and 4,4,5,5-tetramethyl-2-(*p*-tolyl)-1,3,2-dioxaborolane (469 mg, 2.15 mmol) in THF (80 mL) and a separate solution of $NaHCO_3$ (1.68 g, 20.00 mmol) in water (20 mL) were degassed for 30 min. $Pd(PPh_3)_4$ (33 mg, 0.03 mmol) was added to the organic solution which was again degassed for 30 min. The aqueous solution was added to the organic and the reaction mixture was stirred under argon at 80 °C for 18 h. Brine (100 mL) was added and the organic product was extracted with $CH_2Cl_2$ (3 x 100 mL). The organic fractions were dried over $MgSO_4$ and concentrated *in vacuo*. The product was purified *via* column chromatography ($SiO_2$, eluent hexane) and the relevant organic fractions collected and concentrated *in vacuo* to yield the product (226 mg, 0.73 mmol, 51%). $^1$H NMR (600 MHz, $CDCl_3$) δ 7.83 (d, *J* = 1.4 Hz, 1H, TMSCC*H*), 7.61 (dd, *J* = 8.0, 1.4 Hz, 1H, $CF_3$CC*H*CH), 7.32 (d, *J* = 8.0 Hz, 1H, $CF_3$CCHC*H*), 7.22 (d,

*J* = 7.8 Hz, 2H, $CH_3CCHCH$), 7.16 (d, *J* = 7.8 Hz, 2H, $CH_3CCH$), 2.43 (s, 3H, $CH_3CCHCH$), 0.04 (s, 9H, $SiCH_3$).

**3-methyl-4'-(trifluoromethyl)-1,1'-biphenyl**

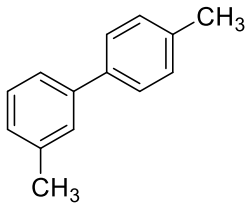


A solution of 1-bromo-3-methylbenzene (500 mg, 2.92 mmol) and 4,4,5,5-tetramethyl-2-(*p*-tolyl)-1,3,2-dioxaborolane (955 mg, 4.38 mmol) in THF (160 mL) and a separate solution of $NaHCO_3$ (3.36 g, 40.00 mmol) in water (40 mL) were degassed for 30 min. $Pd(PPh_3)_4$ (68 mg, 0.06 mmol) was added to the organic solution which was again degassed for 30 min. The aqueous solution was added to the organic and the reaction mixture was stirred under argon at 80 °C for 18 h. Brine (200 mL) was added and the organic product was extracted with $CH_2Cl_2$ (3 x 200 mL). The organic fractions were dried over $MgSO_4$ and concentrated *in vacuo* to yield the product (452 mg, 2.48 mmol, 85%). $^1$H NMR (600 MHz, $CDCl_3$) δ 7.49 (d, *J* = 7.9 Hz, 2H, $CH_3CCHCHC$), 7.41 – 7.37 (m, 2H, $CH_3CCHCHCH$ and $CH_3CCHC$), 7.32 (dd, *J* = 7.5, 7.5 Hz, 1H, $CH_3CCHCHCH$), 7.25 (d, *J* = 7.9 Hz, 2H, $CH_3CCHCHC$), 7.15 (d, *J* = 7.5 Hz, 1H, $CH_3CCHCHCH$), 2.42 (s, 3H, $CH_3$), 2.40 (s, 3H, $CH_3$). All spectroscopic data is in accordance with literature values.[206]

**4-bromo-3,4'-dimethyl-1,1'-biphenyl**

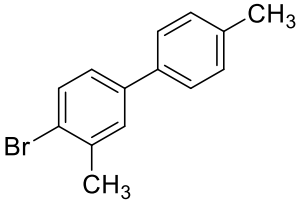


3-methyl-4'-(trifluoromethyl)-1,1'-biphenyl (100 mg, 0.55 mmol), $I_2$ (3 mg, 0.01 mmol) and $CH_2Cl_2$ (5 mL) were stirred at 0 °C under argon for 30 min. $Br_2$ (0.034 mL, 0.66 mmol) in $CH_2Cl_2$ (0.66 mL) was added and the reaction mixture was stirred at 0 °C under argon in the dark for 3 h. The reaction mixture was quenched with saturated $Na_2SO_3$ solution (50 mL) and the product was extracted with $CH_2Cl_2$ (3 x 50 mL), dried over $MgSO_4$ and concentrated *in vacuo*. The product was purified *via* column chromatography ($SiO_2$, eluent hexane) and the relevant

organic fractions collected and concentrated *in vacuo* to yield the product (68 mg, 0.26 mmol, 47%). $^{1}$H NMR (600 MHz, $CDCl_3$) δ 7.57 (d, *J* = 8.2 Hz, 1H, BrCC*H*), 7.47 – 7.43 (m, 3H, BrCCHC*H* and $CH_3CCHCH$), 7.26 – 7.23 (m, 3H, $BrCC(CH_3)CH$ and $CH_3CCH$), 2.46 (s, 3H, $CH_3$), 2.40 (s, 3H, $CH_3$); $^{13}$C NMR (151 MHz, $CDCl_3$) δ 140.5, 138.2, 137.5, 137.4, 132.7, 129.7, 129.5, 126.9, 126.0, 123.8, 23.2, 21.2.

**2-bromo-4-methylaniline**

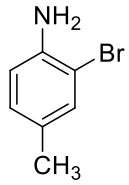


NBS (1.74 g, 9.80 mmol) was added to a solution of 4-methylaniline (1.0 g, 9.33 mmol) in $CHCl_3$ (20 mL) and the reaction mixture was stirred at 70 °C under argon in the dark for 2 h. The reaction mixture was concentrated *in vacuo*, the product was purified *via* column chromatography ($SiO_2$, eluent $Et_2O$:hexane (1:20 to 1:1)) and the relevant organic fractions collected and concentrated *in vacuo* to yield the product (884 mg, 4.75 mmol, 51%). $^{1}$H NMR (600 MHz, $CDCl_3$) δ 7.24 (d, *J* = 1.2 Hz, 1H, BrCC*H*), 6.92 (dd, *J* = 8.1, 1.2 Hz, 1H, $CH_3CCHCH$), 6.69 (d, *J* = 8.1 Hz, 1H, $NH_2CCH$), 3.93 (s, 2H, $NH_2$), 2.23 (s, 3H, $CH_3$); MS ($Cl^+$) m/z 186, 188 $(MH)^+$. All spectroscopic data is in accordance with literature values.[207]

**4',5-dimethyl-[1,1'-biphenyl]-2-amine**

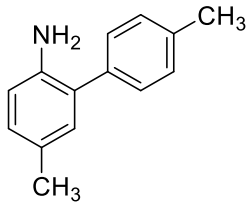


A solution of 2-bromo-4-methylaniline (800 mg, 4.30 mmol), 4,4,5,5-tetramethyl-2-(*p*-tolyl)-1,3,2-dioxaborolane (1.41 g, 6.45) in THF (200 mL) and a separate solution of $NaHCO_3$ (4.62 g, 55.00 mmol) in water (50 mL) were degassed for 30 min. $Pd(PPh_3)_4$ (99 mg, 0.09 mmol) was added to the organic solution which was again degassed for 30 min. The aqueous solution was added to the organic and the reaction mixture was stirred under argon at 80 °C for 18 h. Brine (200 mL) was added and the organic product was extracted with $CH_2Cl_2$ (3 x 200 mL). The

organic fractions were dried over $MgSO_4$ and concentrated *in vacuo*. The product was purified *via* column chromatography ($SiO_2$, eluent EtOAc:hexane 1:20 to 1:1) and the relevant organic fractions collected and concentrated *in vacuo* to yield the product (195 mg, 0.99 mmol, 23%). $^1$H NMR (600 MHz, $CDCl_3$) δ 7.35 (d, *J* = 8.2 Hz, 2H, $CH_3CCHCH$), 7.25 (d, *J* = 8.2 Hz, 2H, $CH_3CCHCH$), 6.98 – 6.94 (m, 2H, $NH_2CCHCH$ and $NH_2CCCH$), 6.70 (d, *J* = 7.6 Hz, 1H, $NH_2CCH$), 2.40 (s, 2H, $CH_3$), 2.28 (s, 2H, $CH_3$). All spectroscopic data is in accordance with literature values.[208]

**4'-methyl-[1,1'-biphenyl]-2-amine**

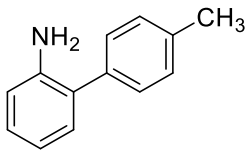


A solution of 2-bromoaniline (0.47 mL, 4.17 mmol), 4,4,5,5-tetramethyl-2-(*p*-tolyl)-1,3,2-dioxaborolane (1.0 g, 4.59 mmol) in THF (250 mL) and a separate solution of $K_2CO_3$ (2.31 g, 16.68 mmol) in water (60 mL) were degassed for 30 min. $Pd(PPh_3)_4$ (96 mg, 0.08 mmol) was added to the organic solution which was again degassed for 30 min. The aqueous solution was added to the organic and the reaction mixture was stirred under argon at 80 °C for 18 h. Brine (200 mL) was added and the organic product was extracted with $CH_2Cl_2$ (3 x 200 mL). The organic fractions were dried over $MgSO_4$ and concentrated *in vacuo*. The product was purified *via* column chromatography ($SiO_2$, eluent $CHCl_3$:hexane 0:1 to 1:0) and the relevant organic fractions collected and concentrated *in vacuo* to yield the product (764 mg, 4.17 mmol, 100%). $^1$H NMR (600 MHz, $CDCl_3$) δ 7.36 (d, *J* = 7.9 Hz, 2H, $CH_3CCHCH$), 7.26 (d, *J* = 7.9 Hz, 2H, $CH_3CCHCH$), 7.15 (ddd, *J* = 7.7, 7.7, 1.5 Hz, 1H, $NH_2CCHCH$), 7.13 (dd, *J* = 7.7, 1.5 Hz, 1H, $NH_2CCHCHCHCH$), 6.83 (ddd, *J* = 7.7, 7.7, 1.1 Hz, 1H, $NH_2CCHCHCH$), 6.77 (dd, *J* = 7.7, 1.1 Hz, 1H, $NH_2CCH$), 3.76 (s, 2H, $NH_2$), 2.41 (s, 3H, $CH_3$). All spectroscopic data is in accordance with literature values.[209]

**2-bromo-4'-methyl-1,1'-biphenyl**

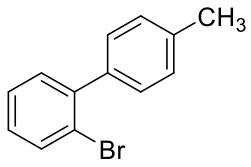


A solution of 1-bromo-2-iodobenzene (778 mg, 2.75 mmol), 4,4,5,5-tetramethyl-2-(*p*-tolyl)-1,3,2-dioxaborolane (500 mg, 2.29 mmol) in DME (10 mL) and a separate solution of $K_2CO_3$ (1.58 g, 11.46 mmol) in water (2 mL) were degassed for 30 min. $Pd(PPh_3)_4$ (32 mg, 0.05 mmol) was added to the organic solution which was again degassed for 30 min. The aqueous solution was added to the organic and the reaction mixture was stirred under argon at 85 °C for 18 h. Brine (50 mL) was added and the organic product was extracted with $CH_2Cl_2$ (3 x 50 mL). The organic fractions were dried over $MgSO_4$ and concentrated *in vacuo*. The product was purified *via* column chromatography ($SiO_2$, eluent hexane) and the relevant organic fractions collected and concentrated *in vacuo* to yield the product (284 mg, 1.15 mmol, 50%). $^1$H NMR (600 MHz, $CDCl_3$) δ 7.67 (dd, *J* = 8.0, 0.9 Hz, 1H, BrCC*H*), 7.37 – 7.30 (m, 4H, $CH_3$CCHC*H* and BrCCHCHC*H* and BrCCHCHCHC*H*), 7.25 (d, *J* = 7.8 Hz, 2H, $CH_3$CC*H*), 7.19 (ddd, *J* = 8.0, 7.1, 2.1 Hz, 1H, BrCCHC*H*), 2.42 (s, 3H, C*H*$_3$); MS ($Cl^+$) m/z 264, 266 $(M + NH_4)^+$; HRMS 246.0039 calculated for $C_{13}H_{11}{}^{79}Br$ found 246.0038. All spectroscopic data is in accordance with literature values.[210]

**5-bromo-2-iodobenzoic acid**

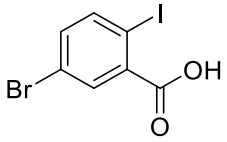


Methyl-2-iodobenzoate (10 mL, 68.08 mmol) in $H_2SO_4$ (200 mL) at 0 °C was treated with NBS (13.33 g, 74.89 mmol). The reaction mixture was heated to 80 °C and stirred for 18 h. The reaction mixture was allowed to cool and poured slowly into $H_2O$ (500 mL) at 0 °C. The product was extracted with $CH_2Cl_2$ (3 x 250 mL), washed with brine (2 x 250 mL), dried over $MgSO_4$ and concentrated *in vacuo*. The product was taken into the next reaction without further purification (20.0 g, 61.17 mmol, 90%).$^1$H NMR (400 MHz, $CDCl_3$) δ 8.14 (d, *J* = 2.4 Hz, 1H, C(OOH)CC*H*), 7.91 (d, *J* = 8.4 Hz, 1H, ICC*H*CHCBr), 7.34 (dd, *J* = 8.4, 2.4 Hz, 1H, ICCHC*H*CBr); MS ($EI^+$) *m/z* 326, 328 ($M^+$). All spectroscopic data is in accordance with literature values.[211]

**Methyl-5-bromo-2-iodobenzoate**

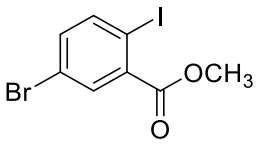


5-bromo-2-iodobenzoic acid (1.0 g, 3.07 mmol), $H_2SO_4$ (0.4 mL) and MeOH (10 mL) were stirred at 70 °C for 18 h. The reaction mixture was allowed to cool and concentrated *in vacuo*. The product was extracted with EtOAc (3 x 50 mL) and brine (50 mL), dried over $MgSO_4$ and concentrated *in vacuo*. The product was taken into the next reaction without further purification (1.05 g, 3.08 mmol, 100%). $^1$H NMR (600 MHz, $CDCl_3$) δ 7.95 (d, *J* = 2.4 Hz, 1H, C(OOMe)CC*H*), 7.84 (d, *J* = 8.4 Hz, 1H, ICC*H*CHCBr), 7.29 (dd, *J* = 8.4, 2.4 Hz, 1H, ICCHC*H*CBr), 3.94 (s, 3H, C*H*$_3$); MS ($Cl^+$) *m/z* 358, 360 (M + $NH_4^+$). All spectroscopic data is in accordance with literature values.[212]

**4,4,5,5-tetramethyl-2-(thiophen-2-yl)-1,3,2-dioxaborolane**

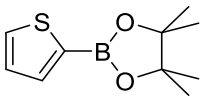


1.6 M $^n$BuLi in hexanes (40.8 mL, 65.3 mmol) was added slowly to thiophene (5.0 g, 59.4 mmol) in THF (50 mL) at -78 °C under argon and the reaction mixture was allowed to warm to rt and stirred for 30 min. 2-isopropoxy-4,4,5,5-tetramethyl-1,3,2-dioxaborolane (12.12 mL, 59.4 mmol) was added at -78 °C and the reaction mixture was again allowed to warm to rt and stirred for 30 min. The reaction mixture was concentrated *in vacuo*, passed through a plug of silica using $CH_2Cl_2$ as eluent and concentrated *in vacuo* to yield the product (9.30 g, 44.26 mmol, 75%). $^1$H NMR (600 MHz, $CDCl_3$) δ 7.66 (d, *J* = 3.6 Hz, 1H, SC*H*CHCH or SCHCHC*H*), 7.64 (d, *J* = 4.5 Hz, 1H, SCHCHC*H* or SC*H*CHCH), 7.20 (dd, *J* = 4.5, 3.6 Hz, 1H, SCHC*H*CH), 1.35 (s, 12H, C*H*$_3$). All spectroscopic data is in accordance with literature values.[213]

**Methyl 5-bromo-2-(thiophen-2-yl)benzoate**

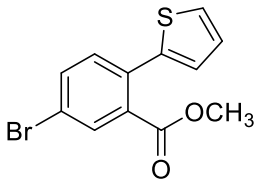


Methyl-5-bromo-2-iodobenzoate (514 mg, 1.51 mmol), 4,4,5,5-tetramethyl-2-(thiophen-2-yl)-1,3,2-dioxaborolane (265 mg, 1.26 mmol) and THF (10 mL) were degassed with argon for 30 mins. $Pd(PPh_3)_4$ (29 mg, 0.03 mmol) was added and the reaction mixture was further degassed for 30 mins. Degassed $K_2CO_3$ (871 mg, 6.30 mmol) in $H_2O$ (2 mL) was added and the reaction mixture was heated to 80 °C for 64 h. The reaction mixture was allowed to cool, concentrated *in vacuo*, dissolved in $CH_2Cl_2$ (50 mL), washed with brine (3 x 50 mL), dried over $MgSO_4$ and concentrated *in vacuo*. The product was purified *via* column chromatography ($SiO_2$, Eluent 5 to 50% $CH_2Cl_2$ in Hexane) and the organic fractions collected and concentrated *in vacuo* to yield the product (309 mg, 1.04 mmol, 69%). $^1$H NMR (400 MHz, $CDCl_3$) δ 7.86 (t, *J* = 2.2 Hz, 1H, C(OOMe)CC*H*), 7.61 (dd, *J* = 8.3, 2.2 Hz, 1H, BrCC*H*CH), 7.38 – 7.34 (m, 2H, BrCCHC*H* and SC*H*CHCH), 7.09 – 7.00 (m, 2H, SCHCHC*H* and SCHC*H*CH), 3.75 (s, 3H, C*H*$_3$); MS ($Cl^+$) *m/z* 314, 316 ($M + NH_4^+$); HRMS 313.9845 calculated for $C_{12}H_9O_2SBr^{79}$ + $NH_4$ found 313.9846.

**5-bromo-2-(thiophen-2-yl)benzoic acid**

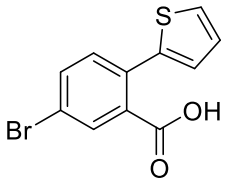


Methyl-5-bromo-2-(thiophen-2-yl)benzoate (3.22 g, 10.8 mmol), NaOH (1.30 g, 32.4 mmol) and EtOH (150 mL) were stirred at 85 °C for 3 h. The reaction mixture was concentrated *in* vacuo and the product was extracted with $CH_2Cl_2$ (3 x 200 mL) and 2M HCl solution (200 mL), dried over $MgSO_4$ and concentrated *in vacuo*. The product was taken into the next reaction without further purification (2.60 g, 9.18 mmol, 85%). $^1$H NMR (600 MHz, $CDCl_3$) δ 8.03 (s, 1H, COOHCC*H*), 7.67 (d, *J* = 8.3 Hz, 1H, BrCC*H*CH), 7.39 (dd, *J* = 4.9, 1.4 Hz, 1H, SC*H*), 7.37 (d, *J* = 8.3 Hz, 1H, BrCCHC*H*), 7.11 – 7.05 (m, 2H, SCHC*H* and SCHCHC*H*); MS ($Cl^+$) *m/z* 300, 302 ($M + NH_4^+$); HRMS 299.9688 calculated for $C_{11}H_7O_2S^{79}Br$ + $NH_4$ found 299.9689.

**6-bromo-4*H*-indeno[1,2-*b*]thiophen-4-one**

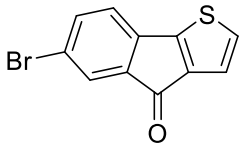


Thionyl chloride (4 mL) was added to 5-bromo-2-(thiophen-2-yl)benzoic acid (100 mg, 0.35 mmol) under argon at 0 °C. DMF (0.1 mL) was added and the reaction mixture was stirred for 2 h at rt under argon. The reaction mixture was concentrated *in vacuo,* added to a suspension of $AlCl_3$ (0.4 g) in $CH_2Cl_2$ (8 mL) at 0 °C and stirred at rt for 18 under argon. The product was extracted with $CH_2Cl_2$ (3 x 50 mL) and 2M HCl solution (50 mL), dried over $MgSO_4$ and concentrated *in vacuo*. The product was purified *via* column chromatography ($SiO_2$, eluent 5 to 50% $CH_2Cl_2$ in hexane) and the relevant organic fractions collected and concentrated *in vacuo* to yield the product (89 mg, 0.34 mmol, 97%). $^1$H NMR (400 MHz, $CDCl_3$) δ 7.56 (d, *J* = 1.7 Hz, 1H, BrCC*H*C), 7.48 (dd, *J* = 7.8, 1.7 Hz, 1H, BrCC*H*CH), 7.22 (d, *J* = 4.9 Hz, 1H, SC*H*), 7.13 (d, *J* = 4.9 Hz, 1H, SCHC*H*), 7.02 (d, *J* = 7.8 Hz, 1H, BrCCHC*H*).

**(*R*,*S*)-6-bromo-4-(4'-methyl-[1,1'-biphenyl]-2-yl)-4*H*-indeno[1,2-*b*]thiophen-4-ol**

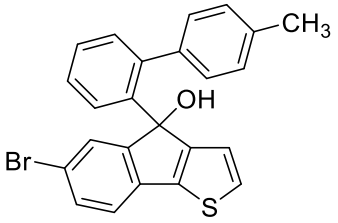


1.6 M $^n$BuLi in hexanes (0.36 mL, 0.58 mmol) was added slowly to 2-bromo-4'-methyl-1,1'-biphenyl (131 mg, 0.53 mmol) in THF (5 mL) at -78 °C under argon. The reaction mixture was stirred for 30 min. 6-bromo-4*H*-indeno[1,2-*b*]thiophen-4-one (140 mg, 0.53 mmol) in THF (5 mL) was added and the reaction mixture was stirred at rt for 1 h. The reaction mixture was concentrated *in vacuo* and the product was purified *via* column chromatography ($SiO_2$, eluent $CH_2Cl_2$:hexane 1:9 to 1:0) and the relevant organic fractions collected and concentrated *in vacuo* to yield the product (200 mg, 0.46 mmol, 87%). $^1$H NMR (600 MHz, $CDCl_3$) δ 8.34 (dd, *J* = 7.6, 1.4 Hz, 1H, OHCCC*H*CHCHCH), 7.51 (ddd, *J* = 7.6, 7.6, 1.5 Hz, 1H, OHCCCHC*H*CHCH), 7.33 (ddd, *J* = 7.6, 7.6, 1.4 Hz, 1H, OHCCCHCHC*H*CH), 7.26 – 7.21 (m, 2H, OHCCCHCHCHC*H* and BrCC*H*C), 7.17 (d, *J* = 4.9 Hz, 1H, SC*H*), 6.95 (dd, *J* = 7.4, 1.3 Hz, 1H, BrCC*H*CH), 6.80 (d, *J* = 4.9

Hz, 1H, SCHC*H*), 6.70 (d, *J* = 7.4 Hz, 1H, BrCCHC*H*), 6.59 (br d, *J* = 31.0 Hz, 2H, $CH_3CCHCH$), 6.11 (d, *J* = 8.1 Hz, 2H, $CH_3CCH$), 2.27 (s, 1H, O*H*), 2.19 (s, 3H, $CH_3$); MS ($Cl^+$) *m/z* 432, 434 ($M^+$).

**(*R*,*S*)-6'-bromo-2-methylspiro[fluorene-9,4'-indeno[1,2-*b*]thiophene]**

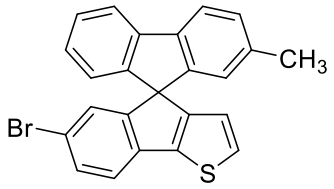


Concentrated HCl solution (5 drops) was added to (*R*,*S*)-6-bromo-4-(4'-methyl-[1,1'-biphenyl]-2-yl)-4H-indeno[1,2-b]thiophen-4-ol (200 mg, 0.46 mmol) in AcOH (50 mL) and the reaction mixture was stirred at rt for 10 mins. The reaction mixture was poured into $H_2O$ (500 mL) and the precipitate was filtered and washed with $H_2O$ (500 mL). The product was purified *via* column chromatography ($SiO_2$, eluent $CH_2Cl_2$:hexane 1:9 to 1:1) and the relevant organic fractions collected and concentrated *in vacuo* to yield the product (130 mg, 0.31 mmol, 67%). $^1$H NMR (600 MHz, $CDCl_3$) δ 7.78 (d, *J* = 7.6 Hz, 1H, CHCHCHC*H*CCCH), 7.71 (d, *J* = 7.8 Hz, 1H, $CH_3CCHCH$), 7.42 – 7.39 (m, 2H, BrCC*H*CH and $CH_3CCHCH$), 7.37 (ddd, *J* = 7.6, 7.4, 1.0 Hz, 1H, CHCHC*H*CHCCCH), 7.26 (d, *J* = 4.9 Hz, 1H, SC*H*), 7.19 (d, *J* = 6.9 Hz, 1H, BrCCHC*H*), 7.11 (ddd, *J* = 7.4, 7.4, 1.0 Hz, 1H, CHC*H*CHCHCCCH), 6.77 (d, *J* = 7.4 Hz, 1H, C*H*CHCHCHCCCH), 6.75 (d, *J* = 1.7 Hz, 1H, $CH_3CCHC$), 6.59 (s, 1H, BrCC*H*C), 6.47 (d, *J* = 4.9 Hz, 1H, SCHC*H*), 2.25 (s, 3H, $CH_3$).

**(*R*,*S*)- 2',6'-dibromo-2-(bromomethyl)spiro[fluorene-9,4'-indeno[1,2-*b*]thiophene]**

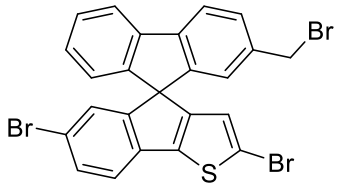


(*R*,*S*)-6'-bromo-2-methylspiro[fluorene-9,4'-indeno[1,2-*b*]thiophene] (130 mg, 0.31 mmol), NBS (61 mg, 0.34 mmol), 25% benzoyl peroxide solution in $H_2O$ (12 mg, 0.04 mmol) and $CHCl_3$ (5 mL) were stirred at 85 °C under argon for 18 h. The reaction mixture was concentrated *in vacuo* and the product was purified *via* column chromatography ($SiO_2$, eluent $CH_2Cl_2$:hexane 1:9 to 1:1) and the relevant organic fractions collected and concentrated *in vacuo* to yield the product (80 mg, 0.16 mmol, 52%). $^1$H NMR (400 MHz, $CDCl_3$) δ 7.82 – 7.77 (m, 2H, CHCHCHC*H*CCCH and $CH_2CCHCH$), 7.49 – 7.37 (m, 3H, CHCHC*H*CHCCCH and $CH_2CCHCH$ and

BrCC*H*CH), 7.34 (d, *J* = 8.1 Hz, 1H, BrCCHC*H*), 7.17 (ddd, *J* = 7.4, 7.4, 1.0 Hz, 1H, CHC*H*CHCHCCCH), 6.81 – 6.77 (m, 2H, C*H*CHCHCHCCCH and BrCC*H*C), 6.74 (d, *J* = 1.7 Hz, 1H, $CH_2CCHC$), 6.49 (s, 1H, SCC*H*), 4.41 (d, *J* = 1.6 Hz, 2H, $CH_2$).

**(*R*,*S*)- 2',6'-dibromospiro[fluorene-9,4'-indeno[1,2-*b*]thiophene]-2-carbaldehyde**

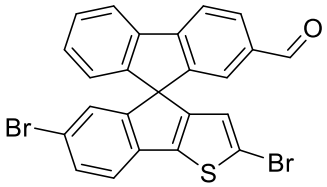


(*R*,*S*)- 2',6'-dibromo-2-(bromomethyl)spiro[fluorene-9,4'-indeno[1,2-*b*]thiophene] (80 mg, 0.14 mmol), $NaHCO_3$ (1.0 g) and DMSO (5 mL) were stirred at 110 °C under argon for 18 h. The reaction mixture was poured into $H_2O$ (50 mL) and the product was extracted with $CH_2Cl_2$ (3 x 50 mL) and concentrated *in vacuo*. The product was taken into the next reaction without further purification (69 mg, 0.14 mmol, 100%). $^1$H NMR (600 MHz, $CDCl_3$) δ 9.89 (s, 1H, C*H*O), 7.97 (d, *J* = 7.8 Hz, 1H, OCHCCHC*H*), 7.93 (d, *J* = 7.8 Hz, 1H, OCHCC*H*CH), 7.90 (d, *J* = 7.8 Hz, 1H, CHCHCHCHCCC*H*), 7.48 – 7.42 (m, 3H, BrCC*H*CH and CHC*H*CHCHCCCH and CHCHC*H*CHCCCH), 7.36 (d, *J* = 8.2 Hz, 1H, BrCCHC*H*), 7.33 (s, 1H, OCHCC*H*C), 6.87 (d, *J* = 7.5 Hz, 1H, C*H*CHCHCHCCCH), 6.71 (s, 1H, BrCC*H*C), 6.47 (s, 1H, SCC*H*).

**(*R*,*S*)- 2',6'-dibromospiro[fluorene-9,4'-indeno[1,2-*b*]thiophene]-2-carbonitrile**

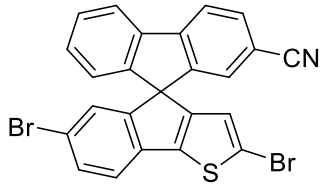


28% ammonium hydroxide solution (1.0 mL) and $I_2$ (89 mg, 0.35 mmol) were added to a solution of (*R*,*S*)- 2',6'-dibromospiro[fluorene-9,4'-indeno[1,2-*b*]thiophene]-2-carbaldehyde (69 mg, 0.16 mmol) in acetonitrile (4 mL) and THF (1 mL). The reaction mixture was allowed to stir for 18 h. The reaction was quenched with saturated $Na_2SO_3$ solution (50 mL) and the product was extracted with $Et_2O$ (2 x 50mL), dried over $MgSO_4$ and concentrated *in vacuo* to give an off white powder (8 mg, 0.02 mmol, 10%). $^1$H NMR (400 MHz, $CDCl_3$) δ 7.92 – 7.85 (m, 2H, NCCCHC*H* and CHCHCHC*H*CCCH), 7.70 (dd, *J* = 7.9, 1.5 Hz, 1H, NCCC*H*CH), 7.49 – 7.42 (m, 2H, BrCC*H*CH and CHCHC*H*CHCCCH), 7.36 (d, *J* = 8.0 Hz, 1H, BrCCHC*H*), 7.27 (ddd, *J* = 7.6, 7.6,

1.1 Hz, 2H, CHC*H*CHCHCCCH), 7.08 (d, *J* = 1.5 Hz, 1H, NCCC*H*C), 6.86 (d, *J* = 7.6 Hz, 1H, C*H*CHCHCHCCCH), 6.70 (d, *J* = 1.6 Hz, 1H, BrCC*H*C), 6.46 (s, 1H, SCC*H*).

# References


1. Hiorns, R. C.; Boucher, R. J.; Duhlev, R.; Hellwich, K.-H.; Hodge, P.; Jenkins, A. D.; Jones, R. G.; Kahovec, J.; Moad, G.; Ober, C. K.; Smith, D. W.; Stepto, R. F. T.; Vairon, J.-P.; Vohlídal, J., *Polym Int,* **2013,** *62* (1), I-II.
2. Kafafi, Z., *Organic electroluminescence*. CRC Press: Boca Raton, 2005.
3. Shirakawa, H.; Louis, E. J.; MacDiarmid, A. G.; Chiang, C. K.; Heeger, A. J., *J Chem Soc Chem Commun,* **1977,** (16), 578-580.
4. Burroughes, J. H.; Bradley, D. D. C.; Brown, A. R.; Marks, R. N.; Mackay, K.; Friend, R. H.; Burns, P. L.; Holmes, A. B., *Nature,* **1990,** *347*, 539.
5. Thejo Kalyani, N.; Dhoble, S. J., *Renew Sust Energ Rev,* **2012,** *16* (5), 2696-2723.
6. Geffroy, B.; le Roy, P.; Prat, C., *Polym Int,* **2006,** *55* (6), 572-582.
7. Ahmad, J.; Bazaka, K.; Anderson, L. J.; White, R. D.; Jacob, M. V., *Renew Sust Energ Rev,* **2013,** *27*, 104-117.
8. Klauk, H., *Chem Soc Rev,* **2010,** *39* (7), 2643-2666.
9. Alexander J. C. Kuehne, M. C. G., *Chem Rev,* **2016,** *116* (21), 12823–12864.
10. Borek, C.; Hanson, K.; Djurovich, P. I.; Thompson, M. E.; Aznavour, K.; Bau, R.; Sun, Y.; Forrest, S. R.; Brooks, J.; Michalski, L.; Brown, J., *Angew Chem Int Edit,* **2007,** *46* (7), 1109-1112.
11. Stephen C. Moratti, D. D. C. B., Raoul Cervini, Richard H. Friend, Neil C. Greenham, Andrew B. Holmes, *Proc Spie,* **1994,** *2144*, 108-114.
12. Hung, L. S.; Chen, C. H., *Mat Sci Eng R,* **2002,** *39* (5), 143-222.
13. van Dijken, A.; Perro, A.; Meulenkamp, E. A.; Brunner, K., *Org Electron,* **2003,** *4* (2), 131-141.
14. Saxena, K.; Jain, V. K.; Mehta, D. S., *Optical Materials,* **2009,** *32* (1), 221-233.
15. Halls, J. J. M.; Walsh, C. A.; Greenham, N. C.; Marseglia, E. A.; Friend, R. H.; Moratti, S. C.; Holmes, A. B., *Nature,* **1995,** *376*, 498.
16. Lu, L.; Yu, L., *Adv Mater,* **2014**, *Advance article* DOI:10.1002/adma.201400384.
17. Xinpeng Jiang, X. G., Jiang Peng, Dahui Zhao, Yuguo Ma, *ACS Appl Mater Interfaces,* **2016,** *8* (18), 11441-11449.
18. Tomas Serevičius, R. K., Povilas Adomėnas, Ona Adomėnienė, Gediminas Kreiza, Vygintas Jankauskas, Karolis Kazlauskas, Arūnas Miasojedovas, Vygintas Jankus, Andy Monkman, and Saulius Juršėnas, *J Phys Chem,* **2017,** *121* (15), 8515-8524.
19. Zhao, J.; Ji, S.; Guo, H., *RSC Adv,* **2011,** *1* (6), 937-950.
20. Peet, J. K., J. Y.; Coates, N. E.; Ma, W. L.; Moses, D.; Heeger, A. J.; Bazan, G. C., *Nat Mater,* **2007,** *6* (7), 497-500.
21. Shockley, W.; Queisser, H. J., *J Appl Phys,* **1961,** *32* (3), 510-519.
22. Baldo, M. A.; Adachi, C.; Forrest, S. R., *Phys Rev B,* **2000,** *62* (16), 10967-10977.
23. Ford, T. A.; Avilov, I.; Beljonne, D.; Greenham, N. C., *Phys Rev B,* **2005,** *71* (12), 125212.
24. Umeyama, T.; Imahori, H., *J Mater Chem A,* **2014**, *Advance article* DOI:10.1039/C3TA15387H.
25. Wasielewski, M. R., *Chem Rev,* **1992,** *92* (3), 435-461.
26. Yella, A.; Lee, H.-W.; Tsao, H. N.; Yi, C.; Chandiran, A. K.; Nazeeruddin, M. K.; Diau, E. W.-G.; Yeh, C.-Y.; Zakeeruddin, S. M.; Grätzel, M., *Science,* **2011,** *334* (6056), 629-634.
27. Zhao, Q.; Huang, C.; Li, F., *Chem Soc Rev,* **2011,** *40* (5), 2508-2524.
28. Ethirajan, M.; Chen, Y.; Joshi, P.; Pandey, R. K., *Chem Soc Rev,* **2011,** *40* (1), 340-362.
29. Imahori, H.; Yamada, H.; Guldi, D. M.; Endo, Y.; Shimomura, A.; Kundu, S.; Yamada, K.; Okada, T.; Sakata, Y.; Fukuzumi, S., *Angew Chem Int Edit,* **2002,** *41* (13), 2344-2347.

30. Ryan, A.; Tuffy, B.; Horn, S.; Blau, W. J.; Senge, M. O., *Tetrahedron,* **2011,** *67* (43), 8248-8254.
31. Huang, X.; Zhu, C.; Zhang, S.; Li, W.; Guo, Y.; Zhan, X.; Liu, Y.; Bo, Z., *Macromolecules,* **2008,** *41* (19), 6895-6902.
32. Umeyama, T.; Takamatsu, T.; Tezuka, N.; Matano, Y.; Araki, Y.; Wada, T.; Yoshikawa, O.; Sagawa, T.; Yoshikawa, S.; Imahori, H., *J Phys Chem C,* **2009,** *113* (24), 10798-10806.
33. Lindsey, J. S.; Hsu, H. C.; Schreiman, I. C., *Tetrahedron Lett,* **1986,** *27* (41), 4969-4970.
34. Lindsey, J. S.; Schreiman, I. C.; Hsu, H. C.; Kearney, P. C.; Marguerettaz, A. M., *J Org Chem,* **1987,** *52* (5), 827-836.
35. Lindsey, J. S.; Wagner, R. W., *J Org Chem,* **1989,** *54* (4), 828-836.
36. Cammidge, A. N.; Öztürk, O., *Tetrahedron Lett,* **2001,** *42* (2), 355-358.
37. Filatov, M. A.; Lebedev, A. Y.; Vinogradov, S. A.; Cheprakov, A. V., *J Org Chem,* **2008,** *73* (11), 4175-4185.
38. Littler, B. J.; Ciringh, Y.; Lindsey, J. S., *J Org Chem,* **1999,** *64* (8), 2864-2872.
39. Spellane, P. J.; Gouterman, M.; Antipas, A.; Kim, S.; Liu, Y. C., *Inorg Chem,* **1980,** *19* (2), 386-391.
40. Minaev, B.; Baryshnikov, G.; Agren, H., *Phys Chem Chem Phys,* **2014,** *16* (5), 1719-1758.
41. Baldo, M. A.; O'Brien, D. F.; You, Y.; Shoustikov, A.; Sibley, S.; Thompson, M. E.; Forrest, S. R., *Nature,* **1998,** *395* (6698), 151-154.
42. Sudhakar, M.; Djurovich, P. I.; Hogen-Esch, T. E.; Thompson, M. E., *J Am Chem Soc,* **2003,** *125* (26), 7796-7797.
43. Lane, P. A.; Palilis, L. C.; O'Brien, D. F.; Giebeler, C.; Cadby, A. J.; Lidzey, D. G.; Campbell, A. J.; Blau, W.; Bradley, D. D. C., *Phys Rev B,* **2001,** *63* (23), 235206.
44. Chen, X.; Liao, J.-L.; Liang, Y.; Ahmed, M. O.; Tseng, H.-E.; Chen, S.-A., *J Am Chem Soc,* **2003,** *125* (3), 636-637.
45. Sandee, A. J.; Williams, C. K.; Evans, N. R.; Davies, J. E.; Boothby, C. E.; Köhler, A.; Friend, R. H.; Holmes, A. B., *J Am Chem Soc,* **2004,** *126* (22), 7041-7048.
46. Morgado, J.; Cacialli, F.; Friend, R. H.; Iqbal, R.; Yahioglu, G.; Milgrom, L. R.; Moratti, S. C.; Holmes, A. B., *Chem Phys Lett,* **2000,** *325* (5–6), 552-558.
47. Iqbal, R.; Moratti, S. C.; Holmes, A. B.; yahioglu, G.; Milgrom, L. R.; cacialli, F.; Morgado, J.; friend, R. H., *J Mater Sci-Mater El,* **2000,** *11* (2), 97-103.
48. Morgado, J.; Cacialli, F.; Iqbal, R.; Moratti, S. C.; Holmes, A. B.; Yahioglu, G.; Milgrom, L. R.; Friend, R. H., *J Mater Chem,* **2001,** *11* (2), 278-283.
49. Fenwick, O.; Sprafke, J. K.; Binas, J.; Kondratuk, D. V.; Di Stasio, F.; Anderson, H. L.; Cacialli, F., *Nano Lett,* **2011,** *11* (6), 2451-2456.
50. Li, P.; Fenwick, O.; Yilmaz, S.; Breusov, D.; Caruana, D. J.; Allard, S.; Scherf, U.; Cacialli, F., *Chem Commun,* **2011,** *47* (31), 8820-8822.
51. Steckler, T. T.; Fenwick, O.; Lockwood, T.; Andersson, M. R.; Cacialli, F., *Macromol Rapid Comm,* **2013,** *34* (12), 990-996.
52. Steckler, T. T.; Lee, M. J.; Chen, Z.; Fenwick, O.; Andersson, M. R.; Cacialli, F.; Sirringhaus, H., *J Mater Chem C,* **2014,** *2* (26), 5133-5141.
53. Tregnago, G.; Fléchon, C.; Choudhary, S.; Gozalvez, C.; Mateo-Alonso, A.; Cacialli, F., *Appl Phys Lett,* **2014,** *105* (14), 143304.
54. Day, N. U.; Wamser, C. C.; Walter, M. G., *Polym Int,* **2015,** *64* (7), 833-857.
55. Hou, Q.; Zhang, Y.; Li, F.; Peng, J.; Cao, Y., *Organometallics,* **2005,** *24* (19), 4509-4518.
56. Zhuang, W.; Zhang, Y.; Hou, Q.; Wang, L.; Cao, Y., *J Polym Sci Pol Chem,* **2006,** *44* (13), 4174-4186.
57. Cho, N. S.; Hwang, D.-H.; Lee, J.-I.; Jung, B.-J.; Shim, H.-K., *Macromolecules,* **2002,** *35* (4), 1224-1228.
58. Dennler, G.; Scharber, M. C.; Brabec, C. J., *Adv Mater,* **2009,** *21* (13), 1323-1338.

59. Deng, Y. Y.; Sirringhaus, H., *Phys Rev B,* **2005,** *72* (4), 045207.
60. Kahveci, Z.; Martínez-Tomé, M. J.; Mallavia, R.; Mateo, C. R., *ACS Appl Mater Interfaces,* **2017,** *9* (1), 136-144.
61. Freeman, D. M. E.; Tregnago, G.; Rodriguez, S. A.; Fallon, K. J.; Cacialli, F.; Bronstein, H., *J Org Semiconductors,* **2015,** *3* (1), 1-7.
62. Freeman, D. M. E.; Minotto, A.; Duffy, W.; Fallon, K. J.; McCulloch, I.; Cacialli, F.; Bronstein, H., *Polym Chem-UK,* **2016,** *7* (3), 722-730.
63. Yu, L.; Muthukumaran, K.; Sazanovich, I. V.; Kirmaier, C.; Hindin, E.; Diers, J. R.; Boyle, P. D.; Bocian, D. F.; Holten, D.; Lindsey, J. S., *Inorg Chem,* **2003,** *42* (21), 6629-6647.
64. Jiang, B.; Jones, W. E., *Macromolecules,* **1997,** *30* (19), 5575-5581.
65. Kwong, R. C.; Sibley, S.; Dubovoy, T.; Baldo, M.; Forrest, S. R.; Thompson, M. E., *Chem Mater,* **1999,** *11* (12), 3709-3713.
66. Ponterini, G.; Serpone, N.; Bergkamp, M. A.; Netzel, T. L., *J Am Chem Soc,* **1983,** *105* (14), 4639-4645.
67. Becker, K.; Lupton, J. M.; Feldmann, J.; Nehls, B. S.; Galbrecht, F.; Gao, D. Q.; Scherf, U., *Adv Funct Mater,* **2006,** *16* (3), 364-370.
68. Hou, Q.; Zhang, Y.; Li, F. Y.; Peng, J. B.; Cao, Y., *Organometallics,* **2005,** *24* (19), 4509-4518.
69. Zhuang, W. L.; Zhang, Y.; Hou, Q.; Wang, L.; Cao, Y., *J Polym Sci Pol Chem,* **2006,** *44* (13), 4174-4186.
70. Singh-Rachford, T. N.; Castellano, F. N., *Coordin Chem Rev,* **2010,** *254* (21–22), 2560-2573.
71. Zhao, J.; Wu, W.; Sun, J.; Guo, S., *Chem Soc Rev,* **2013,** *42* (12), 5323-5351.
72. Monguzzi, A.; Tubino, R.; Hoseinkhani, S.; Campione, M.; Meinardi, F., *Phys Chem Chem Phys,* **2012,** *14* (13), 4322-4332.
73. Monguzzi, A.; Tubino, R.; Meinardi, F., *Phys Rev B,* **2008,** *77* (15), 155122.
74. Lee, S. H.; Ayer, M. A.; Vadrucci, R.; Weder, C.; Simon, Y. C., *Polym Chem-UK,* **2014,** *5* (24), 6898-6904.
75. Dzebo, D.; Börjesson, K.; Gray, V.; Moth-Poulsen, K.; Albinsson, B., *J Phys Chem C,* **2016,** *120* (41), 23397-23406.
76. Wilson, C. J.; Wilson, D. A.; Boyle, R. W.; Mehl, G. H., *J Mater Chem C,* **2013,** *1* (1), 144-150.
77. Maiti, N. C.; Mazumdar, S.; Periasamy, N., *J Phys Chem B,* **1998,** *102* (9), 1528-1538.
78. Xia, Z.-Y.; Su, J.-H.; Wong, W.-Y.; Wang, L.; Cheah, K.-W.; Tian, H.; Chen, C. H., *J Mater Chem,* **2010,** *20* (38), 8382-8388.
79. Li, Y.; Rizzo, A.; Salerno, M.; Mazzeo, M.; Huo, C.; Wang, Y.; Li, K.; Cingolani, R.; Gigli, G., *Appl Phys Lett,* **2006,** *89* (6), 061125.
80. Sun, Y.; Borek, C.; Hanson, K.; Djurovich, P. I.; Thompson, M. E.; Brooks, J.; Brown, J. J.; Forrest, S. R., *Appl Phys Lett,* **2007,** *90* (21), 213503.
81. Che, C.-M.; Hou, Y.-J.; Chan, M. C. W.; Guo, J.; Liu, Y.; Wang, Y., *J Mater Chem,* **2003,** *13* (6), 1362-1366.
82. Lai, S.-W.; Hou, Y.-J.; Che, C.-M.; Pang, H.-L.; Wong, K.-Y.; Chang, C. K.; Zhu, N., *Inorg Chem,* **2004,** *43* (12), 3724-3732.
83. Egbe, D. A. M.; Türk, S.; Rathgeber, S.; Kühnlenz, F.; Jadhav, R.; Wild, A.; Birckner, E.; Adam, G.; Pivrikas, A.; Cimrova, V.; Knör, G.; Sariciftci, N. S.; Hoppe, H., *Macromolecules,* **2010,** *43* (3), 1261-1269.
84. Kimyonok, A.; Tekin, E.; Haykır, G.; Turksoy, F., *J Lumin,* **2014,** *146*, 186-192.
85. Dou, L.; Liu, Y.; Hong, Z.; Li, G.; Yang, Y., *Chem Rev,* **2015,** *115* (23), 12633-12665.
86. Kalinowski, J., *Mater Sci-Poland,* **2009,** *27* (3), 735.
87. Lin, Y. L.; Koch, M.; Brigeman, A. N.; Freeman, D. M. E.; Zhao, L.; Bronstein, H.; Giebink, N. C.; Scholes, G. D.; Rand, B. P., *Energ Environ Sci,* **2017,** *10*, 1465-1475.

88. McCulloch, I. H., Martin; Bailey, Clare; Genevicius, Kristijonas; MacDonald, Iain; Shkunov, Maxim; Sparrowe, David; Tierney, Steve; Wagner, Robert; Zhang, Weimin; Chabinyc, Michael L.; Kline, R. Joseph; McGehee, Michael D.; Toney, Michael F., *Nat Mater,* **2006,** *5* (4), 328-333.
89. Grein, F., *J Phys Chem A,* **2002,** *106* (15), 3823-3827.
90. Wolfle, T.; Gorling, A.; Hieringer, W., *Phys Chem Chem Phys,* **2008,** *10* (37), 5739-5742.
91. O'Sullivan, M. C.; Sprafke, J. K.; Kondratuk, D. V.; Rinfray, C.; Claridge, T. D. W.; Saywell, A.; Blunt, M. O.; O'Shea, J. N.; Beton, P. H.; Malfois, M.; Anderson, H. L., *Nature,* **2011,** *469* (7328), 72-75.
92. Kondratuk, D. V.; PerdigãoLuís, M. A.; EsmailAyad, M. S.; O'Shea, J. N.; Beton, P. H.; Anderson, H. L., *Nat Chem,* **2015,** *7* (4), 317-322.
93. Rousseaux, S. A. L.; Gong, J. Q.; Haver, R.; Odell, B.; Claridge, T. D. W.; Herz, L. M.; Anderson, H. L., *J Am Chem Soc,* **2015,** *137* (39), 12713-12718.
94. Liu, L.; Fortin, D.; Harvey, P. D., *Inorg Chem,* **2009,** *48* (13), 5891-5900.
95. Jiang, F.-L.; Fortin, D.; Harvey, P. D., *Inorg Chem,* **2010,** *49* (6), 2614-2623.
96. Lamare, S.; Aly, S. M.; Fortin, D.; Harvey, P. D., *Chem Commun,* **2011,** *47* (39), 10942-10944.
97. Shomura, R.; Sugiyasu, K.; Yasuda, T.; Sato, A.; Takeuchi, M., *Macromolecules,* **2012,** *45* (9), 3759-3771.
98. Zenkina, O.; Altman, M.; Leitus, G.; Shimon, L. J. W.; Cohen, R.; van der Boom, M. E., *Organometallics,* **2007,** *26* (18), 4528-4534.
99. Schilz, M.; Plenio, H., *J Org Chem,* **2012,** *77* (6), 2798-2807.
100. Nowak-Król, A.; Plamont, R.; Canard, G.; Edzang, J. A.; Gryko, D. T.; Balaban, T. S., *Chem-Eur J,* **2014**, 1488-1498.
101. Boyarskiy, V. P.; Ryabukhin, D. S.; Bokach, N. A.; Vasilyev, A. V., *Chem Rev,* **2016,** *116* (10), 5894-5986.
102. Colvin, M. T.; Smeigh, A. L.; Giacobbe, E. M.; Conron, S. M. M.; Ricks, A. B.; Wasielewski, M. R., *J Phys Chem A,* **2011,** *115* (26), 7538-7549.
103. Chappell, J.; Lidzey, D. G.; Jukes, P. C.; Higgins, A. M.; Thompson, R. L.; O'Connor, S.; Grizzi, I.; Fletcher, R.; O'Brien, J.; Geoghegan, M.; Jones, R. A. L., *Nat Mater,* **2003,** *2* (9), 616-621.
104. Köhler, A.; Bässler, H., *Mat Sci Eng R,* **2009,** *66* (4–6), 71-109.
105. Uoyama, H.; Goushi, K.; Shizu, K.; Nomura, H.; Adachi, C., *Nature,* **2012,** *492* (7428), 234-238.
106. Zhang, Q.; Li, B.; Huang, S.; Nomura, H.; Tanaka, H.; Adachi, C., *Nat Photon,* **2014,** *8* (4), 326-332.
107. Yang, Z.; Mao, Z.; Xie, Z.; Zhang, Y.; Liu, S.; Zhao, J.; Xu, J.; Chi, Z.; Aldred, M. P., *Chem Soc Rev,* **2017,** *46* (3), 915-1016.
108. Endo, A.; Sato, K.; Yoshimura, K.; Kai, T.; Kawada, A.; Miyazaki, H.; Adachi, C., *Appl Phys Lett,* **2011,** *98* (8), 083302.
109. Köhler, A.; Beljonne, D., *Adv Funct Mater,* **2004,** *14* (1), 11-18.
110. Köhler, A.; Wilson, J. S.; Friend, R. H.; Al-Suti, M. K.; Khan, M. S.; Gerhard, A.; Bässler, H., *J Chem Phys,* **2002,** *116* (21), 9457-9463.
111. DeRosa, C. A.; Samonina-Kosicka, J.; Fan, Z.; Hendargo, H. C.; Weitzel, D. H.; Palmer, G. M.; Fraser, C. L., *Macromolecules,* **2015,** *48* (9), 2967-2977.
112. Nikolaenko, A. E.; Cass, M.; Bourcet, F.; Mohamad, D.; Roberts, M., *Adv Mater,* **2015,** *27* (44), 7236-7240.
113. Nobuyasu, R. S.; Ren, Z.; Griffiths, G. C.; Batsanov, A. S.; Data, P.; Yan, S.; Monkman, A. P.; Bryce, M. R.; Dias, F. B., *Adv Opt Mater,* **2016**, 597-607.

114. Luo, J.; Xie, G.; Gong, S.; Chen, T.; Yang, C., *Chem Commun,* **2016,** *52* (11), 2292-2295.
115. Zhu, Y.; Zhang, Y.; Yao, B.; Wang, Y.; Zhang, Z.; Zhan, H.; Zhang, B.; Xie, Z.; Wang, Y.; Cheng, Y., *Macromolecules,* **2016,** *49* (11), 4373-4377.
116. Lee, S. Y.; Yasuda, T.; Komiyama, H.; Lee, J.; Adachi, C., *Adv Mater,* **2016,** *28* (21), 4019-4024.
117. Lee, S. Y.; Yasuda, T.; Yang, Y. S.; Zhang, Q.; Adachi, C., *Angew Chem Int Edit,* **2014,** *53* (25), 6402-6406.
118. Jankus, V.; Aydemir, M.; Dias, F. B.; Monkman, A. P., *Adv Sci,* **2016,** *3* (1), 1500221.
119. Wang, X.; Zhao, L.; Shao, S.; Ding, J.; Wang, L.; Jing, X.; Wang, F., *Polym Chem-UK,* **2014,** *5* (22), 6444-6451.
120. Jankus, V.; Aydemir, M.; Dias, F. B.; Monkman, A. P., *Advanced Science,* **2016,** *3* (1), 1500221-n/a.
121. Freeman, D. M. E.; Musser, A. J.; Frost, J. M.; Stern, H. L.; Forster, A. K.; Fallon, K. J.; Rapidis, A. G.; Cacialli, F.; McCulloch, I.; Clarke, T. M.; Friend, R. H.; Bronstein, H., *J Am Chem Soc,* **2017**.
122. Nakagawa, T.; Ku, S.-Y.; Wong, K.-T.; Adachi, C., *Chem Commun,* **2012,** *48* (77), 9580-9582.
123. Nakanotani, H. H., Takahiro; Furukawa, Taro; Masui, Kensuke; Morimoto, Kei; Numata, Masaki; Tanaka, Hiroyuki; Sagara, Yuta; Yasuda, Takuma; Adachi, Chihaya, *Nat Commun,* **2014,** *5*, 4016.
124. Jiang, W.-F.; Wang, H.-L.; Wang, A.-G.; Li, Z.-Q., *Synthetic Commun,* **2008,** *38* (12), 1888-1895.
125. Poriel, C.; Barrière, F.; Thirion, D.; Rault-Berthelot, J., *Chem-Eur J,* **2009,** *15* (48), 13304-13307.
126. Couture, C.; Paine, A. J., *Can J Chem,* **1985,** *63* (1), 111-120.
127. Hixson, S. S.; Franke, L. A.; Gere, J. A.; Xing, Y. D., *J Am Chem Soc,* **1988,** *110* (11), 3601-3610.
128. Bondarenko, L.; Dix, I.; Hinrichs, H.; Hopf, H., *Synthesis,* **2004,** *2004* (16), 2751-2759.
129. Stambuli, J. P.; Kuwano, R.; Hartwig, J. F., *Angew Chem Int Edit,* **2002,** *41* (24), 4746-4748.
130. Luh, T.-Y.; Leung, M.-k.; Wong, K.-T., *Chem Rev,* **2000,** *100* (8), 3187-3204.
131. Zhu, Z.; Bai, Y.; Lee, H. K. H.; Mu, C.; Zhang, T.; Zhang, L.; Wang, J.; Yan, H.; So, S. K.; Yang, S., *Adv Funct Mater,* **2014,** *24* (46), 7357-7365.
132. King, S. M.; Hintschich, S. I.; Dai, D.; Rothe, C.; Monkman, A. P., *J Phys Chem C,* **2007,** *111* (50), 18759-18764.
133. Aydemir, M.; Jankus, V.; Dias, F. B.; Monkman, A. P., *J Phys Chem C,* **2015,** *119* (11), 5855-5863.
134. Hintschich, S. I.; Rothe, C.; King, S. M.; Clark, S. J.; Monkman, A. P., *J Phys Chem B,* **2008,** *112* (51), 16300-16306.
135. dos Santos, P. L.; Dias, F. B.; Monkman, A. P., *J Phys Chem C,* **2016,** *120* (32), 18259-18267.
136. Kang, T. E.; Cho, H.-H.; Cho, C.-H.; Kim, K.-H.; Kang, H.; Lee, M.; Lee, S.; Kim, B.; Im, C.; Kim, B. J., *ACS Appl Mater Interfaces,* **2013,** *5* (3), 861-868.
137. Neumann, K.; Schwarz, C.; Köhler, A.; Thelakkat, M., *J Phys Chem C,* **2014,** *118* (1), 27-36.
138. Hong, Y.; Lam, J. W. Y.; Tang, B. Z., *Chem Commun,* **2009,** (29), 4332-4353.
139. Zhang, Q.; Komino, T.; Huang, S.; Matsunami, S.; Goushi, K.; Adachi, C., *Adv Funct Mater,* **2012,** *22* (11), 2327-2336.

140. Rajamalli, P.; Senthilkumar, N.; Gandeepan, P.; Huang, P.-Y.; Huang, M.-J.; Ren-Wu, C.-Z.; Yang, C.-Y.; Chiu, M.-J.; Chu, L.-K.; Lin, H.-W.; Cheng, C.-H., *J Am Chem Soc,* **2016,** *138* (2), 628-634.
141. Kasha, M., *Discuss Faraday Soc,* **1950,** *9* (0), 14-19.
142. Stern, H. L.; Musser, A. J.; Gelinas, S.; Parkinson, P.; Herz, L. M.; Bruzek, M. J.; Anthony, J.; Friend, R. H.; Walker, B. J., *P Natl Acad Sci USA,* **2015,** *112* (25), 7656-7661.
143. Korovina, N. V.; Das, S.; Nett, Z.; Feng, X.; Joy, J.; Haiges, R.; Krylov, A. I.; Bradforth, S. E.; Thompson, M. E., *J Am Chem Soc,* **2016,** *138* (2), 617-627.
144. Pensack, R. D.; Ostroumov, E. E.; Tilley, A. J.; Mazza, S.; Grieco, C.; Thorley, K. J.; Asbury, J. B.; Seferos, D. S.; Anthony, J. E.; Scholes, G. D., *J Phys Chem Lett,* **2016,** *7* (13), 2370-2375.
145. Bakulin, A. A.; Morgan, S. E.; Kehoe, T. B.; Wilson, M. W. B.; Chin, A. W.; Zigmantas, D.; Egorova, D.; Rao, A., *Nat Chem,* **2016,** *8* (1), 16-23.
146. Saragi, T. P. I.; Spehr, T.; Siebert, A.; Fuhrmann-Lieker, T.; Salbeck, J., *Chem Rev,* **2007,** *107* (4), 1011-1065.
147. Samanta, P. K.; Kim, D.; Coropceanu, V.; Brédas, J.-L., *J Am Chem Soc,* **2017,** *139* (11), 4042-4051.
148. Kaji, H.; Suzuki, H.; Fukushima, T.; Shizu, K.; Suzuki, K.; Kubo, S.; Komino, T.; Oiwa, H.; Suzuki, F.; Wakamiya, A.; Murata, Y.; Adachi, C., *Nat Commun,* **2015,** *6*.
149. Wang, T.; Weerasinghe, K. C.; Sun, H.; Hu, X.; Lu, T.; Liu, D.; Hu, W.; Li, W.; Zhou, X.; Wang, L., *J Phys Chem C,* **2016,** *120* (21), 11338-11349.
150. Kaiser, C.; Schmiedel, A.; Holzapfel, M.; Lambert, C., *J Phys Chem C,* **2012,** *116* (29), 15265-15280.
151. Bandi, V.; Gobeze, H. B.; Lakshmi, V.; Ravikanth, M.; D'Souza, F., *J Phys Chem C,* **2015,** *119* (15), 8095-8102.
152. Kozlowski, M.; Yoon, T., *J Org Chem,* **2016,** *81* (16), 6895-6897.
153. Field, J. E.; Muller, G.; Riehl, J. P.; Venkataraman, D., *J Am Chem Soc,* **2003,** *125* (39), 11808-11809.
154. Yang, Y.; da Costa, R. C.; Fuchter, M. J.; Campbell, A. J., *Nat Photon,* **2013,** *7* (8), 634-638.
155. Riehl, J. P.; Richardson, F. S., *Chem Rev,* **1986,** *86* (1), 1-16.
156. Dyreklev, P.; Berggren, M.; Inganäs, O.; Andersson, M. R.; Wennerström, O.; Hjertberg, T., *Adv Mater,* **1995,** *7* (1), 43-45.
157. Grell, M.; Bradley, D. D. C., *Adv Mater,* **1999,** *11* (11), 895-905.
158. Grell, M.; Oda, M.; Whitehead, K. S.; Asimakis, A.; Neher, D.; Bradley, D. D. C., *Adv Mater,* **2001,** *13* (8), 577-580.
159. Sherson, J. F.; Krauter, H.; Olsson, R. K.; Julsgaard, B.; Hammerer, K.; Cirac, I.; Polzik, E. S., *Nature,* **2006,** *443* (7111), 557-560.
160. Wagenknecht, C.; Li, C.-M.; Reingruber, A.; Bao, X.-H.; Goebel, A.; Chen, Y.-A.; Zhang, Q.; Chen, K.; Pan, J.-W., *Nat Photon,* **2010,** *4* (8), 549-552.
161. Farshchi, R.; Ramsteiner, M.; Herfort, J.; Tahraoui, A.; Grahn, H. T., *Appl Phys Lett,* **2011,** *98* (16), 162508.
162. Richardson, R. D.; Baud, M. G. J.; Weston, C. E.; Rzepa, H. S.; Kuimova, M. K.; Fuchter, M. J., *Chem Sci,* **2015,** *6* (7), 3853-3862.
163. Yang, Y.; da Costa, R. C.; Smilgies, D.-M.; Campbell, A. J.; Fuchter, M. J., *Adv Mater,* **2013,** *25* (18), 2624-2628.
164. Savoini, M.; Biagioni, P.; Lakhwani, G.; Meskers, S. C. J.; Duò, L.; Finazzi, M., *Opt. Lett.,* **2009,** *34* (22), 3571-3573.
165. Dektar, J. L.; Hacker, N. P., *J Org Chem,* **1991,** *56* (5), 1838-1844.
166. Sergeyev, N. M.; Sandor, P.; Sergeyeva, N. D.; Raynes, W. T., *J Magn Reson Ser A,* **1995,** *115* (2), 174-182.

167. Raynes, W. T.; Sergeyev, N. M.; Sandor, P.; Grayson, M., *Magn Reson Chem,* **1997,** *35* (2), 141-143.
168. Lungerich, D.; Reger, D.; Hölzel, H.; Riedel, R.; Martin, M. M. J. C.; Hampel, F.; Jux, N., *Angew Chem Int Edit,* **2016,** *55* (18), 5602-5605.
169. Guan, D.; Han, L.; Wang, L.; Song, H.; Chu, W.; Sun, Z., *Chem Lett,* **2015,** *44* (6), 743-745.
170. Harada, N.; Watanabe, M.; Kuwahara, S.; Sugio, A.; Kasai, Y.; Ichikawa, A., *Tetrahedron-Asymmetr,* **2000,** *11* (6), 1249-1253.
171. Hoye, T. R.; Jeffrey, C. S.; Shao, F., *Nat Protoc,* **2007,** *2* (10), 2451-2458.
172. Allen, D. A.; Tomaso, A. E.; Priest, O. P.; Hindson, D. F.; Hurlburt, J. L., *J Chem Educ,* **2008,** *85* (5), 698.
173. Chen, B.-S.; Resch, V.; Otten, L. G.; Hanefeld, U., *Chem-Eur J,* **2015,** *21* (7), 3020-3030.
174. Ott, R.; Sauber, K., *Tetrahedron Lett,* **1972,** *13* (37), 3873-3878.
175. Helmchen, G.; Nill, G., *Angew Chem Int Edit,* **1979,** *18* (1), 65-66.
176. Corey, E. J.; Noe, M. C., *J Am Chem Soc,* **1996,** *118* (45), 11038-11053.
177. deMello, J. C.; Wittmann, H. F.; Friend, R. H., *Adv Mater,* **1997,** *9* (3), 230-232.
178. Brown, T. M.; Cacialli, F., *J Polym Sci Pol Phys,* **2003,** *41* (21), 2649-2664.
179. Kim, J. S.; Granstrom, M.; Friend, R. H.; Johansson, N.; Salaneck, W. R.; Daik, R.; Feast, W. J.; Cacialli, F., *J Appl Phys,* **1998,** *84* (12), 6859-6870.
180. Marsitzky, D.; Vestberg, R.; Blainey, P.; Tang, B. T.; Hawker, C. J.; Carter, K. R., *J Am Chem Soc,* **2001,** *123* (29), 6965-6972.
181. Li, Q.; Guo, H.; Ma, L.; Wu, W.; Liu, Y.; Zhao, J., *J Mater Chem,* **2012,** *22* (12), 5319-5329.
182. Kim, J.-H.; Kim, H. U.; Mi, D.; Jin, S.-H.; Shin, W. S.; Yoon, S. C.; Kang, I.-N.; Hwang, D.-H., *Macromolecules,* **2012,** *45* (5), 2367-2376.
183. Seo, K. D.; Lee, M. J.; Song, H. M.; Kang, H. S.; Kim, H. K., *Dyes Pigments,* **2012,** *94* (1), 143-149.
184. Zhang, Q.; Peng, H.; Zhang, G.; Lu, Q.; Chang, J.; Dong, Y.; Shi, X.; Wei, J., *J Am Chem Soc,* **2014,** *136* (13), 5057-5064.
185. Kleinbeck, F.; Toste, F. D., *J Am Chem Soc,* **2009,** *131* (26), 9178-9179.
186. Golovanov, A. A.; Latypova, D. R.; Bekin, V. V.; Pisareva, V. S.; Vologzhanina, A. V.; Dokichev, V. A., *Russ J Org Chem+,* **2013,** *49* (9), 1264-1269.
187. Serra, A.; Pineiro, M.; Santos, C. I.; Rocha Gonsalves, A. M. d. A.; Abrantes, M.; Laranjo, M.; Botelho, M. F., *Photochem Photobiol,* **2010,** *86* (1), 206-212.
188. Chhun, C.; Richard-Daniel, J.; Kempf, J.; Schmitzer, A. R., *Org Biomol Chem,* **2013,** *11* (36), 6023-6028.
189. Murakami, K.; Yamamoto, Y.; Yorimitsu, H.; Osuka, A., *Chem-Eur J,* **2013,** *19* (28), 9123-9126.
190. Balaban, T. S.; Goddard, R.; Linke-Schaetzel, M.; Lehn, J.-M., *J Am Chem Soc,* **2003,** *125* (14), 4233-4239.
191. Kim, J. S.; Song, M.; Park, J. S.; Yoon, M.; Yoon, H. W.; Kim, A. J.; Lee, J. W.; Gal, Y.-S.; Jin, S.-H., *Mol Cryst Liq Cryst,* **2011,** *538* (1), 223-231.
192. Higuchi, H.; Ishikura, T.; Mori, K.; Takayama, Y.; Yamamoto, K.; Tani, K.; Miyabayashi, K.; Miyake, M., *B Chem Soc Jpn,* **2001,** *74* (5), 889-906.
193. Cahiez, G.; Gager, O.; Moyeux, A.; Delacroix, T., *Adv Synth Catal,* **2012,** *354* (8), 1519-1528.
194. Balasaravanan, R.; Duraimurugan, K.; Sivamani, J.; Thiagarajan, V.; Siva, A., *New J Chem,* **2015,** *39* (9), 7472-7480.
195. Xiong, J.-F.; Luo, S.-H.; Huo, J.-P.; Liu, J.-Y.; Chen, S.-X.; Wang, Z.-Y., *J Org Chem,* **2014,** *79* (17), 8366-8373.

196. Zhang, X.; Ji, X.; Su, R.; Weeks, B. L.; Zhang, Z.; Deng, S., *ChemPlusChem,* **2013,** *78* (7), 703-711.
197. Xiao, H.; Yin, H.; Wang, L.; Ding, L.; Guo, S.; Zhang, X.; Ma, D., *Org Electron,* **2012,** *13* (9), 1553-1564.
198. Wong, K.-T.; Ku, S.-Y.; Cheng, Y.-M.; Lin, X.-Y.; Hung, Y.-Y.; Pu, S.-C.; Chou, P.-T.; Lee, G.-H.; Peng, S.-M., *J Org Chem,* **2006,** *71* (2), 456-465.
199. Dong, C.-G.; Hu, Q.-S., *J Am Chem Soc,* **2005,** *127* (28), 10006-10007.
200. Xiao, H.; Yin, H.; Zhang, X., *Org Lett,* **2012,** *14* (20), 5282-5285.
201. Shi, L.; He, C.; Zhu, D.; He, Q.; Li, Y.; Chen, Y.; Sun, Y.; Fu, Y.; Wen, D.; Cao, H.; Cheng, J., *J Mater Chem,* **2012,** *22* (23), 11629-11635.
202. Rumer, J. W.; Dai, S.-Y.; Levick, M.; Biniek, L.; Procter, D. J.; McCulloch, I., *J Polym Sci Pol Chem,* **2013,** *51* (6), 1285-1291.
203. Bárta, O.; Císařová, I.; Štěpnička, P., *Eur J Inorg Chem,* **2017,** *2017* (2), 489-495.
204. Lv, J.; Liu, Q.; Tang, J.; Perdih, F.; Kranjc, K., *Tetrahedron Lett,* **2012,** *53* (39), 5248-5252.
205. Zhang, L.; Jiao, L., *J Am Chem Soc,* **2017,** *139* (2), 607-610.
206. Luan, Y.-X.; Zhang, T.; Yao, W.-W.; Lu, K.; Kong, L.-Y.; Lin, Y.-T.; Ye, M., *J Am Chem Soc,* **2017,** *139* (5), 1786-1789.
207. Moghaddam, F. M.; Tavakoli, G.; Saeednia, B.; Langer, P.; Jafari, B., *J Org Chem,* **2016,** *81* (9), 3868-3876.
208. Hartmann, M.; Daniliuc, C. G.; Studer, A., *Chem Commun,* **2015,** *51* (15), 3121-3123.
209. Ke, H.; Chen, X.; Zou, G., *J Org Chem,* **2014,** *79* (15), 7132-7140.
210. Minard, C.; Palacio, C.; Cariou, K.; Dodd, R. H., *Eur J Org Chem,* **2014,** *2014* (14), 2942-2955.
211. Ravnsbæk, J. B.; Jacobsen, M. F.; Rosen, C. B.; Voigt, N. V.; Gothelf, K. V., *Angew Chem Int Edit,* **2011,** *50* (46), 10851-10854.
212. Zhou, N.; Wang, L.; Thompson, D. W.; Zhao, Y., *Org Lett,* **2008,** *10* (14), 3001-3004.
213. Ochiai, H.; Uetake, Y.; Niwa, T.; Hosoya, T., *Angew Chem Int Edit,* **2017,** *56* (9), 2482-2486.

# Appendices

## Appendix 1: Deep-red electrophosphorescence from a platinum(II)–porphyrin complex copolymerised with polyfluorene for efficient energy transfer and triplet harvesting

*Journal of Organic Semiconductors*, 2015
Vol. 3, No. 1, 1–7, http://dx.doi.org/10.1080/21606099.2015.1047473



# Deep-red electrophosphorescence from a platinum(II)–porphyrin complex copolymerised with polyfluorene for efficient energy transfer and triplet harvesting

David M.E. Freeman[a†], Giulia Tregnago[b†], Silvia Araguas Rodriguez[b], Kealan J. Fallon[a], Franco Cacialli[b*] and Hugo Bronstein[a*]

[a]*Department of Chemistry, University College London, London WC1H 0AJ, UK;* [b]*Department of Physics and Astronomy, London Centre for Nanotechnology, University College London, London WC1E 6BT, UK*

(*Received 13 March 2015; final version received 29 April 2015* )

A series of polyfluorene-based polymers with a range of weight percentages (w/w) of a platinum(II)-containing porphyrin, 5,15-dimesityl-10,20-diphenylporphyrinato platinum(II) (**MPP(Pt)**), were synthesised and incorporated into organic light-emitting diodes. All polymers showed emission predominantly in the red/NIR region with only those polymers with porphyrin w/w of less than 2% showing residual tails at wavelengths lower than 600 nm, indicating increased emission from the porphyrin as w/w increases. The 2% loading of **MPP(Pt)** gave the highest efficiency LED (0.48%) and light output (2630 mW/m$^2$).

**Keywords:** conjugated polymer; OLED; triplet harvesting; porphyrin; fluorene



## 1. Introduction

Phosphorescent emitters are of great interest in organic light-emitting diodes (OLEDs) due to their potential to achieve near to 100% internal quantum efficiency.[1] Upon incorporation of heavy metal atoms with strong spin–orbit coupling such as platinum(II) or iridium(III), the system is distorted such that radiative transitions from triplet states, that is, where $\Delta S \neq 0$, become feasible. Intersystem crossing from any excited singlet state is also more favourable, resulting in radiative decay from $T_1$ regardless of the original spin of the exciton. Since the first investigation of the electroluminescence (EL) from Pt(II)–porphyrin complexes [2] and Ir(ppy)$_3$,[3] many groups have reported the use of such complexes in blend with a polymer host. However, phosphorescent dopant aggregation and phase separation are disadvantages of blend architecture, due to the increased phosphorescent quenching rate.[4,5] While synthetically more challenging, copolymerisation overcomes these disadvantages.[6,7] Having the dopant covalently bonded to the polymer will both increase the rate of energy transfer and reduce loss processes by maintaining the absorbing and emitting moieties at fixed distance, thus preventing intermolecular interaction between dopant molecules. Solubility of the whole system is also increased facilitating low-cost solution-processed device fabrication. In particular, the incorporation of Pt(II)-complexed porphyrins into host polymers has been demonstrated to be a viable route, that is, as a side chain in 2-methoxy-5-(20-ethylhexyloxy)-1,4-phenylene vinylene (MEH-PPV). [8–10] These materials are promising candidates for deep-red [11] OLEDs with spectral components extending even into the near-infrared (NIR),[12–15] the focus of increasing attention for application in the biomedical, security and communication sectors. Still few investigations have been reported for the incorporation of Pt(II)–porphyrin directly in the polymer backbone.[16–18] Of the few previously reported polymers, porphyrins are generally incorporated by the $\beta$-pyyrollic position.[16,18] Meso incorporation into a polyfluorene polymer has previously been achieved by Xiang but was studied only in the context of oxygen sensing and was synthesised via a less controlled (compared to Suzuki) Yamamoto reaction.[17]

Here, we investigate the inclusion of Pt(II)–porphyrin, a dimesityl diphenyl porphyrin platinum (**MPP-Pt**) in a polyfluorene host polymer, poly(9,9-di-*n*-octylfluorenyl-2,7-diyl) (PFO) where the phosphorescent dopant is covalently linked to the fluorescent host via phenyl groups (**PF-MPP(Pt)**). We also characterised the steady-state and time-resolved photoluminescence (PL) of the materials, which were then incorporated in light-emitting diodes.

*Corresponding author. Emails: f.cacialli@ucl.ac.uk; h.bronstein@ucl.ac.uk
†These authors contributed equally to this work.

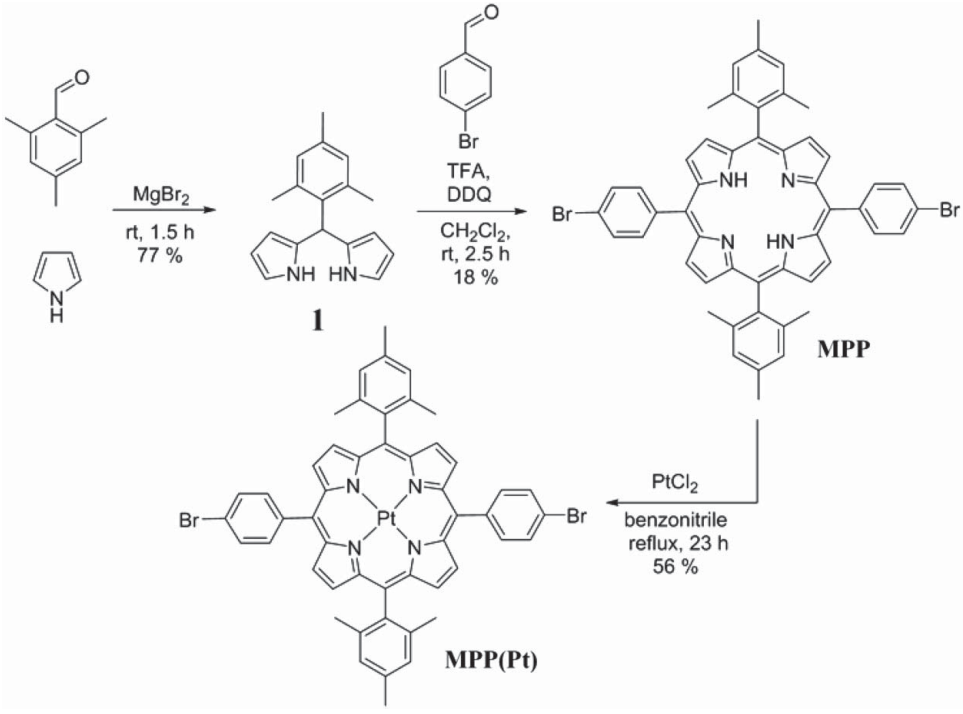


Scheme 1. Synthesis of **MPP(Pt)**.

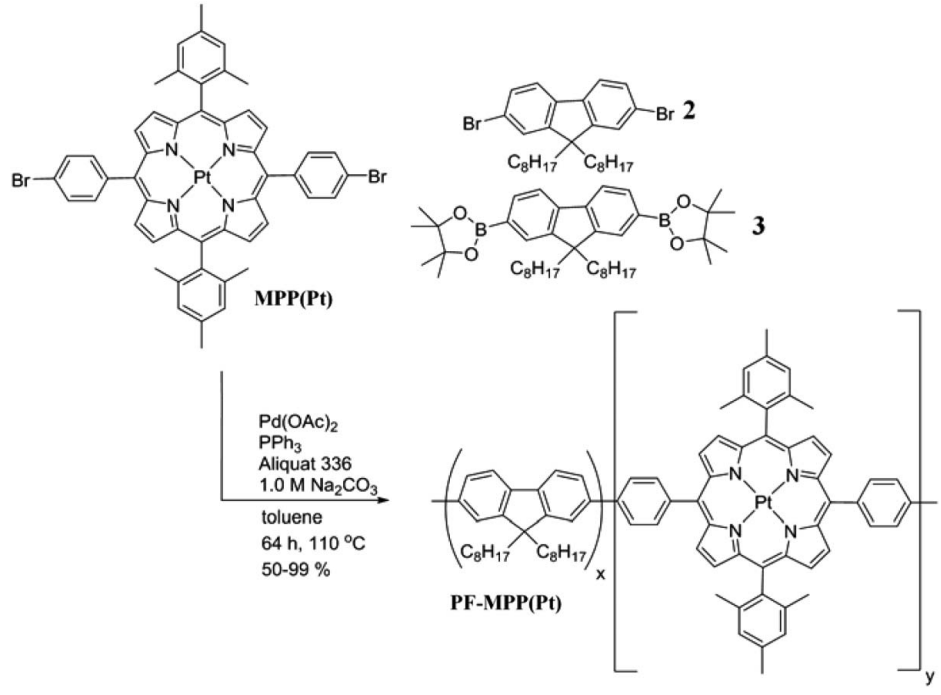


Scheme 2. Suzuki–Miyaura polymerisation of **2**, **3** and **MPP(Pt)** to form **PF-MPP(Pt)**.

## 2. Synthesis

The polymer that forms the basis of this work, **PF-MPP(Pt)**, was prepared via Suzuki–Miyaura cross-coupling reaction of monomers **2**, **3** and **MPP(Pt)** (Scheme 2). Flourene monomers **2** and **3** were synthesised from a literature procedure from fluorene.[19] **MPP(Pt)** was synthesised as in Scheme 1 in three steps from pyrrole and mesitaldehyde using a modified procedure of Lindsey that allows the synthesis of trans-$A_2B_2$ porphyrins from a relevant dipyrromethane and aldehyde.[20] Mesityldipyrromethane **1** was formed by stirring mesitaldehyde with $MgBr_2$ using pyrrole as

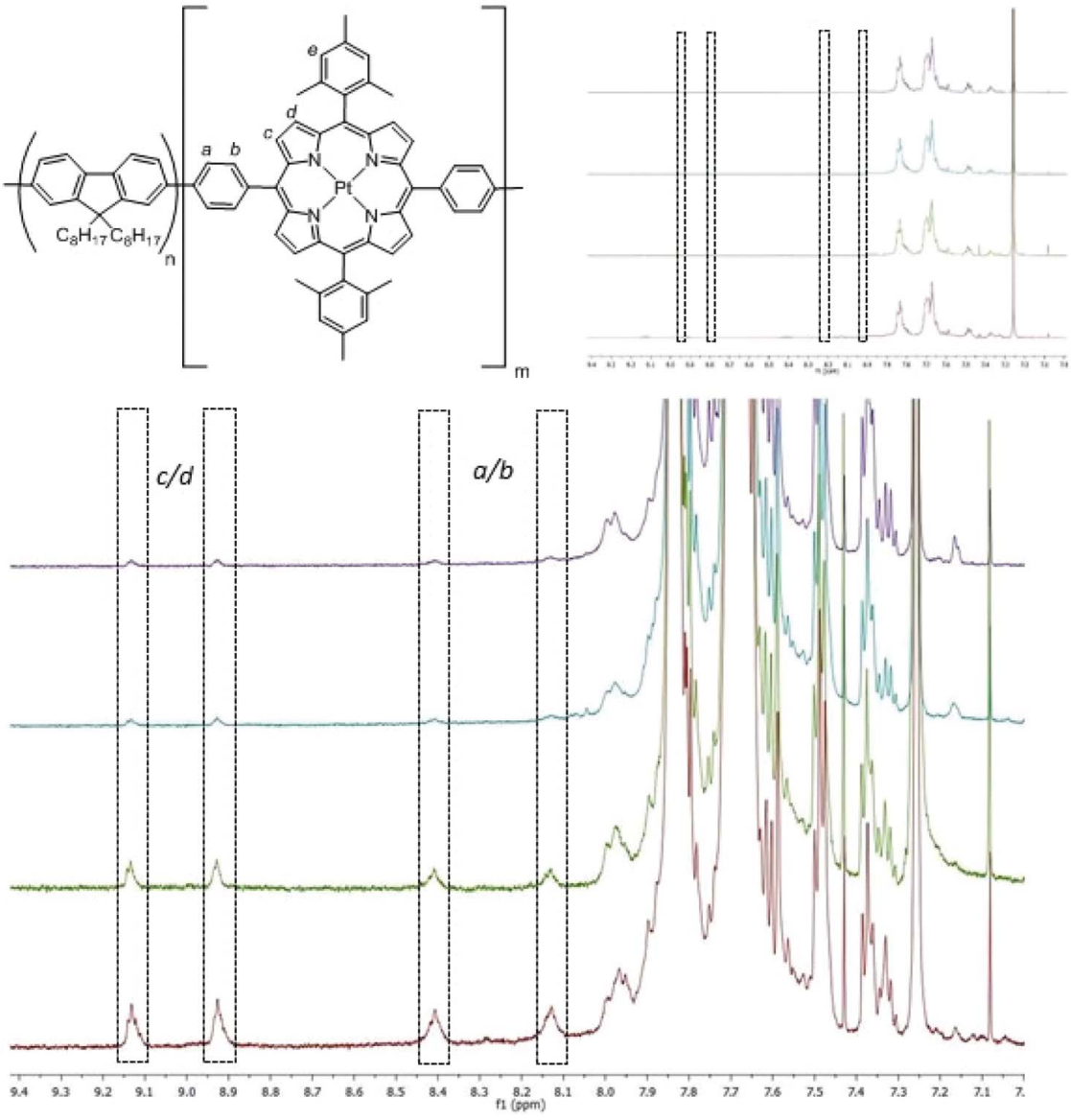


Figure 1. $H^1$ NMR spectra in $CDCl_3$ of **PF-MPP(Pt)** containing 0.5% (**P1**, purple, top), 1.0% (**P2**, cyan, second from top), 2.0% (**P3**, green, second from bottom) and 5.0% (**P4**, maroon, bottom) w/w of **MPP(Pt)**. PF observed peaks (top right) were set to the same level. Peaks corresponding to porpyhin protons are shown in dotted boxes.



solvent. Dipyrromethane **1** was subsequently reacted with bromobenzaldehyde in the presence of TFA and oxidised with DDQ to give **MPP** as purple crystals. Complexation of the free base porphyrin with $PtCl_2$ in refluxing benzonitrile resulted in **MPP(Pt)** as a red powder.

Suzuki polymerisation of the monomers was realised using $Pd(OAc)_2$ with $PPh_3$ as catalyst in the presence of Aliquat 336 and base (Scheme 2). **PF-MPP(Pt)** was prepared with **MPP(Pt)** in several weight percentages (w/w), controlled by varying the ratio of the monomers. The amount of diboronic ester fluorene **3** was always constant while the ratio of fluorene dibromide **2** and **MPP(Pt)** was varied to control the w/w of porphyrin in the final polymer. **MPP(Pt)** was incorporated with w/w of 0.5%, 1.0%, 2.0% and 5.0% into **PF MPP(Pt)**, giving a range of products that were analysed together (**P1**, **P2**, **P3** and **P4**, respectively). The novel polymers were isolated as dark red solids and were purified by Soxhlet extraction using acetone, hexane and finally chloroform. Gel permeation chromatography of the polymers showed a molecular weight ($M_w$) of 15.0–23.0 kDa with PDIs of 1.6–1.9.

Attempts to determine the percentage incorporation of **MPP(Pt)** into each of the polymers were made by $^1H$ NMR spectroscopy. Figure 1 shows how the ratio of porphyrin to PFO signals changes with increasing porphyrin incorporation and it can clearly be seen that the percentage incorporation increases with increased porphyrin feed ratio, and does so in a manner concurrent with the feed

Table 1. Synthetic results of polymerisation.

| Polymer | Incorporation ratio: w/w porphyrin (%)[a] | Incorporation ratio: Feed ratio[b] | $M_n$ (kDa)[c] | $M_w$ (kDa)[c] | PDI[c] |
|---|---|---|---|---|---|
| **P1** | 0.5 | 0.2 | 8.0 | 15 | 1.8 |
| **P2** | 1.0 | 0.3 | 11 | 20 | 1.8 |
| **P3** | 2.0 | 0.9 | 11 | 17 | 1.6 |
| **P4** | 5.0 | 2.2 | 12 | 23 | 1.9 |

[a]Determined by reaction stoichiometry.
[b]Determined by $^1$H NMR spectroscopy.
[c]Determined by SEC(PS) using PhCl eluent.

ratios. The estimated incorporation values are shown in Table 1 and are based on the ratio between the alkyl protons closest to fluorene and the most downfield pyrrolic proton peaks, these being the most isolated. As the feed ratio is increased, so does the incorporation ratio by an equivalent amount. This shows good evidence that the polymers are as expected relative to each other and represent a good range of porphyrin incorporation. The values are lower than the corresponding feed ratio, however, low incorporation to feed ratios have been shown before on similar systems.[21] It is thought that this discrepancy is primarily a result of errors associated with the NMR spectra integration, rather than lower than the expected porphyrin incorporation, due to the good solubility of **MPP(Pt)** in toluene. By comparing the **MPP(Pt)** peaks in the polymers to monomeric **MPP(Pt)** and **MPP**, the peaks may be tentatively identified. The four protons *a–d* come at 8.1, 8.4, 8.9 and 9.1 ppm and can be seen as the intensity of the aromatic region is increased. All four shifts are further downfield than **MPP(Pt**) as a monomer. Proton *e* is expected to be under the much larger PFO peaks. The furthest downfield peaks (8.9 and 9.1 ppm) have been assigned as *c* and *d* and the remaining peaks at 8.1 and 8.4 ppm have been assigned as *a* and *b*. These assignments are based on the ordering of peaks of previous compounds (heteroaromatic protons were further downfield than aromatic). As the level of porphyrin incorporation into the polymer is increased from 0.5% to 5.0%, the relative intensities of the proton peaks increase, qualitatively showing that the four porphyrin-containing polymers have a good range of w/w.

Methods for spectroscopy and LEDs are reported in the Electronic Supplementary Information (ESI).

The energy levels and molecular orbitals of **PF-MPP(Pt)** were calculated by DFT B3LYP *in silico* using basis set 6–31G* for C, H and N and LanL2DZ for Pt. Figure 2 shows the HOMO and LUMO levels of an approximation of a porphyrin-containing portion of the polymer. To reduce calculation times, the octyl chains of PF have been replaced with methyl groups.

What is most apparent from the MO calculations is the degree of localisation of the molecular orbitals to either the porphyrin or fluorene portion of the molecule. The twist from porphyrin to phenyl to fluorene is such that conjugation across the entire molecule is broken. While this will have an overall negative impact on mobilities of the system, it does mean that the basic electronic characteristics of both moieties are likely to be only mildly affected. However, the HOMO, and to a smaller degree the LUMO, do both show a mild degree of delocalisation from the porphyrin to the main polymer chain, despite the large twist. It is expected therefore that energy transfer will be more facilitated than the analogous blend of porphyrin and PFO. Significant LUMO contribution from the Pt d-orbitals can be observed indicating that its role not only facilitates intersystem crossing but that the electronic transitions have metal-to-ligand charge transfer characteristic.

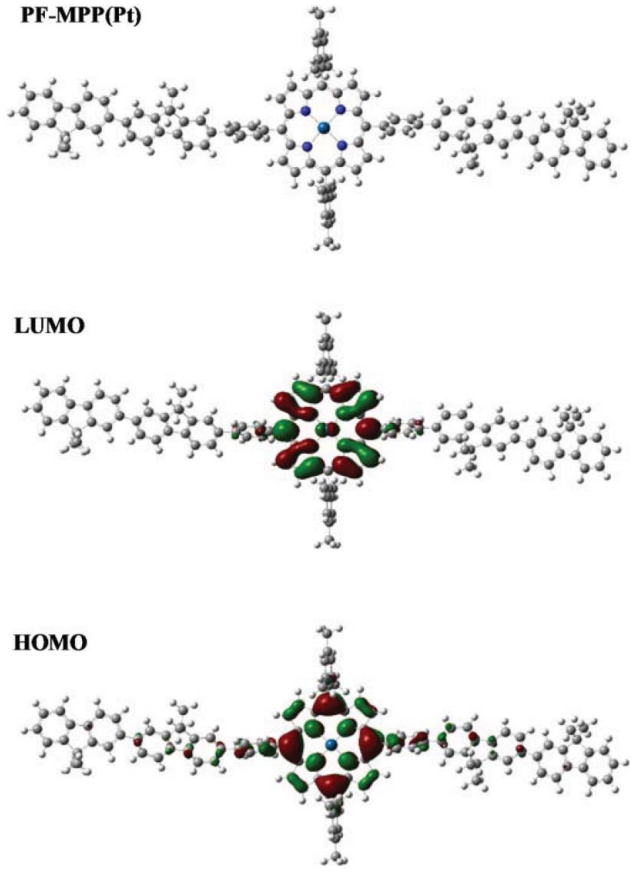


Figure 2. HOMO and LUMO levels of **PF-MPP(Pt)**.

## 3. Results and discussion

We report the absorption and emission spectra for the copolymers **P1–P4** thin films in Figure 3(b) and 3(c). The copolymers show an intense featureless band at 380 nm due to the absorption of the PFO host polymer. In addition, the samples show two features at about 512 and 540 nm that we attribute to the Q-bands of the metalloporphyrin.[22] These bands increase in intensity as the concentration of **MPP-Pt**

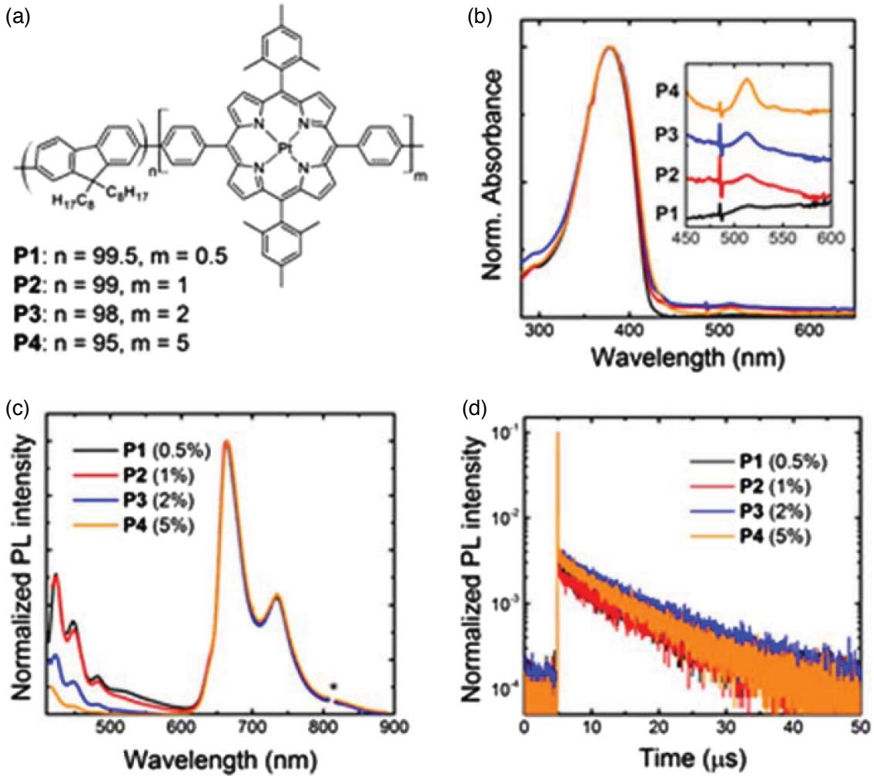


Figure 3. (a) Chemical structure of the PFO-MPP(Pt) copolymers with different MPP(Pt) loading: 0.5% for P1, 1% for P2, 2% for P3 and 5% for P4. (b) Normalised absorption spectra of the copolymers film on fused silica glass. The inset shows MPP(Pt) absorption features, the curves are stacked with Y-offset following the increase in the MPP(Pt) content. (c) Normalised PL spectra of the copolymer films. The '*' indicates the monochromator second-order transmission of the excitation wavelength. (d) PL time decay taken at the most intense peak emission wavelength of the MPP(Pt) (665 nm) following excitation at 371 nm.

increases and are clearly distinguishable for loadings as low as 1%.

Interestingly, given the small dopant loading, the PL spectra show a dominant emission in the red and NIR region with three components at about 665, 735 and 805 nm and an emission shoulder at 645 nm that we assign to the **MPP(Pt)** segment. The copolymers also present a lower intensity emission at shorter wavelengths with vibronic peaks at ~442, 467 and 497 nm that we assign to PFO. Interestingly, when increasing the porphyrin content, the intensity of these peaks reduces relative to the porphyrin emission, therefore suggesting an efficient energy transfer from PFO to the porphyrin. Indeed, the good spectral overlap between the **MPP(Pt)** absorption and the PFO emission (Fig. S1) corroborates this hypothesis: both the Soret band (peaking at 402 nm) and the Q-band of the Pt(II)–porphyrin significantly overlap with the PFO emission. We also note a weak fluorescence emission band between 500 and 600 nm that can be related to the presence of fluorenone defects or aggregates/excimers whose presence is further validated by the TCSPC data.[23,24] In fact, the radiative lifetime of PFO taken at 550 nm (Fig. S2) can be fit with a bi-exponential function yielding time constants of ~400 ps and 6.6 ns that are consistent with PFO exciton and fluorenone excimer respectively.[25] The radiative lifetime taken near the peak emission wavelength of the PFO (440 nm) also confirms the presence of efficient energy transfer from the PFO to the porphyrins. In fact, the lifetime of the pure PFO of about ~400 ps is reduced upon loading with the **MPP(Pt)** and drops below the instrument detection limit (~150 ps). The PL lifetime taken at the emission wavelength of the **MPP(Pt)** emission (665 nm) are reported in Figure 3(d). The copolymers show lifetime decays in the microsecond scale indicating the triplet nature of the emissive state. Specifically, we found time constants of 9.3 μs (**P1**), 9.2 μs (**P2**), 9.2 μs (**P3**) and 8.6 μs (**P4**).

The PL efficiency is around 4.9% for the **MPP(Pt)** loading of 0.5% (**P1**) and slightly decreases (4.5%) upon increasing the amount of porphyrin up to 2% (**P2-P3**). A drop to a PL efficiency of 2.5% is seen for higher porphyrin content (**P4**). The trend is consistent with the lifetime values suggesting an increase in the non-radiative deactivation of the exciton for porphyrin concentrations higher than 2%. Note that although these values may appear relatively low in absolute terms, they are comparable to values reported in the literature for similar polymers.[18]

We also incorporated the copolymers in LEDs with ITO/PEDOT:PSS as anode and Ca/Al as cathode. We report the EL spectra in Figure 4(a) in which we note that

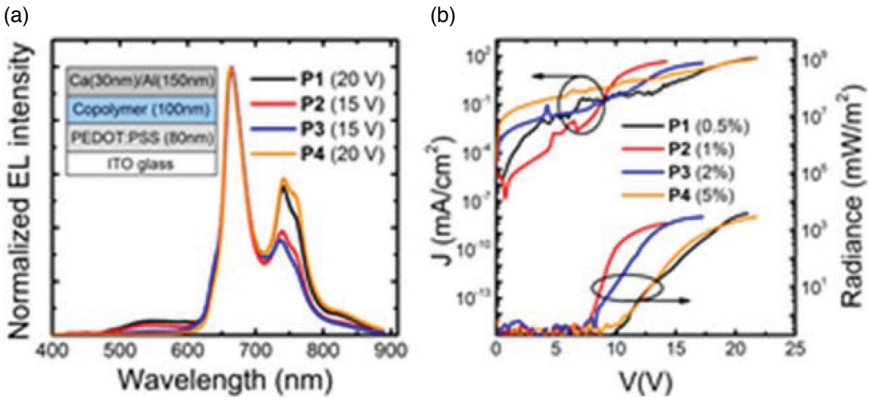


Figure 4. (a) Normalised EL spectra for the copolymers. The LED structure is reported. (b) LED characteristics: current density and radiance versus voltage. The active layer thickness is ~100 nm and the device area is 3.5 $mm^2$.

Table 2. Summary of LEDs performances.

| Copolymer | EQE[a] (%) | $V_{on}$[b] (V) | Radiance[a] ($mW/m^2$) | Luminance[a] ($Cd/m^2$) |
|---|---|---|---|---|
| **P1** | 0.17 ± 0.01 | 10.7 ± 0.2 | 986 ± 61 | 14.8 ± 0.7 |
| **P2** | 0.28 ± 0.04 | 7.6 ± 0.2 | 1486 ± 221 | 23.8 ± 2.9 |
| **P3** | 0.48 ± 0.01 | 8.3 ± 0.3 | 2630 ± 38 | 31.1 ± 0.8 |
| **P4** | 0.28 ± 0.04 | 9.3 ± 0.4 | 1390 ± 56 | 9.9 ± 0.4 |

[a]Measured at 30 $mA/cm^2$.
[b]Intercept of the *I*–*V* curve with the *x*-axis in a semi-log plot.

the copolymers display an emission predominantly in the red and NIR region. In particular, the EL of **P1** peaks at 665, 736 and 818 nm with a shoulder at 642 nm. We do not observe any shifts of the EL for higher **MPP(Pt)** loadings nor compared to the PL spectra. For copolymer **P1** and **P2**, however, we note a weak EL emission at wavelength below 600 nm. When increasing the content of porphyrin, the intensity of the emission tail decreases with little or no intensity left for loading above 1%. Such emission may be related to oxidative defects on the PFO [23] and to the emission from **MPP(Pt)** singlet state, as reported for similar Pt(II)–porphyrin complexes at 580 nm.[26,27] For **MPP(Pt)** loadings above 1%, copolymers show a pure electrophosphorescence (**P3** and **P4**).

The current–voltage and radiance–voltage characteristics are shown in Figure 4(b), and a summary of the LEDs performance is reported in Table 2. The 2% loading of **MPP(Pt)** (**P3**) gives the highest efficiency LED (0.48%) and light output (2630 $mW/m^2$). The result is particularly encouraging compared to what has been reported in the literature up to now, especially when taking into account that the LEDs are not optimised for charge collection and extraction.[16,18] We note an overall improvement of the performance (i.e. lower turn-on voltage, higher efficiency and light output) when increasing the porphyrin loading up to 2%. However, the LEDs performance lowers when the loading exceeds 5%. Given the partial overlap of the **MPP(Pt)** absorption with the PFO emission, we speculate that the EL emission at low voltages is mainly due to charge trapping in the **MPP(Pt)** segment rather than energy transfer. However, upon a further increase in the applied voltage, charges can be injected directly into the PFO levels and can subsequently migrate to the **MPP(Pt)** moiety and contribute to the phosphorescence emission.

## 4. Conclusions

We have prepared a series of conjugated copolymers containing **MPP(Pt)**, a platinum(II)-complexed porphyrin, directly into the PFO backbone via the meso position. Emission of the polymers at 665 nm was shown to have a lifetime decay on the microsecond scale, indicating phosphorescence for all porphyrin-containing polymers, with decreased fluorescence from the PFO backbone as the w/w of **MPP(Pt)** was increased. The polymers were incorporated into OLEDs, and 2% w/w of **MPP(Pt)** was shown to have an efficiency of 0.48% and a light output of 2630 $mW/m^2$. Pure **MPP(Pt)** electrophosphorescence is achieved for loading as low as 2%.

## Acknowledgements

We thank the EC Seventh Framework Programmes (No. 264694 (GENIUS), N. 607585 (OSNIRO), N. 643238 (SYNCHRONICS)), the Royal Society and the EPSRC. F.C. gratefully acknowledges the Wolfson Foundation and the Royal Society for the award of a Wolfson-Royal Society Merit Award.

## Disclosure Statement

No potential conflict of interest was reported by the author(s).

## Supplemental data

Supplemental data for this article can be accessed 10.1080/21606099.2015.1047473.

## References

[1] Minaev B, Baryshnikov G, Agren H. Principles of phosphorescent organic light emitting devices. Phys Chem Chem Phys. 2014;16:1719–1758.

[2] Baldo MA, O'Brien DF, You Y, Shoustikov A, Sibley S, Thompson ME, Forrest SR. Highly efficient phosphorescent emission from organic electroluminescent devices. Nature. 1998;395:151–154.

[3] Baldo MA, Thompson ME, Forrest SR. High-efficiency fluorescent organic light-emitting devices using a phosphorescent sensitizer. Nature. 2000;403:750–753.

[4] Lane PA, Palilis LC, O'Brien DF, Giebeler C, Cadby AJ, Lidzey DG, Campbell AJ, Blau W, Bradley DDC. Origin of electrophosphorescence from a doped polymer light emitting diode. Phys Rev B. 2001;63:235206.

[5] Sudhakar M, Djurovich PI, Hogen-Esch TE, Thompson ME. Phosphorescence quenching by conjugated polymers. J Am Chem Soc. 2003;125:7796–7797.

[6] Chen X, Liao JL, Liang Y, Ahmed MO, Tseng HE, Chen SA. High-efficiency red-light emission from polyfluorenes grafted with cyclometalated iridium complexes and charge transport moiety. J Am Chem Soc. 2003;125:636–637.

[7] Sandee AJ, Williams CK, Evans NR, Davies JE, Boothby CE, Kohler A, Friend RH, Holmes AB. Solution-processible conjugated electrophosphorescent polymers. J Am Chem Soc. 2004;126:7041–7048.

[8] Morgado J, Cacialli F, Friend RH, Iqbal R, Yahioglu G, Milgrom LR, Moratti SC, Holmes AB. Tuning the red emission of a soluble poly(p-phenylene vinylene) upon grafting of porphyrin side groups. Chem Phys Lett. 2000;325:552–558.

[9] Iqbal R, Moratti SC, Holmes AB, Yahioglu G, Milgrom LR, Cacialli F, Morgado J, Friend RH. Synthesis of porphyrin-PPV copolymers for application in LEDs. J Mater Sci –Mater Electron. 2000;11:97–103.

[10] Morgado J, Cacialli F, Iqbal R, Moratti SC, Holmes AB, Yahioglu G, Milgrom LR, Friend RH. Förster energy transfer and control of the luminescence in blends of an orange-emitting poly(p-phenylenevinylene) and a red-emitting tetraphenylporphyrin. J Mater Chem. 2001;11:278–283.

[11] Fenwick O, Sprafke JK, Binas J, Kondratuk DV, Di Stasio F, Anderson HL, Cacialli F. Linear and cyclic porphyrin hexamers as near-infrared emitters in organic light-emitting diodes. Nano Lett. 2011;11:2451–2456.

[12] Li P, Fenwick O, Yilmaz S, Breusov D, Caruana DJ, Allard S, Scherf U, Cacialli F. Dual functions of a novel low-gap polymer for near infra-red photovoltaics and light-emitting diodes. Chem Commun. 2011;47:8820–8822.

[13] Steckler TT, Fenwick O, Lockwood T, Andersson MR, Cacialli F. Near-infrared polymer light-emitting diodes based on low-energy gap oligomers copolymerized into a high-gap polymer host. Macromol Rapid Comm. 2013;34:990–996.

[14] Steckler TT, Lee MJ, Chen Z, Fenwick O, Andersson MR, Cacialli F, Sirringhaus H. Multifunctional materials for OFETs, LEFETs and NIR PLEDs. J Mater Chem C. 2014;2:5133–5141.

[15] Tregnago G, Flechon C, Choudhary S, Gozalvez C, Mateo-Alonso A, Cacialli F. Virtually pure near-infrared electroluminescence from exciplexes at polyfluorene/hexaazatrinaphthylene interfaces. Appl Phys Lett. 2014;105:143304.

[16] Hou Q, Zhang Y, Li FY, Peng JB, Cao Y. Red electrophosphorescence of conjugated organoplatinum(II) polymers prepared via direct metalation of poly(fluorene-co-tetraphenylporphyrin) copolymers. Organometallics. 2005;24:4509–4518.

[17] Xiang H, Zhou L, Feng Y, Cheng J, Wu D, Zhou X. Tunable fluorescent/phosphorescent platinum(II) porphyrin–fluorene copolymers for ratiometric dual emissive oxygen sensing. Inorg Chem. 2012;51:5208–5212.

[18] Zhuang WL, Zhang Y, Hou Q, Wang L, Cao Y. High-efficiency, electrophosphorescent polymers with porphyrin–platinum complexes in the conjugated backbone: synthesis and device performance. J Polym Sci Pol Chem. 2006;44:4174–4186.

[19] Yang R, Tian R, Yan J, Zhang Y, Yang J, Hou Q, Yang W, Zhang C, Cao Y. Deep-red electroluminescent polymers: synthesis and characterization of new low-band-gap conjugated copolymers for light-emitting diodes and photovoltaic devices. Macromolecules. 2005;38:244–253.

[20] Lindsey JS. Synthetic routes to meso-patterned porphyrins. Acc Chem Res. 2009;43:300–311.

[21] Jiang B, Jones WE. Synthesis and characterization of a conjugated copolymer of poly(phenylenevinylene) containing a metalloporphyrin incorporated into the polymer backbone. Macromolecules. 1997;30:5575–5581.

[22] Mink LM, Neitzel ML, Bellomy LM, Falvo RE, Boggess RK, Trainum BT, Yeaman P. Platinum(II) and platinum(IV) porphyrin complexes: synthesis, characterization, and electrochemistry. Polyhedron. 1997;16:2809–2817.

[23] Becker K, Lupton JM, Feldmann J, Nehls BS, Galbrecht F, Gao DQ, Scherf U. On-chain fluorenone defect emission from single polyfluorene molecules in the absence of intermolecular interactions. Adv Funct Mater. 2006;16:364–370.

[24] Pei QB, Yang Y. Efficient photoluminescence and electroluminescence from a soluble polyfluorene. J Am Chem Soc. 1996;118:7416–7417.

[25] Sims M, Bradley DDC, Ariu M, Koeberg M, Asimakis A, Grell M, Lidzey DG. Understanding the origin of the 535 nm emission band in oxidized poly(9,9-dioctylfluorene): the essential role of inter-chain/inter-segment interactions. Adv Funct Mater. 2004;14:765–781.

[26] Kwong RC, Sibley S, Dubovoy T, Baldo M, Forrest SR, Thompson ME. Efficient, saturated red organic light emitting devices based on phosphorescent platinum(II) porphyrins. Chem Mater. 1999;11:3709–3713.

[27] Ponterini G, Serpone N, Bergkamp MA, Netzel TL. Comparison of radiationless decay processes in osmium and platinum porphyrins. J Am Chem Soc. 1983;105:4639–4645.

# Appendix 2: Highly red-shifted NIR emission from a novel anthracene conjugated polymer backbone containing Pt(II) porphyrins

# Appendix 3: Synthesis and Exciton Dynamics of Donor-Orthogonal Acceptor Conjugated Polymers: Reducing the Singlet–Triplet Energy Gap